UNIVERSITÉ DE STRASBOURG

UNIVERSITÈ DE STRASBOURG

Ecole Doctorale des Sciences de la Vie et de la Santé

THÈSE

présentée pour obtenir le grade de

Docteur de l'Université de Strasbourg

Discipline : Sciences du Vivant

Domaine : Aspects Moléculaires et Cellulaires de la Biologie

par

Namrata JAIN

Vecteurs de Gènes Non-Viraux Basés sur de Nouveaux Bolaamphiphiles Dissymétriques

Soutenue le 21 décembre 2010 devant la commission d'examen :

Pr. Philippe BARTHÉLÉMY	**Rapporteur externe**
Dr. Patrick MIDOUX	**Rapporteur externe**
Dr. Michel BESSODES	**Examinateur**
Dr. Guy ZUBER	**Rapporteur interne**
Dr. Andrey KLYMCHENKO	**Examinateur**
Dr. Guy DUPORTAIL	**Directeur de thèse**

UMR CNRS 7213, Faculté de Pharmacie, ILLKIRCH

UNIVERSITÉ DE STRASBOURG

UNIVERSITÈ DE STRASBOURG

Ecole Doctorale des Sciences de la Vie et de la Santé

THÈSE

présentée pour obtenir le grade de

Docteur de l'Université de Strasbourg

Discipline : Sciences du Vivant

Domaine : Aspects Moléculaires et Cellulaires de la Biologie

par

Namrata JAIN

Non-Viral Gene Delivery Vectors Based on New Unsymmetrical Bolaamphiphiles

Soutenue le 21 décembre 2010 devant la commission d'examen :

Pr. Philippe BARTHÉLÉMY	**Rapporteur externe**
Dr. Patrick MIDOUX	**Rapporteur externe**
Dr. Michel BESSODES	**Examinateur**
Dr. Guy ZUBER	**Rapporteur interne**
Dr. Andrey KLYMCHENKO	**Examinateur**
Dr. Guy DUPORTAIL	**Directeur de thèse**

UMR CNRS 7213, Faculté de Pharmacie, ILLKIRCH

My thesis project was performed in the Laboratoire de Biophotonique et Pharmacologie, directed by Prof. Yves MELY. I am grateful to him for providing me the opportunity to work in his lab.

I would like to express my heartfelt gratitude to Director of my thesis Dr. Guy DUPORTAIL for his help, guidance and support during my research. He has been generous with his time and knowledge. I would like to express my deepest gratitude and sincere appreciation to my co-Director Dr. Andrey S. KLYMCHENKO for his supervision, inspiration and encouragement for monitoring my research. It has been a privilege to study with him.

I am greatly honoured by the kind acceptance of Prof. Philippe BARTHÉLÉMY, Dr. Patrick MIDOUX, Dr. Michel BESSODES and Dr. Guy ZUBER as members of jury for my thesis and would like to thanks them for serving as my advisory committee.

Special thanks to Dr. Valérie GOLDSCHMIDT for her guidance and support with cellular studies, and Dr. Youri ARNTZ for his help with AFM studies. I would like to extend my gratitude to Dr. Hugues de ROCQUIGNY for his help with HPLC, Dr. Sebnem ERCELEN for preliminary structural characterisation and cellular studies, Dr. Ludovic RICHERT and Dr. Romain VAUCHELLES for fluorescence imaging studies. I thank to the groups of Dr. J.-S. REMY and Dr. B. FRISCH for help with luminometry and DLS measurements.

I would like to thank all my friends in the lab Kamal Kant SHARMA, Viktoriia POSTUPALENKO, Oleksandr KUCHERAK, Beata BASTA, Zeinab DARWICH, Julien GODET, Vanille GRENIER, Armelle JOUONANG, Jacques LUX and Hussein FTOUNI for their constant help, encouragement and our great discussions. I wish them all the best of luck in their future endeavours. I would also like to thank master's students Nada KRAYEM and Ludovic JOUANOLOU with whom I worked.

On a personal note, I would like to thank my family and friends who have supported me along the way in my pursuit for my goals.

The potential of gene therapy to treat genetic disorders relies strongly on the efficiency of delivery vectors. The failure of viral gene therapy clinical trails due to toxicity, immunogenicity and carcinogenicity raised serious safety concerns and strongly motivated a non-viral approach. However, non-viral gene delivery, mainly based on lipids and polymers, is currently ineffective for *in vivo* applications due to poor structural control of their DNA complexes and lack of serum stability.

The research conducted for this thesis was aimed at the design and synthesis of unsymmetrical bolaamphiphiles as a new family of non-viral vectors. For this purpose, several new bolaamphiphiles (bolas) were obtained by multi-step organic synthesis, bearing neutral sugar residue (mannoic, gluconic, lactonic acid or PEG group) and mono- or oligo-cationic ammonium-based headgroups, connected by different hydrophobic spacers. Within this design, a positively charged headgroup is expected to bind DNA, the hydrophobic spacer should drive the formation of a monolayer membrane shell around DNA, while the neutral group is to be exposed outside that will prevent further aggregation of the complexes. Our different structural characterization measurements showed that the self-assembly of bola, their interaction with DNA and the morphology of the bolaplexes depend strongly on the bola structure. While the first two generations of bolas lack the essential features of nonviral vectors, the final third generation was found highly promising. The latter showed strong interaction with DNA and formation of small DNA complexes (~100 nm) at low N/P, while at higher N/Ps it was significantly larger due to neutralization of their surface charge. Atomic Force Microscopy studies revealed a rod shaped or spherical nano-structural morphology of the bolaplexes. Their transfection efficiency and intracellular trafficking were tested in different cell lines. Significant transfection efficiency was observed in the presence of helping agents like DOPE or chloroquine suggesting that the key barrier for their internalization is the endosomal escape. Some bolaplex formulations showed transfection efficiency comparable to the best commercial transfection agents. Finally, all bolas showed low cytotoxicity. Thus, the present work validates a new concept for construction of nonviral vectors featuring controlled small size, high efficiency and low cytotoxicity.

We believe that the bola structure could be further modified to enhance transfection efficiency by favouring endosomal escape without use of any helping agent.

Table of Contents

ABBREVIATIONS

AAV	Adeno-associated virus
AFM	Atomic Force Microscope
1,8-ANS	1-Anilinonaphthalene-8-Sulfonic Acid
ASGPR	Asialoglycoprotein receptors
BC	Bicinchoninic Acid
BOP	(Benzotriazol-1-yloxy)tris(dimethylamino)phosphonium hexafluorophosphate
bp	Base pair
CAR	Coxsackie and Adenovirus Receptor
Cbz	Benzyloxy Carbonyl
Ch	Cholesterol
CMC	Critical micelle concentration
CT-DNA	Calf Thymus DNA
DIEA	N,N-Diisopropylethylamine
DLS	Dynamic Light Scattering
DMEM	Dulbecco's modified eagle's medium
DMF	Dimethyl formamide
DMSO	Dimethyl sulfoxide
DOPC	Dioleoylphosphatidylcholine
DOPE	Dioleoyl phosphatidylethanolamine
EtBr	Ethidium bromide
EM	Electron Microscopy
FBS	Fetal bovine serum
HCl	Hydrochloric acid
HIV	Human Immunodeficiency Virus
HOBt	1-hydroxybenzotriazole
HSV	Herpes simplex virus
kb	Kilo base
kbp	Kilo base pair
Luc	Luciferase

LL	Lactonolactone
LUV	Large unilamellar vesicles
LC-MS	Liquid chromatography-mass spectrometry
MES	2-(N-morpholino)-ethane sulphonic acid
MLM	Monolayer membrane
MS	Mass Spectrometry
MTT	3-(4,5-dimethyl-2-thiazolyl)-2,5-diphenyltetrazolium bromide
NLS	Nuclear localization signal
NMR	Nuclear Magnetic Resonance
Opti-MEM	Reduced Serum Media
PAM	Polyamidoamine
PBS	Phosphate buffer saline
pCMV-Luc	Plasmid encoding the photinus pyralis luciferase gene under the control of the cytomegalovirus promoter
pDNA	Plasmid DNA
Pd	Palladium
Pd-C	Palladium on carbon
PE	Posphatidylethanolamine
PEG	Polyethylene glycol
PEI	Polyethylenimine
PLL	Poly(l-lysine)
RLU	Relative light units
RME	Receptor-mediated endocytosis
RT	Room Temperature
TAE	Tris-acetate-ethylenediaminetetraacetic acid buffer
TFA	Trifluoroacetic acid
TfR	Transferrin receptor
THF	Tetrahydrofuran
YOYO-1	1,1'-(4,4,8,8-tetramethyl-4,8 diazaundecamethylene)bis[4-[[3-methylbenz-1,3-oxazol-2-yl]methylidine]-1,4 dihydroquinolinium] tetraiodide

GENERAL INTRODUCTION

Gene therapy is a rapidly developing area of research representing a fundamentally new way to treat a disease. Genetic material (genes) used in such a therapy should express a protein or interfere with its synthesis inside the cell. Replacing a defective gene with a normal gene and thus restoring the lost gene function in the patient's body is the essence of gene therapy.

The success in gene therapy strongly relies on the efficiency of delivery vectors. An ideal vector should be able to protect gene from all cellular barriers for effective delivery to the nucleus, should have the ability to regulate expression of the gene of interest and minimize toxicity by targeting specific cells. A variety of gene delivery vectors, viral and non-viral vectors, have been developed in past decades. Although viral vectors are highly efficient in transfecting cells, there are several concerns that limit their use to deliver DNA therapeutics in humans. The major concern is the toxicity of the viruses and their potential for generating a strong immune response. All these concerns make non-viral vectors, based on lipids and polymers, an attractive alternative. Their key advantages over viral vectors are: simplicity of use, large-scale production, ability to carry DNAs of large size, and lack of immune response. Their complexes with DNA (lipoplexes and polyplexes, respectively) show high efficiency *in vitro*, though their application for gene therapy *in vivo* remains a challenge. One of the key problems with these vectors is the poor structural control of their complexes with DNA.

The vast majority of natural and synthetic lipids studied so far are "monopolar" amphiphiles, i.e. molecules presenting one polar headgroup and generally two hydrophobic chains. However, bipolar amphiphiles, which are analogues of lipids presenting polar groups at the two opposite sides of the hydrophobic chain(s), so-called bolaamphiphiles (bolas), became the matter of intensive research only in the recent years. A remarkable feature of bolas is that, in contrast to bilayer membranes formed by lipids, they can form monolayer membranes due to the presence of membrane-spanning hydrophobic chains responsible for enhanced physical stability of bola membranes. In nature, they are mainly present in archaebacteria and ensure the integrity of the bacterial membrane at critical temperature and pH. In this context, unsymmetrical bolas, bearing

two different polar headgroups, can assemble in a parallel fashion to form asymmetric membranes (in form of vesicles or nanotubes) that will present different functional groups on each side.

In the case of membranes generated by unsymmetrical bolas bearing positively charged inner and neutral outer headgroups, the inner surface can be used to wrap the DNA molecule. While the outer surface, being inert to DNA, would prevent further oligomerization of the complex and could be utilized for efficient exposure of the biological signal for specific targeting. However, only a few reports have used this approach until now. Though the design of organic molecules forming nanotubes is well developed, only limited attempts have been made to use these nanostructures as gene delivery vehicles. Thus, in line with their ability to interact with DNA, these bola-molecules can be used as gene delivery vectors, a domain for which "monopolar" cationic lipids and other cationic agents are currently maintaining a dominant position.

In this project, we synthesized several new bolaamphiphiles, bearing neutral sugar and positive amine headgroups, connected by different hydrophobic spacers. Self-assembly of these bolaamphiphiles in aqueous solutions were determined by a number of physico-chemical methods: Dynamic Light Scattering (DLS), Gel Electrophoresis, Atomic Force Microscopy (AFM), Electron Microscopy and Fluorescence Microscopy. In addition, transfection efficiency and cytotoxicity was evaluated *in vitro*

Thus, this work introduces new bolaamphiphile-based non-viral vectors and provides interesting insights for further improvements of their efficiency.

Bibliographic Review

1. GENE THERAPY

1.1 Overview and Historical Prospective

The double-helix model of DNA proposed by 'Watson and Creek' in 1953 (*1*) and the concepts of chromosomes, genes, etc., opened a whole new vista of permutations and combinations in the treatment of various hereditary diseases. Rapid developments of recombinant DNA technology permitted the preparation of large quantities of therapeutic proteins. However, after the discovery of nucleic acids by Miescher, and other important findings - like the search for transforming factors (*2*) and chemical analysis of DNA, it was realized that genetic information is transferred via DNA and not by genetic proteins or complex polysaccharides. The transfer of this genetic material to a target cell in order to achieve a clinical benefit is termed as "Gene Therapy" and was first proposed by Friedman and Roblin in 1972 (*3*).

Gene therapy brings about tremendous potential in the treatment of various diseases and disorders as the defective or absent genes, responsible for the disease, are removed or replaced with a 'healthy' or working gene so that the enzyme or protein requirement of the body is fulfilled, resulting in elimination of the disease (*4*). Originally conceived as an approach to treat autosomal recessive Mendelian disorders, it is now being applied to a broad range of diseases such as cancers, infections and degenerative disorders (*5*). After diagnosis of the problem and construction of appropriate plasmids, gene therapy requires effective and safe transfection and gene expression. Transfection describes the transfer of genetic material into the cell nucleus, and gene expression indicates the subsequent synthesis of the encoded protein by the cell. Due to safety, legal and ethical issues, gene transfer in humans is presently permitted only in somatic cells and not in germline cells.

In more general terms, Gene therapy can be redefined as a method which provides, to patient's somatic cells, the genetic information required for producing specific therapeutic proteins to correct or modulate diseases. It involves the three independent steps of administration, delivery and expression (*6*). Introduction of DNA into the body refers to administration while delivery consists of the translocation of genetic material from the site of administration to the nucleus of the target cell. Finally, expression

determines the production of the therapeutic protein in the cell. The purpose of somatic gene therapy is to overcome the limitations associated with direct administration of therapeutic proteins, including low bioavability, systemic toxicity, instability and high cost of manufacturing.

This research has gained significant attention over the past two decades as a potential method for treating genetic disorders such as severe combined immunodeficiency (*7*), cystic fibrosis (*8*) and Parkinson's disease (*9*), as well as an alternative method to traditional chemotherapy used in treating cancer (*10*). Early gene therapy studies represented the feasibility of genetic manipulation as a novel treatment for disease. The first experiments on cloning of mammalian genes in the late 1970s and early 1980's are commonly seen as the precursors of gene therapy resulting in the first human gene therapy trial in 1989 (*11*). A major setback for gene therapy was the death of Jesse Gelsinger in 1999 during a clinical trial due to an adenovirus-based gene vector (*12*). Another unfortunate case occurred in 2002 when two children, treated for X-linked severe combined immunodeficiency (SCID-X1), developed leukemia (*13*). However, the treatment was successful in seven other patients. Most recently, a clinical trial on retinal dystrophy was performed and improved visual function was observed (*14, 15*). So far, more than 1500 clinical trials have been conducted in humans, where cancer related diseases account for the largest number (~65%) of all clinical trials treated by gene therapy (Figure 1.1). Cardiovascular diseases are the most common cause of death in western countries and 9% of all the clinical trials have been directed against these diseases and 8 % against monogenic diseases.

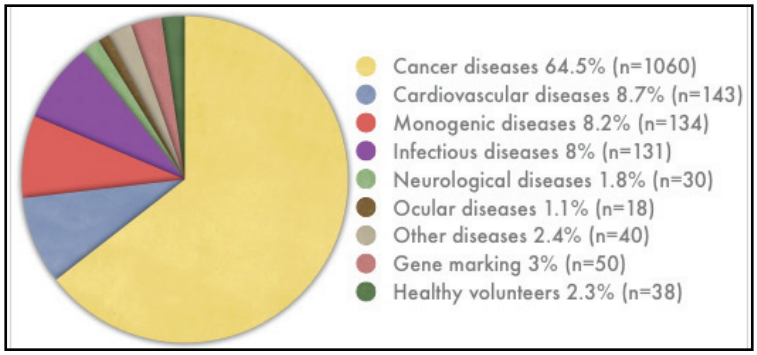

Figure 1.1. Indication addressed by gene therapy clinical trials (2010) modified from (http://www.wiley.co.uk/genetherapy/clinical/).

The two different strategies, *in vitro* and *in vivo*, for delivering therapeutic transgene will be discussed in the following section.

1.2 In Vitro (or Ex-Vivo) and In Vivo Gene Therapy

In vitro gene therapy involves removing tissues from the patient, transfecting (or virally-infecting) the cells in culture, and then reimplanting the genetically altered cells to the patient. This delivery strategy is more common, but at the same time problematic, since it requires (i) a mitotic cell population; (ii) a tissue culture method and (iii) a cell transplantation technology. However, this approach has several advantages: (i) gene transfer efficiency is generally high; (ii) the transduced cells can be enriched if the vector has a specific marker gene and (iii) transduction efficiency can be assessed before re-implantation.

On the other hand, *in vivo* gene therapy requires the transgene to achieve specific cell targeting, either through direct tissue injection (brain tumors) and biolistics (dermal DNA vaccination) or by receptor-mediated processes (cell specific DNA carriers), within the body.

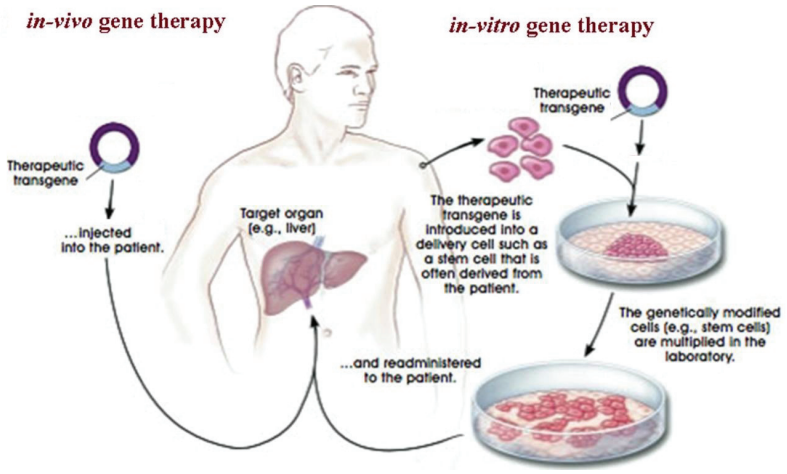

Figure 1.2. Strategies for delivering therapeutic transgene into patient.

Importantly, none of these strategies involves reproductive germline cells, therefore the genetic alteration will not be transmitted to the next generation. At present, gene therapy strategies, both *in vitro* and *in vivo*, are mainly focused on the development of transgene carrier with less toxicity and prolonged and controlled expression, thereby widening the potential application of the therapy to a high spectrum of medical fields. However, several barriers need to be overcome for successful application of gene therapy into efficient therapeutics. These barriers will be discussed briefly in the next section.

2. GENE DELIVERY BARRIERS

Circumventing the biological barriers to gene delivery is a considerable challenge, as it requires the successful transport of the transgene from the site of administration to the nucleus of the target cells where it becomes available to the transcription machinery or capable of blocking the expression of the defected genes (*16*). The biodistribution or pharmacokinetics of a gene is determined by its interaction with the body, a factor that relies on both physicochemical and biological properties. Although efficient and target-specific gene transfer is difficult to achieve, the route of administration determines the number of barriers that need to be overcome for successful gene transfer. These barriers fall into two main classes known as extracellular barriers and intracellular barriers.

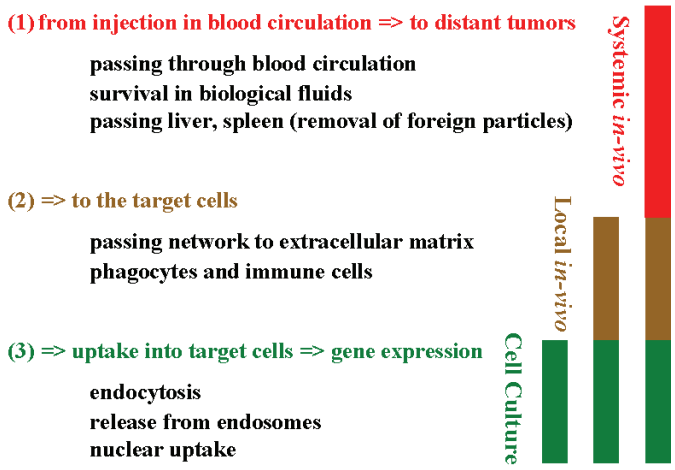

Figure 1.3. Multiple barriers for targeted gene expression.

2.1 Extracellular Barriers

Successful *in vivo* gene transfer could be achieved by overcoming the extracellular barriers. These biodistribution barriers for systemic gene delivery include physiochemical hindrances (such as particle size and surface charge), interaction with blood components, recognition by immune system and nonspecific uptake.

Once in blood stream, transgene is exposed to serum inactivation and degradation by nucleases. Therefore, some carrier molecules should be used to encapsulate DNA which are capable of protecting and rendering DNA inaccessible to these degradative enzymes. Protection could also be achieved by encapsulation in protein capsules, by condensation of DNA using cationic carrier system or by entrapping in controlled release hydrogels. Thus, steric stabilization can be achieved by creating a 'brush' layer of "carriers" on the surface of gene, thereby decreasing non-specific interactions.

Control of size and surface charge play an important role for *in vivo* gene transfer. The structure of the blood capillary wall varies among organs and tissues like in discontinuous capillaries of the liver, spleen, and bone marrow sinusoid, large inter-endothelial junctions, where fenestrations are of up to 150 nm (*17*). Moreover, strong positive charge on the particles facilitates non-specific interactions to the extracellular matrix, cell surfaces and plasma proteins (all negatively charged), whereas strong negative charge can cause scavenging by phagocytosis via the macrophage polyanion receptor.

Additionaly, nonspecific uptake need to be reduced by attaching targeting ligands such as antibodies (*18*) and peptides (*19*) to the surface of the DNA delivery carrier. Therefore, the stabilization of genome by a carrier molecule should allow specific cell types to be targeted by utilizing the interactions between surface receptors and ligand-containing gene delivery carrier systems. These ligands can be small molecules (e.g. folate, galactose, etc.) or peptides and proteins (e.g. transferrin and antibodies).

Thus, the most essential need for efficient gene delivery is to provide steric stabilization of gene (as mentioned above), i.e. by controlling the size and surface charge, for extended circulation time (*20*) and to minimize the nonspecific interactions (*21, 22*) and a requirement to place the targeting ligand at the surface of the particle to provide for effective and specific binding to cell surface receptors.

In the following section, various ligands for specific targeting with respect to their advantages and mechanism of gene delivery will be reviewed.

2.1.1 Specific targeting

An encouraging technique to achieve specific, efficient and safe gene delivery involves binding of targeting gene delivery vehicle to a cell-specific receptor or surface marker for subsequent uptake and transport to the nucleus for expression and thus permitting selective delivery directly to the patient's cells *in vivo*. This concept of targeted delivery was proposed by Paul Ehrlich at the end of the 20th century and was named as the "magic bullet" concept. Based on the various specific interactions discovered in biology, several antibodies or ligands have been investigated to achieve active targeting effect to the corresponding antigen- or receptor-overexpressing organs, tissues, or cells (*23-27*).

Specific targeting may be achieved in two ways: First, tissue or tumor-specific promoters may be engineered into the expression vector carrying the gene of interest to ensure site-specific expression. Second, the vector-containing vehicle may be constructed to deliver the exogenous DNA to the target cells (*28, 29*).

Specificity of gene vectors in recognizing the target cells only and exploiting the proper intracellular trafficking routes are the key issues in their optimization. In this respect, ligand-receptor mediated delivery systems that have the potential to direct cell-specific gene transfer have received major attention in the past few years, as the naturally occurring ligands and their receptors are not only able to achieve site-specific targeting to ligand-specific biosites, but they are also biodegradable, non-toxic and non-immunogenic (*30*). Coupling of such growth factors, antibodies or antibody-fragments to DNA

complexes not only offers the possibility to deliver gene to the targeted cell, but also facilitates internalization of the complexes via receptor-mediated endocytosis (RME).

The most widely used preexisting targeting ligands are based on endogenous molecules, which are already present in the body. Preexisting ligands are often relatively easily available and the receptor and its distribution are fairly well studied (*31*). The use of the vitamin folic acid as a ligand is an example of the effective use of the natural receptor substrate for targeting. The receptor for folic acid is overexpressed in a number of human tumors, including cancers of the ovary, kidney, uterus, testis, brain, colon, lung, and myelocytic blood cells (*32*).

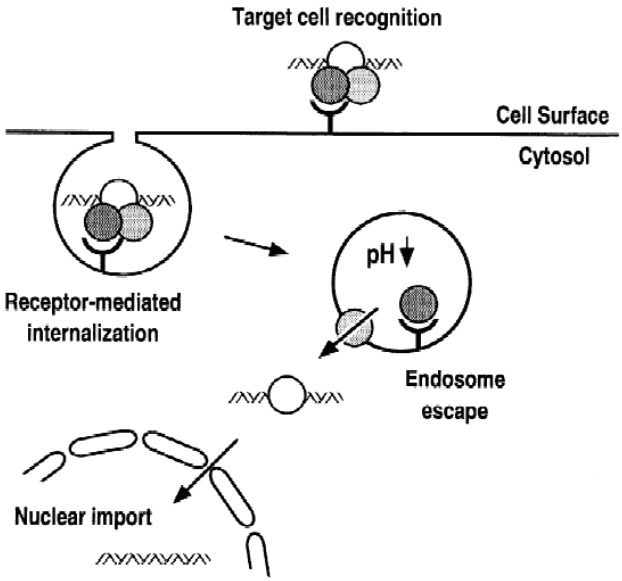

Figure 1.4. Functions facilitating transport of DNA across cellular barriers: ligands interacting with cell surface receptors facilitate target-cell specific uptake via receptor-mediated endocytosis. In the low pH environment of the endosomal compartment an endosomolytic activity mediates the release of the DNA complex into the cytosol. Active nuclear transport mechanisms could enhance transfection efficiency and allow successful gene transfer in non-dividing cells. These activities might be attached to DNA complexes individually or reside in distinct functional domains of chimeric DNA-carrier proteins (*33*).

Moreover, Transferrin receptor (TfR) has been used as a target to deliver a wide range of therapeutic agents (*26, 34*). Other ligands that have been examined in this regard include insulin (*35, 36*), asialoorosomucoid (*37*), and many others (*38*). The asialoorosomucoid receptor, the earliest lectin exploited for this purpose, is expressed in hepatocytes (*39*) and in the model human hepatocellular carcinoma cell line HepG2 where each cell displays around 200,000 receptors (*40*). Wu and co-workers were the first to couple asialoorosomucoid to PLL for receptor-mediated gene delivery to hepatocytes (*37, 41*). This approach was extended by utilizing a large number of different ligands (*42*).

At the last, targeting the delivery system have been extensively proposed using macromolecular carriers with monoclonal antibodies (*43*) or carbohydrates (*44, 45*) as target signals. Since the feasibility of using carbohydrate as a ligand to target protein receptors at sites of localization, termed 'glycotargeting', was first demonstrated in 1971 (*46*), the potential of using carbohydrates to create a truly targeted (or actively-targeted) delivery system became more clear. Among them, carbohydrate receptors in the liver, i.e., asialoglycoprotein receptors (ASGPR) in hepatocytes and mannose receptors in Kupffer and liver endothelial cells were reported by Ashwell and Harford (*47*). Several other macromolecular carriers like galactose (*48, 49*) have been developed as a targetable moiety for liver-specific chemical agent delivery (*50, 51*). Moreover, lactose has also been proposed for specific interaction with the asialoglycoprotein (ASGP) receptors over-expressed on hepatocyte membranes (*52-54*) and several other sugar-containing conjugates have been used as a target permitting organ specific therapy of liver diseases (*55*).

After successful gene transfer through extracellular barriers, the gene reach to the second class of barriers, known as intracellular barriers, which need to be overcome by both *in vivo* and *in vitro* gene delivery systems.

2.2 Intracellular Barriers

Cell surface and its interior acts as intracellular barriers for successful transgene expression, which need to be overcome in order to develop regulated transport of relevant molecules to the cell interior and then towards the nucleus.

Various intracellular barriers will be discussed in this section.

2.2.1 Cellular uptake and endosomal escape

Cell is the basic functional unit of life and an elaborate structure of barriers that serve to maintain its delicate homeostasis. It is defined by a plasma membrane composed of a phospholipid bilayer and proteins, containing different cell organelles. One of its major characteristics is the separation of genetic material from the rest of the cell, called the cytoplasm, by a nuclear membrane. The nuclear envelope is composed of double lipidic bilayer membrane which fuses at regular intervals, forming nuclear pores, and thus allowing nucleus-cytoplasm trade in both directions. Thus, cell acts as is a system of walls and doorways for foreign intruders, like transgene.

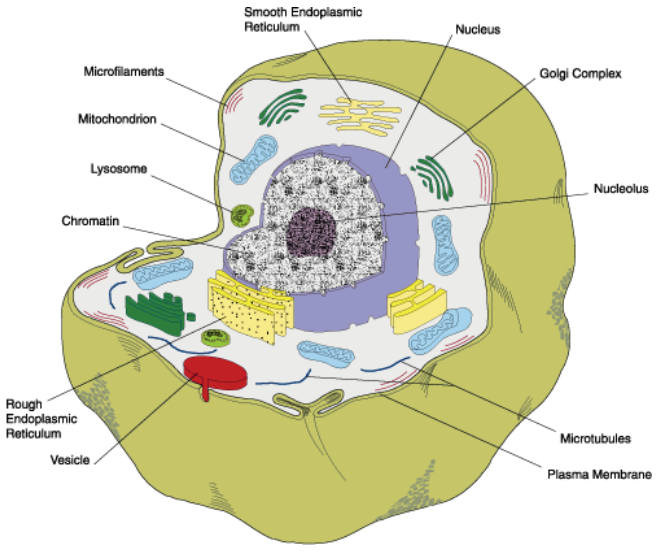

Figure 1.5. Basic structure of eukaryotic cell.

Considering the cellular features, the interaction of DNA with the cellular membranes is typically very low due to their relatively high negative charge density (*56*). Therefore, steric stabilization of the gene by a cationic carrier could result in its binding to the negatively charged cellular membrane. Moreover, eukaryotic cells uptake molecules of the outside world by a variety of different mechanisms and target them to specific organelles within the cytoplasm. These processes are collectively termed as endocytosis. Cells use three major types of endocytosis: phagocytosis, pinocytosis and receptor-mediated endocytosis (RME) (Figure 1.6).

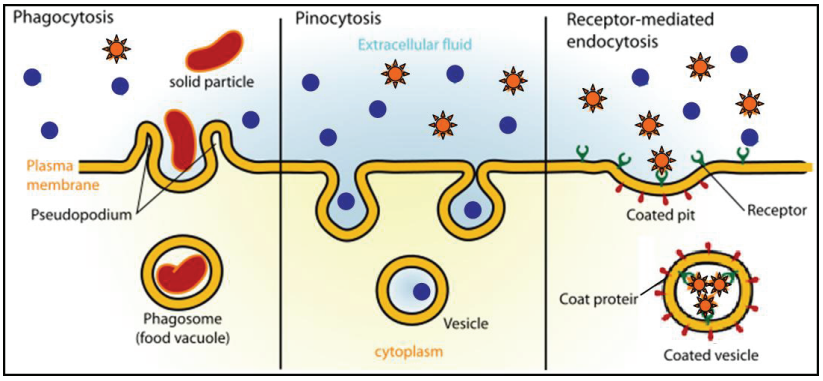

Figure 1.6. Cellular uptake by endocytosis (Cell Biology Wiki, 2009 Lecture 6, http://php.med.unsw.edu.au/cellbiology/index.php?title=2009_Lecture_6).

Phagocytosis (or "cellular eating") involves uptake of large particles while pinocytosis (or "cellular drinking") involves the ingestion of fluid and solutes via small vesicles. Some specific molecules are often transported through receptor-mediated endocytosis. In this case, the molecules first bind to the specific receptors on the plasma membrane where the interior portion of the receptor protein is embedded. The protein clathrin then coats the inside of the membrane in the area of the pit. When an appropriate collection of molecules gathers in the coated pit, the pit deepens and seals off to form a coated vesicle, which carries the molecule into the cell. This is the best-characterized mechanism for gaining entry into the cell. After internalization, these molecules are delivered to early endosomes, where efficient sorting occurs (*57*). Some of the molecules, in particular recycling receptors, are rapidly recycled back to the plasma membrane for reutilization. However, the inability to escape the endosomal compartment presumably

results in trafficking via late endosomes to lysosomal compartments where the DNA is eventually degraded. Thus, including the uptake of extracellular nutrients, the endocytic mechanisms serve other important cellular functions like regulation of cell-surface receptor expression, maintenance of cell polarity, and antigen presentation. However, efficient endosomal escape is necessary for effective delivery (*56*).

2.2.2 Cytosolic mobility and nuclear entry

On endosomal escape, DNA must cross the cytosol and nuclear membrane to gain access to the transcriptional machinery of the nucleus. The high viscosity of cytosol leads to a decrease of plasmid mobility (*58*). Moreover, the diffusion coefficient of DNA in the cytoplasm is inversely related to the size of the plasmid, suggesting that smaller plasmids may easily transport to reach nucleus.

There are three possible routes for DNA transport to the nucleus: 1. it can pass into the nucleus through nuclear pores, 2. it can become physically associated with chromatin during mitosis when the nuclear envelope breaks down or 3. it could traverse the nuclear envelope. Of these three possibilities, the latter seems to be least favorable with no experimental support (*56*). Transport of plasmid DNA by nuclear pores has been implicated in numerous studies, particularly when the plasmid contains specific sequences recognized by host cell transcription factors (*59*). Nuclear pores are embedded in the nuclear envelope at high surface densities (3000–4000 pores/nucleus) (*60*)and exist in at least two conformational states. The closed state permits the passive diffusion of molecules of < 9 nm in diameter, whereas the open state facilitates transport of particles of size < 26 nm (*61, 62*).

Covalent modification of DNA by the attachment of nuclear localization sequence or signal (NLS) has been demonstrated to increase nuclear translocation of DNA (*63*). The use of peptide nucleic acids to non-covalently attach NLS by the formation of site-specific DNA triplexes has also been reported (*64*). The most widespread mechanism by which DNA is thought to gain access to the nucleus is by association with nuclear material on breakdown of the nuclear envelope during mitosis. Thus, the dividing cells

often exhibit higher transfectability than non-mitotic cells, indicating that plasmid DNA can reach the nucleus during nuclear envelope disassembly (*65*).

3. GENE DELIVERY VECTORS

The susceptibility of DNA and other nucleic acids to nuclease degradation and the unknown abundance of nucleases present in the pathway of *in vitro* or *in vivo* administered genes generally call for a delivery vector/system that will provide an initial packaging. Thus, the main objective in gene therapy is the development of efficient and non-toxic gene carriers that can encapsulate and deliver foreign genetic materials into the specific cell types. In this quest, the use of nucleic acid as drugs for gene therapy purpose has led to the development of sophisticated and efficient DNA carriers, called gene delivery vectors. These packaging vectors should not only protect the genes through the delivery process, but also preserve the activity of the nucleic acid drugs.

Thus, an ideal vector should have: 1. low antigenic potential, high capacity and high transduction efficiency; 2. allow controlled and targeted transgene expression; 3. of a reasonable expense and 4. be safe for both patients and the environment.

In the following sections gene delivery vectors has been categorised, with respect to their advantages as well as disadvantages and the mechanism of gene delivery, as viral and non-viral vectors.

3.1 Viral Vectors

Viruses are intra-cellular parasites that infect cells, often with great specificity to a particular cell type. Viral vectors are biological systems derived from those naturally evolved viruses capable of transferring their genetic materials into the host cells. These are one of the major vehicles used in gene therapy to get their carrier sequences expressed in the proper host. The recombinant viral vectors can transduce the cell type it would normally infect, by replacing genes that are needed for the replication phase of viral life cycle (the non-essential genes) with foreign genes of interest. The modification

of viruses for the delivery of exogenous genes was first reported in 1968 using the tobacco mosaic virus. To produce such recombinant viral vectors the non-essential genes are provided in trans, either integrated into the genome of the packaging cell line or on a plasmid.

Nowadays, viruses are employed in more than 60 % of human clinical gene therapy trials worldwide. Gene therapy using viral systems has made significant progress for the treatment of diseases, such as cancer (*66*), AIDS (*67*), and dystrophy (*68*). The most commonly used gene transfer vehicles in clinical trials are adenovirus and retrovirus vectors (Figure 1.7).

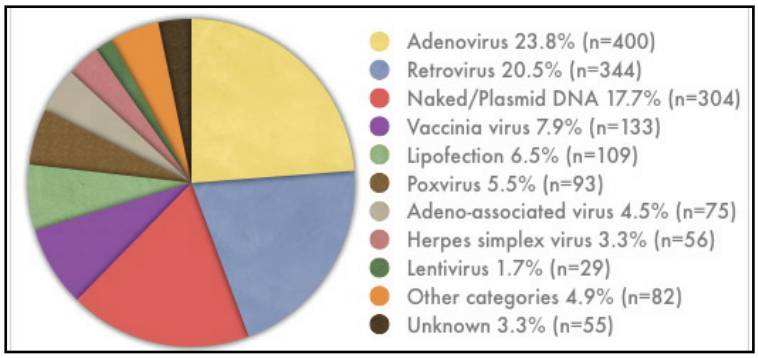

Figure 1.7. Vectors used in gene therapy clinical trials (2010) modified from (http://www.wiley.co.uk/ genetherapy/clinical/)

Though a number of viruses have been developed as gene delivery vectors, only retrovirus, adenovirus, adeno-associated virus and herpes simplex virus based vectors will be discussed in the following sections.

3.1.1 Retrovirus (including lentivirus)

Retroviruses are enveloped single-stranded RNA viruses, with wide applications in gene transfer protocols. The ability of retroviral vectors to successfully deliver foreign genetic materials was first described in 1981 (*69, 70*). The most commonly used retroviral vectors are based on the moloney murine leukaemia virus (Mo-MLV) and have varying

cellular tropisms, depending on the receptor binding surface domain (SU) of the envelope glycoproteins. Their structure consists of a diploid genome of about 7-10 kb, composed of four gene regions known as gag, pro, pol and env encoding the structural proteins, viral protease, integrase and viral reverse transcriptase, and envelope glycoproteins, respectively. Following entry into the target cells, the RNA genome is reversed-transcribed into a double-stranded DNA proviral genome, which further forms a pre-integration complex with the viral integrase and transported to nucleus (*71*). Inside nucleus, proviral genome is integrated into the host chromosomal genome, where the host's transcriptional machinery gives rise to expression of viral genes.

The advantages of retroviral vectors include the ability to transduce dividing cells, the inability to express any immunogenic viral proteins and long-term transgene expression in humans (*72*). On the other hand, their disadvantages are the random insertion into the host genome, which could possibly cause oncogene activation or tumor-suppressor gene inactivation; the limited insertion capacity (8 kb); the inability to transduce non-dividing cells and their inactivation by human complement (*73*).

To overcome the drawbacks of retroviruses, vectors derived from lentivirus have been constructed as they have the ability to infect and express their genes in both mitotic and post-mitotic cells. Additionally, they have two virion proteins (matrix and Vpr) that can transport the pre-integration complex across the nuclear membrane in the absence of mitosis (*74*). The most commomly used lentivirus is the human immunodeficiency viruses (HIV) that possess all the advantages of retroviral vectors alongwith the additional ability to transduce post-mitotic cells.

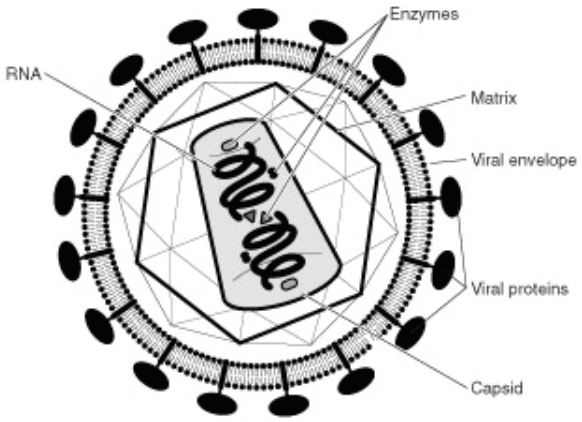

Figure 1.8. Basic Structure of retroviral particle.

3.1.2 Adenovirus

Adenoviruses are non-enveloped double-stranded DNA viruses (36 kb) that can infect both dividing and non-dividing cell (*75, 76*). They are infectious human viruses (*77*), which often cause mild respiratory illness, kerato-conjunctivitis or gastroenteritis. Their structure consists of icosahedral capsids composed of 240 hexon capsomeres forming the 20 triangular faces of the icosahedron, and 12 penton capsomeres with spike-shaped protrusions located at the 12 vertices (Figure 1.9). Histon-like viral core proteins are associated with the DNA package within the capsid (*78, 79*).

The process of virus entry into the cell is mediated by the attachment of the fiber knob protein to a high-affinity cell-surface receptor called the Coxsackie and Adenovirus Receptor (CAR) (*80*) and then further progressed by an interaction between cell-surface integrins with the capsid (*81*). The adenovirus virion is endocytosed and a subsequent decrease in endosomal pH causes a conformational change to the virion capsid proteins, resulting in the release of the capsid into the cytoplasm. The capsid is then transported to the nucleus and the genome is released which further undergoes replication and transcription. Adenoviral vectors have been widely used for cancer therapy (*82-84*).

Adenoviruses vectors present other additional advantages like a relatively large transgene capacity and a high efficiency of gene transfer without integration into the host genome supplemented by easy manipulations. However, the durations of *in vivo* transgene expression and immunogenicity are limited.

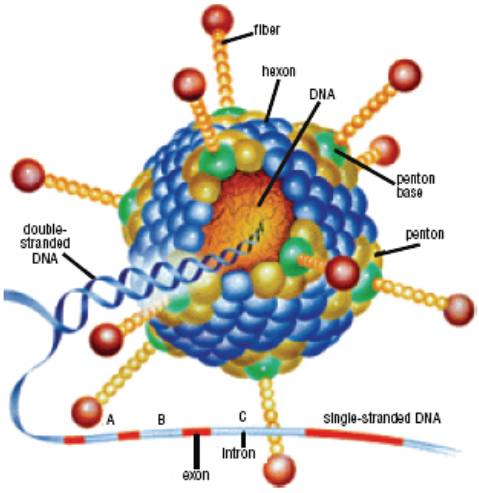

Figure 1.9. Basic structure of adenovirus particle (*85*).

3.1.3 Adeno-Associated viruses

Adeno-associated viruses (AAVs) are human parvoviruses that normally require a helper virus, such as adenovirus, to mediate a productive infection (*86*). Their structure consists of a short, linear, single-stranded DNA genome (*87*) composed of two open reading frames (ORFs), rep (regulation) and cap (structure), and two small (145 bp) inverted terminal repeats (ITRs) (*88*). Similar to adenoviruses, AAVs can infect both dividing and non-dividing cells. Their DNA, however, integrate into the host cell genome in a similar way as retroviruses (*89*).

The main drawback, however, is the need for helper viruses for their production (*90, 91*) which may result in contaminated AAV vectors during preparation. This disadvantage was overcame by inducing viral replication through genotoxic stimuli such as heat shock, chemicals or irradiation (*92*). In fact, AAV-mediated gene transduction and antitumor effects *in vitro* and *in vivo* were significantly enhanced when combined with UV and gamma radiation treatments (*93-95*). In addition to replication difficulties, the packaging capacity of this vector is very limited (< 5.0 kb) (*96*), which is a major limitation of this vector system.

3.1.4 Herpes simplex virus

HSV-1 is an enveloped, double-stranded DNA virus with a genome of 152 kb encoding more than 80 genes. The virus genome is almost 15 and 4 times bigger than that of lentivirus and adenovirus respectively, ranking at the top of viral vector's capacity. These features provide multiple sites of foreign gene insertion, making HSV a large capacity vector capable of harboring at least 30 kb of non-HSV sequences representing large single genes or multiple transgenes that may be coordinately or simultaneously expressed (*97*). HSV vectors have been used to infect a wide variety of cell types, including neurons (*98, Lowenstein, 1995 #155, 99*), muscle (*100*), brain tumours (*101*), liver (*102*), pancreatic islets (*103*) and pituitary cells (*104*).

A most attractive feature is the efficient infectivity of HSV for a large number of cell types, which results in efficient gene transduction. Limitations of these vectors include the lack of experience with recombinant herpes viruses in patients, difficulties related to long-term transgene expression in certain tissues including brain and difficulties related to vector targeting, since the mechanism of HSV attachment and entry is complex, involving multiple viral envelope glycoproteins (*105*). Although recent vector modifications have made HSV vectors less toxic (*106, 107*), the potential therapeutic application of HSV vectors, except for cancer gene therapy (*108*), may be limited.

3.2 Non-Viral Vectors

Although viral vectors have demonstrated excellent gene transfer and expression, there are several concerns regarding the use of viruses to deliver DNA therapeutics in humans. The limitations associated with viral vectors in terms of their limited capacity of transgenic materials, induction of strong immune response, inability to transfect non-dividing cells and significant toxicity (*89, 96*) have led to the search for alternative approaches. Thus, the transfer of genetic material using viral- based vectors is followed by the development of non-viral systems. Non-viral vectors, also called non-biological gene delivery systems, can be traced back to the work of Avery, MacLeod, and McCarthy, in 1944 which showed that genes were transferred by nucleic acids (*109*). Several studies in the early 1960s reported changes in cellular phenotype following exogenous DNA exposure.

Non-Viral vectors are particularly suitable with respect to simplicity and ease of large scale production. Moreover, they lack innate immune response with certain exceptions (*110*). The first non-viral technique to gain wide acceptance was calcium phosphate-mediated transfection. This system has undergone little change since being well characterized in the early 1970s. It was not until the advent of cationic liposomes in 1988 that non-viral vectors offered an efficient means to transfer genes into cells.

In the past decade, non-viral gene transfer vectors have been actively studied in order to obtain structural entities with minimum size and defined shape. The final size of a gene transfer vector did not depend on the plasmid DNA length, while the gene transfer capacity is said to be effected (*111*). Moreover, non-viral systems are cationic in nature. They interact with negatively charged DNA through electrostatic interactions. The total charge however maintains a positive net value, enabling the carrier to efficiently interact with the negatively charged cell membranes and internalize into the cell, which occurs mainly through the endocytosis pathway (*112*).

Non-viral gene delivery systems consist of following categories:

3.2.1 Naked DNA

Simple injection of plasmid DNA directly into a tissue without additional help from either a chemical agent or a physical force is able to transfect cells. In 1990, Wolff and colleagues were the first to report effective expression of intramuscularly injected naked plasmid DNA in myofibers (*113*). The level of gene expression, although relatively low, was sufficient for vaccination. Local injection of plasmid DNA into the muscle (*113*), liver (*114-116*), skin (*117*), or airway instillation into the lungs (*118*) leads to low-level gene expression. Nevertheless, gene transfer with naked DNA is attractive because of its simplicity and lack of toxicity. Practically, airway gene delivery and intramuscular injection of naked DNA for the treatment of acute diseases and DNA-based immunization, respectively, are the two areas that are likely to benefit from naked DNA-mediated gene transfer, provided that further improvements are made in delivery efficiency and duration of transgene expression (*119*).

A broad application of naked DNA-mediated gene transfer may not be conceivable because DNA, being large in size and highly hydrophilic, is efficiently kept out of the cells by several extracellular and intracellular barriers. Therefore, various manipulations have been used to improve the efficiency of the method and several physical methods like electroporation, gene gun, ultrasound, high pressure injection, etc. have been established. In this section, I will focus mainly on the methods of electroporation and gene gun.

3.2.2 Electroporation

Electroporation is the application of high voltage to a mixture of DNA and cells in suspension and was first described in 1960s (*120*). The cell-DNA suspension is placed between two electrodes and subjected to an electrical pulse. In this case, DNA enters the cells through holes formed in the cellular membrane during the electrical pulse and gets trapped within the cytoplasm upon termination of the electrical pulse. For efficient gene transfer, electroporation depends upon the nature of the electrical pulse, the distance between the electrodes, the ionic strength of the suspension buffer, and the nature of the cells. Best results have often been obtained from rapidly proliferating cells. Electroporation is a versatile method that has been extensively tested in many types of tissues *in vivo (121, 122)*, among which skin and muscles are the most extensively investigated, although the system should work in any tissues into which a pair of electrodes can be inserted. Because of the necessity of using electrodes, electroporation is difficult to be designed for *in vivo* applications. However, in the recent years, DNA electrotransfer to muscle tissue has reached clinical advancement with 8 on-going clinical trials (*123*).

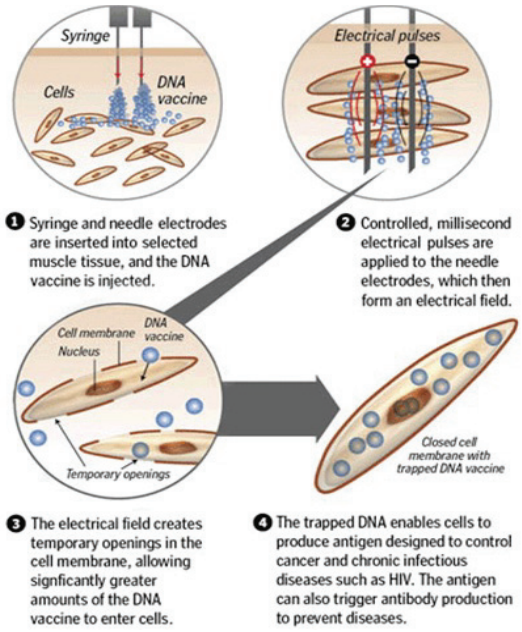

Figure 1.10. Basic steps involved in electroporation (http://www.inovio.com/images/IMG_how_ep_delivers.gif).

Major drawbacks of electroporation for *in vivo* applications are: 1. limited effective range of ~1 cm between the electrodes, which makes it difficult to transfect cells in a large area of tissues; 2. a surgical procedure is required to place the electrodes deep into the internal organs; 3. high voltage applied to tissues can result in irreversible tissue damage as a result of thermal heating (*124*). For example, electroporation of mammalian cells is an inefficient technique since many cells do not survive the high voltage nature of this procedure. However, some of these concerns may be solved by optimizing the design of electrodes, their spatial arrangement, the field strength, and the duration and frequency of electric pulses.

3.2.3 Gene gun

Particle bombardment through a gene gun is an ideal method for gene transfer to skin, mucosa, or surgically exposed tissues within a confined area (*125*). DNA is deposited on the surface of gold particles, which are then accelerated by pressurized gas and expelled onto cells or tissues. The momentum allows the gold particles to penetrate a few millimeters deep into a tissue and release DNA into cells on the path (*119*). Further improvements could include chemical modification of the surface of the gold particles to allow higher capacity and better consistency for DNA coating, and fine-tuning of the expelling force for precise control of DNA deposition into cells in various tissues (*126*).
The major advantage of gene-gun mediated gene transfer is that it does not require the use of complex delivery systems. However, a disadvantage is the shallow penetration of DNA into the tissues.

3.2.4 Cationic lipid based vectors

Felgner pioneered gene delivery using cationic lipids in 1987 (*127*) and since their introduction as gene carriers, cationic liposomes have become one of the most studied non-viral vectors. The idea was to neutralize the negative charge of plasmids with positively charged lipids to capture plasmids more efficiently and to deliver DNA into the cells. The ability to chemically synthesize a wide variety of liposomes have resulted in a highly adaptable and flexible system capable of gene delivery both *in vitro* and *in vivo*. Since the liposome technology is better understood, it should be possible to produce vectors with improved *in vivo* gene delivery for specific targeting. Studies involving protein-DNA-liposome complexes were already showing promise in the ability to target DNA into the specific cells. However, compared to viral vectors, they demonstrate decreased transgene expression, and are relatively transient due to cellular degradation and a lack of stable integration into the host genome (*128*).

In aqueous media, cationic lipids are assembled into a bilayer vesicular-like structure (liposomes). Liposomes are first arranged into multilamellar vesicles, while unilamellar vesicles could be obtained by sonication (*129*), detergent removal (*130*) or extrusion through porous membranes (*131, 132*). However, more recently, cationic lipid emulsions have been described and evaluated as possible non-viral gene carriers (*133, 134*).

One of the most frequently cited cationic lipids "lipofectin", is commercially available and first reported by Felgner in 1987 to deliver genes *in vitro*. Lipofectin is a mixture of N-[1-(2, 3-dioleyloyx) propyl]-N-N-N-trimethyl ammonia chloride (DOTMA) and DOPE (a helper lipid) with 100% loading efficiency of its DNA complexes. The lipid :DNA ratio and overall lipid concentrations used in forming these complexes are extremely important for efficient gene transfer. It has been used to deliver linear DNA, plasmid DNA, and RNA to a variety of cells *in vitro*. Following intravenous administration of lipofectin-DNA complexes, both the lung and liver showed marked affinity for uptake of these complexes and transgene expression. Moreover, a large number of other cationic lipids have been synthesised and studied for gene delivery (*135-141*). In the series of various of cationic lipids, DC-Chol, *N*-[1-(2,3-

dimyristyloxy)propyl]-*N,N*-dimethyl-*N*-(2-hydroxyethyl) ammonium bromide and N,N,N-trimethyl-2-bis[(1-oxo-9-octadecenyl)oxy]-(Z,Z)-1propanaminium methyl sulfate have been used in human clinical trails by local injection (*142*).

Due to the close correlation between the structure and related biological activity of the cationic lipids as gene delivery vectors, their structure, complexes with DNA, effect of helper lipid in transgene delivery and structure/activity relationship will be summarized in the following sections.

3.2.4a Structure of cationic Lipid

Their structure is composed of three basic domains: a hydrophobic anchor (consisting of one or two fatty acid side chains), a linker and a positive charged headgroup thus making them amphiphilic molecules.

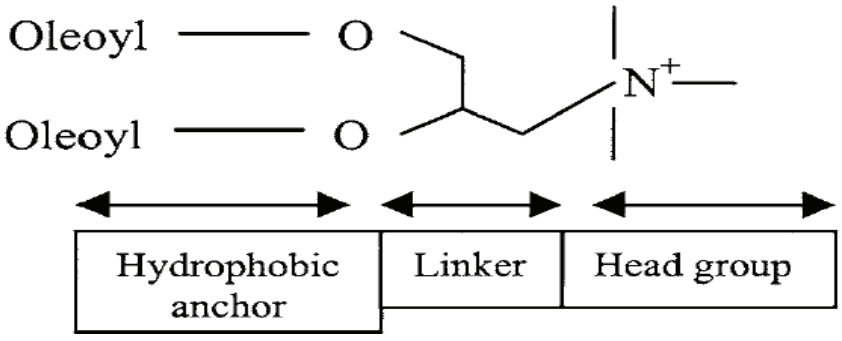

Figure 1.11. Schematic presentation of a cationic lipid (*143*).

For example 1,2-dioleoyl-3-trimethylammonium-propane (DOTAP), a commonly used cationic lipid for gene delivery, consists of two unsaturated diacyl side chains (oleoyl), ester linker and propyl ammonium headgroup (*144*).

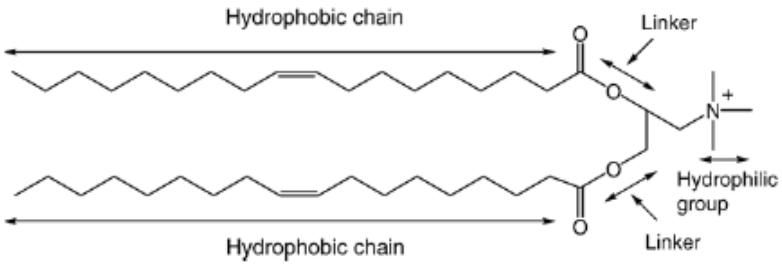

Figure 1.12. DOTAP lipid with its three basic domains (*89*).

A) Hydrophobic anchor

There are two major types of hydrophobic moieties, namely aliphatic chains and cholesterol-based derivatives. For aliphatic chains, single-tailed cationic lipids are more toxic and less efficient than their double-tailed counterparts (*145*).

Single-chain hydrocarbons, like cetyl trimethylammonium bromide (CTAB) and 6-lauroxyhexyl ornithinate (LHON) are better known as surfactants because of their ability to form micelles in solution. Studies revealed that CTAB/DNA complexes remain trapped on the external plasma membrane surface, which is a major limiting step in transfection. However, their interaction with anionic vesicles, that mimic the cytoplasmic facing monolayer of plasma membrane, showed a high transfection efficiency due to destabilization of endosomal membrane by cationic surfactants (*146*). Their use in gene therapy is limited due to their toxicity (*145*).

The majority of synthesized cationic lipids, like DOTMA and DOTAP, contain double chain hydrocarbons. Oleoyl chain (C18:1) is the most frequently used unsaturated acyl chain, whereas C14, C16 and C18 are the commonly used saturated hydrocarbon chains. The importance of the alkyl chain length in transfection activity was studied *in vitro* by Felgner at al (*135*), who varied the alkyl chain length in a homologous series of hydroxyethyl quaternary ammonium derivatives. It was observed that the alkyl chain length can influence the transfection activity. Usually, double-chain hydrocarbons are capable of forming liposomes by themselves, but they are often used with helper phospholipids, like DOPE, in cationic lipid transfection formulations.

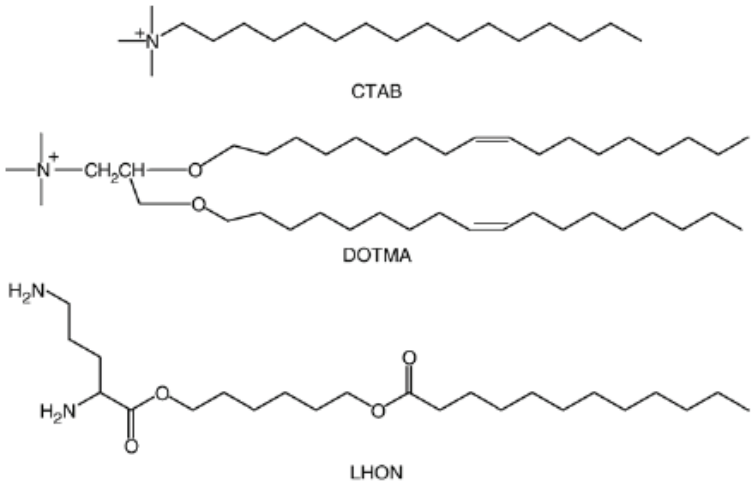

Figure 1.13. Chemical structures of CTAB, DOTMA and LHON.

B) Linker

The linker represents any chemical part between the hydrophobic anchor and the headgroup. It ensures the optimal contact between the cationic headgroup and the negatively charged phosphates of the DNA. Most of the linker bonds are ether, ester or amide bond. Although compounds with ether linker render better transfection efficiency, they are too stable to be biodegraded thus causing toxicity. Cationic lipids with ester bonds such as DOTAP in the linker zone are more biodegradable and associated with less cytotoxicity in cultured cells (*147-149*), but those with amide linkers are liable to decompose in the circulation system.

C) Headgroup

The cytotoxic effect is associated with the cationic nature of the vectors, which is mainly determined by the structure of its hydrophilic headgroup. The headgroup often consists of primary, secondary, tertiary amines or quaternary ammonium salts, but guanidino and imidazole groups have also been tried (*150*).

To improve the transfection efficiency, chemical modifications of the headgroup were performed by several groups. Felgner et al (*135*) synthesized a series of 2,3-

dialkyloxy quaternary ammonium compounds containing a hydroxyl moiety on the quaternary amine. These compounds are more efficient in transfection than DOTMA, which lacks a hydroxyl group on the quaternary amine. This suggests that the hydroxyl group could improve the compaction of DNA. Moreover, DNA can form hydrogen bonds with the lipid, and the hydroxyl group can enhance the membrane hydration. Meanwhile, by varying the chain length of the hydroxyl-alkyl moiety, keeping the remaining structure unchanged, the activity of lipid decreases with the increase in the hydroxyl-alkyl chain length. It was speculated that an increase in the number of carbon atoms in the hydroxyl-alkyl chain, providing more flexibility to the terminal hydroxyl group, could lead to an inefficient interaction with DNA. To design lipids containing a headgroup well adapted for interacting with the phosphate groups of DNA, Vigneron et al (*151*) synthesized divalent cationic cholesterol derivatives like bis-guanidinium cholesterol, which are able to form hydrogen bonds with nucleic acid bases. These compounds were found to be very efficient to transfect a variety of mammalian cell lines.

3.2.4b Structure of cationic lipid/DNA complexes

Characterization of the structure of the lipid/DNA complex (lipoplex) is gaining more interest, based on the idea that a better understanding of the molecular assembly of DNA and cationic lipids should help to establish correlations with their biological activity. Indeed, the transfection efficiency of a given lipoplex highly depends on its structural and physicochemical properties.

Lipoplexes form spontaneously when cationic liposomes are mixed with DNA. The process involves an initial rapid association of polycationic liposomes and polyanionic DNA through electrostatic interaction (*152*), followed by a slower lipid rearrangement process. The structure of lipoplexes is influenced by multiple factors, including the charge ratio, the concentration of individual lipids and DNA, the structure of the cationic lipid and the helper lipid, the physical aggregation state of the lipids (multilamellar, unilamellar liposomes, or micelles), the salt concentration, and the method of preparation (*153-155*). Lipoplexes were then described as aggregates of cationic liposomes surrounding DNA molecules that coexist with tubular structures composed of DNA

molecules coated by lipid bilayers, giving rise to the so-called "spaghetti-meatballs" model.

However, liposomes composed of DOPC (a helper lipid) and DOTAP (1:1) mixed with plasmid DNA revealed that liposomes and DNA are rearranged in a multilamellar structure, with DNA intercalated between the bilayers. The mixture of cationic liposomes with DNA results in a topological transition from the liposomal structure to a liquid-crystalline, condensed and globular structure, consisting of DNA monolayers, characterized by a uniform interhelical spacing, which are sandwiched between cationic lipid bilayers. This structure was designated the L_{α}^{C} structure. Dan (*156*) was able to predict the interhelical spacing of complexed DNA molecules by using a simple theoretical model that allows the identification of the forces governing DNA adsorption on cationic lamellae, and thus provide some support to the experimental observations made by Rädler.

The replacement of DOPC by DOPE in DOPC/DOTAP liposomes leads to a transition from the multilamellar structure (L_{α}^{C}) to an inverted hexagonal phase (H_{II}^{C}) which consists of DNA coated by cationic lipid monolayers arranged on a two-dimensional hexagonal lattice (*157*). This inverted hexagonal structure was in close agreement with studies performed by May and Ben-Shaul (*158*) suggesting that the so-called "honeycomb" structures consisting of a bundle of plasmid DNA.

In conclusion, the final structure of the lipoplexes seems to depend on the liposome composition. Despite the various morphologies for the lipoplexes presented in the literature, it is not yet possible to accurately define the conditions or factors that determine each of them. In fact, it could not be excluded that the different structures coexist in the same preparation and that the differences involved in the complex preparation, which may result from the various techniques that have been used to study the lipid bilayers and thus to assess the lipoplexes morphology.

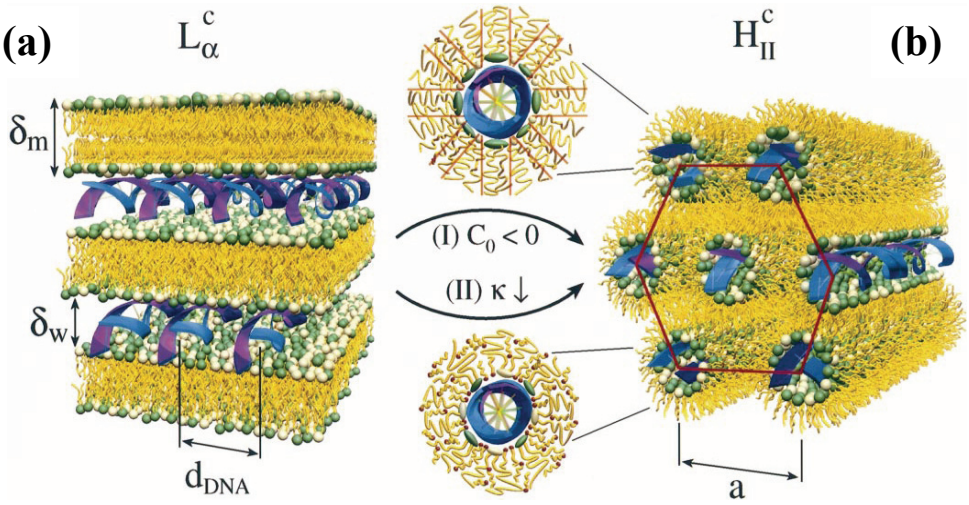

Figure 1.14. Multilamellar and hexagonal arrangement of lipids with DNA. L_α^C: lamellar phase; H_{II}^C: columnar inverted hexagonal phase; a: unit cell spacing; δ_m: bilayer thickness; δ_w: water gap; d_{DNA}: interaxial DNA-DNA spacing (*157, 159*).

3.3.4c Effect of helper lipid/co-lipid

Co-lipids, also called helper lipids, are in most cases required for stabilization of liposome complex by facilitating membrane fusion and help to destabilize the endosome (*135, 160*). Inclusion of these neutral lipids, like dioleoylphosphatidylcholine (DOPC), dioleoylphosphatidylethanolamine (DOPE) (*161, 162*) and cholesterol (Chol) (*163, 164*), into the cationic liposomes has been a common practice in cationic liposome-mediated transfection (*127, 135, 165-167*).

Spontaneous mixing between cationic lipids and cellular lipids in the membrane of the endocytic vesicles is crucial to the endosome-releasing process. Spontaneous lipid mixing in endosomes becomes more profound when a non-bilayer-forming lipid such as DOPE is used as the helper lipid, rather than a bilayer-forming lipid, DOPC. In many cases, an equimolar mixture of a cationic lipid and DOPE ensures an efficient transfection (*135*).

Inclusion of DOPE is believed to increase membrane fluidity and facilitate lipid exchange and membrane fusion between lipoplexes and the endosomal membrane (*162, 168*). A high local concentration of DOPE, which has a strong tendency to form an inverse hexagonal phase, may lead to a nonbilayer lipid structure and cause membrane perturbation and endosome destruction. However, some multivalent lipids present an intrinsic transfection activity, and a helper lipid does not have a major impact on overall transfection activity, indicating that multivalent cationic lipids work on a different mechanism. In addition, several studies have also shown that inclusion of cholesterol into cationic liposomes can enhance the transfection activity at lower cationic lipid to DNA ratios (*144, 163, 164, 169*). Despite the fact that DOPE is found to be effective in enhancing the transfection activity of liposomes *in vitro*, the same may not be efficient for systemic gene delivery indicating that the optimal composition of DNA/liposome complexes is likely to be condition dependent.

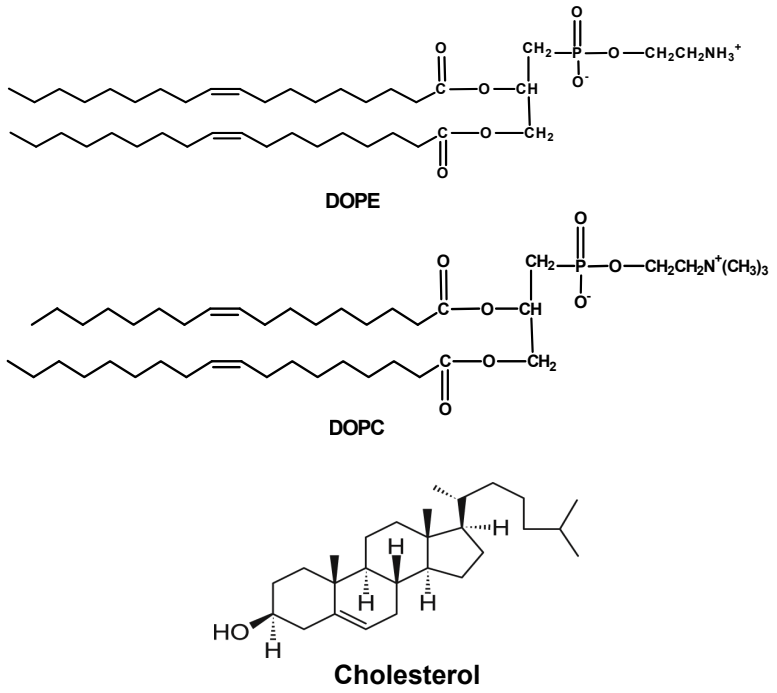

Figure 1.15. Chemical structure of commonly used helper lipids, DOPE, DOPC and cholesterol.

3.2.4d Structure/activity relationship

Due to the complex factors affecting gene transfer, no clear conclusions have been obtained about the possible relationship between cationic lipid structure/composition and lipoplex transfection activity (*89*). The levels of transfection among different cell lines, for example, may significantly vary with the same lipoplex formulations (*170*). More importantly, the correlation between *in vitro* and *in vivo* experiments is not always obtained (*171, 172*). However, the addition of helper lipids increases the transfection ability of lipoplexes both *in vitro* and *in vivo*. Among the most commonly used colipids, DOPE is more efficient *in vivo*, while Cholesterol enhances *in vitro* lipoplex transfection (as discussed in Section 3.3.4c).

Moreover, the transfection efficiency of lipoplexes is affected by physicochemical parameters like the size and structure of the cationic lipid, the charge ratio between the cationic lipid and the DNA, the structure and proportion of the helper lipid in the complexes (*119*).

3.2.5 Polymer based vectors

Despite the cationic liposomes are the most probable alternative to viral delivery systems and their application for gene delivery, they cannot condense DNA efficiently, especially those composed of monovalent cationic lipids, resulting in a heterogeneous size distribution of the complex. Thus, the major disadvantage of cationic liposomes as gene delivery systems is their relatively low transfection efficiency. As an alternative, cationic polymers at physiological pH can be combined with DNA to form complexes, polyplexes, capable of gene transfer into the targeted cells (*89*). This DNA packaging could be achieved by electrostatic interaction, encapsulation or adsorption (Figure 1.16)

The most obvious difference between cationic polymers and cationic lipids is that they do not contain a hydrophobic moiety and are completely soluble in water (*173*). Compared with cationic liposomes, they have the advantage of compressing DNA molecules to a relatively small size (*174, 175*), which can be crucial for gene transfer as small particle size may be favorable for improving the transfection efficiency.

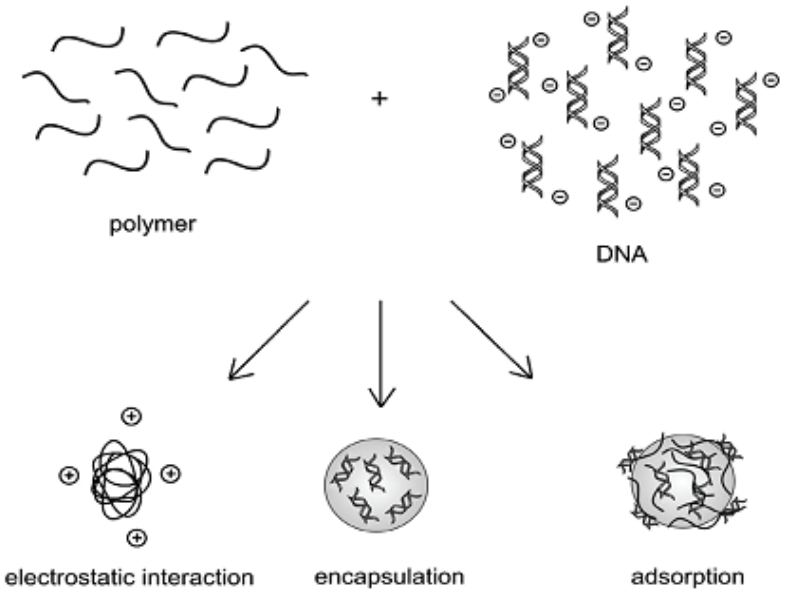

Figure 1.16. Gene packaging: The three main strategies employed to package DNA are via (1) electrostatic interaction, (2) encapsulation within or (3) adsorption onto biodegradable nano or microspheres (*176*).

Polyplexes based transfection systems have advantages, but they are not ideal as these systems suffer from problems in the control of their molecular weight distribution, their dispersity, and other quality control issues (*177*) resulting in low transfection capabilities. Moreover, some polymers have inherent potent pharmacological properties that make them unfavourable for human use (*178*). However, modifications to these polymers such as molecular weight, geometry (linear vs. branched) and ligand attachment can be easily achieved (*173*), opening the way to extensive structure/function relationship studies.

The most widely studied polymers for gene delivery vectors include poly(L-lysine) (PLL), poly (ethylenimine) (PEI) and biodegradable polycations.

3.2.5a Poly(L-lysine)-based vectors

Poly-L-lysine (PLL) polymers are one of the first cationic polymers employed for gene transfer (*37*). They are linear polypeptides with amino acid lysine as the repeating unit, thus possessing a biodegradable nature which is a useful property for *in vivo* applications. However, once into the circulatory system, PLL polyplexes are rapidly bound to plasma proteins and hence cleared from the circulation resulting in lower transfection efficiency.

The gene transfer activity of PLL polyplexes without the use of receptor-mediated strategies is poor (*179*) unless endosomolytic or lysosomotropic agents, like chloroquine, are added (*180, 181*).

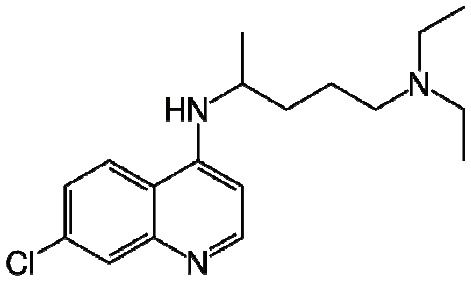

Figure 1.17. Chemical structure of Chloroquine.

Chloroquine (CQ), N'-(7-chloroquinolin-4-yl)-N,N-diethyl-pentane-1,4-diamine, was discovered in 1934 by Hans Andersag and co-workers. Is a weak base with two pK values (10.2 and 8.1) (*182*). Owing to this property, it passes through the plasma membrane and accumulates in acidic compartment in a pH dependent manner (*183*). It raises the pH of acidic compartments of endocytotic pathway, inducing a reduction of the delivery to lysosomes and of the intravesicular degradarion of endocytosed material (*184*). This addition, however, causes an increase in toxicity.

The necessity of using chloroquine for PLL-based gene delivery is an important drawback with respect to the cationic lipids. Many PLL polymers with different molecular weights were tested and evaluated for gene transfer (*185-187*). It has been shown that DNA condensation and transfection efficiency increased with increase in

molecular weight of PLL, but alongwith undesired enhanced toxicity (*188*). Okuda et al (*189, 190*) reported high transfection efficiency of dendritic poly(L-lysine) of the 6th generation (KG6), without significant toxicity or cell specificity.

Earlier experiments with complexes of lipidic PLL and DNA have been found to be more efficient *in vitro* than the cationic liposomes (*191, 192*). Moreover, the creation of amphiphilic PLL, by linking both PEG and palmitoyl groups to the polymer, reduced toxicity without compromising the gene delivery efficiency (*179*). Cellular uptake and gene transfer in the presence (*193*) or absence (*181*) of targeting ligands is however still dependant on the presence of a positively charged polyplex (*193*), presumably to allow interaction with the negatively charged cell surface and subsequent endosomal uptake.

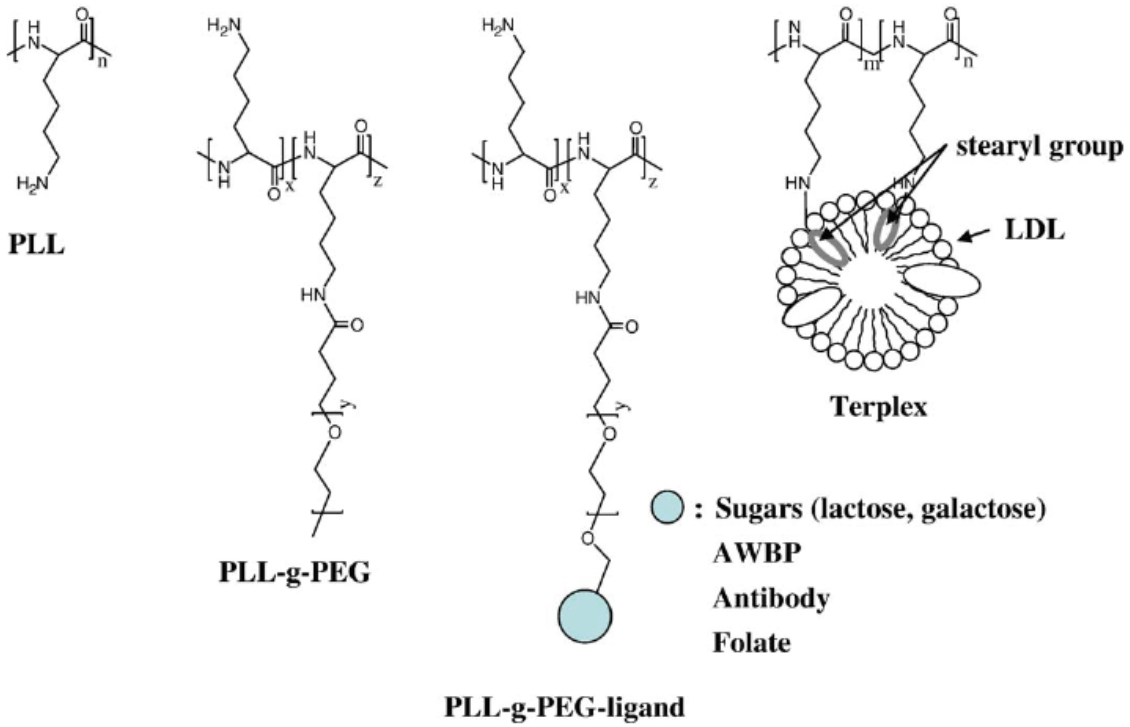

Figure 1.18. Chemical structures of PLL-based gene carriers. PEG, polyethyleneglycol; AWBP, arterial wall binding protein; LDL, low-density lipoprotein.

3.2.5b Polyethylenimine-based vectors

Polyethylenimine (PEI), a commercially available cationic polyamine first introduced by Boussif et al. (*194*), is one of the most successful and widely studied gene delivery polymers (*195-197*) with high transfection efficiency, but together with high cytotoxicity (*198*). PEI polymers can have linear or a branched topology (Figure 1.19) and are available in a wide range of molecular weights.

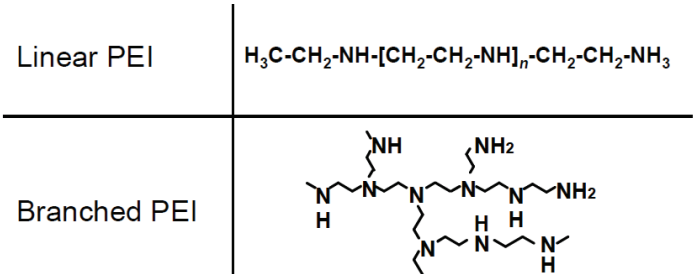

Figure 1.19. Structure of linear and branched PEI.

Unlike PLL, this polymer shows efficient gene transfer without the need for endosomolytic or lysosomotropic agents. PEI is endocytosed by cells and is also believed to facilitate endosomal escape (*199, 200*). Alongwith the requirement of positive charge for a transgene vector, many other factors affect the efficiency/cytotoxicity profile of PEI polyplexes such as molecular weight, degree of branching, ionic strength of the solution, zeta potential and particle size (*196, 201*). One study, for instance, showed that low molecular weight (10 kDa), moderately branched polymer resulted in efficient delivery with low toxicity in comparison with commercial high molecular weight PEI (*202*).

Godbey et al. (*195*) reported that there were mainly two types of cytotoxicity associated with PEI-mediated cell transfection, immediate toxicity in case of free PEI and delayed toxicity in the cellular processing of PEI/DNA complexes (*203*). When administered in the circulatory system, the free PEIs interacted with negatively charged serum proteins (such as albumin) and red blood cells, precipitated in huge clusters and adhered to the cells surface (*202*). This effect could destabilize the plasma-membrane and induces immediate toxicity. But, this toxicity decreases when PEI form complexes with DNA. The delayed toxicity by PEI/DNA complex can be related to the release of DNA

and restoration of free PEI during internalization into the cell's cytoplasm. In cell culture, free PEI interacts with cellular components and inhibits normal cellular process that causes several changes to cells, like cell shrinking, reduced number of mitoses and vacuolization of the cytoplasm.

However, higer transfection efficiency with low cytotoxicity can be achieved by using targeting ligands, like polyethylene glycol (PEG). For instance, Kircheis et al. (*201*) showed that PEGylated PEI polyplexes attached to tumor-specific ligand transferrin resulted in five-fold increase in the transfection efficiency with lower toxicity in comparison with PEGylated (transferrin free) PEI polyplexes.

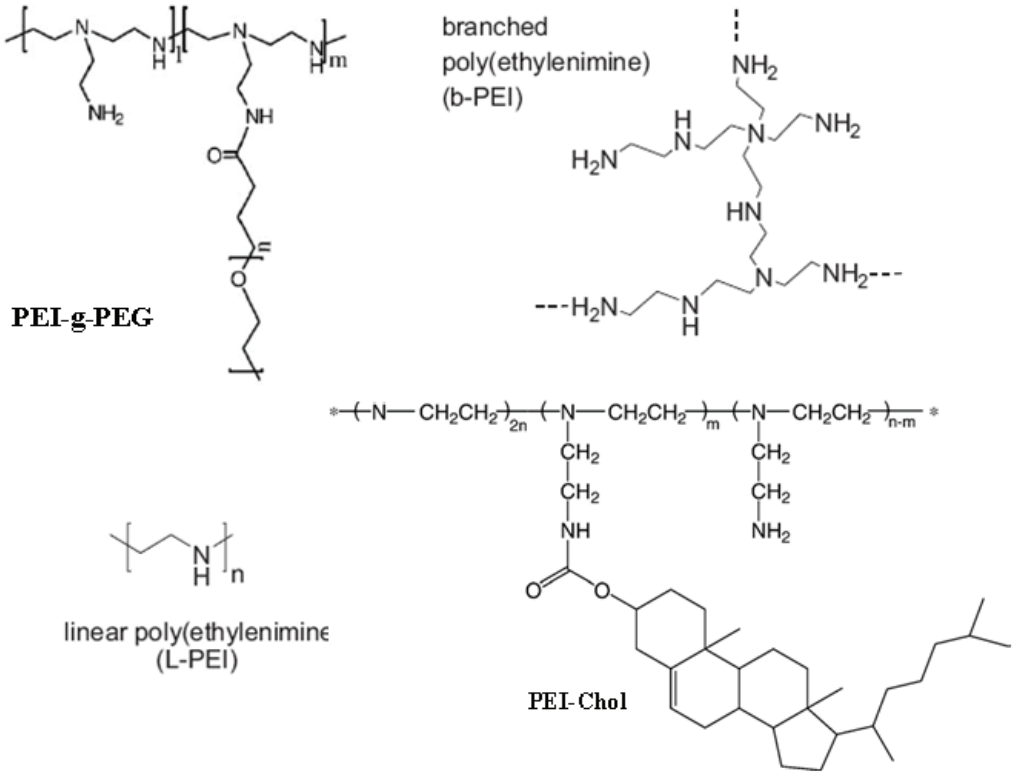

Figure 1.20. Chemical structures of polyethylenimine (PEI)-based gene delivery vectors.

Han et al. synthesized a water soluble PEI-Chol lipopolymer for gene delivery to combine the advantages of both cationic polymer and liposome (*204*). PEI-Chol is an amphiphilic lipopolymer due to hydrophilic and hydrophobic nature of PEI and cholesterol, respectively. It may form micelles or micellar aggregates at higher concentrations, depending on the hydrophilic–hydrophobic balance between the cationic headgroup and the lipid tail. This lipopolymer was found to be non-toxic to a variety of cells (*205, 206*).

3.2.5c Biodegradable polycations

The backbone linkages of most polymeric gene carriers consist either of –C–C– or amide bonds, which are not degraded in physiological conditions. Consequently, these non-viral carriers are not easily removed by physiological clearance systems and, therefore, can possibly accumulate within cells or tissues to elicit further cytotoxicity. To address the problems, several biodegradable polycations have been synthesized and evaluated as potential gene carriers.

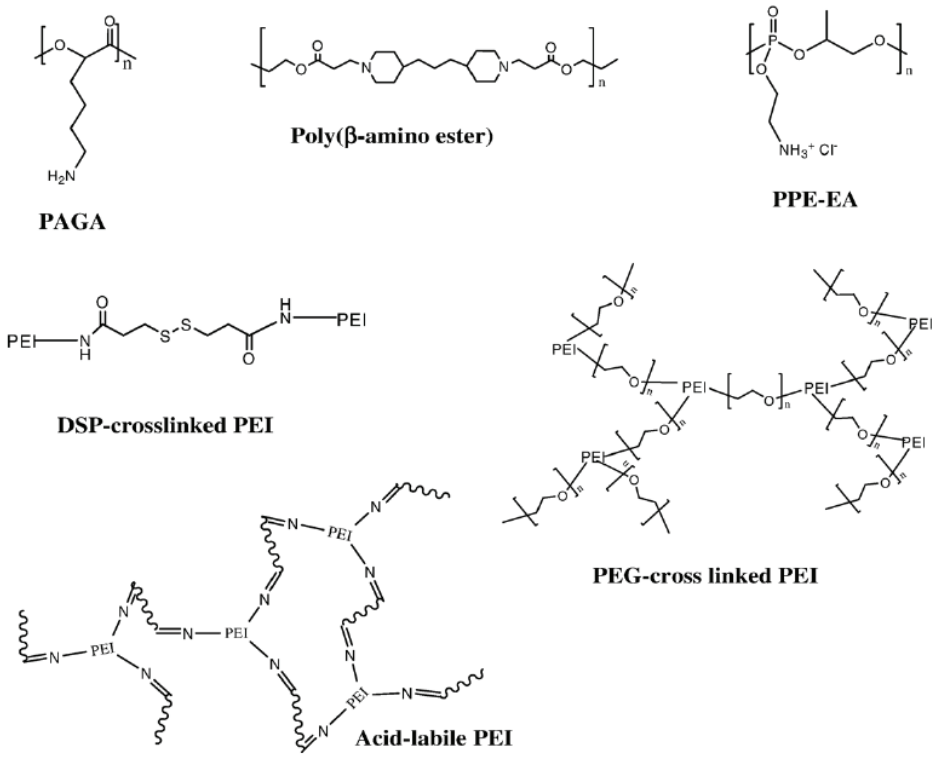

Figure 1.21. Gene carriers based on degradable cationic polymers.

In this context, several of these polycations like poly(α-[4-aminobutyl]-L-glycolic acid) (PAGA) (*207*), poly (β-amino ester)s (*208*), poly(2-aminoethyl propylene phosphate) (PPE-EA) (*209*), DSP, dithiobis(succinimidylpropionate) and degradable PEIs (*198, 210*) were investigated. Generally, the biodegradable polycations showed much less cytotoxicity and higher (or comparable) transfection efficiency compared to unmodified polycations, such as PLL or PEI (*211*).

4. Intracellular Trafficking of Lipoplexes and Polyplexes

While the first generation of cationic lipids was already highly efficient *in vitro*, the cationic polymers became popular only after introduction of a second generation of cationic polymers, such as polyethylenimines. Starting with a relatively low cationic lipid- and polymer-mediated transfection, significant progress was achieved over the past decade regarding their complex formation, binding and entry into the cells, and transportation of the plasmid DNA into the nucleus.

In this section, I will focus on the gradual progress of both lipoplexes and polyplexes in the elucidation of cellular pathways and the steps that lead to transgene expression. At each step, both vectors will be compared and their differences will be highlighted.

4.1 Cellular Binding and Uptake

The cell membrane is negatively charged owing to its high content of glycoproteins and glycolipids containing negatively charged sialic acid residues that can display various types of receptors and antigens, depending on the function of the cell. It is generally accepted that interaction of lipoplexes or polyplexes with cells in culture, in the absence of serum, is non-specific and involves mainly electrostatic interactions between the positively charged complexes and the negatively charged cell surface (Figure 1.22). However, only few data on the possible roles of the different cell surface components (cell matrix components, phospholipids, glycoproteins) are available.

Endocytosis has been established as the main mechanism allowing internalization of the lipoplexes and polyplexes inside the cell. The role of this clathrin-mediated pathway in the internalization was evidenced by microscopy analysis using endocytosis-interfering drugs (*212, 213*). Nevertheless, the exact nature of the endocytotic vesicles and the influence of serum and extracellular matrix components on the type of endocytosis involved are still a matter of debate.

Moreover, another study revealed that the direct fusion with the cell membrane and/or fluid phase endocytosis may also contribute to the cellular uptake of the lipoplexes (*212*) (Figure 1.24). However, this fusion results in the exclusion of the DNA at the cell surface and thereby does not result in its entry into the cell (*214*).

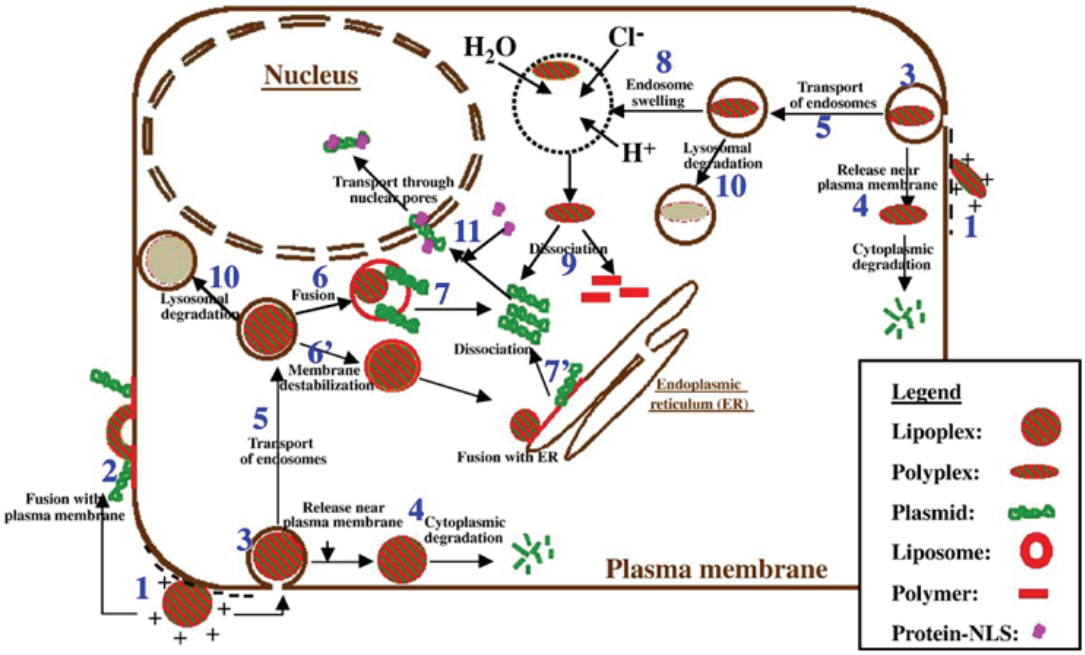

Figure 1.22. Summary of the steps involved in lipoplex- and polyplex-mediated transfection. Lipoplexes and polyplexes are represented by a disc and an ellipse, respectively, of red (representing lipid or polymer) and green (representing plasmid DNA) (*173*).

4.2 Endosomal Escape

The endocytic pathway for lipoplexes and polyplexes entry into the cells raises the question of the mechanisms responsible for the release of the complexes into the cytosol, a step that precedes nuclear localization of DNA. Endosomes undergo a relatively rapid maturation ending by fusion with lysosomes, an issue which is not expected to be productive for transfection. The plasmid may become degraded while reaching the lysosomes. Accordingly, for productive transfection, the plasmid needs to acquire an access to the cytosol at an earlier stage, presumably by escaping from (early) endosomal compartments. The chemical structure of the vector plays a crucial role in this endosomal escape.

4.2.1 Lipoplexes

The fusion of the lipoplexes with the endosomal membranes results in the release of DNA into the cytoplasm, which was evidenced by several studies (*162, 168, 214, 215*), and a mechanism for this fusion has been proposed by Xu and Szoka (*216*), on the basis of the established ability of membrane phospholipids to flip from one bilayer leaflet to the other. In this model (Figure 1.23), the endosomal membrane enveloping a cationic lipoplex becomes destabilized by the complex, thus enabling anionic lipids facing the cytoplasmic side of the membrane to flip and face the endosomal lumen. These anionic lipids mix with the cationic lipids of the lipoplex, laterally diffuse into the complex and form charge neutral ion pairs with the lipids of the complex. This process displaces the transgene from the cationic lipids, and releases the transgene into the cytoplasm.

However, DOPE-containing lipoplexes present a transition from bilayer to inverted hexagonal structures (*157, 217*), which, due to their instability, rapidly fuse to anionic vesicles in the membrane and release DNA. Several studies have questioned the role of fusion in transfection, however, no obvious correlation was found between fusion of lipoplexes with cells and transfection efficiency (*214, 215*). Moreover, the role of the fusogenic helper lipid DOPE was not limited to fusion but also concerned the cellular

uptake of lipoplexes and the dissociation of transgene from lipids (*218*). This role of the helper lipid can also vary depending on the cationic lipid and the target cells.

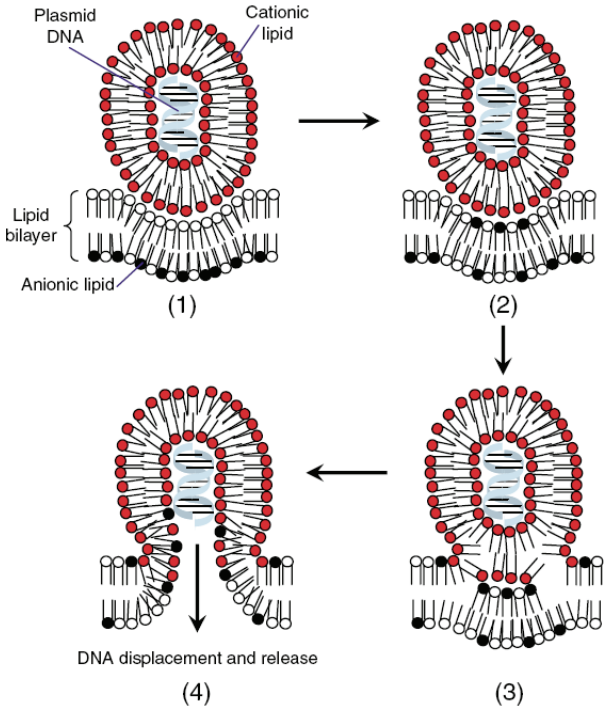

Figure 1.23. Proposed mechanism of endosomolysis by lipoplex. Flip-flop. The lipoplex becomes endocytosed (1), and destabilizes the membrane, inducing flipping of anionic lipids from the cytoplasm to face the endosomal lumen (2). The anionic lipids form charge neutral ion pairs with cationic lipids of the complex (3), thus displacing the DNA and releasing it into the cytoplasm (4) (*219*).

Considering the large surface occupied by the cationic lipid bilayer over the endosome membrane surface, most of the cationic charges could not be neutralized and the transgene would be expected to be only partially released into the cytoplasm. In agreement, undissociated lipoplexes were observed in the cell cytosol by electron microscopy(*220, 221*). This leads Ruysschaert and colleagues (*222*) to propose that lipoplexes escape from endosomes into the cell cytosol by a detergent-like destabilization mechanism of the endosomal membranes. Once released into the cytosol, the lipoplexes dissociate after interaction and/or fusion with the cytosolic membrane network, i.e., the endoplasmic reticulum, Golgi, mitochondria, and nuclear membrane to release transgene.

4.2.2 Polyplexes

Cationic polymers are devoided of a hydrophobic domain and therefore cannot fuse/destabilize the endosome by direct interaction with the endosomal membrane as it is the case for cationic lipids. Behr and colleagues proposed a "proton sponge" hypothesis that lead to endosomal disruption and the high transfection efficiency in case of polyamidoamine (PAM) (*223*) and PEI (*194*) probably due to incorporated titratable amines into these branched polymers. This hypothesis (Figure 1.26) postulates that at physiological pH one upon six nitrogen atoms are protonated, while the proportion increases upon lowering the pH, e.g. in endosomes, and generates a charge gradient, which induces a Cl^- influx. The increase in Cl^- concentration induces a water influx and ultimately an endosomal swelling and rupture. Indirect evidence that supported their hypothesis included the remarkable decrease in the transfection efficiency of PEI containing polyplexes when the cells were treated with drugs that prevent endosome acidification, such as chloroquine (*200, 224*). Subcellular fractionation and confocal analysis applied to a pancreatic carcinoma cell line incubated with PEI/DNA polyplexes revealed that the polyplexes accumulated mainly in the lysosomes (*225*). Studies also revealed that these polyplexes attach themselves to the surface of the lysosomal membrane, from which they succeed to enter into the cytoplasm through local membrane damage and thus supporting the idea that the transit of PEI polyplexes in an acidic compartment is a prerequisite to their escape into the cytoplasm. In another study, the effects of the polymers PEI and PAM (containing protonable amines) to those of PLL (which is devoid of protonable amines) on pH, Cl^- concentration, and volume of endosomes after transfection of CHO cells was compared (*226*). Whereas PEI and PAM induced a remarkable increase in the Cl^- concentration and volume of the polyplex-containing endosomes, PLL had no significant effect thus confirming the "proton sponge" hypothesis.

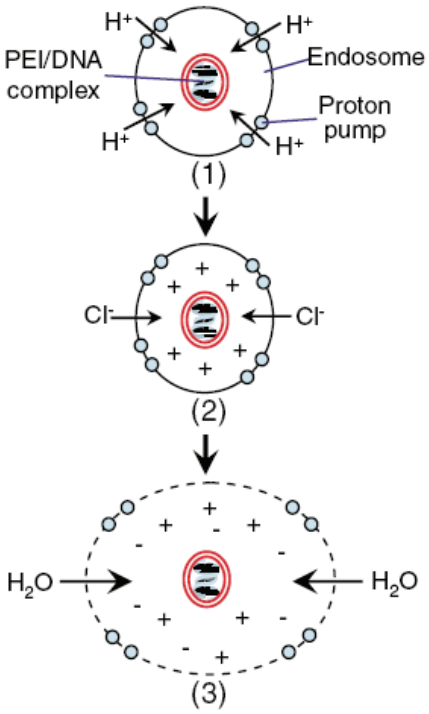

Figure 1.24. Proton sponge hypothesis. The polyplex considerably favours proton accumulation in the endosome (1), inducing a passive chloride influx (2), and causing an osmotic swelling and an endosomal rupture (3) (*219*).

In fact, the first generation of cationic polymers, such as polylysine or polyarginine, was quite inefficient in terms of endosomal escape and transfection efficiencies. This led to the development of strategies that enhance the endosomal destabilization by polyplexes, like co-incubation of adenovirus particles and polyplexes with the cells to be transfected (*227*). Adenovirus has intrinsic endosomal rupture properties that allow it to escape from endosomes with a high efficiency. This allowed an increase in the transfection efficiency but required the use of a large number of adenovirus particles per cell, eventually causing high toxicity. To circumvent this limitation, adenovirus was coupled directly to the cationic polymers via enzymatic or biochemically-based linkage (*228, 229*). However, the use of this method *in vivo* was again limited by the toxicity and immune response toward adenovirus particles.

4.3 Nuclear Entry

Once released into the cytoplasm, the DNA has to move into the nucleus to be transcribed. Several studies established that among cells showing cytoplasmic plasmid delivery only those with the evidence of nuclear plasmid localization resulted in efficient transgene expression (*230-232*). The narrow functional diameter of the nuclear pores (~ 25 nm) limits the nuclear translocation of plasmid DNA. Moreover, the stability of the DNA in the cytoplasm is compromised by the cytoplasmic nucleases. For instance, the half-life of DNA in the cytoplasm of HeLa cells was estimated to be 90 min (*233, 234*). It is not surprising that the nuclear translocation efficiency of plasmid DNA has been estimated to be about 1/1000 (*235*).

Even though, two main mechanisms were proposed to explain how plasmid DNA (released either from a lipoplex or from a polyplex) enters into the nucleus: (1) a passive DNA entry into the nucleus during cell division when the nuclear membrane is temporarily disintegrated; (2) an active transport of the DNA through the nuclear pores. It should be emphasized that these two mechanisms are not mutually exclusive in a given cell type.

4.3.1 Lipoplexes

As with the other steps involved in intracellular gene delivery by lipoplexes, the knowledge of DNA trafficking to the nucleus is still scarce. Assuming that DNA is lipid-free, a rapid movement to the nucleus appears to be required in order to avoid its degradation by nucleases, as indicated by the finding that free DNA microinjected into the cytoplasm is degraded within a short time (*236*).

In the absence of cell division, whether DNA penetrates the nuclear membrane through pores by a passive diffusion process or through active transport mechanisms involving, for example, its non-specific association with receptors for NLS, remains to be clarified. The former mode of entry by a passive diffusion process is unlikely to occur, since pores act as a size exclusion sieve avoiding the free exchange of macromolecules larger than 70 kDa, which is significantly lower than the molecular weight of DNA. It

seems that partial coating of DNA with lipid would be advantageous at this stage, not only to reduce the size of the plasmid but also to ensure its protection against cytoplasmic nucleases. Moreover, it can be speculated that traces of cationic lipid still associated with DNA may play a role in the destabilization of the nuclear membrane. However, so far no evidence has been reported to support this hypothesis. Studies showed that microinjection of free plasmids into the nucleus results in gene expression, whereas microinjection of lipoplexes does not, suggesting that total lipid coating of DNA inhibits transcription (*237*). Therefore, it would be highly favourable to have a complete DNA uncoating at the interface of the nuclear membrane, just prior to DNA injection into the nucleus.

4.3.2 Polyplexes

Although the transport of the polyplexes through the cytoplasm to the nucleus is poorly understood, there is some evidence that polycations protect DNA from cytosol nucleases thus resulting in a higher probability for nuclear entry (*238*). Intact PEI/DNA polyplexes were found in the nucleus, indicating that it may not be necessary for the polycation to separate from DNA prior to nuclear entry (*195, 225, 239*). Due to efficient nuclear transport, modifications of polycations with NLS or the inclusion in the plasmid of nucleotide sequences presenting an affinity for cellular proteins, such as transcription factors, greatly enhanced the transfection efficiency (*240-242*).

5. BOLAAMPHIPHILE-BASED VECTORS

5.1 General Introduction

As discussed above, synthetic cationic lipids and polymers became acceptable alternatives to viruses as DNA carrier and transfection agents due to their low immunogenicity and higher cargo carrying capacity. Furthermore, they can be readily prepared and handled. However, they lack sufficient stability for *in vivo* applications. Since the discovery of the DOTMA and its *in vitro* transfection ability, a large array of molecules has been developed to improve the low transfection rates, usually observed *in vivo* by using synthetic carriers. This loss of activity is in part due to the extra- and intra-cellular barriers that have to be by-passed to induce the final gene expression.

Thus, a promising alternative consists in using unsymmetrical bolaamphiphiles that form monolayer membrane, which are potentially more stable than conventional liposomes and are less likely to fuse with each other due to reduced lipid exchange (Figure 1.25) (*243, 244*).

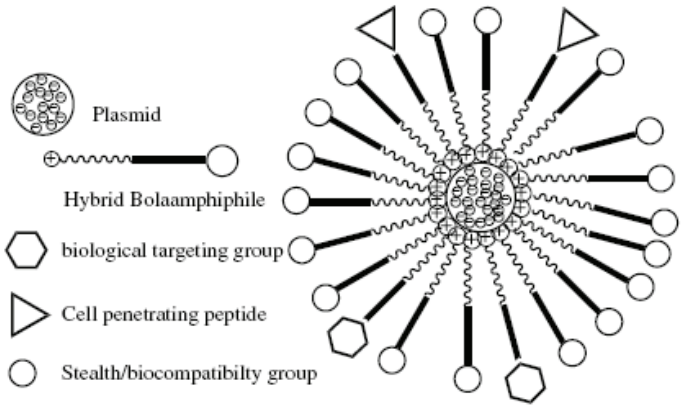

Figure 1.25. Schematic representation of a polyfunctionalized bolaplex (bola-DNA complex) (*245*).

Bipolar amphiphiles, which are the analogues of lipids presenting polar groups at the two opposite sides of the hydrophobic chain(s), called bolaamphiphiles (bolas), have progressively gained importance in recent years because of their ability to provide well-defined supramolecular structures and advanced biomaterials. They are also known as "bolaform amphiphiles" or "bolaphiles".

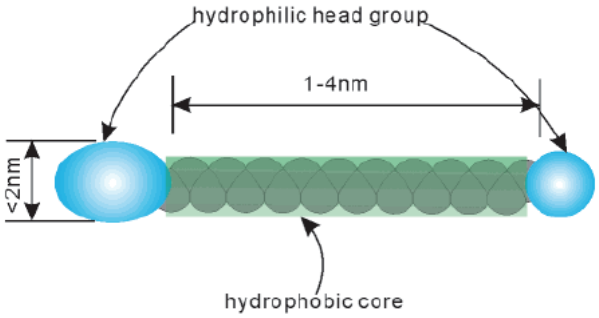

Figure 1.26. Schematic presentation of a bolaamphiphile (bola). Green and blue coloring indicates hydrophobic and hydrophilic parts respectively (*246*).

Heteroditopic 1,ω-bipolar amphiphiles, so-called unsymmetrical bolaamphiphiles, in which two different hydrophilic end groups are connected by a hydrophobic spacer that has one or two alkyl chains, are one of the cell membrane components of thermophilic and acidophilic Archaebacteria (Fig. 1.27) (*247, 248*). These organisms can sustain harsh environments such as high salt concentrations, extreme temperatures or very acidic environments (*249-251*). The archaebacteria bolaamphiphiles are composed of acid-stable ether linkages letting them to survive in acidic media; chiral methylated centers inducing twisting to form helical structures; pseudo-rotating cyclopentane units replacing the chemically sensitive cis-double bonds responsible for higher growth temperature adaptation, by providing necessary rigidity and stability of the membrane (*246*). In addition to that, they have been known to form highly stable monolayer lipid membranes (MLMs) (*246, 252, 253*). These advantageous properties of bipolar membrane-spanning lipids make them attractive candidates as delivery vector systems (*254*) or supported membrane biosensor devices (*255*).

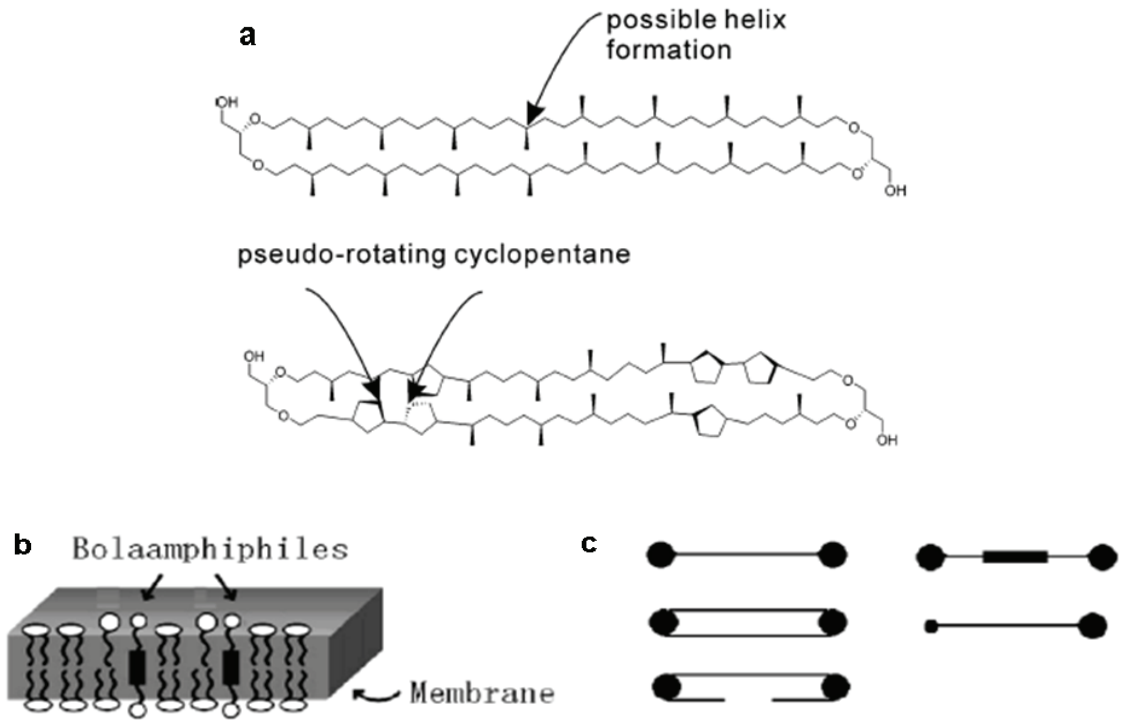

Figure 1.27. (a) Structural formula of typical bolas from archaebacteria (*246*). (b) Conformation of bolas in the membrane of Archaea; (c) illustration of structure of bolas. The skeleton structures represent symmetrical bolas with flexible single, double, half-loop (left column top down), rigid (right upper), spacer chain, and asymmetrical headgroups (right down) (*256*).

5.2 Self-Assembly of Bolaamphiphiles

Molecular self-assembly and self-organization are becoming increasingly significant in the elucidation of life processes, and to the generation of new supramolecular structures and molecular materials. As a consequence, the most important inspirations for the conceptual development of such structures and materials are those provided by biological cells, which exemplify the assembly of a variety of different sizes and functions (*257*). In this respect, archaebacteria, which proliferate under extreme conditions, provide a rich source of inspiration.

However, archaebacteria bolaamphiphiles are both difficult to isolate and difficult to synthesize. To overcome these limitations, many different synthetic analogs have been prepared and studied. These analogs comprise a hydrophobic skeleton, consisting of one, two or three alkyl chains, a steroid, or a porphyrin, and two water-soluble groups, one at each end (*246*). Among the different approaches that have been used to synthesize bolaamphiphiles are condensation and substitution reactions of commercial α,ω-diols, -dihalides, and -diamines with dicarboxylates.

For example, Okahata and Kunitake (1979) succeeded in preparing vesicle with monolayer membranes from a single-chain bipolar ammonium salt. Other symmetrical bolaamphiphiles have been synthesized with two viologen headgroups (*244*). The synthesis of bipolar amphiphiles with cyclic structures that aggregated into vesicles has also been described. Depending on the molecular parameters, bolaamphiphiles can form micelles, multilayered sheets, vesicles, rings, or a variety of microstructures with cylindrical geometry, such as rods, tubules, ribbons, and helices (*258*). Recent studies have shown that in aqueous solution some single chain bolaamphiphiles form spherical vesicles (*259*) but others form tube-like vesicles (*260*) or fibrous (*261*) structures.

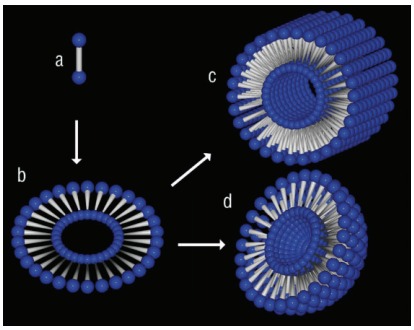

Figure 1.28. Proposed molecular model for the self-assembly of the bolaamphiphile. Single peptide molecules (a) aggregate together in the form of a micelle (b) and self-assemble into cylindrical (c) or spherical (d) nanostructures with a hydrophilic core and surface (*262*).

Unsymmetrical bola lipids with polar headgroups of different sizes may exhibit an unsymmetrical or a symmetrical type arrangement depending on a parallel or antiparallel molecular packing within the monolayer as shown in Figure 1.29 (*263*). Great emphasis has been aimed to control the polymorphism of bolaamphiphiles because the molecular packing affects not only the self-assembled morphologies like solid fibers and tubes, but also their dimensions from nanometers to micrometers (*258, 260, 264, 265*).

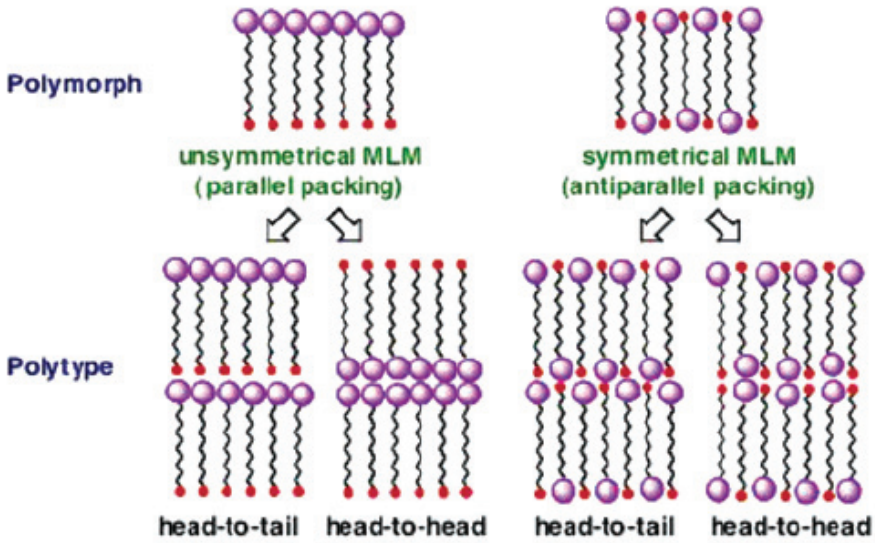

Figure 1.29. Formation of monolayer lipid membranes (MLMs) from unsymmetrical bolaamphiphiles and resultant structures formed by the stacking of the MLMs (*265*).

5.3 Effect of Hydrophobic Spacer Chain Length and Headgroup

Over the past decade, the results obtained from synthetic bola molecules have demonstrated the existence of complex relationships between spacer's chain composition and headgroups that considerably influence the structure of their supramolecular aggregates (*257, 266, 267*). Consequently, the rational design of well-defined functional bolaamphiphiles continues to be challenging in order to analyze the mechanisms involved in molecular self-assembly and to develop new advanced materials. The major contribution of bolas to supramolecular chemistry lies in the combination of asymmetric arrangements of α,ω-headgroups and the formation of cooperative hydrogen-bond or π-π interaction chains. The headgroups differentiate between binding to a solid surface and interactions with solvents or solutes, while the internal connectivity provides the chemical and physical stability of solid surfaces (*246*).

Shimizu suggested the odd-even effect on the self-assembly morphology of bolas, as the hot aqueous solutions of even-numbered **1(n)** compounds (n= 14, 16, 18 and 20) became slightly opaque and viscous upon cooling indicating their self-assembly, while on the other hand, the odd numbered compounds **1(13)** yielded only colorless crystalline solids (Figure 1.30) (*268, 269*).

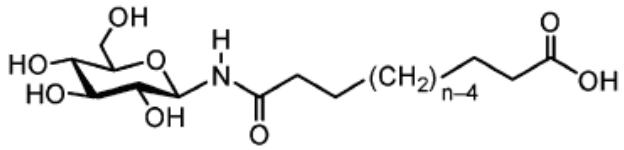

1(*n*), *n* = 12, 13, 14, 16, 18, and 20

Figure 1.30. Synthetic unsymmetrical bolaamphiphiles **1**(***n***) with an oligo-methylene chain having a 1-glucosamide moiety and a carboxylic acid headgroups (*265*).

Transmission electron microscopic (TEM) observations revealed nanotube formation by the former compounds. Moreover, the bola **1(12)** packs into a symmetrical MLM, but **1(14)** packs into an unsymmetrical MLM with a head-to-tail interface, as determined by single-crystal structure analysis. Importantly, the diameter of the obtained MLM tubular structures correlated well with the lengths of the alkyl chain. XRD pattern

further indicated the effect of chain length on the MLM polymorph of the tubular assemblies due to the difference in membrane fluidity. Although, shortening the oligomethylene chain increases the molecular fluidity, it transforms into a random orientation for very short chain lengths, as found for the shortest-chain **1**(**12**) nanotube (Figure 1.31a). Alternatively, the molecule forms a symmetrical MLM, as in the **1**(**12**) crystal, in which antiparallel packing best compensates for the dipole moment and the void arising from the bulky headgroup (Figure 1.31b). Thus, the chain length effects MLMs formation, as in the case of **1**(***n***).

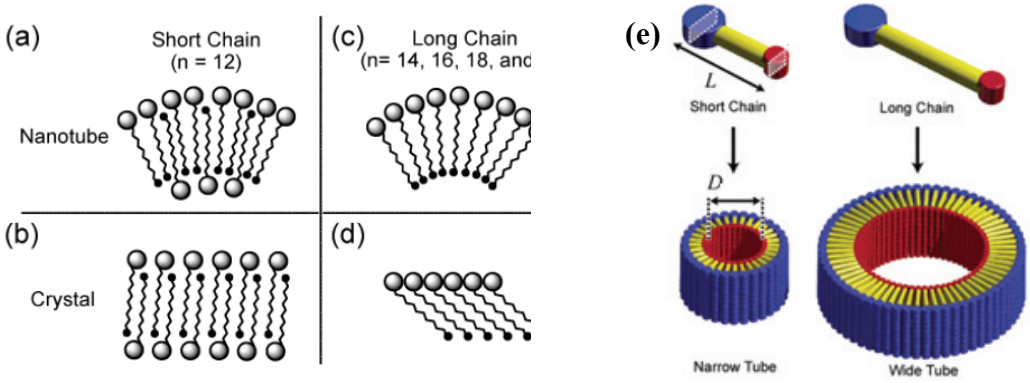

Figure 1.31. (a-d) Schematic illustration of the effect of the chain length on molecular packing in tubular assemblies and crystals of unsymmetrical bolaamphiphiles. (e) Schematic models of unsymmetrical bolaamphiphiles 1(n) with a short and a long oligomethylene chain and the tubular assemblies from each model (*265*).

Additionaly, bolaamphiphiles with an electroneutral and an electropositive headgroup can present several key advantages as coating amphiphiles for negatively charged polyelectrolytes such as nucleic acids. However, cationic DNA carriers suffer from severe limitations due to their rapid clearance from the blood together with their strong cytotoxicity particularly of a hepatic nature (*238, 270, 271*). In the case of the unsymmetrical bolaamphiphiles, one may assume that if the bolaplexes are endowed with a non-ionic outer surface, then their non-specific interactions as well as cytotoxicity, would be reduced, hence enhancing their transfection efficiency particularly for *in vivo* applications.

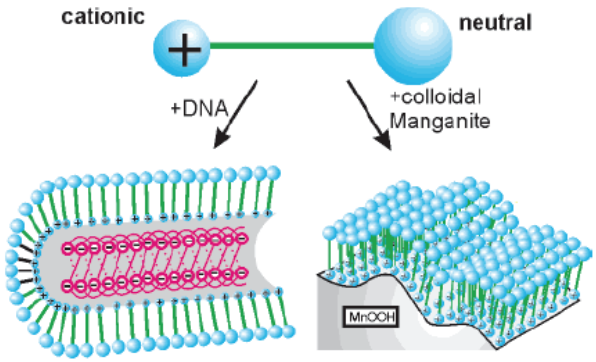

Figure 1.32. Bolas with an electroneutral and a positively charged headgroup may be used to neutralize surface charges of polyelectrolytes or colloids as anticorrosive monolayers or a solvent for hydrophobic molecules (*246*).

Carbohydrate residue was probably the most well-established neutral headgroup used for bolaamphiphiles. Unsymmetrical bolas with D-glucose and carboxylic acid headgroups are known to form nanotube structures (*265*). Use of electroneutral ligands like mannose (*272-274*), lactose (*275*) and various carbohydrates (*276-278*) can induce receptor mediated endocytosis. Various other sugar residues have also been used as a functional group for gene transfer (*279*).

5.4 Bolas as Gene Delivery Vectors

Aiming at the goals of efficient delivery of genetic material to target specific cells and its effective expression within the cell, bolaamphiphiles could be an attractive alternative to existing non-viral vectors. One approach that would allow to complex DNA and to functionalize the surface carrier through membrane targeting or crossing agents lies in using dissymmetric (unsymmetrical) bolaamphiphiles. Since they are known to self-organize as monolamellar membranes likely to close up as vesicles, thus a parallel assembly of that bolas around the DNA might be expected for instance, by using a cationic polar head (dedicated to the complexation of nucleic acids) and a second non-ionic glycosylated polar head. Moreover, the application of an adapted formulation composed of bolaamphiphiles first functionalized with targeting or membrane crossing agents would improve the *in vivo* efficiency of these DNA carriers.

The potentialities of this family of compounds in DNA vectorization technologies have been studied, but none of them studied the correlations between their structures, phase behaviour and DNA complexation and transfection activities (*280-286*).

So far, α-galacto-*ώ*-polycationic bola (Gal-CLs) were reported (*285*) to mediate a specific gene transfer, *in vitro*, into cells expressing ASGP (human HepG2 and murine BNL-CL2 hepatocytes). Various cell-targeting ligands, including galactosylated residues, were conjugated to the DNA complexes in order to trigger receptor-mediated gene delivery.

Recently, a series of dissymmetric hemifluorocarbon bolaamphiphiles were evaluated for DNA complexation as well as *in vitro* gene transfer carrier (*245*). These compounds showed remarkable modularity which favours variations in a number of their structural subunits: (i) a cationic polar head derived from amino acids such as lysine or histidine to complex DNA by electrostatic interactions, (ii) a glycosylated non-ionic polar head made of galactosyl or lactobionamide units to ensure surface neutrality of the complex and the possible targeting of membrane cells bearing specific lectins (in particular hepatocytes membranes) (*283*) and (iii) a hemifluorinated hydrophobic part linked to two polar caps through amide bounds.

α-galacto-*ώ*-spermine bolas (GalSper) has also been reported for effective receptor-mediated gene transfer (*284*). Moreover, Galactose-spermine double-chain asymmetric bolaamphiphiles have been synthesized for gene delivery and C6, C7, C8, and C10 amide dispermine bolaamphiphiles have been synthesized as inhibitors of spermidine transport in breast cancer cells (*287*). Spermine bolaamphiphiles may thus have important biomedical applications yet their self-assembly has not been sufficiently studied. While the C8 and C10 alkyl spermine bolaamphiphiles of the current report did not self-assemble in aqueous media, the C12 compound self-assembled into particulate structures of 20 nm (*288*).

In the present work, we synthesized a new series of such bolaamphiphile molecules, optimized to enhance the solubility and DNA coating efficiency, in order to form stable nano-structures with possible applications in gene delivery. The positive charge on one end of the bola should tightly bind to the poly-anion in aqueous solution. Therefore, we selected ammonium headgroups as they are common in biological systems. In addition to

that, an electroneutral, water soluble headgroup on the other end should prevent precipitation, which is invariably observed with α,ω-dicationic bolaamphiphiles (*289, 290*). Moreover, the coated nucleic acid should be useful in transfection, since the vesicles with neutral surface should pass biological membranes. Considering all these factors, sugar acid residues like gluconic, mannoic and lactose were used as neutral headgroups, as several biological systems are known to contain carbohydrate selective receptors.

6. IDEAL VECTOR

Although many advances have been achieved in the field of gene transfer, the ability to deliver recombinant DNA both selectively and efficiently to a specific cell-type *in vivo* still remains a big challenge. Thus the development of gene therapy vector with sufficient targeting ability, transfection efficiency and safety must be achieved before its routine application in humans.

The potential applications of gene therapy in the treatment of disease are currently limited by the inability to adequately deliver genes to target tissues and to maintain their expression. Because different tissues have diverse biological properties, and since even the most developed of vector systems has its limitations, it is unrealistic to imagine that one vector will eventually emerge as the most suitable for all gene therapy applications. Rather, successful gene therapy likely lies with the ability to create highly specialized "designer" vectors that safely incorporate specific advantageous characteristics from several viruses to address specific features of a disease and the target tissue for treatment.

Therefore, an ideal vector system should have at least the following characteristics: (i) specificity for the targeted cells; (ii) resistance to metabolic degradation and/or attack by the immune system; (iii) safety, i.e., minimal side effects; and (iv) ability to express, in an appropriately regulated fashion, the therapeutic gene for as long as required.

Materials and Methods

1. Synthesis of Bolaamphiphiles

All chemicals and solvents were purchased from Sigma-Aldrich. Mass spectra were measured using Mass Spectrometer Mariner System 5155. LC-MASS was performed on Agilent, 1956 B/MSD. ^{1}H-NMR spectra were recorded on Bruker 300 MHz spectrometer.

1.1 First Generation Bolas

A) Synthesis of M-C8-C12-EDA

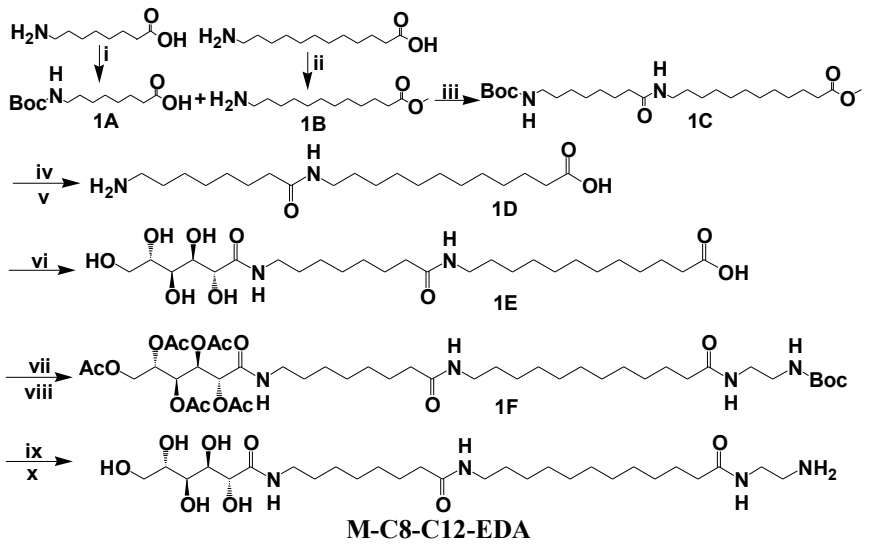

Reagents: (i) Boc_2O, DMF, CH_2Cl_2, 20 h; (ii) $SOCl_2$, MeOH, 20 h; (iii) BOP, HOBt, DIEA, DMF, CH_2Cl_2, 24 h; (iv) NaOH, EtOH, 24 h; (v) TFA, CH_2Cl_2, 4 h; (vi) Mannoic acid lactone, MeOH, DIEA, 70 °C, 24 h; (vii) C_5H_5N, $(CH_3CO)_2O$, 45 h; (viii) N-Boc-ethylenediamine, BOP, HOBt, DIEA, DMF, CH_2Cl_2, 20 h; (ix) NaOH, EtOH, 20 h; (x) TFA, CH_2Cl_2, 2 h.

Scheme 1.1. Synthesis of **M-C8-C12-EDA.**

8-tert-Butoxycabonylamino-octanoic acid (1A). Amino group of 8-aminooctanoic acid (31.4 mmol, 5 g) was protected by Boc using di-tert-butyl dicarbonate (34.6 mmol, 7.54 g) in the solution of DMF (30 ml) and dichloromethane (40 ml).Then, DIEA (94.2 mmol, 16.38 ml) was added and the reaction mixture was stirred for 20 h at RT. The solvent was evaporated and product was crystallized from dichloromethane. The precipitate was

filtered off and dried to give compound **1A** (7.5 g, 92 %). ^{1}H NMR ($CDCl_3$, 300 MHz): δ 4.55 (s, 1H), 3.07 (t, 2H), 2.3 (t, 2H), 1.67-1.5 (t, 4H), 1.56-1.37 (t, 9H), 1.37-1.21 (m, 6H).

12-Amino-dodecanoic acid methyl ester (1B). Thionyl chloride (103.4 mmol, 7.5 ml) was added drop-wise to 100 ml of methanol at 0 °C and the mixture was stirred for another 20 min. Then, 10 g of 12-aminododecanoic acid (46.5 mmol) was added and reaction mixture was stirred for 20 h at RT. The solvent was evaporated and product was crystallized from heptane to give compound **1B** (10 g, 94 %). ^{1}H NMR (DMSO, 300 MHz): δ 7.89 (s, 2H), 3.68 (s, 3H), 2.75 (t, 2H), 2.28 (t, 2H), 1.58-1.15 (m, 18H).

12-(8-Tert-Butoxycarbonylamino-octanoylamino)-dodecanoic acid methyl ester (1C). Compound **1B** (6.5 mmol, 1.5 g) was coupled with **1A** (7.2 mmol, 1.87 g) using BOP (7.2 mmol, 3.18 g), HOBt (8.9 mmol, 1.2 g) and DIEA (25.9 mmol, 4.5 ml) in DMF (15 ml) and dichloromethane (30 ml). The reaction mixture was stirred for 24 h at RT. Then the solvents were evaporated and product was crystallized from ethyl acetate : heptane (8:2). The precipitate was filtered off and dried to give compound **1C** (2.5 g, 81 %). ^{1}H NMR ($CDCl_3$, 300 MHz): δ 5.41 (s, 1H), 4.48 (s, 1H), 3.65 (s, 3H), 3.21 (t, 2H), 3.08 (t, 2H), 2.29 (t, 2H), 2.13 (t, 2H), 1.69-1.15 (m, 39H). LC-MS: (m/z) Found $[M+1]^+$ = 371.2 (calcd for $C_{26}H_{50}N_2O_5^+$ - $C_{10}H_{18}O_4$ (2Boc) = 371.2).

12-(8-Amino-octanoylamino)-dodecanoic acid (1D). Methyl ester of **1C** (4.3 mmol, 2 g) was hydrolyzed using 1 M NaOH (70 mmol, 1.3 ml) in 50 ml of ethanol. Solvent was evaporated after 24 h of stirring and water was poured into the reaction flask. Then the pH was neutralized using 1 M HCl and the resultant precipitate was filtered, dried and 1 g (2.2 mmol) of the obtained crystals was further reacted with 5 ml of TFA in 5 ml dichloromethane for removal of Boc. Solvents were evaporated after 4 h of stirring to obtain compound **1D** (0.71 g, 91 %).

12-[8-(2,3,4,5,6-Pentahydroxy-hexanoylamino)-octanoylamino]-dodecanoic acid (1E). 0.3 g (0.84 mmol) of **1D** was mixed with L-mannoic-γ-lactone (1.1 mmol, 0.21 g) in 15 ml of methanol. Then, DIEA (8.5 mmol, 1.5 ml) was added and the reaction mixture was stirred at 70°C for about 24 h. Solvent was removed and the product was crystallized from ethanol, filtered off and dried to obtain compound **1E** (0.32 g, 71 %). ^{1}H NMR (DMSO, 300 MHz): δ 7.85 (d, 1H), 7.72 (d, 1H), 4.77-4.32 (m, 3H), 3.9 (d,

1H), 3.67-3.6 (d, 2H), 3.59-3.52 (m, 1H), 3.5-3.42 (m, 2H), 3.1-2.94 (m, 4H), 2.19 (t, 2H), 2.02 (t, 2H); 1.55-1.33 (m, 8H), 1.31-1.13 (m, 18H).

Acetic acid 2,3,4,5-tetraacetoxy-5-{7-[11-(2-tert-butoxycarbonylamino-ethylcarbamoyl)-undecylcarbamoyl]-heptylcarbamoyl}-pentyl ester (1F). All sugar hydroxyl groups of **1E** (0.28 mmol, 0.15 g) were acetylated using acetic anhydride (6.4 mmol, 0.6 ml) in the presence of pyridine (12 mmol, 1 ml). After 45 h of stirring at RT, the solution was poured in water and the product was extracted with ethyl acetate and dried with sodium sulfate. 0.1 g (0.13 mmol) of the obtained acetylated compound was further coupled with Boc-ethylenediamine (0.16 mmol, 26 mg) using BOP (0.15 mmol, 65 mg), HOBt (1.9 mmol, 25 mg) and DIEA (0.54 mmol, 0.093 ml) in DMF (3 ml) and dichloromethane (5 ml). The reaction mixture was stirred 20 h at RT. Then the solvents were evaporated and product **1F** (0.1 g, 84 %) was purified by column chromatography using dichloromethane : methanol (9:1). ^{1}H NMR ($CDCl_3$, 300 MHz): δ 6.34 (s, 1H), 6.2-6.14 (t, 1H), 5.66-5.43 (m, 3H), 5.14-5.06 (m, 2H), 3.35-3.12 (m, 6H), 2.16-1.92 (m, 18H), 1.6-1.44 (m, 4H), 1.43-1.35 (m, 9H), 1.34-1.08 (m, 24H).

12-[8-(2,3,4,5,6-Pentahydroxy-hexanoylamino)-octanoylamino]-dodecanoic acid (2-amino-ethyl)-amide (M-C8-C12-EDA). Deacetylation of **1F** (0.03 mmol, 50 mg) was done using 1 M NaOH (13 mmol, 0.25 ml) in 2 ml of ethanol. After 20 h of stirring at RT, the solvent was removed and obtained reaction mixture was further reacted with 1 ml TFA in 1 ml of CH_2Cl_2 to remove Boc group. Solvent was evaporated after 2 h of stirring at RT to afford the final product **M-C8-C12-EDA** (25 mg, 77 %). LC-MS: (m/z) Found $[M+1]^+ = 577.5$ (calcd for $C_{28}H_{56}N_4O_8^+ = 577.4$).

B) Synthesis of G-C12-EDA

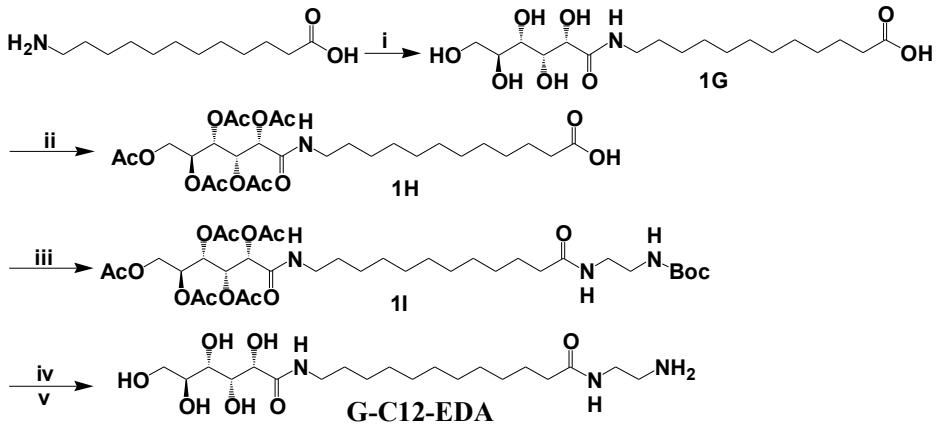

Reagents: (i) Gluconic acid lactone, MeOH, DIEA, 70 °C, 20 h; (ii) C_5H_5N, $(CH_3CO)_2O$, 20 h;
(iii) N-Boc-ethylenediamine, BOP, HOBt, DIEA, DMF, CH_2Cl_2, 10 h;
(iv) NaOH, EtOH, 8 h; (v) TFA, CH_2Cl_2, 2 h.

Scheme 1.2. Synthesis of **G-C12-EDA.**

12-(2,3,4,5,6-Pentahydroxy-hexanoylamino)-dodecanoic acid (1G). Amino group of 12-Amino-dodecanoic acid (0.93 mmol, 0.2 g) was coupled with δ-gulonic-γ-lactone (1.1 mmol, 0.2 g) in 10 ml methanol. Then DIEA (4.65 mmol, 0.8 ml) was added and solvent was evaporated after 20 h of stirring at 70 °C. Water was poured in to the reaction flask and was further acidified by 1 M HCl, where precipitate was formed. Then, it was filtered out and dried to obtain compound **1G** (0.25 g, 68 %). ^{1}H NMR (DMSO, 300 MHz): δ 7.71 (s, 1H), 3.91 (d, 1H), 3.67-3.52 (m, 3H), 3.49-3.31 (m, 2H), 3.09 (t, 2H), 2.18 (t, 2H), 1.57-1.37 (m, 4H), 1.33-1.17 (m, 14H).

12-(2,3,4,5,6-Pentaacetoxy-hexanoylamino)-dodecanoic acid (1H). All sugar hydroxyl groups of **1G** (0.25 mmol, 0.1 g) were acetylated using acetic anhydride (2.6 mmol, 0.25 ml) in the presence of pyridine (12 mmol, 1 ml). After 20 h of stirring at RT, the solution was poured in water and the product was extracted with ethyl acetate and dried over sodium sulfate. Then the solvent was removed to obtain product **1H** (0.11 g, 72 %). ^{1}H NMR ($CDCl_3$, 300 MHz): δ 6.18 (s, 1H), 5.73-5.41 (m, 3H), 5.23 (d, 1H), 4.26 (t, 1H), 4.02 (t, 1H), 3.26 (t, 2H), 2.4-2.3 (t, 2H), 2.18-1.92 (m, 15H), 1.7-1.1 (m, 18H).

Acetic acid 2,3,4-triacetoxy-1-acetoxymethyl-4-[11-(2-tert-butoxycarbonylamino-ethylcarbamoyl)-undecylcarbamoyl]-butyl ester (1I). Acetylated compound **1H** (0.09 mmol, 55 mg) was coupled with Boc-ethylenediamine (0.1 mmol, 0.017 g) using BOP

(0.09 mmol, 41 mg), HOBt (0.1 mmol, 15 mg) and DIEA (11 mmol, 2 ml) in DMF (1 ml) and dichloromethane (5 ml). The reaction mixture was stirred for 10 h at RT. Then the solvents were evaporated and product **1I** (64 mg, 94 %) was purified by column chromatography using ethyl acetate. ^{1}H NMR ($CDCl_3$, 300 MHz): δ 6.19 (t, 2H), 5.74-5.45 (m, 3H), 5.22 (d, 1H), 4.95 (s, 1H), 4.30-4.25 (m, 1H), 4.13-3.98 (m, 4H); 3.37-3.19 (m, 4H), 2.17-1.97 (m, 15H), 1.65-1.45 (m, 4H), 1.44-1.37 (m, 9H); 1.33-1.22 (m, 14H).

12-(2,3,4,5,6-Pentahydroxy-hexanoylamino)-dodecanoic acid (2-amino-ethyl)-amide (G-C12-EDA). Deacetylation of **1I** (0.07 mmol, 50 mg) was done using 1 M NaOH (30 mmol, 0.55 ml) in 5 ml of ethanol. After 8 h of stirring at RT, the solvent was removed and obtained reaction mixture was further reacted with 5 ml TFA in 5 ml of CH_2Cl_2 for Boc removal. Solvent was evaporated after 2 h of stirring at RT to afford the final product **G-C12-EDA** (21 mg, 72 %). ^{1}H NMR (CD_3OD, 300 MHz): δ 4.23 (d, 1H), 4.09 (s, 1H), 3.86-3.58 (m, 5H), 3.49-3.4 (t, 2H), 3.25-3.17 (t, 2H), 3.05-2.99 (t, 2H), 2.31-2.16 (t, 2H), 1.69-1.44 (m, 4H), 1.39-1.23 (m, 14H). LC-MS: (m/z) Found $[M+1]^+$ = 436.3 (calcd for $C_{20}H_{41}N_3O_7^+$ = 436.3).

C) Synthesis of M-C12-EDA

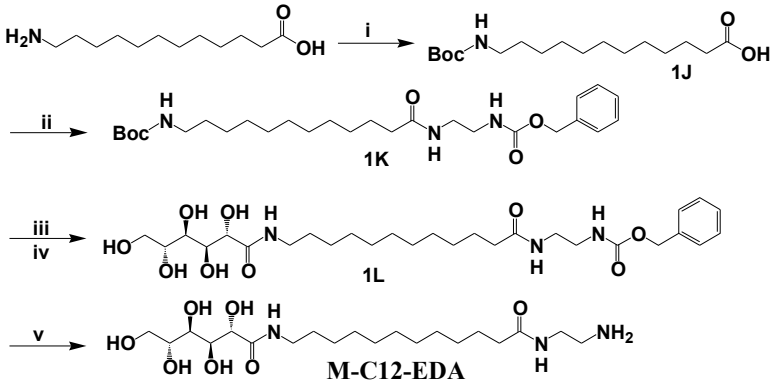

Reagents: (i) Boc_2O, DMF, CH_2Cl_2, 20 h; (ii) $C_{10}H_{14}N_2O_2$, BOP, HOBt, DIEA, DMF, CH_2Cl_2, 24 h; (iii) TFA, CH_2Cl_2, 4 h; (iv) Mannoic acid lactone, MeOH, DIEA, 70 °C, 24 h; (v) Pd-C, MeOH/HCOOH (3/2, v/v), 2 h.

Scheme 1.3. Synthesis of **M-C12-EDA.**

12-Tert-Butoxycabonylamino-dodecanoic acid (1J). Amino group of 12-Amino-dodecanoic acid (9.3 mmol, 2 g) was protected by Boc using di-tert-butyl dicarbonate (10 mmol, 2.2 g) in solution of DMF (10 ml) and dichloromethane (20 ml). Then, DIEA (5.8 mmol, 1 ml) was added and the reaction mixture was stirred for 20 h at RT. The solvent

was evaporated and product was crystallized from dichloromethane. The precipitate was filtered off and dried to give compound **1J** (2.2 g, 75 %). ^{1}H NMR ($CDCl_3$, 300 MHz): δ 4.49 (s, 1H), 3.14-3.01 (m, 2H), 2.47-2.38 (t, 2H), 1.7-1.56 (m, 2H), 1.46-1.4 (m, 9H), 1.36-1.19 (m, 16H).

[11-(2-Benzyloxycarbonylamino-ethylcarbamoyl)-undecyl]-carbamic acid tert-butyl ester (1K). Boc protected 12-amino-dodecanoic acid **(1J)** (1.3 mmol, 0.4 g) was coupled with (2-amino-ethyl)-carbamic acid benzyl ester **(4)** (1.5 mmol, 0.3g) using BOP (1.4 mmol, 0.62 g), HOBt (1.8 mmol, 0.24 g) and DIEA (5.2 mmol, 0.9ml) in DMF (5 ml) and dichloromethane (10 ml). The reaction mixture was stirred for 24 h at RT. Then the solvents were evaporated and product was crystallized from ethyl acetate. The precipitate was filtered off and dried to get compound **1K** (0.46 g, 73 %). ^{1}H NMR ($CDCl_3$, 300 MHz): δ 7.37-7.3 (m, 5H), 6.11 (s, 1H), 5.25 (s, 1H), 5.08 (s, 2H), 4.48 (s, 1H), 3.4-3.25 (m, 4H), 3.06 (d, 2H), 2.17-2.1 (t, 2H), 1.66-1.54 (m, 4H), 1.50-1.35 (m, 9H), 1.32-1.16 (m, 16H).

{2-[12-(2,3,4,5,6-Pentahydroxy-hexanoylamino)-dodecanoylamino]-ethyl}-carbamic acid benzyl ester (1L). Boc group of **1K** (0.61 mmol, 0.3 g) was removed using 2 ml TFA in 2 ml of dichloromethane for 4 h at RT. The solvent was evaporated and 0.15 g (0.38 mmol) of the obtained deprotected amine was mixed with L-mannoic- γ-lactone (0.5 mmol, 90 mg) in 20 ml of methanol. Then, DIEA (3 mmol, 0.52 ml) was added and the reaction mixture was stirred at 70°C for about 24 h. Precipitate was formed during the reaction. It was filtered off and dried to obtain compound **1L** (0.15 g, 68 %). ^{1}H NMR (CD_3OD, 300 MHz): δ 7.74 (d, 2H), 7.46-7.33 (m, 5H), 5.48 (s, 1H), 5.04 (s, 2H), 4.56-4.45 (m, 3H), 3.97-3.76 (m, 2H), 3.2-3.02 (m, 6H), 2.12-2 (t, 2H), 1.58-1.38 (m, 4H), 1.35-1.17 (m, 14H).

12-(2,3,4,5,6-Pentahydroxy-hexanoylamino)-dodecanoic acid (2-amino-ethyl)-amide (M-C12-EDA). Cbz group was removed from 70 mg (0.12 mmol) of **1L** using 50 mg of Pd-C (10%) in 12 ml of methanol and 8 ml of formic acid (methanol : formic acid = 3 : 2) for 2 h at 70 °C. Then the reaction mixture was filtered to remove Pd and the solvent was removed in vacuo. Product was crystallized from ethanol and the precipitate was filtered off and dried to afford the final product **M-C12-EDA** (38 mg, 71 %). ^{1}H NMR (CD_3OD, 300 MHz): δ 8.06 (s, 1H), 4.14 (d, 1H), 3.98 (d, 1H), 3.84-3.58 (m, 4H), 3.48-3.4 (t, 2H),

3.28-3.21 (t, 2H), 3.07-3.01 (t, 2H), 2.27-2.17 (t, 2H), 1.67-1.47 (m, 4H), 1.39-1.24 (m, 16H).LC-MS: (m/z) Found $[M+1]^+ = 436.3$ (calcd for $C_{20}H_{41}N_3O_7^+ = 436.3$).

D) Synthesis of G-C8-C12-EDA

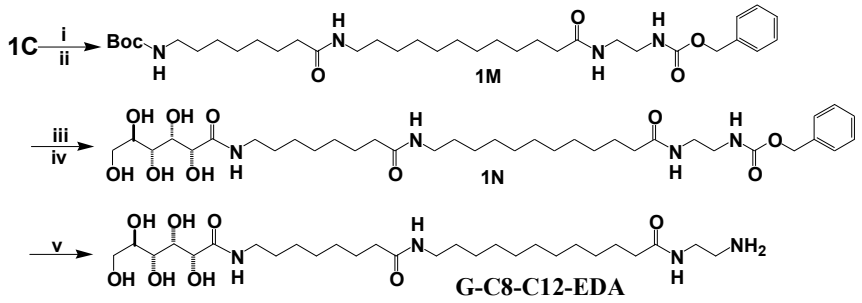

Reagents: (i) NaOH, EtOH, 24 h; (ii) $C_{10}H_{14}N_2O_2$, BOP, HOBt, DIEA, DMF, CH_2Cl_2, 24 h; (iii) TFA, CH_2Cl_2, 4 h; (iv) Gluconic acid lactone, MeOH, DIEA, 70 °C, 24 h; (v) Pd-C, MeOH/HCOOH (3/2, v/v), 2 h.

Scheme 1.4. Synthesis of **G-C8-C12-EDA.**

{7-[11-(2-Benzyloxycarbonylamino-ethylcarbamoyl)-undecylcarbamoyl]-heptyl}-carbamic acid tert-butyl ester (1M). Methyl ester of **1C** (1.5 mmol, 0.7 g) was hydrolyzed using 1 M NaOH (90 mmol, 1.86 ml) in 20 ml of ethanol. Solvent was evaporated after 24 h of stirring and water was poured into the reaction flask. Then the pH was neutralized using 1 M HCl and the resultant precipitate crystals were filtered and dried. 0.4 g (0.88 mmol) of the obtained product was reacted with (2-amino-ethyl)-carbamic acid benzyl ester (**4**) (1 mmol, 0.2 g) using BOP (0.97 mmol, 0.43 g), HOBt (1.2 mmol, 0.16 g) and DIEA (3.5 mmol, 0.61 ml) in DMF (5 ml) and dichloromethane (10 ml). The reaction mixture was stirred for 24 h at RT. Then the solvents were evaporated and product was crystallized from ethyl acetate. The precipitate was filtered off and dried to give compound **1M** (0.48 g, 87 %). ^{1}H NMR ($CDCl_3$, 300 MHz): δ 7.4-7.29 (m, 5H), 6.11 (s, 1H), 5.45 (s, 1H), 5.29 (s, 1H), 5.08 (s, 2H), 4.51 (s, 1H), 3.38-3.31 (m, 4H), 3.25-3.18 (m, 2H), 3.07 (d, 2H), 2.15-2.08 (t, 4H), 1.65-1.5 (m, 8H), 1.46-1.4 (m, 11H), 1.3-1.15 (m, 20H).

(2-{12-[8-(2,3,4,5,6-Pentahydroxy-hexanoylamino)-octanoylamino]-dodecanoyl amino}-ethyl)-carbamic acid benzyl ester (1N). Boc group of **1M** (0.47 mmol, 0.3 g) was removed in dichloromethane (3 ml) in the presence of 3 ml of TFA for 4 h at RT. The solvent was evaporated and 0.2 g (0.38 mmol) of the obtained deprotected amine was

mixed with δ-gulonic-γ-lactone (0.53 mmol, 95 mg) in 20 ml of methanol. Then, DIEA (3 mmol, 0.543 ml) was added and the reaction mixture was stirred at 70°C for about 24 h. Precipitate was formed during the reaction. It was filtered off and dried to obtain compound **1N** (0.2 g, 75 %). ^{1}H NMR (DMSO, 300 MHz): δ 7.77-7.54 (m, 3H), 7.36-7.27 (m, 5H), 5.32 (d, 1H), 4.89 (s, 2H), 4.52-4.28 (m, 4H), 3.97-3.84 (m, 2H), 3.59-3.40 (m, 3H), 3.13-2.93 (m, 8H), 2.07-1.92 (t, 4H), 1.54-1.28 (m, 8H), 1.26-1.12 (m, 20H).

12-[8-(2,3,4,5,6-Pentahydroxy-hexanoylamino)-octanoylamino]-dodecanoic acid (2-amino-ethyl)-amide (G-C8-C12-EDA). Cbz group was removed from 0.14 g (0.2 mmol) of **1N** using 100 mg of Pd-C (10%) in 18 ml of methanol and 12 ml of formic acid (methanol : formic acid = 3 : 2) for 2 h at 70 °C. Then the reaction mixture was filtered to remove Pd and the solvent was removed in vacuo. Product was crystallized from ethanol and the resultant precipitate was filtered off and dried to afford the final product **G-C8-C12-EDA** (80 g, 70 %). ^{1}H NMR (CD_3OD, 300 MHz): δ 4.24 (d, 1H), 4.1 (s, 1H), 3.85-3.61 (m, 5H), 3.51-3.44 (t, 2H), 3.27-3.19 (m, 2H), 3.18-3.07 (m, 4H), 2.29-2.14 (m, 4H), 1.68-1.44 (m, 8H), 1.39-1.23 (m, 20H). LC-MS: (m/z) Found $[M+1]^+ = 577.4$ (calcd for $C_{28}H_{56}N_4O_8^+ = 577.4$).

E) Synthesis of M-C6-C8-C12-EDA

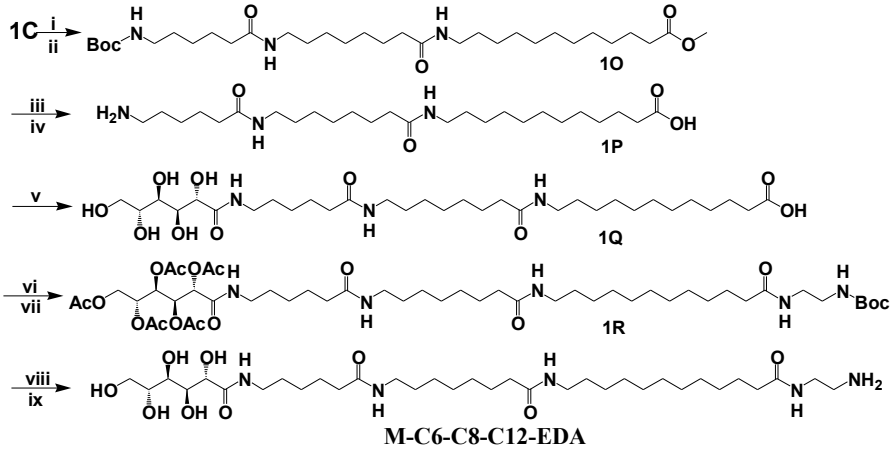

Reagents: (i) TFA, CH_2Cl_2, 4 h; (ii) $C_{11}H_{21}NO_4$, BOP, HOBt, DIEA, DMF, CH_2Cl_2, 24 h; (iii) NaOH, EtOH, 24 h; (iv) TFA, CH_2Cl_2, 4 h; (v) Mannoic acid lactone, MeOH, DIEA, 70 °C, 24 h; (vi) C_5H_5N, $(CH_3CO)_2O$, 48 h; (vii) N-Boc-ethylenediamine, BOP, HOBt, DIEA, DMF, CH_2Cl_2, 20 h; (viii) NaOH, EtOH, 20 h; (ix) TFA, CH_2Cl_2, 2 h.

Scheme 1.5. Synthesis of **M-C6-C8-C12-EDA.**

12-[8-(6-tert-Butoxycarbonylamino-hexanoylamino)-octanoylamino]-dodecanoic acid methyl ester (1O). Boc group of **1C** (2.1 mmol, 1 g) was removed using 5 ml of TFA and 5 ml of dichloromethane for 4 h at RT. The solvent was evaporated and the resulting deprotected amine (2.2 mmol, 0.8 g) was coupled with 6-tert-butoxycarbonylamino-hexanoic acid (2.6 mmol, 0.6 g) using BOP (1.4 mmol, 1 g), HOBt (3 mmol, 0.42 g) and DIEA (11.6 mmol, 2 ml) in DMF (10 ml) and dichloromethane (20 ml). The reaction mixture was stirred 24 h at RT. Then the solvents were evaporated and product was crystallized from ethyl acetate : heptane (8 : 2). The precipitate was filtered off and dried to give compound **1O** (0.84 g, 85 %). ^{1}H NMR ($CDCl_3$, 300 MHz): δ 5.66 (s, 1H), 4.6 (s, 1H), 3.64 (s, 3H), 3.25-3.16 (m, 4H), 3.13-3.03 (m, 2H), 2.32-2.24 (t, 2H), 2.18-2.1 (m, 4H), 1.7-1.55 (m, 6H), 1.51-1.37 (m, 15H), 1.34-1.15 (m, 22H).

12-[8-(6-Amino-hexanoylamino)-octanoylamino]-dodecanoic acid (1P). Methyl ester of **1O** (1.2 mmol, 0.7 g) was hydrolyzed using 1 M NaOH (42 mmol, 0.8 ml) in 20 ml of ethanol. Solvent was evaporated after 24 h of stirring and further reacted with TFA (3 ml) in 3 ml of dichloromethane to remove Boc group. Solvents were evaporated after 4 h of stirring at RT, to obtain compound **1P** (0.5 g, 89 %).

12-{8-[6-(2,3,4,5,6-Pentahydroxy-hexanoylamino)-hexanoylamino]-octanoylamino}-dodecanoic acid (1Q). L-Mannoic-γ-lactone (1.1 mmol, 0.2 g) was added to a solution of **1P** (0.64 mmol, 0.3 g) in 10 ml of methanol. Then, DIEA (5 mmol, 0.9 ml) was added and the reaction mixture was stirred at 70°C for about 24 h. Solvents was removed and the product was crystallized from ethanol. It was filtered off and dried to obtain compound **1Q** (0.3 g, 72 %).

Acetic acid 2,3,4-triacetoxy-1-acetoxymethyl-4-(5-{7-[11-(2-tert-butoxycarbonyl amino-ethylcarbamoyl)-undecylcarbamoyl]-heptylcarbamoyl}-pentylcarbamoyl)-butyl ester (1R). All sugar hydroxyl groups of **1Q** (0.23 mmol, 0.15 g) were acetylated using acetic anhydride (6.4 mmol, 0.6 ml) in the presence of pyridine (12.4 mmol, 1 ml). After 48 h of stirring at RT, the solution was poured in water and the product was extracted with ethyl acetate and dried with sodium sulfate. Then the solvent was removed and 0.1 g (0.12 mmol) of the obtained acetylated compound was further coupled with boc-ethylenediamine (0.16 mmol, 26 mg) using BOP (0.15 mmol, 65 mg), HOBt (0.2 mmol, 25 mg) and DIEA (0.6 mmol, 0.1 ml) in DMF (2 ml) and dichloromethane (5 ml).

The reaction mixture was stirred for 20 h at RT. Then the solvents were evaporated and the product **1R** (0.1 g, 86 %) was purified by column chromatography using ethyl acetate. ^{1}H NMR ($CDCl_3$, 300 MHz): δ 6.48 (s, 1H), 6.38-6.32 (t, 1H), 5.9-5.77 (m, 2H), 5.53-5.44 (t, 2H), 5.24-5.07 (m, 3H), 4.25-4.03 (m, 2H), 3.36-3.14 (m, 8H), 2.69-2.53 (m, 18H), 1.72-1.54 (m, 8H), 1.48-1.37 (m, 9H), 1.35-1.19 (m, 30H).

12-{8-[6-(2,3,4,5,6-Pentahydroxy-hexanoylamino)-hexanoylamino]-octanoylamino}-dodecanoic acid (2-amino-ethyl)-amide (M-C6-C8-C12-EDA). Deacetylation of **1R** (0.1 mmol, 0.1 g) was done using 1 M NaOH (16 mmol, 0.3 ml) in 5 ml of ethanol. After 8 h of stirring at RT, the solvent was removed and obtained reaction mixture was further reacted with 5 ml of TFA in 5 ml of CH_2Cl_2 to remove Boc group. Solvent was evaporated after 2 h of stirring at RT to afford the final product **M-C6-C8-C12-EDA** (50 mg, 72 %). ^{1}H NMR (CD_3OD, 300 MHz): δ 4.13 (d, 1H), 4.00 (d, 1H), 3.8 (d, 1H), 3.77-3.59 (m, 4H), 3.47-3.41 (t, 2H), 3.28-3.23 (m, 4H), 3.19-3.1 (t, 6H), 3.08-3.00 (t, 2H); 2.24-2.11 (m, 6H), 1.52-1.42 (m, 4H), 1.4-1.23 (m, 30H). LC-MS: (m/z) Found $[M+1]^+$ = 690.5 (calcd for $C_{34}H_{67}N_5O_9^+$ = 690.5).

1.2 Second Generation Bolas

A) Synthesis of Orn-C8-C12-G/Orn-C8-C12-L

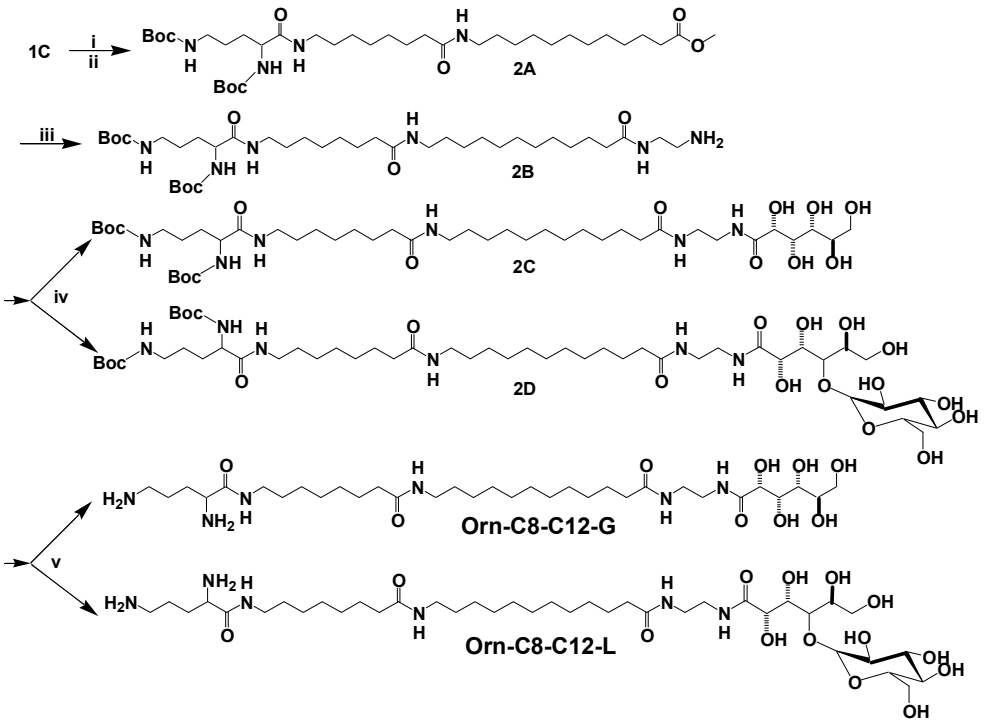

Reagents: (i) TFA, CH_2Cl_2, 1 h; (ii) Boc_2-Ornithine-OH, BOP, HOBt, DIEA, DMF, CH_2Cl_2, 24 h; (iii) $C_2H_8N_2$, 70 °C, 72 h; (iv) Gluconic acid lactone or lactonolactone, MeOH, DIEA, 70 °C, 24 h; (v) TFA, H_2O, 1 h.

Scheme 2.1. Synthesis of **Orn-C8-C12-G** and **Orn-C8-C12-L.**

12-[8-(2,5-Bis-tert-butoxycarbonylamino-pentanoylamino)-octanoylamino]-dodecanoic acid methyl ester (2A). Boc group of **1C** (2.13 mmol, 1 g) was removed in dichloromethane (3 ml) in the presence of 2 ml of TFA for 1 h at RT. The solvent was evaporated and 1 g (2.1 mmol) of the obtained deprotected amine was coupled with 2,5-bis-tert-butoxycarbonyl amino-pentanoic acid (2.2 mmol, 0.72 g) using BOP (2.4 mmol, 1.04 g), HOBt (2.96 mmol, 0.4 g) and DIEA (8.63 mmol, 1.5 ml) in DMF (5 ml) and dichloromethane (15 ml). The mixture was stirred overnight at RT. Then solvent was evaporated and product **2A** (1.3 g, 92 %) was crystallized from acetonitrile. ^{1}H NMR ($CDCl_3$, 300 MHz): δ 6.46 (s, 1H), 5.56 (s, 1H), 5.2 (s, 1H), 4.73 (s, 1H), 4.17 (s, 1H), 3.65 (s, 3H), 3.28-3.04 (m, 6H), 2.28 (t, 2H), 2.13 (t, 2H), 1.66-1.19 (m, 50H). LC-MS: (m/z) Found $[M+1]^+$ = 585.4 (calcd for $C_{36}H_{68}N_4O_8^+$ - $C_{10}H_{18}O_4$ (2Boc) = 585.4).

(1-{7-[11-(2-Amino-ethylcarbamoyl)-undecylcarbamoyl]-heptylcarbamoyl}-4-tert-butoxycarbonylamino-butyl)-carbamic acid tert-butyl ester (2B). The methyl ester **2A** (1.75 mmol, 1.2 g) was reacted with ethylenediamine (150 mmol, 10 ml) for 72 h at 70°C. Then the excess of ethylenediamine was evaporated, the water was added and the product **2B** was filtered (1.2 g, 96 %). ^{1}H NMR (CD_3OD, 300 MHz): δ 3.99 (s, 1H), 3.28-3.13 (m, 6H), 3.06 (t, 2H), 2.73 (t, 2H), 2.24-2.15 (m, 4H), 1.67-1.28 (m, 50H). LC-MS: (m/z) Found $[M+1]^+$ = 713.4 (calcd for $C_{37}H_{72}N_6O_7^+$ = 713.4).

[4-tert-Butoxycabonylamino-4-(7-{11-[2-(2,3,4,5,6-pentahydroxy-hexanoylamino)-ethylcarbamoyl]-undecylcarbamoyl}-heptylcabamoyl)-butyl]-carbamic acid tert-butyl ester (2C). δ-Gulonic-γ-lactone (0.95 mmol, 0.17 g) was added to solution of **2B** (0.56 mmol, 0.4 g) in 30 ml of methanol. Then, DIEA (5.64 mmol, 0.98 ml) was added and the reaction mixture was stirred at 70°C for about 24 h. Solvents were evaporated in vacuo. The obtained compound was crystallized from methanol to get product **2C** (0.15 g, 88 %). ^{1}H NMR (DMSO, 300 MHz): δ 7.83-7.61 (m, 4H), 6.8-6.64 (m, 2H), 5.35 (d, 1H), 4.57-4.26 (m, 5H), 4.0-3.75 (m, 3H), 3.61-3.38 (m, 6H), 3.22-2.81 (m, 11H), 2.06-1.95 (m, 4H), 1.54-1.37 (m, 10H), 1.36-1.32 (m, 18H), 1.31-1.11 (m, 24H). LC-MS: (m/z) Found $[M+1]^+$ = 891.6 (calcd for $C_{43}H_{82}N_6O_{13}^+$ = 891.6).

{4-tert-Butoxycarbonylamino-1-[7-(11-{2-[2,3,5,6-tetrahydroxy-4-(3,4,5-trihydroxy-6-hydroxymethyl-tetrahydro-pyran-2-yloxy)-hexanoylamino]-ethylcarbamoyl}-undecylcarbamoyl)-heptylcarbamoyl]-butyl}-carbamic acid tert-butyl ester (2D). Lactonolactone (**5**) (1 mmol, 0.33 g) was added to solution of **2B** (0.4 mmol, 0.3 g) in 20 ml of methanol. Then, DIEA (6 mmol, 1.05 ml) was added and after 24 h of stirring at 70°C, the solution was poured into water. The product was extracted with butanol and dried with sodium sulfate. Then the solvent was removed to obtain compound **2D** (0.4 g, 91 %).

12-[8-(2,5-Diamino-pentanoylamino)-octanoylamino]-dodecanoic acid[2-(2,3,4,5,6-pentahydroxy-hexanoylamino)-ethyl]-amide (Orn-C8-C12-G). Boc was removed from 0.1 g (0.11 mmol) of **2C** using 1 ml of TFA with 3% of H_2O. After 1h, the solvent was evaporated in vacuo to afford the final product **Orn-C8-C12-G** (0.095 g, 92 %). MS: (m/z) Found $[M+1]^+$ = 691.5 (calcd for $C_{33}H_{67}N_6O_9^+$ = 691.5). MS: (m/z) Found $[M+1]^+$ = 691.5 (calcd for $C_{33}H_{67}N_6O_9^+$ = 691.5).

12-[8-(2,5-Diamino-pentanoylamino)-octanoylamino]-dodecanoic acid {2-[2,3,5,6-tetrahydroxy-4-(3,4,5-trihydroxy-6-hydroxymethyl-tetrahydro-pyran-2-yloxy)-hexanoylamino]-ethyl}-amide (Orn-C8-C12-L). Boc was removed from 0.1 g (0.095 mmol) of **2D** using 1 ml of TFA with 3% of H_2O. After 1h, the solvent was evaporated in vacuo to afford the final product **Orn-C8-C12-L** (75 mg, 92 %). MS: (m/z) Found $[M+1]^+$ = 853.5 (calcd for $C_{39}H_{76}N_6O_{14}^+$ = 853.5).

B) Synthesis of G-C8-C12-DPTA/L-C8-C12-DPTA

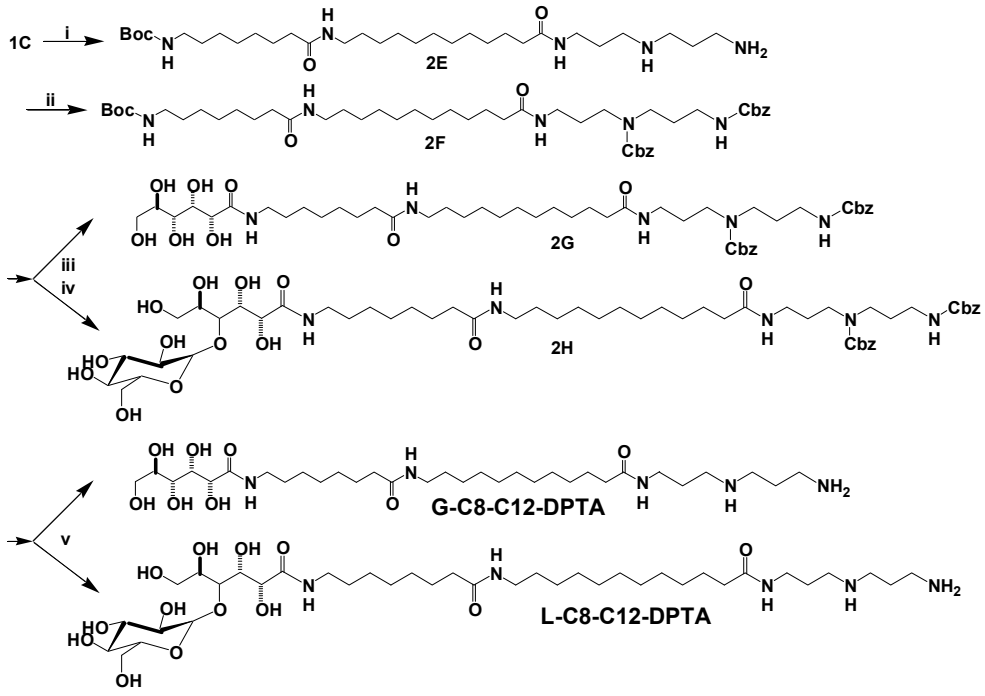

Reagents: (i) DPTA, 72 h, 70 °C; (ii) $C_8H_7ClO_2$, DIEA, THF, 4 h, 0 °C; (iii) TFA, CH_2Cl_2, 4 h; (iv) Gluconic acid lactone or lactonolactone, MeOH, DIEA, 70 °C, 24 h; (v) Pd-C, MeOH/HCOOH (3/2, v/v), 2 h.

Scheme 2.2. Synthesis of **G-C8-C12-DPTA** and **L-C8-C12-DPTA.**

(7-{11-[3-(3-Amino-propylamino)-propylcarbamoyl]-undecylcarbamoyl}-heptyl)-carbamic acid tert-butyl ester (2E). Methyl ester **1C** (6.4 mmol, 3 g) was substituted with bis(3-aminopropyl)amine (0.18 M, 25 ml) for 72 h at 70°C. Precipitate was formed during the reaction. It was filtered off and dried to get the product **2E** (3.2 g, 88 %). ^{1}H NMR (CD_3OD, 300 MHz): δ 3.24-3.17 (t, 2H), 3.17-3.09 (t, 2H), 2.72-2.64 (t, 2H), 2.63-2.53 (m, 4H), 2.19-2.1 (m, 4H), 1.73-1.44 (m, 12H), 1.43-1.27 (m, 9H), 1.36-1.23 (m, 22H).

[7-(11-{3-[Benzyloxycarbonyl-(3-benzyloxycarbonylamino-propyl)-amino]-propylcarbamoyl}-undecylcarbamoyl)-heptyl]-carbamic acid tert-butyl ester (2F). The solution of **2E** (1.75 mmol, 1 g) in 35 ml of THF and 2 ml DIEA (11.5 mmol) was cooled to 0 °C followed by dropwise addition of benzyl chloroformate (8.4 mmol, 1.2 ml). After 4 h of stirring, water was poured into the solution and the product **2F** was extracted with ethyl acetate and further purified by column chromatography using dicholoromethane : methanol (95:5) (1 g, 71 %). ^{1}H NMR ($CDCl_3$, 300 MHz): δ 7.52-7.19 (m, 10H), 6.56 (s, 1H); 5.78 (s, 1H); 5.67 (s, 1H); 5.2-5.0 (m, 4H), 4.6 (s, 1H), 3.41-2.96 (m, 12H), 2.24-2.04 (m, 4H), 1.78-1.66 (m, 4H), 1.64-1.41 (m, 8H), 1.38-1.19 (m, 22H).

(3-Benzyloxycarbonylamino-propyl)-(3-{12-[8-(2,3,4,5,6-pentahydroxy-hexanoyl amino)-octanoylamino]-dodecanoylamino}-propyl)-carbamic acid benzyl ester (2G). Boc group of **2F** (0.84 mmol, 0.7 g) was removed using 2 ml of TFA in dichloromethane (2 ml) for 4 h at RT. The solvent was evaporated and 0.3 g (0.4 mmol) of the obtained deprotected amine was mixed with δ-gulonic-γ-lactone (0.73 mmol, 0.13 g) in 20 ml of methanol. Then, DIEA (4 mmol, 0.7 ml) was added and the reaction mixture was stirred at 70°C for about 24 h. Precipitate was formed during the reaction. It was filtered off and dried to obtain compound **2G** (0.3 g, 81 %). ^{1}H NMR (CD_3OD, 300 MHz): δ 7.4-7.23 (m, 10H), 5.12-5.01 (m, 4H), 4.18 (s, 1H), 4.08 (s, 1H), 3.8-3.58 (m, 4H), 3.25-3.18 (m, 4H), 3.17-3.04 (m, 6H), 2.1-2.04 (m, 4H), 1.78-1.66 (m, 4H), 1.64-1.41 (m, 8H), 1.38-1.19 (m, 22H).

(3-Benzyloxycarbonylamino-propyl)-[3-(12-{8-[2,3,5,6-tetrahydroxy-4-(3,4,5-trihydroxy-6-hydroxymethyl-tetrahydro-pyran-2-yloxy)-hexanoylamino]-octanoylamino}-dodecanoylamino)-propyl]-carbamic acid benzyl ester (2H). Boc group of **2F** (0.84 mmol, 0.7 g) was removed using 2 ml of TFA in dichloromethane (2 ml) for 4 h at RT. The solvent was evaporated and 0.42 g (0.57 mmol) of the obtained deprotected amine was mixed with lactonolactone (**5**) (1 mmol, 0.33 g) in 20 ml of methanol. Then, DIEA (5.8 mmol, 1 ml) was added and after 24 h of stirring at 70°C, the solution was poured in water. The product was extracted with butanol and dried with sodium sulfate. Then the solvent was removed to obtain compound **2H** (0.5 g, 81 %).

12-[8-(2,3,4,5,6-Pentahydroxy-hexanoylamino)-octanoylamino]-dodecanoic acid [3-(3-amino-propylamino)-propyl]-amide (G-C8-C12-DPTA). Cbz was removed from 0.1 g (0.1 mmol) of **2G** using 100 mg of Pd-C (10%) in 12 ml of methanol and 8 ml of formic acid (methanol : formic acid = 3 : 2) for 2 h at 70 °C. Then the reaction mixture was filtered to remove Pd and the solvent was removed in vacuo to afford the final product **G-C8-C12-DPTA** (0.065 g, 92 %). MS: (m/z) Found $[M+1]^+ = 648.4$ (calcd for $C_{32}H_{65}N_5O_8^+ = 648.4$).

12-{8-[2,3,5,6-Tetrahydroxy-4-(3,4,5-trihydroxy-6-hydroxymethyl-tetrahydro-pyran-2-yloxy)-hexanoylamino]-octanoylamino}-dodecanoic acid [3-(3-amino-propylamino)-propyl]-amide (L-C8-C12-DPTA). Cbz was removed from 0.2 g (0.19 mmol) of **2H** using 200 mg of Pd-C (10%) in 24 ml of methanol and 16 ml of formic acid (methanol : formic acid = 3 : 2) for 2 h at 70 °C. Then the reaction mixture was filtered to remove Pd and the solvent was removed in vacuo to afford the final product **L-C8-C12-DPTA** (0.14 g, 93 %). MS: (m/z) Found $[M+1]^+ = 810.4$ (calcd for $C_{38}H_{75}N_5O_{13}^+ = 810.4$).

1.3 Third Generation Bolas

A) Synthesis of Orn-C16-G/Orn-C16-L

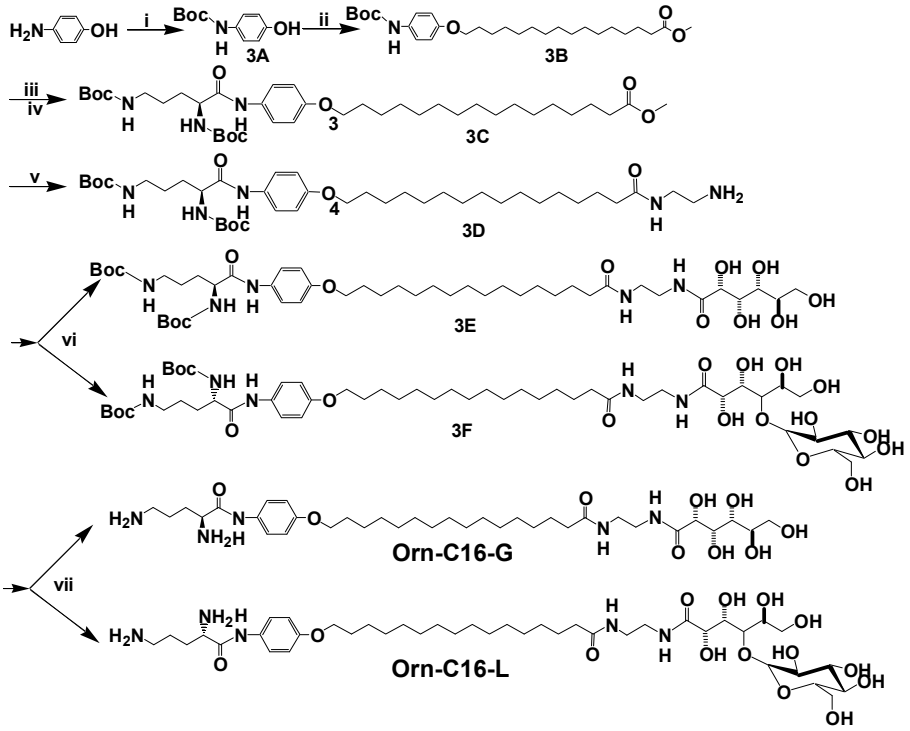

Reagents: (i) Boc_2O, THF; (ii) $C_{17}H_{33}BrO_2$, K_2CO_3, DMF, 12 h; (iii) TFA, H_2O, 1 h;
(iv) Boc_2-Ornithine-OH, BOP, HOBt, DIEA, DMF, CH_2Cl_2, 24 h; (v) $C_2H_8N_2$, 70 °C, 72 h;
(vi) Gluconic acid lactone or lactonolactone, MeOH, DIEA, 24 h; (vii) TFA, H_2O/CH_2Cl_2, 1 h.

Scheme 3.1. Synthesis of **Orn-C16-G** and **Orn-C16-L.**

N-Boc-4-aminophenol (**3A**). 4-Aminophenol (4 g, 36.7 mmol) and Boc_2O (8 g, 36.7 mmol) were dissolved in 30 ml of THF and left stirring overnight. Then water was added and the product was extracted with ethyl acetate and further dried with sodium sulfate. After solvent evaporation in vacuo the crude product **3A** was used without further purification.

16-(4-Tert-butoxycarbonylaminophenoxy)-hexadecanoic acid methyl ester (**3B**). Boc-protected 4-aminophenol (**3A**) (1.8 g, 8.6 mmol) and 16-bromohexadecanoic acid methyl ester (3 g, 8.6 mmol, prepared by methylation of the acid in methanol and thionyl chloride) were dissolved in 10 ml of DMF and supplemented with 1.8 g (13 mmol) of potassium carbonate. After 12 h of stirring at RT, the solution was poured in water and the product was extracted with dichloromethane and dried with sodium sulfate. Then the

solvent was removed and the product was recrystallized from ethanol to obtain product **3B** (1.6 g, 40 %). ^{1}H NMR ($CDCl_3$, 300 MHz): δ 7.24 (d, 2H), 6.82 (d, 2H), 6.4 (s, 1H), 3.91 (t, 2H), 3.67 (s, 3H), 2.31 (t, 2H), 1.82-1.58 (m, 4H), 1.55-1.48 (m, 9H), 1.46-1.2 (m, 24H). LC-MS: (m/z) Found $[M+1]^+$ = 378.2 (calcd for $C_{28}H_{47}NO_5^+$ - $C_5H_9O_2$ (Boc) = 378.3).

16-[4-(2,5-Bis-tert-butoxycaronylamino-pentanoylamino)-phenoxy]-hexadecanoic acid methyl ester (3C). Boc was removed from **3B** (3.14 mmol, 1.5 g) by treating with 5 ml of TFA with 3% H_2O for 1 h at RT. The solvent was evaporated and 1.54 g (3.1 mmol) of the obtained de-protected amine was coupled with 2,5-bis-tert-butoxycarbonyl amino-pentanoic acid (3.57 mmol ,1.15 g) using BOP (3.44 mmol, 1.52 g), HOBt (4.3 mmol, 0.58 g) and DIEA (12.6 mmol, 2.2 ml) in DMF (15 ml) and dichloromethane (30 ml). The mixture was stirred overnight at RT. Then solvent was evaporated and product was crystallized from acetonitrile. The precipitate was filtered off and dried to give compound **3C** (1.6 g, 76 %). ^{1}H NMR ($CDCl_3$, 300 MHz): δ 8.41 (s, 1H), 7.41 (d, 2H), 6.81 (d, 2H), 5.25 (s, 1H), 4.73 (s, 1H), 4.39 (s, 1H), 3.9 (t, 2H), 3.65 (s, 3H), 3.4 (s, 1H), 3.09 (s, 1H), 2.28 (t, 2H), 1.83-1.69 (m, 4H), 1.67-1.53 (m, 4H), 1.47-1.38 (m, 18H), 1.37-1.16 (m, 22H). LC-MS: (m/z) Found $[M+1]^+$ = 491.2 (calcd for $C_{38}H_{65}N_3O_8^+$ - $C_{10}H_{18}O_4$ (2Boc) = 491.2).

(1-{4-[15-(2-Amino-ethylcarbamoyl)-pentadecyloxy]-phenylcarbamoyl}-4-tert-butoxycabonylamino-butyl)-carbamic acid tert-butyl ester (3D). Methyl ester **3C** (0.7 mmol, 0.5 g) was substituted with ethylenediamine (150 mmol, 10 ml) for 72 h at 70°C. Then the excess of ethylenediamine was evaporated, the water was added and the product **3D** was filtered (0.45 g, 87 %). ^{1}H NMR ($CDCl_3$, 300 MHz): δ 8.45 (s, 1H), 7.42 (d, 2H), 6.82 (d, 2H), 6.05 (s, 1H), 5.30 (s, 1H), 4.75 (s, 1H), 4.37 (s, 1H), 3.91 (t, 2H), 3.42-3.25 (m, 3H), 3.16-3.02 (m, 1H), 2.84 (t, 2H), 2.17 (t, 2H), 2.06-1.92 (m, 4H), 1.79-1.7 (m, 2H), 1.67-1.54 (m, 4H), 1.48-1.37 (m, 18H), 1.37-1.20 (m, 20H). LC-MS: (m/z) Found $[M+1]^+$ = 720.4 (calcd for $C_{39}H_{69}N_5O_7^+$ = 720.4).

[4-tert-Butoxylamino-4-(4-{15-[2-(2,3,4,5,6-pentahydroxy-hexanoylamino)-ethylcabamoyl]-pentadecyloxy}-phenylcarbamoyl)-butyl]-carbamic acid tert-butyl ester (3E). δ-Gulonic-γ-lactone (0.23 mmol, 0.04 g) was added to solution of **3D** (0.11 mmol, 0.1 g) in 15 ml of methanol. Then, DIEA (1.4 mmol, 0.24 ml) was added and

reaction mixture was stirred at 70°C for about 24 h. Solvents were evaporated in vacuo. The obtained compound was crystallized from methanol to get product **3E** (0.09 g, 90 %). ^{1}H NMR (CD_3OD, 300 MHz): δ 7.42 (d, 2H), 6.87 (d, 2H), 4.21 (s, 1H), 4.18-4.06 (m, 2H), 3.96 (t, 2H), 3.83-3.6 (m, 5H), 3.09 (t, 2H), 2.19 (t, 2H), 1.86-1.54 (m, 10H), 1.48-1.41 (m, 18H), 1.39-1.26 (m, 22H). LC-MS: (m/z) Found $[M+1]^+$ = 898.57 (calcd for $C_{45}H_{79}N_5O_{13}^+$ = 898.57).

{4-tert-Butoxycarbonylamino-4-[4-(15-{2-[2,3,5,6-tetrahydroxy-4-(3,4,5-trihydroxy-6-hydroxymethyl-tetrahydro-pyran-2-yloxy)-hexanoylamino]-ethylcabamoyl}-pentadecyloxy)-phenylcarbamoyl]-butyl}-carbamic acid tert-butyl ester (3F). Lactonolactone (**5**) (0.24 mmol, 0.08 g) was added to solution of **3D** (0.14 mmol, 0.1 g) in 20 ml of methanol. Then, DIEA (1.4 mmol, 0.24 ml) was added and the reaction mixture was stirred at 70°C for about 24 h. Solvents were evaporated in vacuo and water was poured into the reaction flask. The product **3F** (0.12 g, 81 %) was extracted with butanol and the solvent was evaporated in vacuo. ^{1}H NMR (CD_3OD, 300 MHz): δ 7.43 (d, 2H), 6.84 (d, 2H), 4.49-4.39 (m, 4H), 4.21 (d, 2H), 3.98-3.64 (m, 10H), 3.64-3.42 (m, 4H), 3.08-3.02 (t, 3H), 2.26-2.17 (t, 2H), 1.76-1.5 (m, 8H), 1.48-1.35 (m, 18H), 1.35-1.16 (m, 24H). LC-MS: (m/z) Found $[M+1]^+$ = 1060.62 (calcd for $C_{51}H_{89}N_5O_{18}^+$ = 1060.62).

16-[4-(2,5-Diamino-pentanoylamino)-phenoxy]-hexadecanoicacid[2-(2,3,4,5,6-pentahydroxy-hexanoylamino)-ethyl]-amide (Orn-C16-G). Boc was removed from 50 mg of **3E** using 0.5 ml of TFA with 3 % H2O. After 1 h the solvent was removed to obtain the final product **Orn-C16-G** (27 mg, 90 %). LC-MS (Bruker, HTCultra): (m/z) Found $[M+1]^+$ = 698.4 (calcd for $C_{35}H_{64}N_5O_9^+$ = 698.4).

16-[4-(2,5-Diamino-pentanoylamino)-phenoxy]-hexadecanoicacid{2-[2,3,5,6-tetra hydroxy-4-(3,4,5-trihydroxy-6-hydroxymethyl-tetrahydro-pyran-2-yloxy)-hexanoyl amino]-ethyl}-amide (Orn-C16-L). Boc was de-protected from 50 mg of **3F** using 1 ml of TFA and 2 ml CH_2Cl_2. After 1 h the solvent was removed to obtain the final product **Orn-C16-L** (37 mg, 91 %). LC-MS: (m/z) Found $[M+1]^+$ = 860.2 (calcd for $C_{41}H_{73}N_5O_{14}^+$ = 860.2).

B) Synthesis of Orn-C20-G/Orn-C20-L

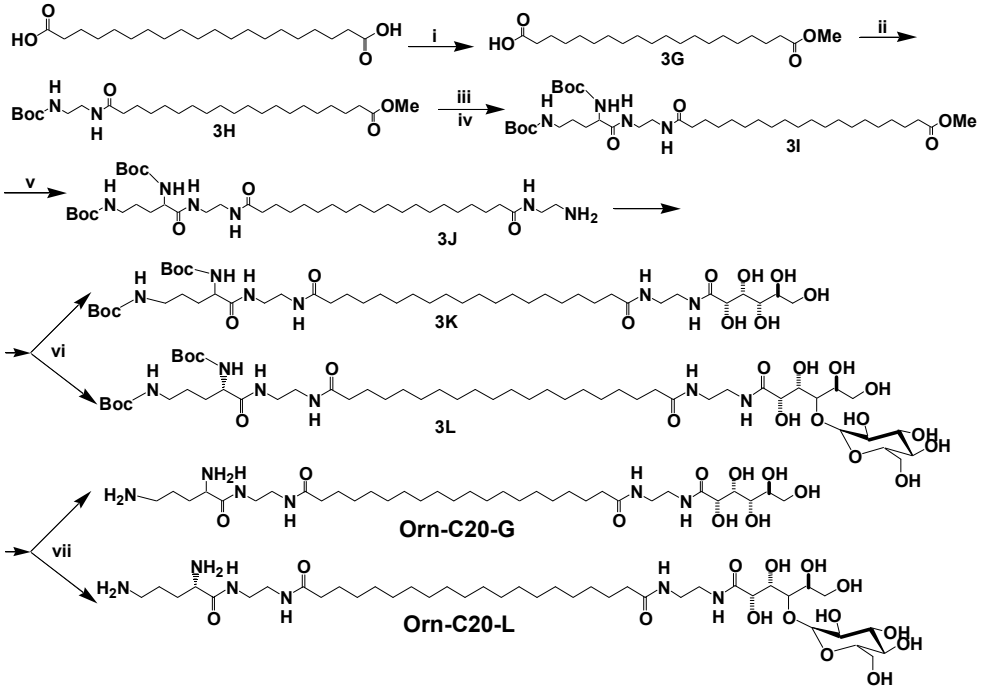

Reagents: (i) MeOH, H_2SO_4, $C_2H_4Cl_2$, 85 °C, 24 h; (ii) N-Boc-ethylenediamine, BOP, HOBt, DIEA, DMF, CH_2Cl_2, 24 h; (iii) TFA, H_2O, 1 h; (iv) Boc_2-Ornithine-OH, BOP, HOBt, DIEA, DMF, CH_2Cl_2, 40 °C, 24 h; (v) $C_2H_8N_2$, 70 °C, 72 h; (vi) Gluconic acid lactone or lactonolactone, MeOH, DIEA, 24 h; (vii) TFA, H_2O/CH_2Cl_2, 1 h.

Scheme 3.2. Synthesis of **Orn-C20-G** and **Orn-C20-L.**

Eicosanedioic acid monomethyl ester (3G). Eicosanedioic acid (14.6 mmol, 5 g) was dissolved in 300 ml of ethylene chloride at 85°C. Methanol (7.4 mmol, 0.59 ml) was added to the clear solution, then H_2SO_4 (1.4 ml) was cautiously added, and the reaction was left to reflux overnight at 85°C. The mixture was concentrated and water was added. Three phases were obtained: aqueous, organic and slurry. To the organic phase, which contained mainly di- and mono-esters, carbon tetrachloride was added and placed in a separate funnel. The organic layer was washed with water, then dried over $MgSO_4$ and evaporated. Product was subjected to column chromatography, where di-ester was eluded with dichloromethane and the monoester **3G** with ethyl acetate (25 % yield). ^{1}H NMR ($CDCl_3$, 300 MHz): 3.65 (s, 3H), 2.36-2.26 (m, 4H), 1.65-1.56 (m, 4H), 1.39-1.19 (m, 28H).

19-(2-tert-Butoxycarbonylamino-ethylcarbamoyl)-nonadecanoic acid methyl ester (3H). *N*-Boc-ethylenediamine (1 mmol, 0.162 g) was coupled with mono-methyl ester **3G** (0.84 mmol, 0.3 g) using BOP (0.93 mmol, 0.41 g), HOBt (1.2 mmol, 0.16 g) and

DIEA (3.4 mmol, 0.6 ml) in DMF (5 ml) and dichloromethane (20 ml). The mixture was stirred overnight at room temperature. Then the solvent was evaporated and the product was crystallized from acetonitrile to give product **3H** (0.3 g, 72 %). ^{1}H NMR (DMSO, 300 MHz): 7.62 (s, 1H), 6.61 (s, 1H), 3.58 (s, 3H), 3.05 (t, 2H), 2.97 (t, 2H), 2.27 (t, 2H), 2.03 (t, 2H), 1.57-1.42 (m, 4H), 1.4-1.33 (m, 9H), 1.32-1.17 (m, 28H). LC-MS: (m/z) Found $[M+1]^+ = 399.2$ (calcd for $C_{28}H_{54}N_2O_5^+ - C_5H_9O_2$ (Boc) = 399.3).

19-[2-(2,5-Bis-tert-butoxycarbonylamino-pentanoylamino)-ethylcarbamoyl]-nonadecanoic acid methyl ester (3I). Boc group was removed from **3H** (0.54 mmol, 0.27 g) by treating with 1 ml of TFA with 3% H_2O for 1 h at RT. The solvent was evaporated and obtained de-protected amine was coupled with 2,5-bis-tert-butoxycarbonyl-aminopentanoic acid (0.62 mmol, 0.207 g) using BOP (0.93 mmol), HOBt (1.2 mmol) and DIEA (3.4 mmol, 0.6 ml) in DMF (10 ml) and dichloromethane (10 ml). The mixture was stirred overnight at 40 °C. Then the solvent was evaporated and the product was crystallized from ethyl acetate. The precipitate was filtered off and dried to give crystals of compound **3I** (0.34 g, 70 %). ^{1}H NMR ($CDCl_3$, 300 MHz): 6.95 (s, 1H), 6.39 (s, 1H), 5.18 (s, 1H), 4.76 (s, 1H), 4.17 (s, 1H), 3.65 (t, 3H), 3.4-3.2 (m, 5H), 3.11-2.99 (m, 1H), 2.28 (t, 2H), 2.15 (t, 2H), 1.87-1.7 (m, 2H), 1.67-1.5 (m, 8H), 1.46-1.38 (m, 18H), 1.34-1.17 (m, 30H). LC-MS: (m/z) Found $[M+1]^+ = 613.4$ (calcd for $C_{38}H_{72}N_4O_5^+ - C_5H_9O_2$ (Boc) = 613.4).

(1-{2-[19-[2-(2-Amino-ethylcarbamoyl)-nonadecanoylamino]-ethylcarbamoyl}-4-tert-butoxycarbonylamino-butyl)-carbamic acid tert-butyl ester (3J). Methyl ester **3I** (0.4 mmol, 0.3 g) was reacted with ethylenediamine (150 mmol 10 ml) for 72 h at 70°C. Then the excess of ethylenediamine was evaporated and water was poured into the reaction flask. Formed precipitate was filtered off to give compound **3J** (0.29 g, 93 %). ^{1}H NMR (CD_3OD, 300 MHz): 3.96 (s, 1H), 3.05 (t, 2H), 2.73 (t, 2H), 2.23-2.16 (m, 4H), 1.67-1.5 (m, 8H), 1.46-1.44 (m, 18H), 1.39-1.23 (m, 30H). LC-MS: (m/z) Found $[M+1]^+ = 741.4$ (calcd for $C_{39}H_{76}N_6O_7^+ = 741.5$).

[4-tert-Butoxycabonylamino-4-(2-{19-[2-(2,3,4,5,6-pentahydroxy-hexanoylamino)-ethylcarbamoyl]-nonadecanoylamino}-ethylcabamoyl)-butyl]-carbamic acid tert-butyl ester (3K). δ-Gulonic-γ-lactone (0.23 mmol, 0.04 g) was added to solution of **3J** (0.13 mmol, 0.1 g) in 10 ml of methanol. Then, DIEA (1.4 mmol, 0.24 ml) was added

and reaction mixture was stirred at 70°C for about 24 h. Solvents were evaporated in vacuo. The obtained compound was crystallized from methanol to give product **3K** (0.095 g, 95 %). ^{1}H NMR (CD_3OD, 300 MHz): 4.21 (s,1H), 4.1 (s, 1H), 3.98 (s, 1H), 3.84-3.59 (m, 5H), 3.07 (t, 2H), 2.25-2.12 (m, 4H), 1.68-1.49 (m, 8H), 1.49-1.4 (m, 18H), 1.4-1.21 (m, 30H). LC-MS: (m/z) Found $[M+1]^+$ = 919.6 (calcd for $C_{45}H_{86}N_6O_{13}^+$ = 919.6).

{4-tert-Butoxycabonylamino-4-[2-(19-{2-[2,3,5,6-tetrahydroxy-4-(3,4,5-trihydroxy-6-hydroxymethyl-tetrahydro-pyran-2-yloxy)-hexanoylamino]-ethylcarbamoyl}-nonadecanoylamino)-ethylcabamoyl]-butyl}-carbamic acid tert-butyl ester (3L). Lactonolactone (**5**) (0.23 mmol, 0.078 g) was added to solution of **3J** (0.14 mmol, 0.1 g) in 20 ml of methanol. Then, DIEA (1.4 mmol, 0.24 ml) was added and reaction mixture was stirred at 70°C for about 24 h. Solvents were evaporated in vacuo and water was poured into the reaction flask. The product **3L** (0.11 g, 75 %) was extracted with butanol and the solvent was evaporated in vacuo. ^{1}H NMR (CD_3OD, 300 MHz): 4.49 (s,1H), 4.36 (s, 1H), 4.22 (s, 1H), 3.95-3.67 (m, 8H), 3.61-3.47 (m, 3H), 3.06-3.02 (t, 2H), 2.21-2.15 (t, 4H), 1.61-1.51 (m, 8H), 1.44-1.43 (m, 18H), 1.42-1.28 (m, 32H). LC-MS: (m/z) Found $[M+1]^+$ = 1081.68 (calcd for $C_{51}H_{96}N_6O_{18}^+$ = 1081.68).

Eicosanedioic acid [2-(2,5-diamino-pentnoylamino)-ethyl]-amide[2-(2,3,4,5,6-pentahydroxy-hexanoylamino)-ethyl]-amide (Orn-C20-G). 40 mg of **3K** was treated with 0.4 ml of TFA with 3 % H2O to remove Boc group. After 1 h the solvent was removed to obtain final compound **Orn-C20-G** (27 mg, 90 %). LC-MS: (m/z) Found $[M+1]^+$ = 719.5 (calcd for $C_{35}H_{71}N_6O_9^+$ = 719.5).

Eicosanedioic acid [2-(2,5-diamino-pentnoylamino)-ethyl]-amide{2-(2,3,5,6-tetrahydroxy-4-(3,4,5-trihydroxy-6-hydroxymethyl-tetrahydro-pyran-2-yloxy)-hexanoylamino]-ethyl}-amide (Orn-C20-L). 50 mg of **3L** was treated with 1 ml TFA and 2 ml CH_2Cl_2 to remove Boc group. After 1 h the solvent was removed to obtain final compound **Orn-C20-L** (38 mg, 93 %). LC-MS: (m/z) Found $[M+1]^+$ = 881.58 (calcd for $C_{41}H_{80}N_6O_{14}^+$ = 881.58).

C) Synthesis of Orn-C12-C16-G

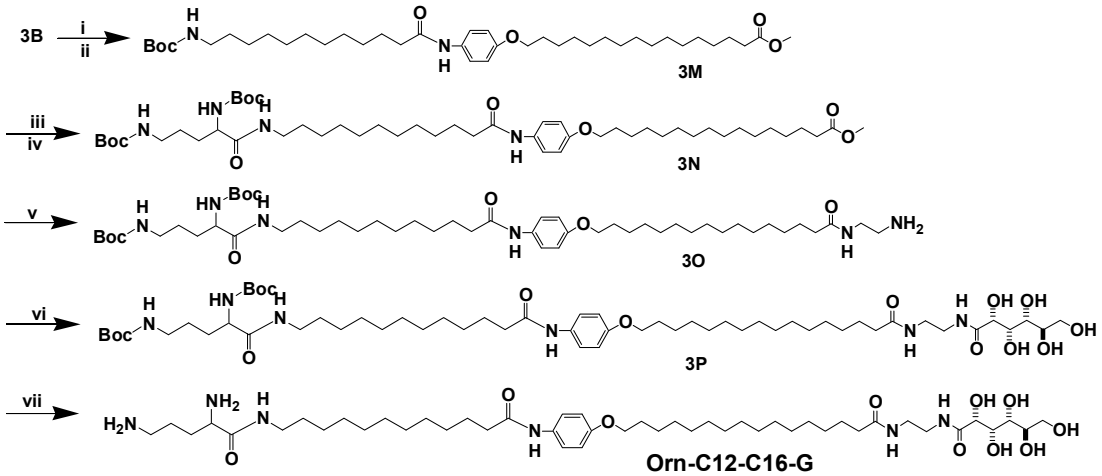

Reagents: (i) TFA, H_2O, 1 h; (ii) $C_{17}H_{33}NO_4$, BOP, HOBt, DIEA, DMF, CH_2Cl_2, 24 h; (iii) TFA, H_2O, 1 h; (iv) Boc_2-Ornithine-OH, BOP, HOBt, DIEA, DMF, CH_2Cl_2, 24 h, 40 °C; (v) $C_2H_8N_2$, 70 °C, 72 h; (vi) Gluconic acid lactone, MeOH, DIEA, 70 °C, 24 h; (vii) TFA, H_2O/CH_2Cl_2, 1 h.

Scheme 3.3. Synthesis of **Orn-C12-C16-G.**

16-[4-(12-tert-Butoxycarbonylamino-dodecanoylamino)-phenoxy]-hexadecanoic id methyl ester (3M). Boc was removed from **3B** (3.14 mmol, 1.5 g) using 5 ml of TFA with 3% H_2O for 1 h at RT. The solvent was evaporated and 0.2 g (0.53 mmol) of the obtained de-protected amine was coupled with 12-tert-butoxycarbonylamino-dodecanoic acid (0.48 mmol ,0.15 g) using BOP (0.45 mmol, 0.2 g), HOBt (0.6 mmol, 0.08 g) and DIEA (1.7 mmol, 0.3 ml) in DMF (5 ml) and dichloromethane (10 ml). The mixture was stirred overnight at RT. Then solvent was evaporated and the product was crystallized from acetonitrile. The precipitate was filtered off and dried to give compound **3M** (0.31 g, 86 %). ^{1}H NMR (DMSO, 300 MHz): δ 9.51 (s, 1H), 7.45 (d, 2H), 6.82 (d, 2H), 3.94-3.87 (t, 2H), 3.58 (s, 3H), 2.93-2.83 (m, 2H), 2.33-2.2 (m, 4H), 1.72-1.62 (m, 2H), 1.6-1.45 (m, 4H), 1.38-1.35 (m, 9H), 1.32-1.29 (m, 22H).

16-{4-[12-(2,5-Bis-tert-butoxycarbonylamino-pentanoylamino)-dodecanoylamino]-phenoxy}-hexadecanoic acid methyl ester (3N). Boc was removed from **3M** (0.37 mmol, 0.25 g) using 3 ml TFA with 3 % H_2O for 1 h at RT. The solvent was evaporated and 0.22 g (0.38 mmol) of the obtained de-protected amine was coupled with 2,5-bis-tert-butoxycarbonyl amino-pentanoic acid (0.39 mmol ,0.13 g) using BOP (0.38 mmol, 0.17 g), HOBt (0.48 mmol, 65 mg) and DIEA (1.4 mmol, 0.24 ml) in DMF (5 ml) and

dichloromethane (10 ml). The mixture was stirred overnight at 40 °C. Then solvent was evaporated and product was crystallized from acetonitrile. The precipitate was filtered off and dried to give compound **3N** (0.3 g, 88 %). ^{1}H NMR ($CDCl_3$, 300 MHz): δ 7.38 (d, 2H), 6.82 (d, 2H), 6.43 (s, 1H), 5.17 (s, 1H), 4.68 (s, 1H), 4.16 (s, 1H), 3.95-3.85 (t, 2H), 3.65 (s, 3H), 3.36-2.97 (m, 4H), 2.33-2.24 (m, 4H), 1.81-1.47 (m, 16H), 1.45-1.38 (m, 18H), 1.37-1.19 (m, 38H).

[1-(11-{4-[15-(2-Amino-ethylcarbamoyl)-pentadecyloxy]-phenylcarbamoyl}-undecylcarbamoyl)-4-tert-butoxycarbonylamino-butyl]-carbamic acid tert-butyl ester (3O). Methyl ester **3N** (0.35 mmol, 0.24 g) was substituted with ethylenediamine (150 mmol, 10 ml) for 72 h at 70°C. Then the excess of ethylenediamine was evaporated and water was poured into the reaction flask, where the product precipitated. It was filtered off and dried to get compound **3O** (0.24 g, 97 %). ^{1}H NMR (CD_3OD, 300 MHz): δ 7.42 (d, 2H), 6.86 (d, 2H), 4-3.9 (t, 3H), 3.28-3.12 (m, 5H), 3.09-3.01 (m, 3H), 2.75-2.68 (t, 2H), 2.38-2.3 (t, 2H), 2.23-2.16 (t, 2H), 1.8-1.58 (m, 8H), 1.55-1.49 (m, 4H), 1.47-1.41 (m, 18H), 1.41-1.26 (m, 38H).

{4-tert-Butoxycarbonylamino-4-[11-(4-{15-[2-(2,3,4,5,6-pentahydroxy-hexanoyl amino)-ethylcarbamoyl]-pentadecyloxy}-phenylcarbamoyl)-undecylcarbamoyl]-butyl}-carbamic acid tert-butyl ester (3P). δ-Gulonic-γ-lactone (0.23 mmol, 41 mg) was added to solution of **3O** (0.045 mmol, 0.1 g) in 10 ml of methanol. Then, DIEA (1.4 mmol, 0.24 ml) was added and reaction mixture was stirred at 70°C for about 24 h. Solvents were evaporated in vacuo and the product was crystallized from methanol to obtain compound **3P** (0.1 g, 84 %). ^{1}H NMR (CD_3OD, 300 MHz): δ 7.4 (d, 2H), 6.85 (d, 2H), 4.05-3.92 (m, 3H), 3.87-3.58 (m, 4H), 3.22-3.11 (m, 2H), 3.1-3.02 (t, 2H), 2.39-2.28 (t, 2H), 2.24-2.12 (t, 2H), 1.8-1.57 (m, 8H), 1.56-1.48 (m, 6H), 1.47-1.41 (m, 18H), 1.41-1.26 (m, 38H).

16-{4-[12-(2,5-Diamino-pentanoylamino)-dodecanoylamino]-phenoxy}-hexadecanoic acid [2-(2,3,4,5,6-pentahydroxy-hexanoylamino)-ethyl]-amide (Orn-C12-C16-G). Boc was removed from 40 mg (0.04 mmol) of **3P** using 2 ml of TFA with 3 % H2O. After 1 h the solvent was removed to obtain the final product **Orn-C12-C16-G** (30 mg, 94 %). MS: (m/z) Found $[M+1]^+ = 895.6$ (calcd for $C_{47}H_{86}N_6O_{10}^+ = 895.6$).

D) Synthesis of 2(Glu-C16)-Orn

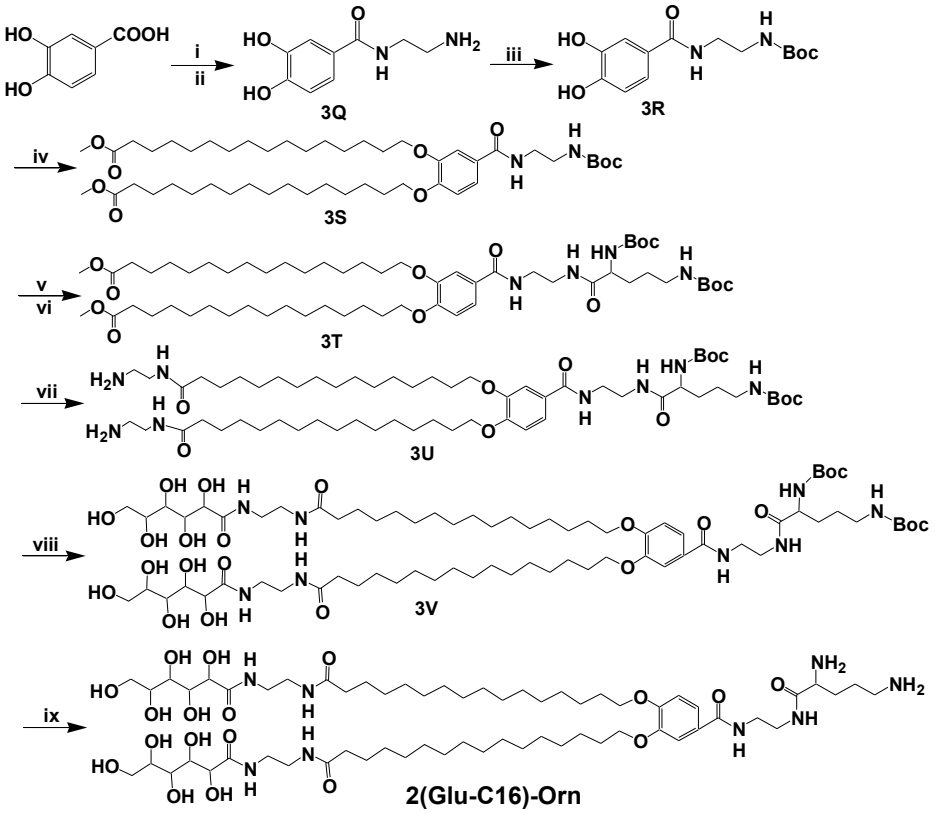

Reagents: (i) $SOCl_2$, MeOH, 20 h; (ii) $C_2H_8N_2$, 24 h, 70°C; (iii) Boc_2O, DMF, 20 h; (iv) $C_{16}H_{31}BrO_2$, K_2CO_3, DMF, 20 h, 50°C; (v) TFA, CH_2Cl_2, 1 h; (vi) Boc_2-Ornithine-OH, BOP, HOBt, DIEA, DMF, CH_2Cl_2, 24 h, 50 °C; (vii) $C_2H_8N_2$, 70°C, 72h; (viii) Gluconic acid lactone, MeOH, DIEA, 24 h, 70 °C; (ix) TFA, H_2O, 1 h.

Scheme 3.4. Synthesis of **2(Glu-C16)-Orn.**

N-(2-Amino-ethyl)-3,4-dihydroxy-benzamide (3Q). Thionyl chloride (0.15 mmol, 10 ml) was added drop-wise to 100 ml of methanol at 0 °C and the mixture was stirred for another 20 min. Then, 10 g of 3,4-dihydroxy-benzoic acid (65 mmol) was added and reaction mixture was stirred for 20 h at RT. The solvent was evaporated and the obtained methyl ester (18 mmol, 3 g) was further reacted with ethylenediamine (0.15 mmol, 10 ml) for 24 h at 70°C. The excess of ethylenediamine was evaporated and the product **3Q** (3.2 g, 91 %) was crystallized from chloroform. ^{1}H NMR (CD_3OD, 300 MHz): δ 7.27 (s, 1H), 7.2 (d, 1H), 6.77 (d, 1H), 3.45-3.38 (t, 2H), 2.9-2.81 (t, 2H), 2.77-2.71 (t, 2H).

[2-(3,4-Dihydroxy-benzoylamino)-ethyl]-carbamic acid tert-butyl ester (3R). Amino group of **3Q** (7.6 mmol, 1.5 g) was protected with Boc group using di-tert-butyl dicarbonate (9.1 mmol, 2 g) in the solution of DMF (10 ml). After 20 h of stirring at RT,

the solution was poured in water and the product was extracted with ethyl acetate and dried with sodium sulphate. Then the solvent was removed to obtain compound **3R** (2 g, 88 %). ^{1}H NMR ($CDCl_3$, 300 MHz): δ 7.98 (s, 2H), 7.48-7.31 (m, 2H); 7.16 (d, 1H); 6.8 (d, 1H), 5.55 (s, 1H), 4.16-4.05 (m, 2H), 3.56-3.16 (m, 4H), 1.44-1.31 (m, 9H).

15-[4-(2-tert-Butoxycarbonylamino-ethylcarbamoyl)-2-(14-methoxycarbonyl-tetradecyloxy)-phenoxy]-pentadecanoic acid methyl ester (3S). 0.7 g (2.4 mmol) of **3R** was coupled with 16-bromohexadecanoic acid methyl ester (4.5 mmol, 1.58 g) using K_2CO_3 (9.5 mmol, 1.31 g) in 10 ml DMF. The reaction mixture was stirred for 20 h at 50 °C and then water was poured into the reaction flask, where the product precipitated. It was filtered out and dried to obtain compound **3S** (1.7 g, 89 %). ^{1}H NMR ($CDCl_3$, 300 MHz): δ 7.43 (s, 1H), 7.31 (d, 1H); 7.11 (s, 1H); 6.85 (d, 1H), 5.02 (s, 1H), 4.11-3.96 (m, 4H), 3.67 (s, 6H), 3.58-3.49 (t, 2H), 3.45-3.34 (t, 2H), 2.36-2.26 (t, 4H), 1.89-1.76 (m, 4H), 1.72-1.55 (m, 4H), 1.54-1.4 (m, 9H), 1.34-1.19 (m, 44H).

15-[4-[2-(2,5-Bis-tert-butoxycarbonylamino-pentanoylamino)-ethylcarbamoyl]-2-(14-methoxycarbonyl-tetradecyloxy)-phenoxy]-pentadecanoic acid methyl ester (3T). Boc group was removed from 1.5 g of **3S** (1.8 mmol) using 2 ml of TFA in 3 ml dichloromethane for 1 h at RT. The solvent was evaporated and 0.7 g (1 mmol) of the obtained deprotected amine was coupled with 2,5-bis-tert-butoxycarbonyl amino-pentanoic acid (0.9 mmol, 0.3 g) using BOP (0.9 mmol, 0.4 g), HOBt (1.1 mmol, 0.15 g) and DIEA (0.04 mmol, 0.6 ml) in DMF (5 ml) and dichloromethane (15 ml). The mixture was stirred overnight at 50 °C. Then the solvent was evaporated and product **3T** (0.9 g, 90 %) was crystallized from acetonitrile. ^{1}H NMR ($CDCl_3$, 300 MHz): δ 7.48-7.23 (m, 3H), 6.75 (d, 1H), 5.42 (s, 1H), 4.9 (s, 1H); 4.11 (s, 1H), 4-3.87 (m, 4H), 3.58 (s, 6H), 3.5-3.34 (m, 4H), 3.15-2.87 (m, 2H), 2.29-2.16 (m, 4H), 1.83-1.63 (m, 4H), 1.6-1.52 (m, 4H), 1.48-1.38 (m, 6H), 1.36-1.3 (m, 18H), 1.29-1.15 (m, 42H).

[1-(2-{3,4-Bis-[14-(2-amino-ethylcarbamoyl)-tetradecyloxy]-benzoylamino}-ethyl carbamoyl)-4-tert-butoxycarbonylamino-butyl]-carbamic acid tert-butyl ester (3U). Methyl ester **3T** (0.3 mmol, 0.3 g) was substituted with ethylenediamine (0.2 mmol, 15 ml) for 72 h at 70°C. Then the excess of ethylenediamine was evaporated and water was poured into the reaction flask, where product precipitated. It was filtered off and dried to obtain compound **3U** (0.3 g, 95 %). ^{1}H NMR (CD_3OD, 300 MHz): δ 7.45 (d, 2H), 6.98

(d, 1H), 4.1-4.01 (t, 4H); 3.27-3.19 (m, 4H), 3.05-2.98 (t, 2H), 2.77-2.68 (t, 4H), 2.24-2.15 (t, 4H), 1.85-1.72 (m, 4H), 1.66-1.47 (m, 10H), 1.46-1.38 (m, 18H), 1.35-1.24 (m, 46H).

{4-[2-(3,4-Bis-{15-[2-(2,3,4,5,6-pentahydroxy-hexanoylamino)-ethylcarbamoyl]-pentadecyloxy}-benzoylamino)-ethylcarbamoyl]-4-tert-butoxycarbonylamino-butyl}-carbamic acid tert-butyl ester (3V). δ-Gulonic-γ-lactone (0.3 mmol, 55 mg) was added to solution of **3U** (0.09 mmol, 0.1 g) in 20 ml of methanol. Then, DIEA (0.02 mmol, 0.32 ml) was added and reaction mixture was stirred at 70°C for about 24 h. Solvents were evaporated in vacuo and the product **3V** (0.1 g, 75 %) was crystallized from methanol.

N-[2-(2,5-Diamino-pentanoylamino)-ethyl]-3,4-bis-{15-[2-(2,3,4,5,6-pentahydroxy-hexanoylamino)-ethylcarbamoyl]-pentadecyloxy}-benzamide (2(Glu-C16)-Orn). Boc was removed from 50 mg (0.034 mmol) of **3V** using 0.5 ml of TFA with 3% H_2O. After 1 h the solvent was removed to obtain the final product **2(Glu-C16)-Orn** (40 mg, 93 %). MS: (m/z) Found $[M/2+1]^+ = 630.4$ (calcd for $(C_{64}H_{114}N_8O_{18}/2)^+ = 630.4$).

E) Synthesis of Orn-C16-PEG

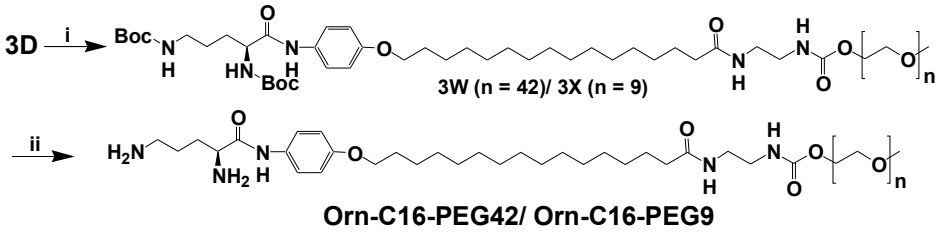

Reagents: (i) N,N-(Dimethyamino)pyridine, NEt_3, DMF, CH_2Cl_2; (ii) TFA, H_2O, 1 h.

Scheme 3.5. Synthesis of **Orn-C16-PEG42/ Orn-C16-PEG9.**

[4-tert-Butoxycarbonylamino-1-(4-{15-[2-(2-methoxy-ethoxycarbonylamino)-ethyl carbamoyl]-pentadecyloxy}-phenylcarbamoyl)-butyl]-carbamic acid tert-butyl ester (3W, 3X). 0.25g (0.35 mmol) of **3D** was coupled with **6 or 7 (Scheme 6)** (0.75 g of 6 or 0.19 mg of 7, 0.36 mmol) using *N,N*-(dimethylamino)pyridine (13 mg, 0.1 mmol) and NEt_3 (0.1 ml, 0.72 mmol) in 10 ml of 1:1 CH_2Cl_2/DMF. The reaction was stirred overnight at RT, then the solvents were removed and the product was purified by column

chromatography using 90:10 CH_2Cl_2/MeOH to get compound **3W or 3X** (700 mg of 3W, 76% and 260 mg of 3X, 64%). **3W:** ^{1}H NMR ($CDCl_3$, 300 MHz): δ 8.56 (s, 1H), 7.42 (d, 2H), 6.79 (d, 2H), 6.36 (s, 1H), 5.6 (s, 1H), 5.33 (m, 1H), 4.86 (s, 1H), 4.39 (s, 1H), 4.18 (t, 2H), 3.89 (m, 2H), 3.62 (m, 206H), 3.35 (s, 3H), 3.1 (m, 2H), 2.37 (s, 2H), 2,13 (t, 2H), 1.41 (d, 18 H), 1.23 (s, 35H). **3X:** ^{1}H NMR ($CDCl_3$, 300 MHz): δ 8.58 (s, 1H), 7.42 (d, 2H), 6.81 (d, 2H), 6.37 (s, 1H), 5.59 (s, 1H), 5.37 (d, 1H), 4.83 (s, 1H), 4.2 (t, 2H), 3.91 (t, 2H), 3.64 (m, 36H), 3.37 (m, 9H), 3.11 (m, 2H), 2.15 (t, 4H), 1.43 (d, 18H), 1.25 (m, 35H).

(2-{16-[4-(2,5-Diamino-pentanoylamino)-phenoxy]-hexadecanoylamino}-ethyl)-carbamic acid 2-methoxy-ethyl ester (Orn-C16-PEG42/ Orn-C16-PEG9). Boc was removed from **3W or 3X** (212 mg of 3W/ 95 mg of 3X, 80.7 μmol) using 2 ml TFA in 2 ml of CH_2Cl_2 and 1% H_2O, for 1 h at RT. The solvent was evaporated to obtain **Orn-C16-PEG42 (**139 mg, 63%) **/ Orn-C16-PEG9 (**62 mg, 75%). **C16-PEG42:** ^{1}H NMR (MeOD, 300 MHz): δ 7.59 (s, 1H), 7.57 (d, 2H), 6.90 (d, 2H), 4.14 (d, 2H), 3.94 (t, 2H), 3.62 (m, 197H), 3.34 (s, 3H), 3.06 (m, 2H), 2.17 (t, 2H), 2.01 (m, 2H), 1.28 (m, 31H). LC-MS: (m/z) Found $[M+23]^+$ = 2449.59 (calcd for $C_{115}H_{223}N_5O_{47}$ = 2426.68). **Orn-C16-PEG9:** ^{1}H NMR ($CDCl_3$, 300 MHz): δ 9.87 (s, 1H), 7.8 (s, 1H), 7.49 (d, 2H), 6.85 (d, 2H), 6.49 (s, 1H), 4.91 (m, 8H), 4.21 (m, 3H), 3.98 (m, 3H), 3.62 (m, 36H), 3.36 (m, 3H), 3.06 (m, 2H), 2.19 (m, 4H), 1.77 (t, 2H), 1.24 (m, 21H). LC-MS: (m/z) Found $[M+1]^+$ = 973.66 (calcd for $C_{49}H_{91}N_5O_{14}$ = 973.58

1.4 Synthesis of Some Intermediates

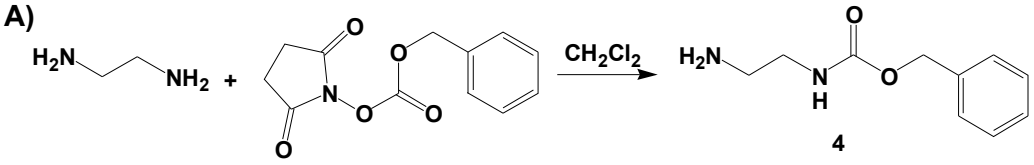

Scheme 4. Synthesis of (2-Amino-ethyl)-carbamic acid benzyl ester **(4).**

(2-Amino-ethyl)-carbamic acid benzyl ester (4). To a solution of ethylene diamine (0.96 mol, 64 ml) in dichloromethane (100 ml), at 5 °C, N-(Benzyloxycarbonyloxy) succinimide (9 g, 36 mmol) was added dropwise over 4 h. Stirring was continued for further 2 h, and then overnight at RT. The resulting mixture was washed with solution of $NaHCO_3$ (2 times), Na_2SO_4 (1 time), dried over anhydrous Mg_2SO_4 and concentrated in vacuo. Diethyl ether was poured into the reaction flask, where di-substituted ethylenediamine precipitated and the product remains suspended in the solution. The precipitate was filtered off to remove the by-product and the rest of the solvent was evaporated to obtain the product **4** (50 %). ^{1}H NMR ($CDCl_3$, 300 MHz): δ 7.45-7.15 (m, 5H), 5.87 (s, 1H), 5.06 (s, 2H), 3.51-3.04 (m, 3H), 2.82-2.63 (t, 1H), 1.95 (s, 1H), 1.74 (s, 1H).

B)

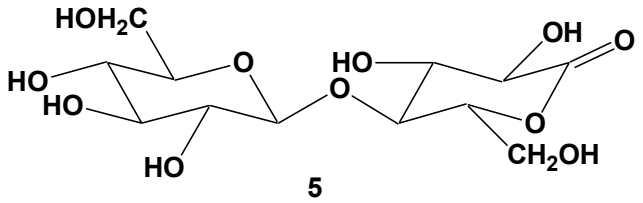

5

Scheme 5. Synthesis of Lactonolactone **(5) (*291*)**.

Lactonolactone (5). (using procedure described in literature) Lactose-monohydrate (12 g, 33 mmol) was dissolved in water (9 ml), diluted with methanol (25 ml) and added to an iodine (17.1 g) solution in methanol (240 ml) at 40 °C. Then, 4 % KOH solution in methanol (400 ml) was added dropwise for 35 min with continuous stirring until the colour of iodine disappeared. After cooling down of solution in ice bath, the precipitated crystalline product was filtered, washed with cold methanol (150 ml) and then cold ether (150 ml) and recrystallized from a mixture (800 ml) of methanol and water (9/1, v/v). The resulting potassium lactonate was then converted to the free acid by passing the aqueous solution through a column of Amberlite IR-120B. The acidic elude was collected and concentrated in vacuo. Repeated evaporation of methanol and ethanol solution converted the lactonic acid into lactonolactone (**5**) (12 g).

C)

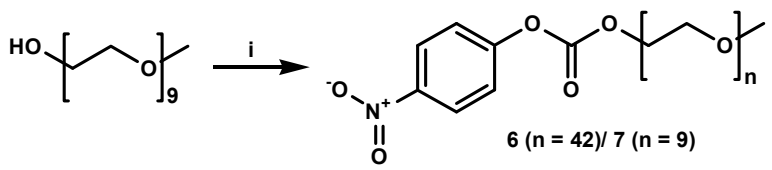

Reagent: (i) 4-nitrophenyl chloroformate, pyridine, CH_2Cl_2, 24 h.

Scheme 6. Synthesis of activated PEG **(6 and 7) (*292*).**

Carbonic acid 2-methoxy-ethyl ester 4-nitro-phenyl ester (6/7). (using procedure described in literature) Pyridine (1.28 ml, 16.0 mmol) was added to a solution of Poly-(ethylene glycol) monomethyl ether (4 g, 2.10 mmol), with a peak MW of 1900, in 40 ml of CH_2Cl_2 followed by addition of 4-nitrophenylchloroformate (1.6 g, 8.0 mmol). The reaction mixture was stirred at room temperature overnight and then precipitated into 400 ml of diethylether two times. The product was dissolved in benzene, pyridinium salts were filtered off, and the resulting solution was precipitated again into diethylether to provide 1.5 g of **(6)** as a white powder.

The same protocol was applied to activate Poly-(ethylene glycol) monomethyl ether (2 g, 5.7 mmol) with a peak MW of 350. But it seems that it is less polar than PEG with MW 1900, so that it did not precipitate in ether. Therefore, after solvent removal it was purified by column chromatography using pure ethyl acetate then CH_2Cl_2/MeOH 95/5 to provide 1.0 g of **(7)** as a yellow film. ^{1}H NMR ($CDCl_3$, 300 MHz): δ 8.28 (d, 2H), 7.39 (d, 2H), 4.43 (t, 2H), 3.81 (t, 2H), 3.64 (m, 31H), 3.54 (t, 2H), 3.37 (m, 3H).

2. *Fluorescent Probes*

2.1 Ethidium Bromide

Ethidium bromide (EtBr) is an intercalating agent commonly used as a nucleic acid stain in molecular biology for agarose gel electrophoresis (Figure 2.1). It exhibits a bright fluorescence upon DNA binding, while its fluorescence intensity is quite low in free-state (*293*).

In our studies, EtBr was used to stain DNA in gel electrophoresis and to study DNA condensation within the bolaplexes. EtBr shows a strong decrease in the fluorescence signal, due to its exclusion from DNA intercalation site, upon DNA condensation. For ethidium bromide (EtBr) exclusion assay, an aliquot of CT-DNA (final concentration 20 μM) was added to the solution of EtBr (final concentration 0.4 μM) in 20mM MES buffer at various pH. After 2 min, increasing quantities of the corresponding bola were added from stock solutions and fluorescence intensity was recorded at 600 nm (excitation at 520 nm) 2 min after each addition.

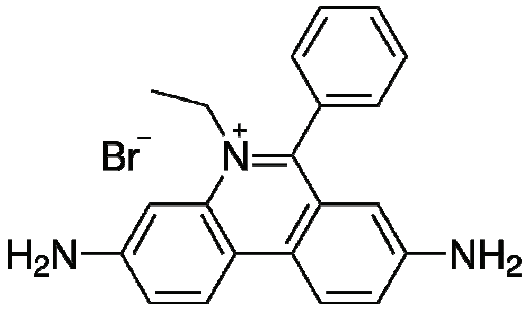

Figure 2.1. Chemical structure of **EtBr** (Ex: 520 nm).

2.2 1,8-ANS

1-Anilinonaphthalene-8-Sulfonic Acid (Figure 2.2) exhibits high binding affinity to the hydrophobic surfaces of proteins. This dye is poorly fluorescent in water while its fluorescence intensity increases significantly upon binding to low polarity regions of a protein surface. These properties make 1,8-ANS well suited for determining the affinity of hydrophobic ligands to their corresponding binding proteins (*294-296*).

In this study, 1,8-ANS was used to investigate the critical aggregation concentration (CAC) of bolas. Increasing quantities of bola aliquot was added to the solution of 1,8-ANS (50 nM) in 20mM MES buffer at various pH. Fluorescence intensity was recorded at 460 nm (excitation at 375 nm) 2 min after each addition.

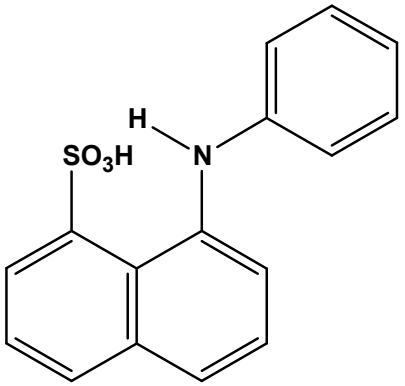

Figure 2.2. Chemical structure of **1,8-ANS** (Ex: 375 nm).

2.3 YOYO-1

YOYO-1 (Molecular Probes, Invitrogen) is a polycyclic +4 cationic bis-intercalator (Figure 2.3). It is a dimer of the nucleic acid stain oxazole yellow and is virtually non-fluorescent in the absence of DNA (*297*). The dimeric cyanine dye exhibits high affinity for nucleic acids, with binding constants between 10^{-10} and 10^{-12} M and forms highly fluorescent complexes with double-stranded DNA, with a fluorescence enhancement of 100-1000 fold.

In this study, YOYO-1 labeled DNA was used to follow the intracellular pathway of bolaplexes by confocal microscopy. For this purpose, YOYO-1 was added to the solution of DNA in milli-Q using molar ratio of 1:50 for YOYO-1/DNA phosphate and vortexed overnight in dark at 4 °C.

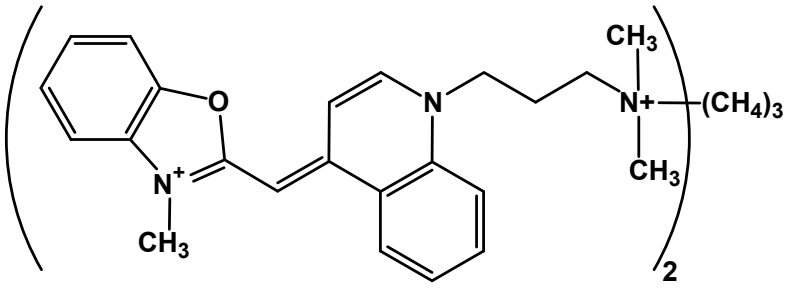

Figure 2.3. Chemical structure of **YOYO-1** (Ex: 480 nm).

3. Plasmids

3.1 Amplification and Purification

The pCMV-Luc (Figure 2.4, 5581 bp) encodes the photinus pyralis luciferase gene under the control of the cytomegalovirus promoter (provided by Dr. Guy Zuber).

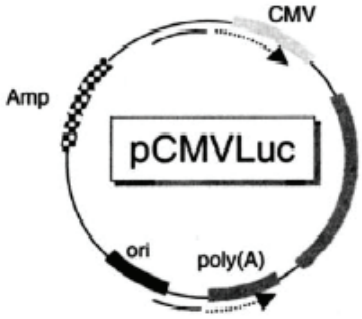

Figure 2.4. Map of pCMV-Luc plasmid (*298*).

A single colony of E. coli was picked from a freshly streaked selective plate and was inoculated to a starter culture of 5 ml Luria Bertani (LB) medium containing 100 μg/ml ampicillin. Incubation was done for about 8 h at 37 °C with vigorous shaking at

220 rpm. The starter culture 1/500 to 1/1000 was then diluted into selective LB medium. The bacteria were further grown at 37 °C for 12-16 h with vigorous shaking (220 rpm). Purification of the plasmids was performed using Plasmid Purification Kit (Invitrogen) The obtained DNA pellet was dried and suspended in TE buffer (included in the kit), followed by its quantification using UV-absorbance spectroscopy. For this purpose, 5 µl DNA stock was diluted in 800 µl Milli-Q and absorbance (OD) was recorded at 260 nm and 280 nm

DNA purity was estimated using the protocol from kit, according to which the extracted DNA is reasonably clean of proteins (if $A_{260}/ A_{280} \geq 1.8$) and this was further confirmed by gel electrophoresis.

3.2 Determination of the Plasmid Concentration

The DNA concentration was determined by absorption spectroscopy, using an extinction coefficient of 6600 M^{-1} cm^{-1} at 260 nm.

DNA (µM) = (A_{260} x dilution factor)/extinction coefficient

The plasmid integrity was checked by electrophoresis on 0.9 % agarose gel (*293*).

4. Preparation of Vector/DNA Complexes

4.1 DNA Complexes with Bolas (bolaplexes)

The complexes of bolaamphiphiles with calf thymus DNA (CT-DNA, Sigma) or pDNA (pCMV-Luc plasmid) were prepared by mixing equal volumes of DNA and bola in 20 mM MES buffer at various pH.

For this preparation, bola stock (20 mM, prepared in DMF and water mixture at various ratios depending on bola solubility) was first diluted in 20mM MES buffer at required concentration and pH. This diluted stock was then added to equal volume of DNA solution in the same buffer. The obtained complexes were used after 30 min of incubation at RT. The final DNA (phosphate) concentration was kept constant, while the

bola concentration was varied to obtain the final N/P ratio. The N/P ratio between bola and DNA was expressed as the molar ratio between all the protonable amino groups of the bola and the phosphate groups of the DNA, respectively.

4.2 DNA Complexes with Bola:DOPE (1:1)

In some formulations, DOPE (1:1 molar ratio with respect to bola) was used as a helper lipid. For this purpose, a mixture of DOPE and bola in ethanol was evaporated in a round bottom flask to obtain a film. Then, MES buffer was added and the samples were hydrated overnight at RT. Later, the samples were vortexed vigorously for 1 min and further sonicated in an ultrasonic bath for 15 min. The obtained suspensions were mixed with an equal volume of pDNA in the buffer to obtain a desired N/P ratio. The obtained complexes were used after 30 min of incubation at RT.

4.3 DNA Complex with jetPEI

jetPEI (PolyPlus) is a powerful reagent that ensures effective and reproducible DNA and oligonucleotide transfection into mammalian cells. It is mainly composed of a linear polyethylenimine and has been shown to provide higher *in vitro* transfection when compared to other agents based on cationic lipids and polymers.

The overall positive charge of the JetPEI/DNA complexes is crucial for efficient transfection. To obtain positively charged complexes, an N/P>3 is required. In order to calculate the N/P ratio, following formula was used, taking into account the volume of JetPEI reagent used for a given amount of DNA.

N/P ratio = 7.5* x µl of JetPEI / 3 x µg of DNA

2 µl JetPEI and 30 µM of DNA were diluted separately in 150 mM NaCl to a final volume of 50 µl each. The solution was vortexed briefly. Then, the JetPEI solution was added to the DNA solution followed by immediate vortex and 30min incubation at RT.

5. Physical Measurements

5.1 Absorption Spectroscopy

Absorption spectra were recorded on a double-beam spectrophotometer Cary 4000 (Varian). The absorbance is characterized by:

$$A = \log(I_0/I)$$

where I_0 and I are the incident and transmitted intensities, respectively.

A correction for the cuvettes also should be done, because the two cuvettes are never perfectly identical. To this end, the baseline of the instrument is first recorded (with both cuvettes filled with the solvents). Then, the DNA/dye is added into the solvent of the sample cuvette and the true absorption spectrum is recorded.

5.2 Steady-State Fluorescence Spectroscopy

Steady-state fluorescence measurements were performed on FluoroMax-3 (Jobin Yvon) or Fluorolog (Jobin Yvon) spectrofluorimeters, which are both a photon counting devices with a linear response in the range of measurements (< 3 Mcps). The source of light is a xenon lamp of 450 watts in fluorolog and 150 watts in fluoromax-3. The correction of the excitation beam is performed with a calibrated photodiode. The wavelength-dependent correction functions for the excitation-emission monochromators and for the photomultiplier response is defined by the manufacturer and is incorporated into the FluoroMax-3 and Fluorolog softwares. The fluorescent spectra are automatically corrected by these calibration functions.

5.3 Dynamic Light Scattering Measurements

Dynamic Light Scattering (DLS) is a technique used for measuring the particle size typically in a sub-micron region. It is based on the principle of Brownian motion and relates this to the size of the particles. Brownian motion is the random movement of particles due to their collision by the solvent molecules that surround them. Normally DLS is concerned with measurement of particles suspended within a liquid. The larger the particle, the slower the Brownian motion will be. Smaller particles are "kicked" further by the solvent molecules and move more rapidly.

The diameter that is measured in DLS is a value that refers to how a particle diffuses within a fluid so it is referred to as a hydrodynamic diameter. The diameter which is obtained by this technique is the diameter of a sphere that has the same translational diffusion coefficient as the particles. The size of the spherical particle is calculated from the translational diffusion coefficient by using the Stokes-Einstein equation:

$$d(H) = \frac{kT}{3\pi\eta D}$$

where:

d (H) = hydrodynamic diameter

D = translational diffusion coefficient

k = Boltzmann's constant

T = absolute temperature

η = viscosity

In a dynamic light scattering instrument, a laser is used as the light source to illuminate the sample cells. For dilute concentrations, most of the laser beam passes through the sample, but some get scattered by the particles within the sample at all angles. In common device, a detector measures the scattered light at 90°. The scattering intensity signal from the detector is processed by a correlator and then analysized by a computer to derive the size information.

Intensity, Volume and Number Distributions

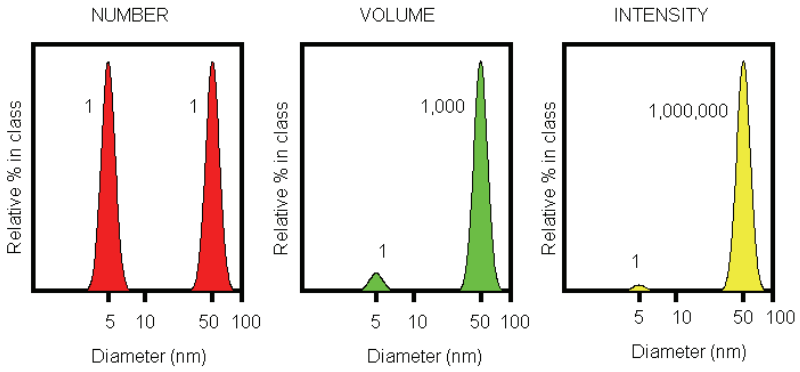

Figure 2.5. Number, volume and intensity distributions of a bimodal mixture of 5 nm and 50 nm lattices present in equal numbers.

A very simple way of describing the difference between the intensity, volume and number distributions is to consider a sample that contains only two sizes of particles (5 nm and 50 nm) but with equal numbers of each size particle (Figiure 2.5).

In number distribution, the two peaks are of the same size (1:1) as there is equal number of particles. While for the volume distribution, the area of the peak for the 50 nm particles is 1000 times larger the peak for the 5 nm (1:1000 ratio). This is because the volume of a 50 nm particle is 1000 times larger that the 5 nm particle (volume of a sphere is equal to $4/3\Pi(r)^3$). Intensity distribution shows that the area of the peak for the 50 nm particles is now 1,000,000 times larger the peak for the 5 nm (1:1000000 ratio). This is because large particles scatter much more light than small particles (the intensity of scattering of a particle is proportional to the sixth power of its diameter (Rayleigh's approximation). In general terms: d(intensity) > d(volume) > d(number).

The basic distribution obtained from a DLS measurement is the intensity and all other distributions are generated from this.

The average size of the bolaplexes was determined with a Zetasizer Nano ZS (Malvern Instruments, Paris, France) with the following specifications: sampling time, 30 s; medium viscosity, 0.8872 cP; refractive index (RI) medium, 1.33; RI particle. 1.59; scattering angle, 90° and temperature, 25 °C. The bolaplexes were prepared as discussed in section 4.1, however the final DNA concentration used was 20 μM. All experiments

were performed using 500 µl of the final volume after 30 min incubation at room temperature.

5.4 Zeta Potential Measurements

The zeta potential is a physical property which characterizes any particle in suspension, and is of importance to optimize the formulations of suspensions and emulsions.

The liquid layer surrounding a particle can be divided into two parts: an inner region (Stern layer), where the ions are strongly bound, and an outer (diffuse) region where the ions are less firmly associated. Within the diffuse layer, the ions and particles form a stable entity. The potential at this boundary (surface of hydrodynamic shear) is the zeta potential (Figure 2.6).

The magnitude of the zeta potential gives an indication of the potential stability of the colloidal system. If all the particles in suspension have a large negative or positive zeta potential then they will tend to repel each other and there will be no tendency for the particles to aggregate. However, if particles have a zeta potential value around zero, then there will be no force to prevent the particles coming together and flocculating. The general dividing line between stable and unstable suspensions is generally taken at either +30 or -30 mV. Particles with zeta potentials more positive than +30 mV or more negative than -30 mV are normally considered stable.

The zeta potential is related to the electrophoretic mobility by the Henry equation:

$$U_E = \frac{2\varepsilon z f(ka)}{3\eta}$$

Where:

U_E = electrophoretic mobility of the particles

z = zeta potential of the particles

ε = dielectric constant of the medium

η = viscosity of the medium

$f(\kappa a)$ = Henry's function

In a zeta potential measurement system, a laser is used as the light source which splits to provide an incident and reference beam. When an electric field is applied to the sample cell, any particles moving through the measurement volume will cause the intensity of light detected to fluctuate with a frequency proportional to the particle speed. This information is processed by a digital signal processor and a computer.

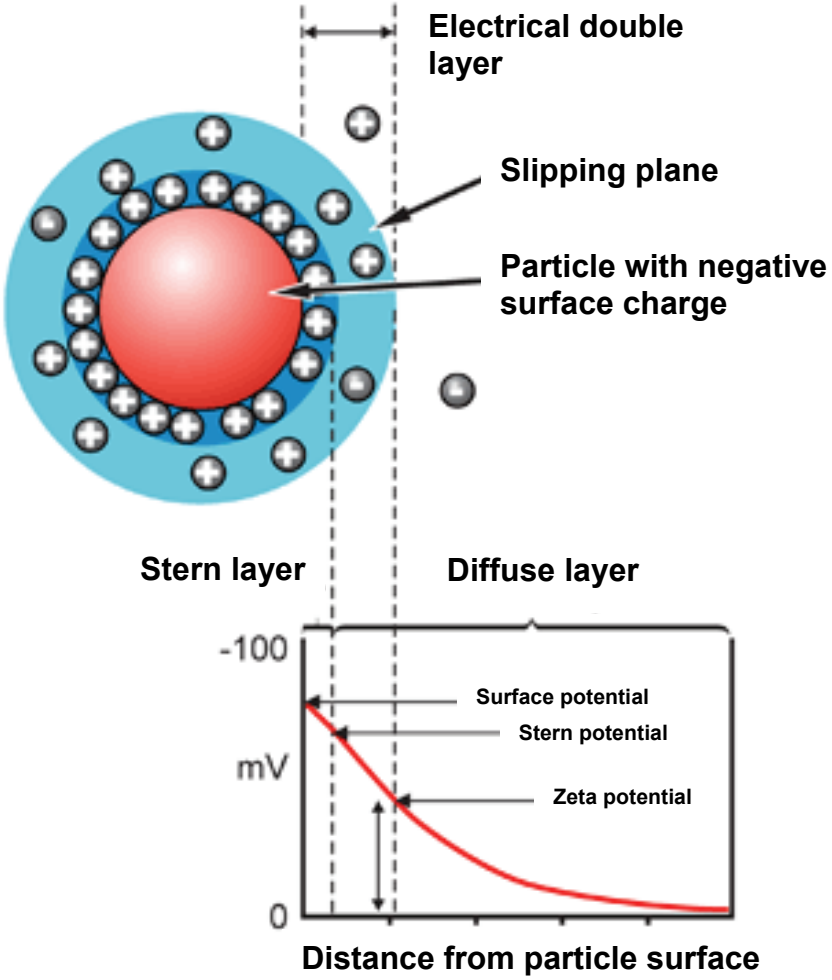

Figure 2.6. Schematic representation of zeta potential.

The zeta potential of the bolaplexes was measured with the following specifications: sampling time, 30 s; medium viscosity, 0.8872 cP; dielectric constant, 78.5 and temperature, 25 °C. The bolaplexes were prepared using CT-DNA as discussed in section 4.1, however the final DNA concentration used was 30 µM. All experiments were performed using 1000 µl of the final volume after 30 min incubation at room temperature.

5.5 Confocal Laser Scanning Microscopy

Optical sectioning of cells was realized using a BIORAD confocal microscope. The system was equipped with a Kr/Ar laser. All observations were carried out with Zeiss LSM 510 microscope using a X40/1.4 oil immersion objective and with 0.4 μm *z*-section intervals. Emitted light was detected with two photomultipliers through selected band pass filters in specific wavelength bands by the Leica spectral detection system.

The intracellular trafficking of the bolaplexes was monitored by confocal microscopy. For these studies, pDNA was labeled with YOYO-1 (*299*). All experiments were performed in liquid conditions at room temperature on an ibidi dish (μ-Dish35mm, ibiTreat, Biovalley). YOYO-1 fluorescence was detected with excitation at 488 nm and an emission band pass filter 506-538 nm (green) (*146*). The intracellular pathway of the complexes was followed by incubating labeled bolaplexes with *HeLa* cells for different time at 37 °C.

5.6 Atomic Force Microscopy (AFM)

Atomic force microscope (AFM) (Figure 2.7) provides a 3D profile of the surface on a nanoscale by measuring forces between a sharp probe (<10 nm) and surface at very short distance (0.2-10 nm probe-sample separation). The probe is supported on a flexible cantilever. The AFM tip "gently" touches the surface and records the small force between the probe and the surface. Attractive or repulsive forces resulting from interactions between the tip and the surface show a positive or negative bending of the cantilever. The bending is detected by means of a laser beam, which is reflected from the back side of the cantilever. The advantages of AFM compared to, for example, electron microscopy are the ease of sample preparation and the possibility to image sample in native conditions in buffer.

AFM measurements were performed using a Solver-Pro-M (NT-MDT) instrument. The measurements were done in 20 mM MES buffer at various pH, using the tapping mode (37 kHz). Cantilevers were NSG03 (NT-MDT). The samples were prepared as for DLS measurements. Then, 100 μL of solution was deposited on the freshly cleaved mica. In some cases, Mg^{2+} ions (*ca* 10 mM) were added to trigger interaction between the bolaplexes and the negatively charged mica surface.

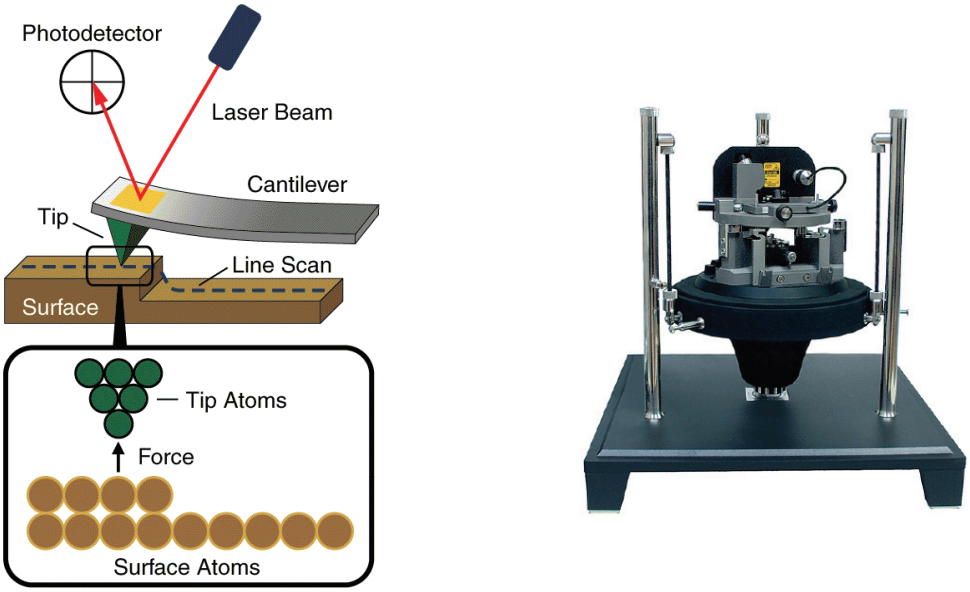

Figure 2.7. AFM: Schematic presentation and Solver-Pro-M (NT-MDT) instrument.

6. *Agarose Gel Electrophoresis*

Agarose gel electrophoresis is used in biochemistry and molecular biology to separate DNA, RNA or protein molecules according to their size. This is achieved by applying an electric field to the gel matrix. The negatively charged DNA fragments are repelled by the negative electrode and attracted by positive electrode. Small molecules move faster and migrate further than larger ones. Molecular weight markers are used to estimate the size of DNA fragment.

The bolaplexes were prepared at different N/P ratios using 60 μM pDNA followed by 30 min incubation at RT. 4 μl of loading dye (6x) was added to 20 μl of the prepared complexes and then 12 μl of this mixture was loaded on 0.9 % agarose gel prepared with 0.5x TAE (Tris-acetate-ethylenediaminetetraacetic acid) buffer. Electrophoresis was carried out with 0.5x TAE buffer at a constant voltage of 100 mV. DNA bands were visualized by UV transilluminator (GeneGenius Imaging System, SYNGENE) after coloration with ethidium bromide (0.5 μg/ml) for 15 min.

7. Cell culture and transfection

7.1 General Conditions and Cell Lines

Dubelcco's modified Eagle medium (DMEM), Opti-MEM, Phosphate-Buffered Saline (PBS) and Penicillin-streptomycin were purchased from Gibco-Invitrogen while Fetal bovine serum (FBS) from Lonza. 75 cm^2 cell culture flasks and 24-well culture plates were purchased from NUNC. The cell lines used for experiments were: HeLa, Cos-7 and HepG2.

Cells were grown in Dulbecco's modified Eagle's medium, supplemented with 10 % fetal bovine serum and 1 % penicillin-streptomycin (complete growth medium) at 37 °C in a humidified atmosphere containing 5 % CO_2. The density of cells seeded in 24-well plates containing complete growth media was: Cos-7 cells – 1 x 10^5 cells/well; HeLa cells – 4 x 10^4 cells/well; HepG2 cells – 8 x 10^4 cells/well.

7.2 Luciferase Assay

The luciferase gene expression was quantified using the Promega's Luciferase Assay System. Light is produced by converting the chemical energy of luciferin oxidation through an electron transition, forming the product molecule oxyluciferin. Firefly luciferase, a monomeric 61 kDa protein, catalyzes luciferin oxidation using $ATP{\cdot}Mg^{2+}$ as a co-substrate.

The luciferase test was performed in the following way. Cells were seeded at above mentioned density, 24 h before transfection. Then, the medium was removed and cells were washed 1 time with PBS (1x). 100 µl of bola-pDNA (1 µg pDNA/well) complexes at different N/P ratios were added to the cells containing 400 µl Opti-MEM or complete growth medium for serum-free and with-serum experiments respectively, followed by 3 h incubation at 37 °C. Chloroquine (100 µM) or DOPE (1:1 equivalent of bola) was used to enhance transfection efficiency in some experiments. For chloroquine addition, an aliquot (final concentration 100 µM) of its stock solution (10 mM in 20 mM MES buffer pH 7) was added to the cells before addition of the complexes. After 3 h, 500 µl of DMEM containing 20 % of FBS was added and cells were harvested for another 21 h. However, for samples with chloroquine, the media was completely replaced with 1 ml of fresh complete growth medium. For 48 h transfection, media was replaced with complete growth media after 24 h of incubation, while for 24 h check cells were preceded directly for luciferase assay.

Luciferase gene expression of lysed cells was quantified using a commercial kit (Invitrogen) and a luminometer (CentroXS^3 LB 960, BERTHOLD Technologies). Before this measurement, the media was removed and cells were washed 3 times with PBS (1x). Then 100 µl of 1x lysis reagent (diluted in Milli-Q from 5x stock) was added to each well followed by 2 min of strong vortex and 30 min incubation at RT. The lysed cells were transferred into eppendorfs and vortexed at 13000 rpm for 6 min. 10 µl of the supernatant was transferred to a 96-well plate from each eppendorf for luminometer measurement (jetPEI sample need to be diluted 10 times before transferring to this plate). Results were expressed as relative light units integrated over 10 s per mg of cell protein lysate (RLU/mg of protein).

7.3 Protein Assay

The bicinchoninic acid (BC) assay is a colorimetric assay, involving the reduction of Cu^{2+} to Cu^{+} by the peptide bonds of proteins. The BC Assay chelates Cu^{+} ions with very high specificity to form a water soluble purple coloured complex. It quantifies the immobilized proteins, for example cells adhering to plates. The reaction should be read at defined time and temperature conditions since the purple coloured copper BC assay complex will continually develop. However, the development is slow enough to allow the processing of numerous samples. The reaction is measured from the optical absorbance of the final Cu^{+} complex at 562 nm. Absorbance is directly proportional to the protein concentration, which is then calculated with a reference curve obtained for a standard protein.

Practically, 15 µl of cell lysate was mixed with 1 ml of BC Assay (A/B = 50:1, A contains bicinchoninic acid; B contains copper (II) sulphate). Then the solutions were incubated at 60 °C for 30 min. All the samples were cooled down to room temperature and the optical absorbance (OD) was measured at 562 nm against the blank (15 µl 1x lysis buffer + 985 µl BC Assay reagent) using Carry 4000 spectrophotometer. Finally, the protein concentration is interpolated from ODs using calibration curve.

For calibration curve, bovine serum albumin (BSA) standard for protein assay (Interchim) was used. 15 µl of 1x lysis buffer was mixed with 1 ml of BC Assay in 6 eppendorfs and then BSA was added to each of them in increasing quantitites (0, 4, 8, 12, 16 and 20 µg respectively) followed by 30 min incubation at RT. Absorbance (OD) was recorded at 562 nm against the blank (15 µl 1x lysis buffer + 985 µl BC Assay reagent) using Carry 4000 spectrophotometer. Finally, calibration curve was plotted for OD_{562} Vs BSA Concentration (µg) and linear regression data was obtained by its linear fit.

7.4 MTT Assay (Cell Viability)

Cytotoxicity of bolas was evaluated using 3-(4,5-dimethyl-2-thiazolyl)-2,5-diphenyltetrazolium bromide (MTT, Sigma-Aldrich) assay. Cells were seeded in 24-well plate and after 24 h of incubation at 37 °C supplemented with bolas, at different concentrations in serum-free Opti-MEM. After incubation for 3 h at 37 °C, 10 % of FBS was added and cells were harvested for another 45 h. Then, the cells were washed with Phosphate Buffer Saline (PBS) and incubated with serum free medium containing 0.5 mg/ml MTT for 3 h at 37 °C. At this step, the yellow MTT is reduced to purple formazan in living cells (Figure 2.8).

Finally, the media was discarded and the obtained formazan crystals were re-suspended in 0.5 ml MTT solvent (Sigma-Aldrich). Absorbance of formazan solution was measured at 570 nm with respect to the background at 690 nm using Cary 4000 spectrophotometer. Viability was expressed as relative absorbance (%) of the sample vs. control cells.

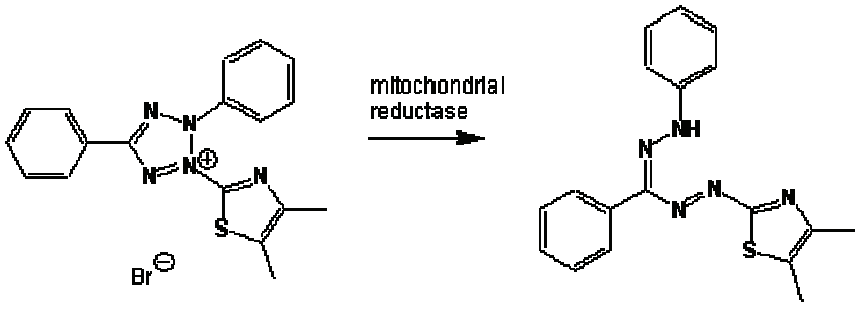

Figure 2.8. Schematic representation of MTT reduction into formazan.

Research Aim

Bipolar amphiphiles, which are the analogues of lipids presenting polar groups at the two opposite sides of the hydrophobic chain(s), called bolaamphiphiles (bolas), have progressively gained importance in recent years because of their ability to provide supramolecular nanostructures. A remarkable feature of bolas is that they can form highly stable monolayer membranes due to presence of membrane-spanning hydrophobic chains, in contrast to bilayer membranes formed by lipids. One of the interesting applications of bolas, which is still in its infancy stage, is gene delivery. In this respect, unsymmetrical bolaamphiphiles bearing positively charged and neutral headgroups could be an attractive alternative to the cationic lipids based vectors.

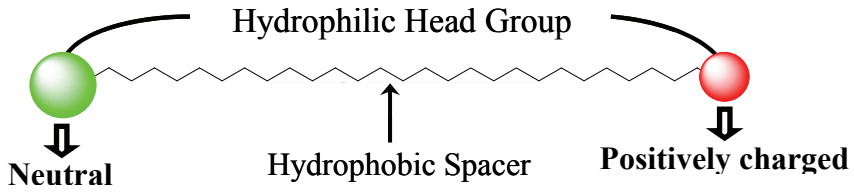

Figure 1.33. Molecular model of bolaamphiphiles.

These molecules could generate asymmetric membranes (in form of vesicles or nanotubes) having positively charged inner and neutral outer surfaces. In such a case, the inner membrane surface can be used to wrap the DNA molecule, while the outer neutral membrane surface, being inert to DNA, would prevent further oligomerization of the complex and could be utilized for efficient exposure of the biological signal for specific targeting.

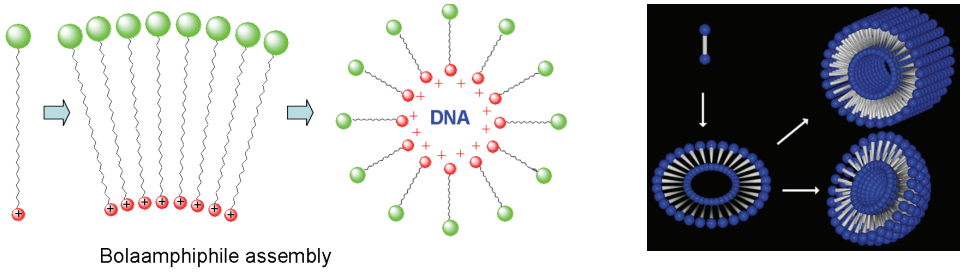

Figure 1.34. Molecular model of bolaamphiphile assembly.

The aim of the presented work was to develop new gene delivery vectors based on bolaamphiphiles capable of forming supramolecular nanostructures hosting a DNA molecule and characterized by the neutral external surface. For this purpose a variety of unsymmetrical bolaamphiphiles bearing cationic and neutral headgroups were synthesized; their self-assembly with DNA was characterized by a variety of instrumental techniques and, finally, the transfection efficiency and cytotoxicity of their bolaplexes was evaluated *in vitro*.

Results and Discussion

1. **First Generation Bolas:** bearing mono-cationic and sugar headgroups

Design and Synthesis

The basic design of bolas is based on a positively charged group and a neutral group connected by a long hydrophobic spacer. Sugar residues, being biocompatible and relatively inert, were used as neutral headgroups while amines were used as cationic headgroups for binding DNA. Different hydrophobic linkers were used in order to optimize hydrophobic, H-bonding and π-stacking interactions on the level of the hydrophobic spacer.

Based on this design, five unsymmetrical bolaamphiphiles were synthesized (Fig. 3.1), bearing either a mannoic or a gluconic acid residue as neutral headgroup and a mono-cationic ammonium group as positively charged headgroup, connected by different hydrophobic linkers: (a) a mono-peptide composed of end-substituted amino acid of 12-carbon atoms, **M-C12-EDA** and **G-C12-EDA**; (b) a dipeptide composed of end-substituted amino acids of 8- and 12-carbon atoms, **M-C8-C12-EDA** and **G-C8-C12-EDA**; (c) a tri-peptide composed of end-substituted amino acids of 6-, 8- and 12-carbon atoms, **M-C6-C8-C12-EDA**.

This design of bolas should force them to assemble in a parallel fashion forming unsymmetrical membranes by favouring intra-molecular hydrogen bonding, where the two opposite sides of the monolayer membrane present different functional groups (Fig. 3.2).

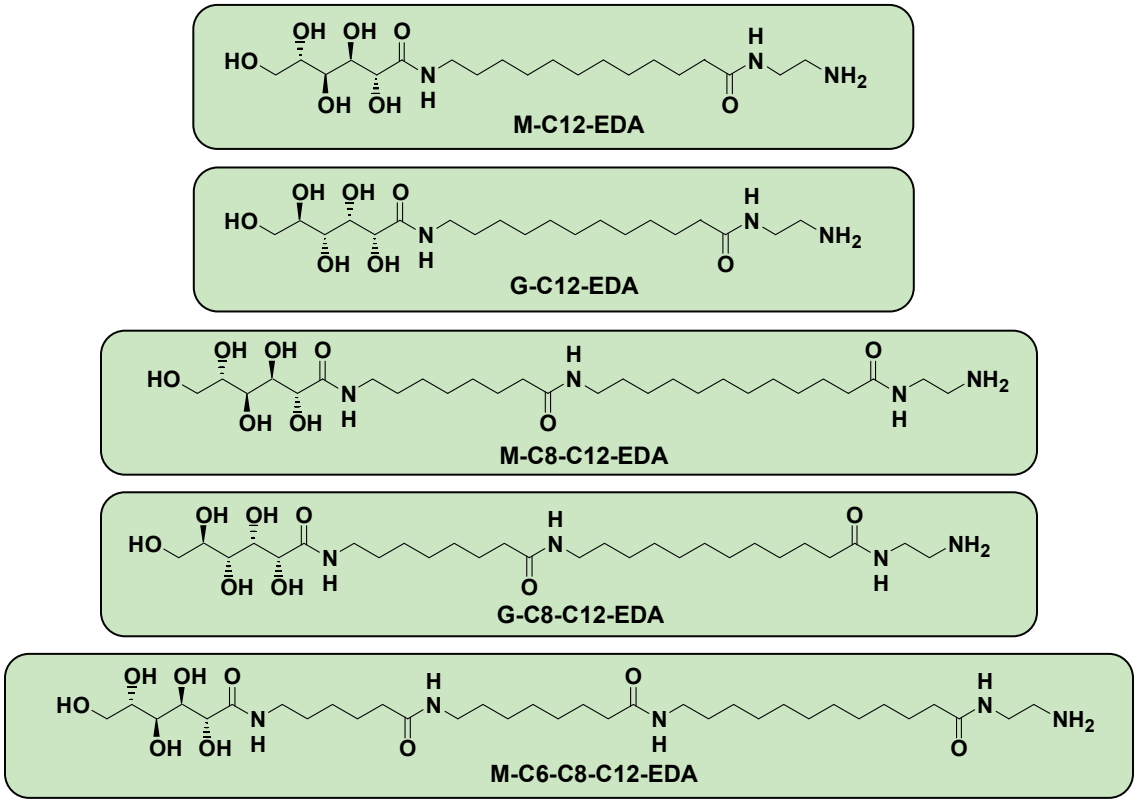

Figure 3.1. Chemical structures of 1st generation bolas.

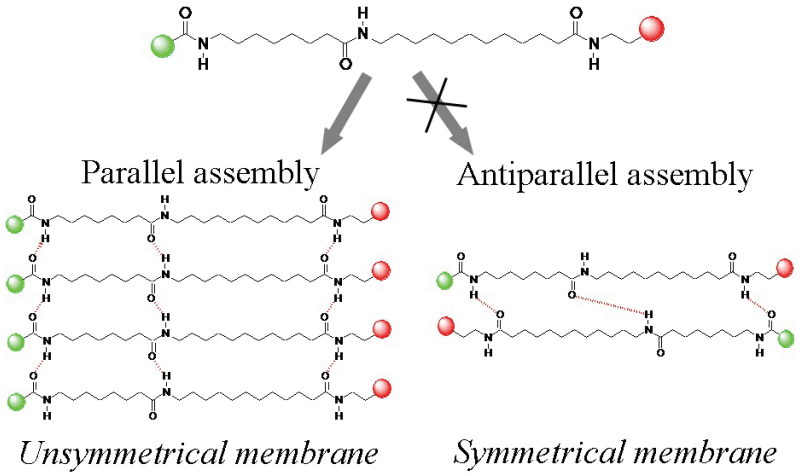

Figure 3.2. Schematic presentation of membrane formation by the assembly of designed bolas.

An example of synthesis of **M-C8-C12-EDA** is presented in Scheme 1.1. Initially, the amino group of 8-aminooctanoic acid was protected with Boc-group (**1A**) and the acid group of 12-aminododecanoic acid was protected with methyl ester (**1B**). Then, the two obtained protected compounds (**1A** and **1B**) were coupled (**1C**) followed by ester hydrolysis and Boc removal. The amino group in the obtained conjugate **1D** was reacted with L-mannoic-γ-lactone and the hydroxyl groups in the sugar conjugate **1E** were protected by acetylation. The latter was then substituted with N-Boc-ethylenediamine followed by deacetylation and Boc-removal, affording final bola **M-C8-C12-EDA**. The yields of the individual steps were systematically >50 % and the obtained final bolas in 100-200 mg quantities were sufficiently pure according to NMR, LC-MS and HPLC techniques.

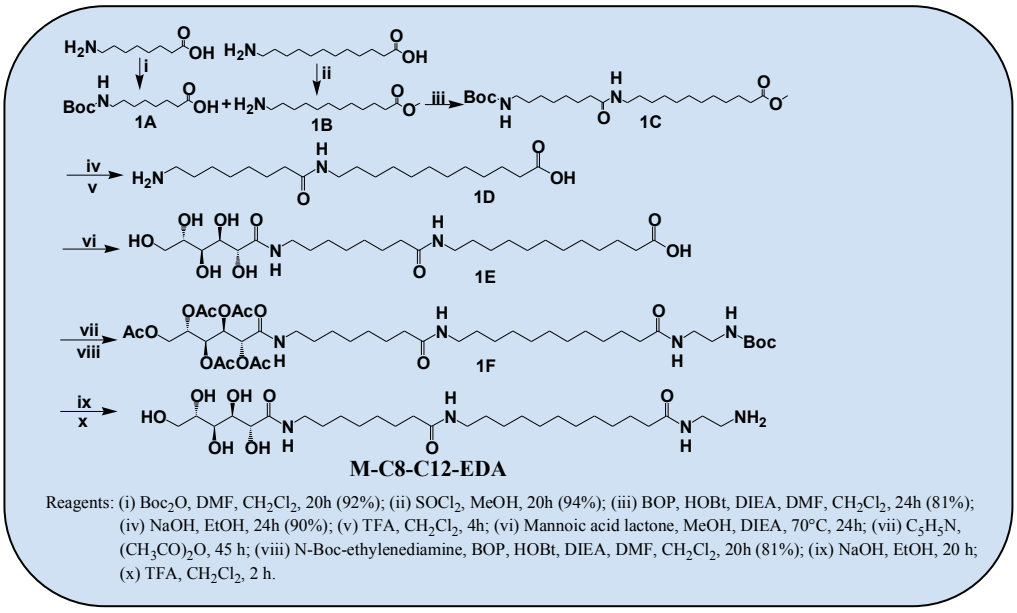

Scheme 1.1. Synthesis of **M-C8-C12-EDA**.

Characterization of Self-Assembly and Interaction with DNA

The obtained bolas were poorly soluble in water. As a general trend, gluconic acid bolas were better soluble in water than mannoic acid bolas. The larger solubility of gluconic-bolas is probably connected with larger space taken by its hydroxyl groups (*300*). Moreover, the solubility decreased with increase in the length of the hydrophobic spacer. Due to the poor solubility of bolas in water, their stock solutions were prepared in DMF. Our first approach of sample preparation was based on direct addition of bola aliquot from the stock solution into 20 mM MES buffer at various pH. The self-assembly of bolas using this approach was first characterized by atomic force microscopy (AFM) in liquid (buffer) phase on a mica surface. It was observed that **M-C8-C12-EDA** and **M-C6-C8-C12-EDA** form spontaneously monolayers on the mica surface at pH 6 (Fig. 3.3a and b respectively). The observed height of the monolayers was close to the lengths of the corresponding molecules, i.e. 3.5 and 4 nm for **M-C8-C12-EDA** and **M-C6-C8-C12-EDA**, respectively. These results suggest that bolas pack together perpendicularly to the mica surface. Within these monolayers, bola molecules self-assemble in a parallel fashion, resulting in unsymmetrical membranes where positive headgroup of the bola interacts to the negatively charged mica surface. The monolayer formation is probably supported by hydrophobic interactions as well as by hydrogen-bonding (Fig. 3.3c), which should favour the hypothesized parallel bola packing. However, **M-C12-EDA** showed fibrous (or tubular) structures (Fig. 3.3d). Absence of membrane structure in this case is probably due to the effect of short hydrophobic chain length. Thus, this approach of direct addition of the unsymmetrical bolas, bearing positively charged and neutral headgroups, generated asymmetric membranes in form of monolayers or fibrous structures.

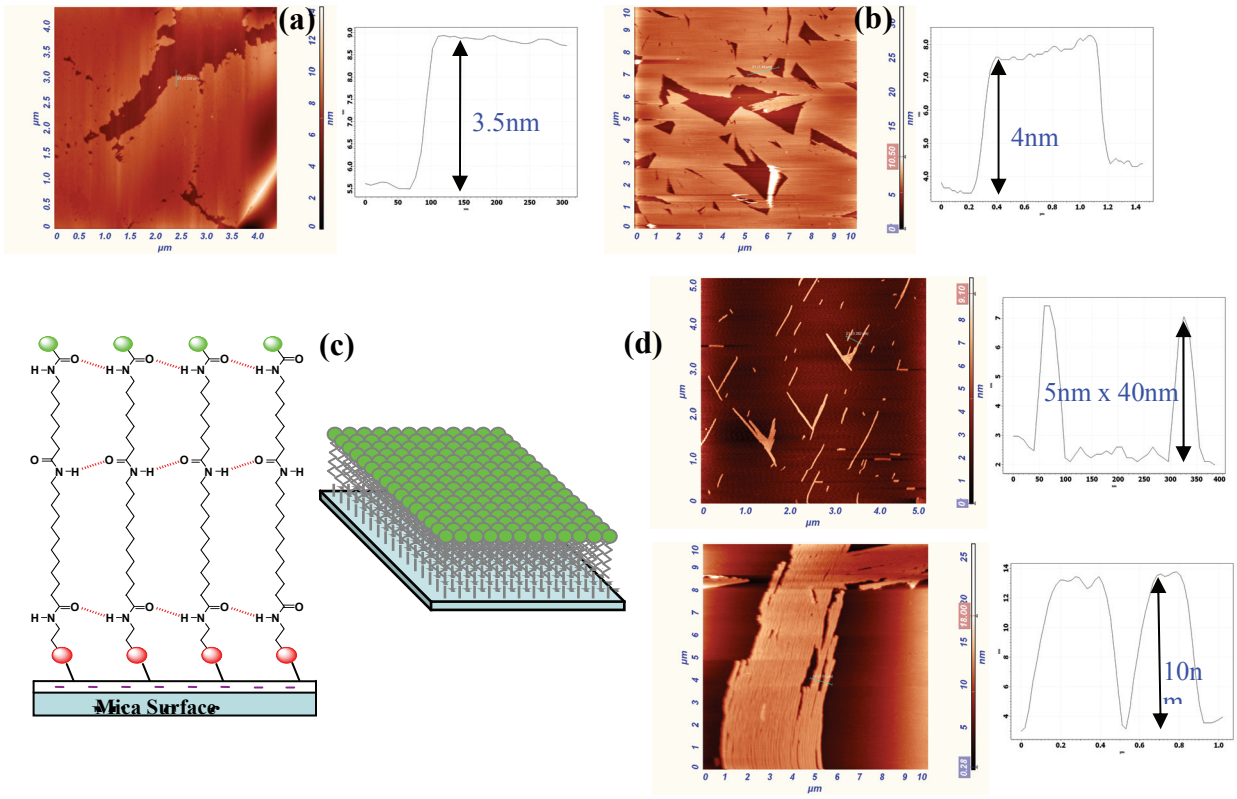

Figure 3.3. AFM images of bolas self-assembly at 100 µM on mica surface, by direct addition of bola stock to MES buffer (pH 6). a**) M-C8-C12-EDA** form 3.5 nm high monolayer , b) **M-C6-C8-C12-EDA** form 4 nm high monolayer, c) Model of bola assembly for monolayer formation , d) **M-C12-EDA** form fibrous structures (or flattened nanotubes on the mica surface), around 5 nm high and 40 nm wide.

To determine the size of the structures formed by bola-assembly in solution, we performed dynamic light scattering (DLS) measurements with **M-C8-C12-EDA,** using the same approach for sample preparation. These studies showed a continuous increase in size with time (Fig. 3.4), indicating that this preparation leads to formation of infinite large structures.

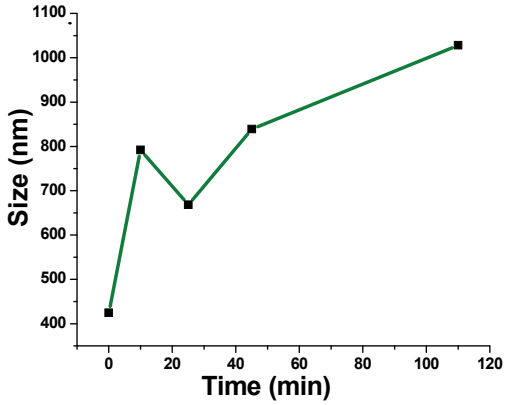

Figure 3.4. DLS data of **M-C8-C12-EDA** at 60 μM with time, prepared by direct addition of bola stock to aqueous buffer (pH 6).

Therefore, due to the observed continuous bola aggregation, this approach of direct addition cannot be efficient for preparation of small nanostructures and compact complexes with DNA. Thus, an alternative methodology of sample preparation was designed for further studies. In this new approach, dry film of the bola stock was prepared in an eppendorf tube, then suspended in 20 mM MES buffer at pH 7 and kept at 100 °C for 20 min. Finally, the samples with and without DNA were prepared by diluting the hot stock solution in cold buffer.

Samples prepared by this new method were first characterized by DLS. These studies showed particle size of <300 nm for most of the bolas. The only exception was M-C8-C12-EDA showing larger particles (*ca* 700 nm). Importantly, the size of bola nanostructures was relatively stable, indicating that this preparation was more appropriate. However, the presence of CT-DNA at N/P 5 (Fig. 3.5) did not modify the size of the nanostructure, thus suggesting that these bolas do not interact with DNA or DNA does not change bola assembly.

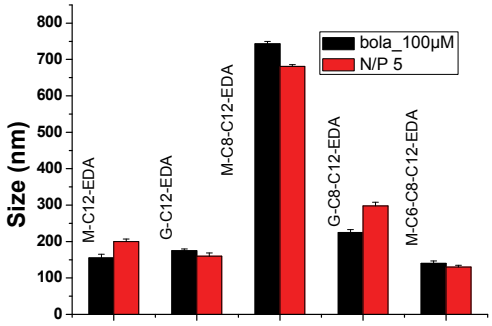

Figure 3.5. DLS data of 1st generation bolas (100 μM) and bolaplexes (N/P 5) in aqueous buffer (pH 7). The final DNA (phosphate) concentration was 20 μM.

According to AFM measurements on the mica surface, **M-C12-EDA** formed short fibers (or flattened tubes) of ~ 200 nm width and height twice that of the bola molecule, while **G-C12-EDA** and **M-C6-C8-C12-EDA** formed desecrate monolayer islands (Fig. 3.6 a1, b1 and c1, respectively). The only exception was **M-C8-C12-EDA** showing continuous network on the surface (Fig. 3.6 d1). Observation of discrete structures on the mica surface for other bolas suggests that some relatively small structures were initially formed in solution, before their deposition on the mica surface. This conclusion is in line with observation of small nanostructures by DLS for all bolas, except **M-C8-C12-EDA**. The obtained results suggest that the second method of preparation allows better control of assembly of bola molecules. However, since all the structures observed by AFM were flat, we assume that the negatively charged mica surface could destroy the native positively charged nanostructures of bolas, originally formed in the solution.

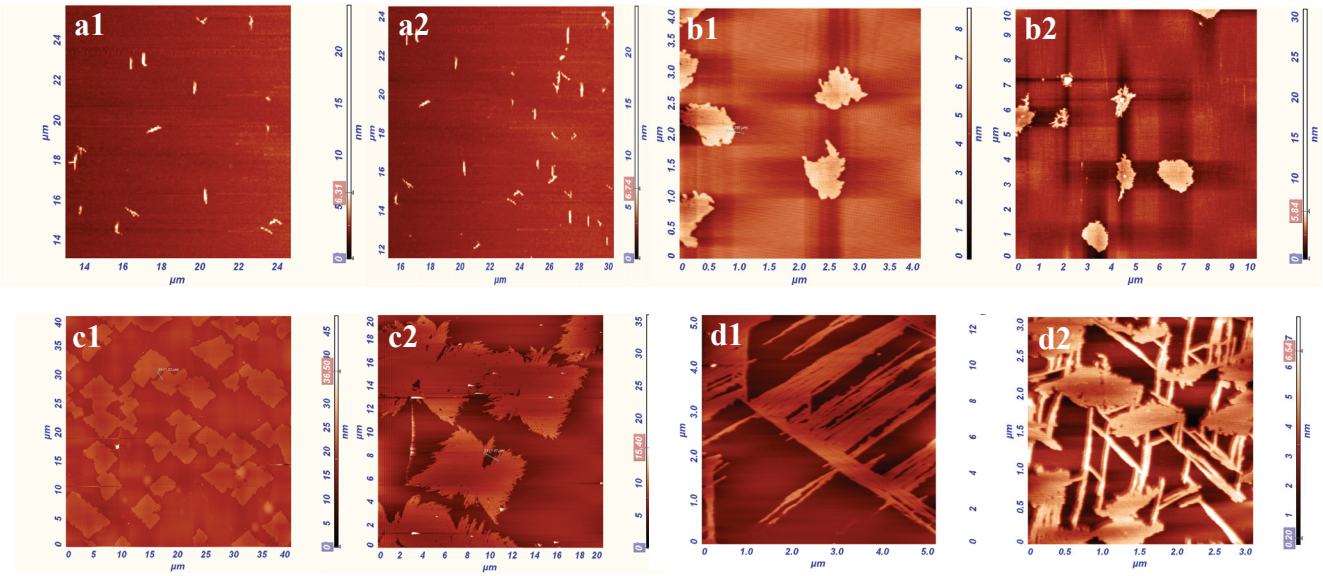

Figure 3.6. AFM images of: a) **M-C12-EDA**, b) **G-C8-C12-EDA**, c) **M-C6-C8-C12-EDA** and d) **M-C8-C12-EDA**; where 1 represent bola alone (100 µM) and 2 represent bolaplexes at N/P 5. Images were obtained by tapping mode. The final DNA (phosphate) concentration was 20 µM.

In addition, we studied assembly of **M-C8-C12-EDA** by film hydration method at pH 11. At this pH, amino groups should not be protonated, which may modify significantly the assembly. Indeed, we found that in these conditions **M-C8-C12-EDA** forms fibrous structures of about ~ 30 nm diameter and 4 nm height according to AFM (Fig. 3.7a). We presumed these fibers as nanotubes being flattened by mica due to the strong electrostatic interactions. To verify the assembly of bola without mica surface we used electron microscopy. We found that **M-C8-C12-EDA** form sheets or nanotubes of about 30 nm diameter (Fig. 3.7b). These observations confirm that this bola is able to form membrane structures. Moreover, these membrane structures can form (with relatively low yield) nanotubes. This nanotube formation is commonly known to occur in two steps, (i) the formation of intermediate bilayer ribbons in solutions through the morphological change of vesicles in a cooling process and (ii) coiling of the solid bilayer ribbon into an open helix, which eventually closes to yield nanotubes by widening of the tape width and maintaining a constant helical pitch (*258*) (Fig. 3.7c).

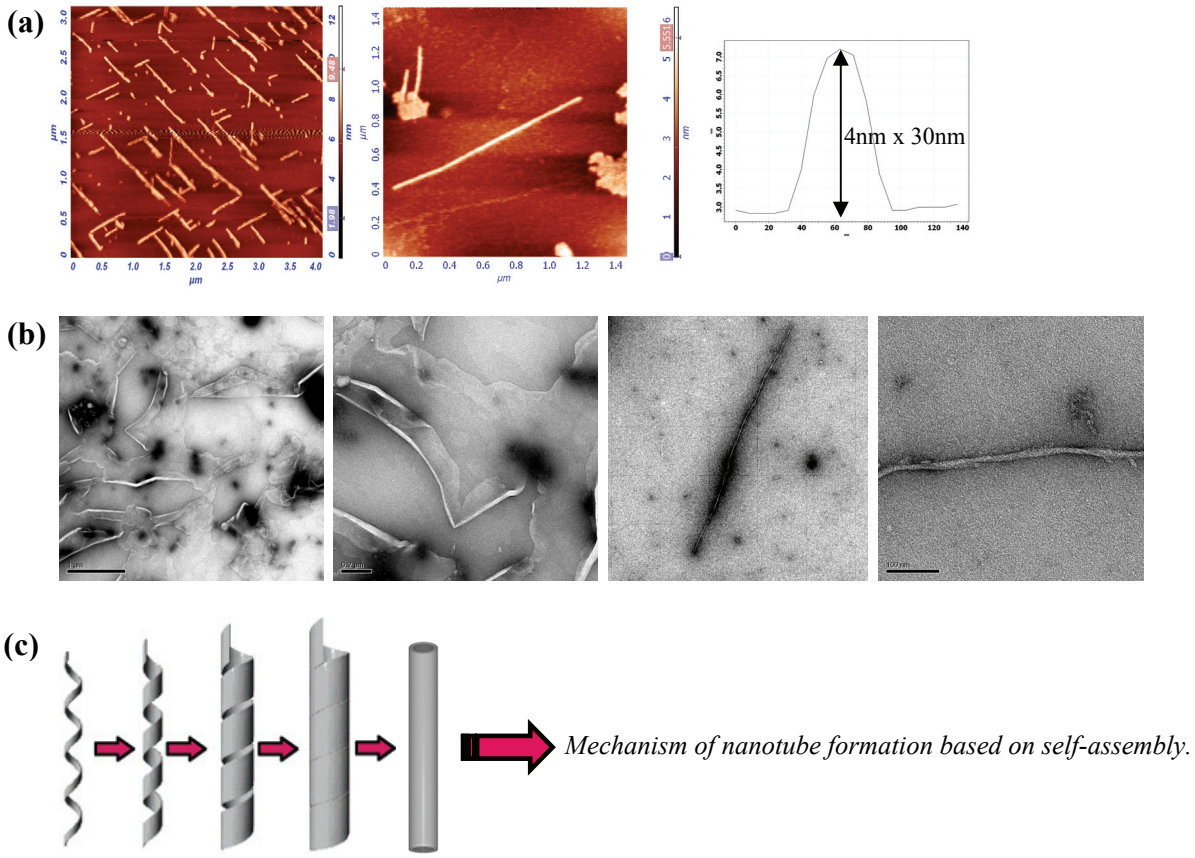

Figure 3.7. M-C8-C12-EDA (30 µM) assembly in aqueous buffer (pH 11) (a) AFM images showing fibrous structures (or flattened tubes) of 30 nm width and 4 nm height, (b) Electron microscopy images showing sheets and nanotubular strcuture of 30 nm diameters, and (c) Schematic presentation of nanotube formation based on self-assembly.

Then, the samples prepared in the presence of calf thymus DNA (CT-DNA) were characterized at pH 7.0. However, as it can be seen from figures 3.6 a2, b2 and c2, the presence of DNA did not change the morphology of bola nanostructures. The change in morphology in the presence of DNA was observed only for **M-C8-C12-EDA**, though the observed structures were polymorphic (Fig. 3.6d). In addition to the fibers of 3.5 nm height and 60 nm width, some complex structures consisting of fibers with varying width, 300-600 nm, were also observed, thus correlating well with the observed large polydisperse structures seen in our DLS measurements.

To further verify the interaction of **M-C8-C12-EDA** with DNA, gel electrophoresis technique was used. It is visible from figure 3.8, that **M-C8-C12-EDA** form complexes with firefly luciferase plasmid DNA (pDNA) only at very high N/P ratios (ratio between cationic groups of bola and phosphate groups of DNA), i.e. ~ 20, indicating rather poor interaction between this bola and DNA.

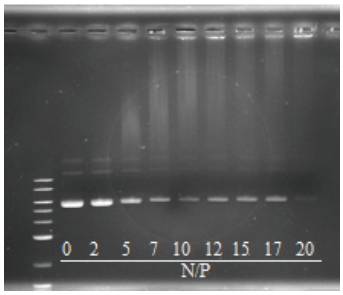

Figure 3.8. Agarose gel electrophoresis (0.9 %) of **M-C8-C12-EDA** complexed with pDNA at different N/P ratios. Band on the left of the gel correspond to 10 kb DNA ladder. The final pDNA (phosphate) concentration was 60 μM, while the bola concentration was varied to obtain the final N/P ratio.

Transfection Efficiency and Cytotoxicity

We performed cellular studies only with **M-C8-C12-EDA** as it showed some interaction with DNA, among the various synthesized bolas. However, we observed no transfection in HeLa cells after 24 or 48 h, when analysed by luciferase assay. This result was further verified by confocal microscopy imaging. It was observed that **M-C8-C12-EDA** complexed with YOYO-1 stained pDNA do not internalize after 4 hrs of incubation in HeLa cells, despite their binding to cell surface (Fig. 3.9a). However, complexes of the commercial transfection agent, jetPEI, with same stained pDNA showed internalization within the same incubation time (Fig. 3.9b).

Finally, we characterized cytotoxicity of **M-C8-C12-EDA**, which was estimated from the total cellular protein measured after transfection with bolaplexes (Fig. 3.9c). The obtained results indicated relatively small cytotoxicity of the bolaplexes, which is much lower than that of jetPEI.

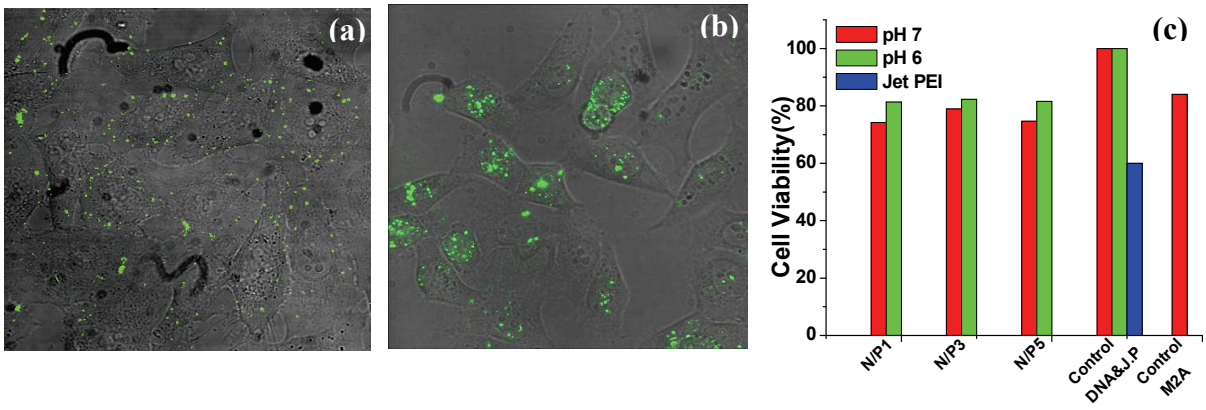

Figure 3.9. (a) Confocal fluorescence image of **M-C8-C12-EDA** complexes with YOYO-1 stained pDNA at N/P 5 after 4 h incubation, (b) Confocal fluorescence image of jetPEI complexes with YOYO-1 stained pDNA after 4 h incubation, and (c) Total protein concentration from the transfection experiments in HeLa cells for **M-C8-C12-EDA** bolaplexes. Data were normalized to 100% for the control non-treated cells. Cells were incubated in serum-free Opti-MEM with a bolaplex composed of plasmid DNA (1 μg per well) at different N/P ratios. After 3 h, the transfection medium was replaced with fresh complete culture medium, and cells were cultured for an additional 45 h. Then cells were lysed and the total protein was estimated using BC assay.

Conclusions

Five new bolaamphiphiles, bearing sugar and cationic headgroups connected by a hydrophobic spacer, were synthesized by multi-step organic synthesis. Due to poor solubility of these bolas in water, two approaches for sample preparation was explored: (1) direct addition of stock solution of bola in DMF into buffer and (2) preparation of bola film, followed by film hydration in the buffer. Self-assembly of bolas using method (1) was characterized by AFM. These studies revealed that some bolas self-assemble into 3-4 nm high monolayer membranes on mica surface, while others form fibers. However, according to DLS, nanostructures formed by method (1) in solution are unstable and grow continuously. In contrast method (2) gave more stable nanostructures, which were observed in AFM as flattened tubes, sheets or fibers. However, these bolas did not interact efficiently with DNA according to gel electrophoresis, AFM and DLS data. Finally, we observed no transfection of their DNA complexes with Luciferase encoding plasmid in HeLa cells, while the cytotoxicity was low.

These results prompted us to make modifications in bola structures in order to increase their solubility and achieve better interaction with DNA. One solution could be to increase the charge of the cationic headgroup. This modification would increase solubility of bolas and may favor their interaction with negatively charged DNA molecules.

2. **Second Generation Bolas:** bearing di-cationic and sugar headgroups

Design and Synthesis

To overcome the difficulties associated with 1st generation bolas, we substituted, as headgroup, the mono-cationic amino group by di-cationic amine residues in order to increase the total positive charge. Di-cationic amine residues should improve bolas affinity to DNA as well as their solubility in water. For this purpose, we selected ornithine and bis(3-aminopropyl)amine residues, featuring two positively charged ammonium groups separated by an appropriate carbon atom distance. The di-peptide, composed of end-substituted amino acids of 8- and 12-carbon, was used as hydrophobic spacer, because it provided the most promising results among all first generation bolas tested. Moreover, since the gluconic residue provided higher solubility to bola molecules than the mannoic one, the former was used as a neutral headgroup. In addition, to further increase the size and hydrophilicity, lactonic acid residue was also selected as a neutral group. This residue was also of interest because it may provide specificity to hepatocytes by receptor mediated pathway involving the asialoglycoprotein receptors on the hepatic (HepG2) cell surfaces (*52-54*). Based on this design, four bolaamphiphiles were synthesized: a) **Orn-C8-C12-G**, b) **Orn-C8-C12-L**, c) **DPTA-C12-C8-G** and d) **DPTA-C12-C8-L** (Fig. 3.10).

An example of synthesis of **Orn-C8-C12-G** is presented in Scheme 2.1. Initially, the amino group of **1C** (see scheme 1.1) was deprotected and substituted with Boc-protected ornithine. The obtained conjugate **2A** was further reacted with ethylene diamine giving **2B.** The latter was then reacted with D-gluconic acid δ-lactone followed by Boc-removal, affording final bola **Orn-C8-C12-G**. The yields of the individual steps were systematically >50 % and the obtained final bolas in 100-200 mg quantities were sufficiently pure according to NMR, LC-MS and HPLC techniques.

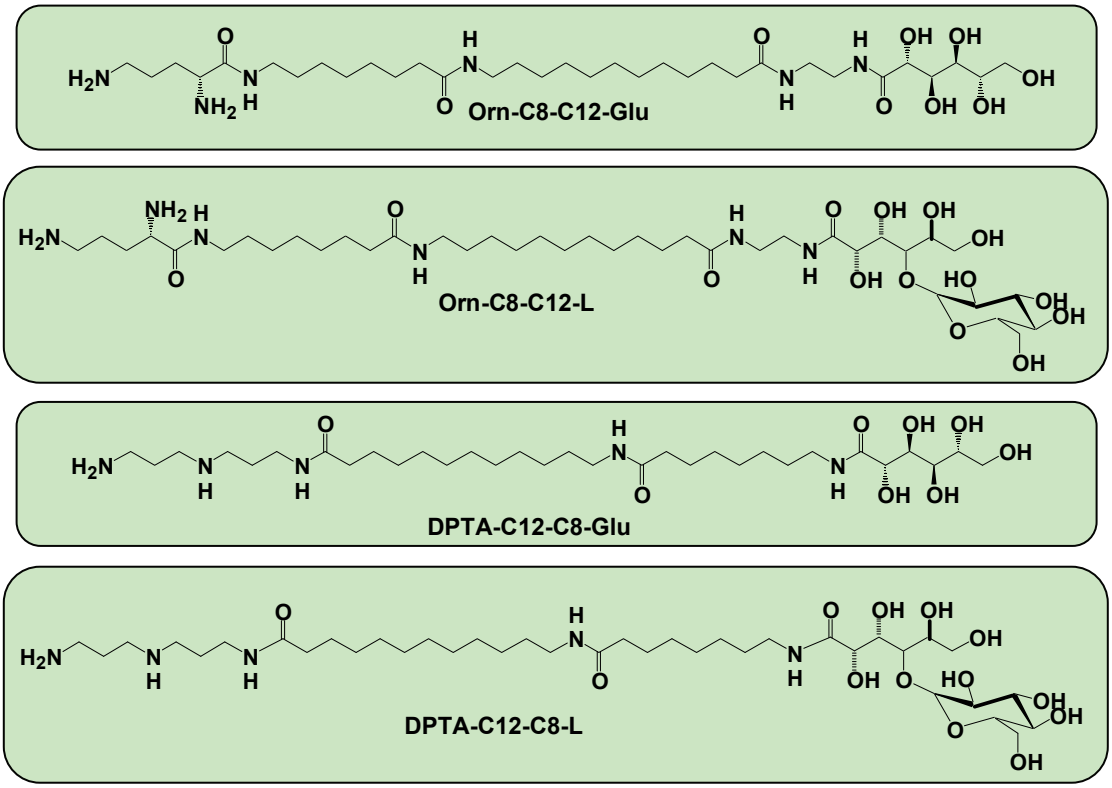

Figure 3.10. Chemical structures of the 2nd generation bolas.

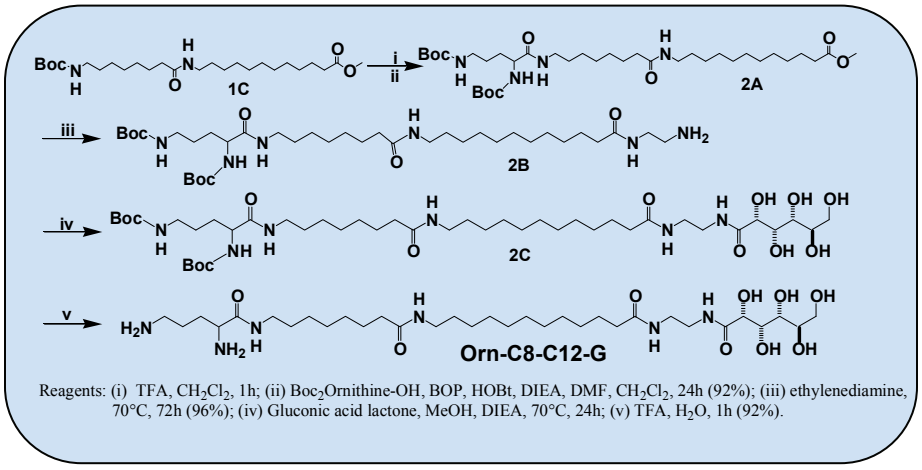

Scheme 2.1. Synthesis of **Orn-C8-C12-G**.

Structural Characterization and DNA Interaction Studies

Bolas of 2nd generation were presenting a significantly better solubility in water, as no any sign of precipitation was observed for bola concentrations up to 1 mM. Thus, additional cationic group increased strongly their solubility. Therefore, we used the previous first method of sample preparation, where stock solution of bola in organic solvent (DMF/water mixture) was directly added to the buffer. Gel electrophoresis was used to study the interactions of bolas with DNA. It was observed that lactonic-bolas do not form complexes with firefly luciferase plasmid DNA (pDNA) (Fig. 3.11 c and d). Moreover, gluconic-bola **DPTA-C12-C8-G** did not show complete complexation even at N/P 20, also suggesting a poor DNA interaction efficiency (Fig. 3.11a). **Orn-C8-C12-G** was the most promising bola to form complexes, but only at high N/P ratios (N/P ≥ 10), which indicates that even with this bola the affinity remains rather weak (Fig. 3.11b). By taking into account that all bolas molecules were bearing the same di-peptide hydrophobic spacer, the stronger interaction of **Orn-C8-C12-G** with DNA could probably be connected to lower hydrophilicity of its headgroups, which in turn favors their self-assembly and their cooperative interaction with DNA.

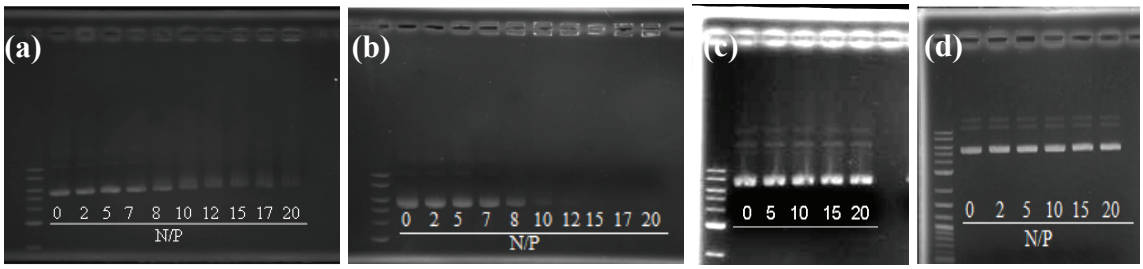

Figure 3.11. Agarose gel electrophoresis (0.9 %) of a) **DPTA-C12-C8-G**, b) **Orn-C8-C12-G**, c) **DPTA-C12-C8-L** and d) **Orn-C8-C12-L** complexed with pDNA at different N/P ratios. Band on the left of each gel corresponds to 10 kb DNA ladder. The final pDNA (phosphate) concentration was 60 μM, while the bola concentration was varied to obtain the final N/P ratio.

The observed poor DNA interaction of two gluconic bolas, **Orn-C8-C12-G** and **DPTA-C12-C8-G**, was further verified by ethidium bromide (EtBr) exclusion assay (Fig. 3.12). Upon DNA condensation, EtBr is expelled from its intercalation site, thus resulting in a strong decrease of its fluorescence intensity. Such a decrease in EtBr fluorescence was visible only above N/P ratio 20, which confirms a very weak interaction with DNA.

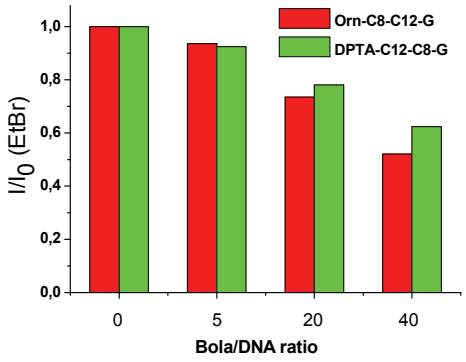

Figure 3.12. Exclusion of EtBr from CT-DNA complexed with bolas at different N/P ratios. The final DNA (phosphate) concentration was 20 μM.

Assembly of bolaamphiphiles was further characterized by DLS. It was observed that, without DNA, the bolas self-assemble to form structures of ~800 and ~ 400 nm sizes for gluconic and lactonic-bolas, respectively (Fig. 3.13). In the presence of DNA, the particle size did not change for N/P 5, confirming the absence of interaction with DNA as shown by gel electrophoresis. At N/P 10, some decrease in size was observed for most of the bolas (except Orn-C8-C12-L). The major problem occurring in these DLS measurements were a relatively low light scattering signal for samples either with or without DNA, so that the obtained size data were not so reliable. We assume that due to their high water solubility, the self-assembly without and with DNA for these compounds is rather poor. Then the DNA complexes, even if they are formed, are not very stable due to low binding affinity. This instability of complexes was further verified by zeta potential measurements. We observed a negative zeta potential for all the studied complexes (Fig. 3.13). Its value decreased with the increase of N/P ratio due to DNA charge compensation. Among the two tested bolas, **Orn-C8-C12-G** showed more efficient DNA negative charge compensation than **DPTA-C12-C8-G**, which is in line with its stronger interaction with DNA suggested by gel electrophoresis. It can be seen

that **Orn-C8-C12-G** was probably able to compensate DNA charge at N/P 10 resulting in complex formation, in line with the gel electrophoresis data.

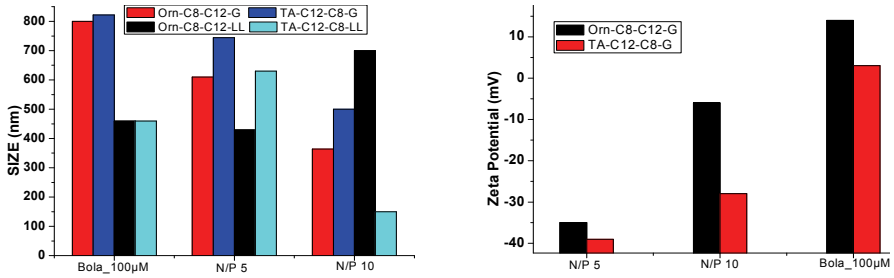

Figure 3.13. DLS and Zeta potential data of 2nd generation bolas (100 µM) and their complexes with DNA at different N/Ps in aqueous buffer (pH 7.4). The final DNA (phosphate) concentration was 20 µM for DLS measurements and 30 µM for zeta potential measuremetns

Despite of these negative results, we performed structural characterization of bola assembly by AFM in liquid (buffer) phase on a mica surface (Fig. 3.14). **Orn-C8-C12-G** alone resulted in spherical structures of 3-10 nm height and 50-100 nm diameter, while with DNA it formed larger particles of 50-100 nm height and 100-300 nm diameters. In contrast, **DPTA-C12-C8-G** did not show any assembly by itself, but showed spherical morphology in presence of DNA with 10-15 nm height and 100-150 nm diameter. These results suggested some interaction of these bolas with DNA. We assume that the negatively charged mica surface helps the bola self-assembly, and may fix some transient bola-DNA complexes at the surface.

Thus, according to our data, it is clear that the self-assembly of the second generation bolas is rather poor compared with bolas of the first generation, so that they could not form stable structures. Moreover, their ability to interact with DNA is also very weak. We assume that both results are related to the much higher solubility of the new generation bolas due to the additional cationic group. Indeed, the additional positively charged group probably shifted the hydrophobic-hydrophilic balance of the bolas towards high hydrophilicity, which drastically weakened the hydrophobic interactions between bolas and thus compromised their self-assembly. The latter should weaken the interactions with DNA, because the formation of cationic amphiphiles is a combination

of amphiphile-DNA and amphiphile-amphiphile interactions. For instance it is known, that cationic detergents form rather weak complexes with DNA, while cationic lipids or oligomeric detergents form highly stable DNA complexes (*301*).

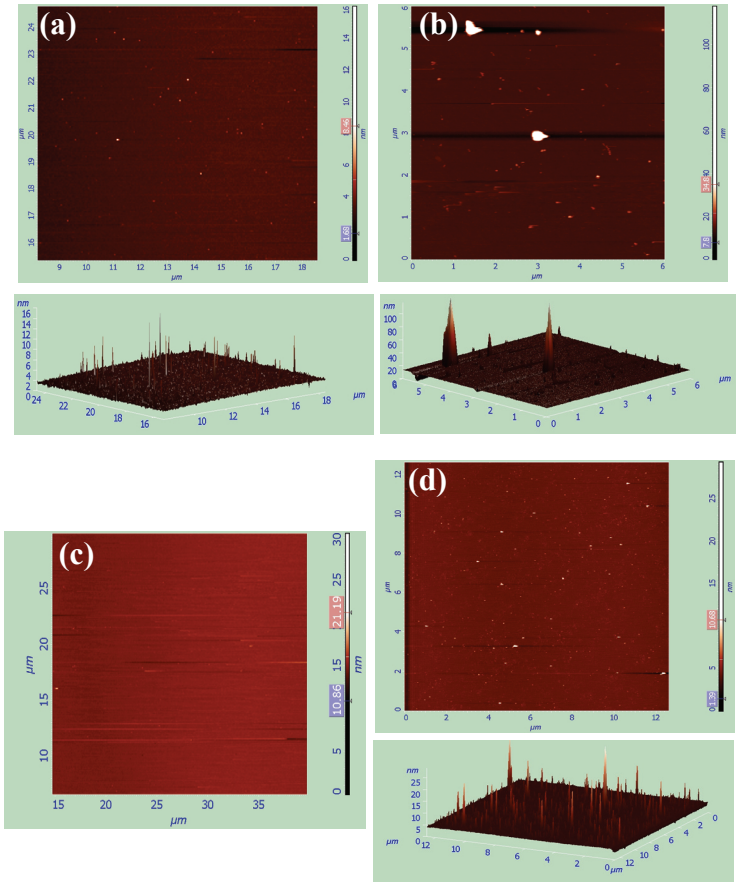

Figure 3.14. AFM images of: a, b) **O-C8-C12-G** (100 μM) and its complexes with DNA at N/P 5 respectively; c, d) **DPTA-C12-C8-G** (100 μM) and its complexes with DNA at N/P 5 respectively. Images were obtained by tapping mode in buffer (pH 7.4). The final DNA (phosphate) concentration was 20 μM.

Transfection Efficiency and Cell Viability

We analysed transfection efficiency of this generation bolas by using luciferase assay, and found no sign of transfection for the bolas, together with high cell viability (> 80 %), when studied in HeLa and COS-7 cell lines. This negative result was expected because of the too low affinity of bolas towards pDNA.

Conclusions

In the second attempt, we synthesized four new bolaamphiphiles which presented a significant improvement in their water-solubility due to additional cationic charge present in the amine headgroup. However, gel electrophoresis data clearly showed poor or even no interaction of bolas with DNA. Only one bola, bearing gluconic and ornithine headgroups showed some interaction with DNA at high N/P ratios (≥10). DLS and AFM studies suggested that the self-assembly of bolas is very poor compared to the bolas of first generation, which appears clearly connected to the additional cationic charge. Therefore, it is not surprising that no transfection was observed when studied in HeLa and COS-7 cells. Thus, due to their additional cationic group, bolas of second generation significantly improved their solubility, but lost their ability to self-assembly and kept a poor affinity to DNA.

These results indicated that the bolas structure need to be further improved in order to enhance DNA complexation. In this 2nd generation of bolas, the di-cationic positive charge might be efficient to bind DNA, but the highly polar amide group present in the hydrophobic spacer may decrease the hydrophobic interactions and thus prevent their self-assembly. Therefore, a further idea was to enhance hydrophobicity of the spacer by removing this amide group.

3. **Third Generation Bolas:** bearing di-cationic & sugar/PEG headgroups and varied hydrophobic spacer

Design and synthesis

Based on the conclusions from the 2nd generation bolas, we need to modify bola structure in order to enhance hydrophobic interactions which could result in better self-assembly and thus enhance DNA interaction efficiency. Considering these properties, bolas bearing either gluconic or lactonic neutral sugar residue and di-cationic ornithine headgroups were synthesized, where the hydrophobic spacer was modified to increase its hydrophobicity. In addition, sugar headgroup was substituted by polyethylene glycol (PEG) headgroup (350 and 2000 Da), which is also neutral, biocompatible and highly inert.

Based on this design, eight bolaamphiphiles were synthesized (Fig. 3.15), presenting different hydrophobic spacers: (a) a long alkyl chain of C20-carbon atoms, **Orn-C20-G** and **Orn-C20-L**; (b) a hydrophobic linker composed of an alkyl chain of C16-carbon atoms and an aromatic unit, **Orn-C16-G**, **Orn-C16-L**, **Orn-C16-PEG2000** and **Orn-C16-PEG350**; (c) a hydrophobic linker composed of an alkyl chain of C12- and C16-carbon atoms on 1,4- C-atoms of an aromatic unit, **Orn-C12-C16-G**; (d) two C16-carbon alkyl chains attached through an aromatic unit, **(2Glu-C16)-Orn**.

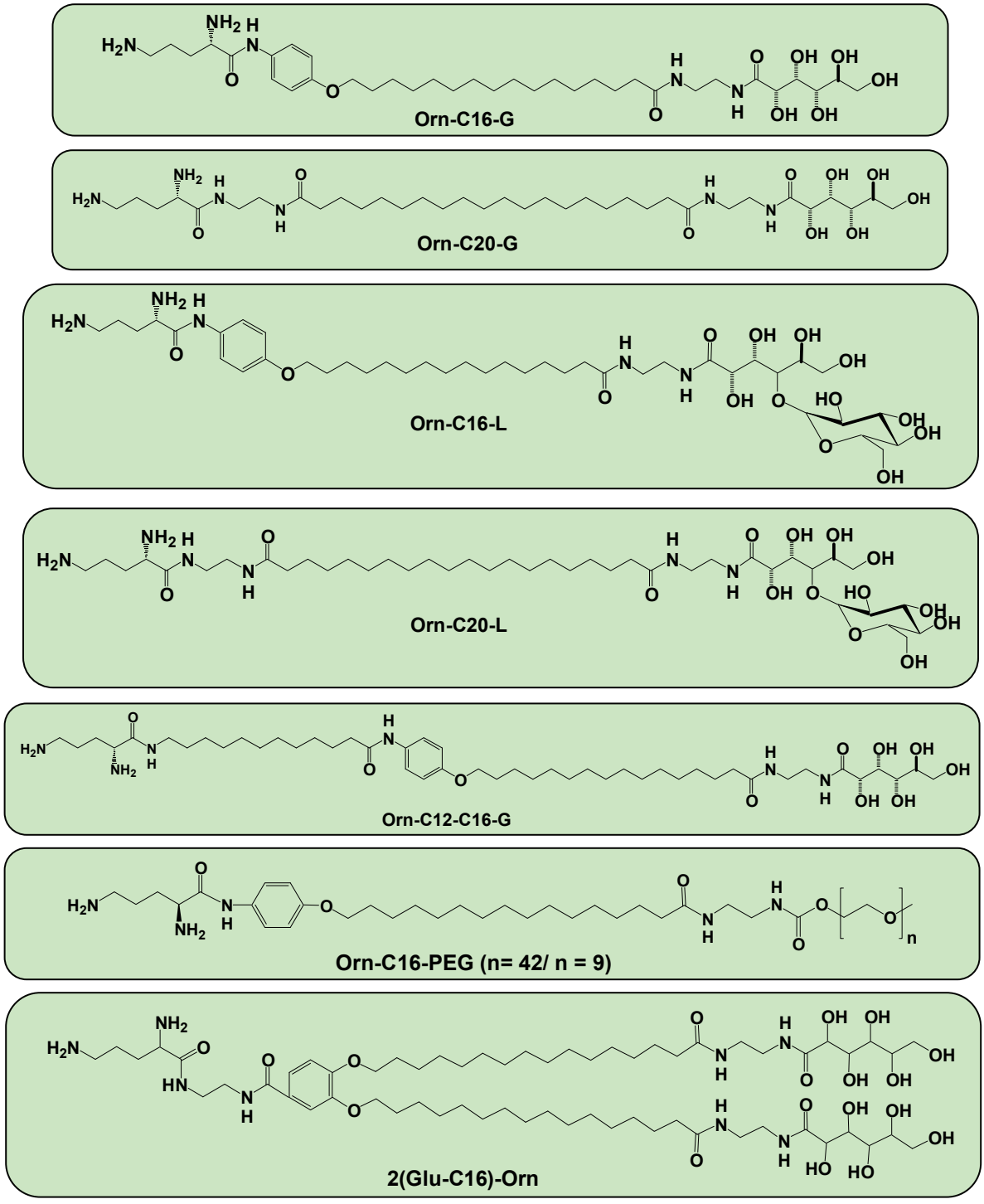

Figure 3.15. Chemical structures of 3rd generation bolas.

The examples of synthesis of **Orn-C16-G**, **Orn-C20-G**, **Orn-C12-C16-G** and **(2Glu-C16)-Orn** are presented below (Schemes 3.1, 3.2, 3.3 and 3.4 respectively). To obtain **Orn-C16-G**, initially, the amino group of 4-aminophenol was protected with Boc-group (**3A**) and its hydroxyl was further reacted with methyl 16-bromohexadecanoate. Then, the amino group in the obtained conjugate **3B** was further deprotected and substituted with Boc-protected ornithine. The obtained conjugate **3C** was further reacted with ethylene diamine giving **3D**. The latter was then reacted with D-gluconic acid δ-lactone followed by Boc-removal, affording final bola **Orn-C16-G** (Scheme 3.1).

For **Orn-C20-G**, one of the acid groups of eicosanedioic acid was protected with methyl group. Then, the obtained mono-methyl ester **3G** was coupled with N-Boc-ethylenediamine. The amino group in the obtained conjugate **3H** was deprotected and substituted with Boc-protected ornithine. The obtained conjugate **3I** was further reacted with ethylene diamine giving **3J**. The latter was then reacted with D-gluconic acid δ-lactone followed by Boc-removal, affording final bola **Orn-C16-G** (Scheme 3.2).

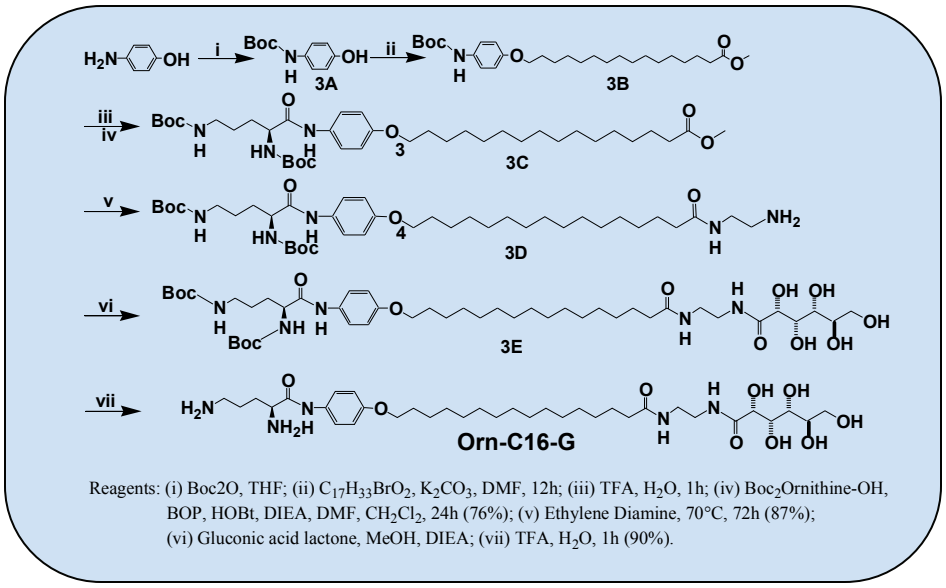

Reagents: (i) Boc2O, THF; (ii) $C_{17}H_{33}BrO_2$, K_2CO_3, DMF, 12h; (iii) TFA, H_2O, 1h; (iv) Boc_2Ornithine-OH, BOP, HOBt, DIEA, DMF, CH_2Cl_2, 24h (76%); (v) Ethylene Diamine, 70°C, 72h (87%); (vi) Gluconic acid lactone, MeOH, DIEA; (vii) TFA, H_2O, 1h (90%).

Scheme 3.1. Synthesis of Orn-C16-G.

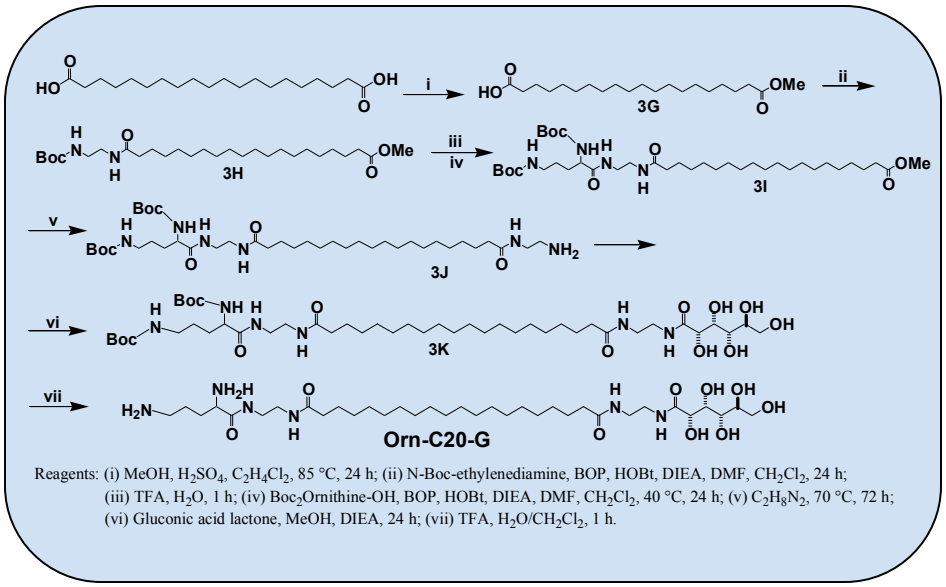

Scheme 3.2. Synthesis of **Orn-C20-G**.

Synthesis of **Orn-C16-L** and **Orn-C20-L** was similar to their corresponding gluconic analogues, Orn-C16-G and Orn-C20-G respectively, while at the last steps lactonic residue was introduced by reacting corresponding amine (**3D** or **3J**) with lactonolactone, followed by the Boc-removal to afford the final bolas.

Synthesis of **Orn-C16-PEG350** and **Orn-C16-PEG2000** was also similar to their corresponding gluconic analogue, Orn-C16-G, while at the last step a PEG group was introduced by reacting corresponding amine (**3D**) with a reactive derivative of PEG. For this purpose, two PEG-monomethyl ethers with different molecular weight (2000 and 350) were activated with 4-nitrophenyl chloroformate and further reacted with compound **3D,** to afford final bolas **Orn-C16-PEG2000** and **Orn-C16-PEG350**.

For **Orn-C12-C16-G**, amino group of **3B** (obtained in scheme 3.1) was deprotected and coupled with 12-tert-butoxycarbonylamino-dodecanoic acid. Then, amino group of the obtained conjugate **3M** was further deprotected and substituted with Boc-protected ornithine. The obtained conjugate **3N** was then reacted with ethylene diamine giving **3O**. The latter was then reacted with D-gluconic acid δ-lactone followed by Boc-removal, affording final bola **Orn-C12-C16-G** (Scheme 3.3).

For **(2Glu-C16)-Orn,** free acid group of 3,4-dihydroxy-benzoic was protected by methyl group followed by reaction with ethylene diamine. Then, amine group of the obtained conjugate **3Q** was protected with Boc to get **3R**. The two hydroxyl groups of 3R were further reacted with 16-bromohexadecanoic acid. Then, the amino group in the obtained conjugate **3S** was further deprotected and substituted with Boc-protected ornithine. The obtained conjugate **3T** was further reacted with ethylene diamine giving **3U**. The latter was then reacted with D-gluconic acid δ-lactone followed by Boc-removal, affording final bola **(2Glu-C16)-Orn** (Scheme 3.4).

The yields of the individual steps were systematically >60 % and the obtained final bolas in 100-200 mg quantities were sufficiently pure according to NMR, LC-MS and HPLC techniques.

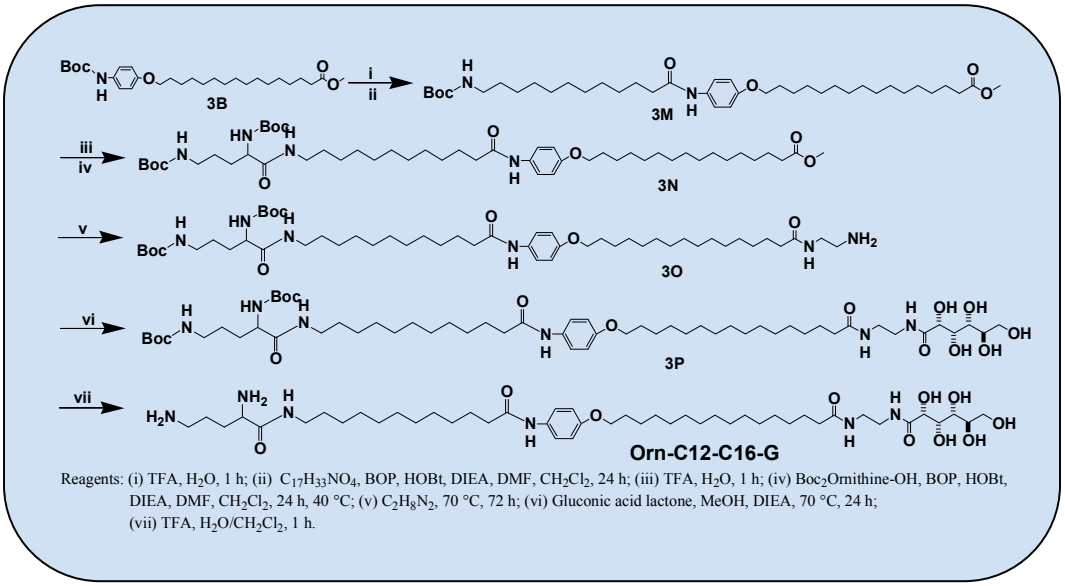

Reagents: (i) TFA, H_2O, 1 h; (ii) $C_{17}H_{33}NO_4$, BOP, HOBt, DIEA, DMF, CH_2Cl_2, 24 h; (iii) TFA, H_2O, 1 h; (iv) Boc_2Ornithine-OH, BOP, HOBt, DIEA, DMF, CH_2Cl_2, 24 h, 40 °C; (v) $C_2H_8N_2$, 70 °C, 72 h; (vi) Gluconic acid lactone, MeOH, DIEA, 70 °C, 24 h; (vii) TFA, H_2O/CH_2Cl_2, 1 h.

Scheme 3.3. Synthesis of **Orn-C12-C16-G.**

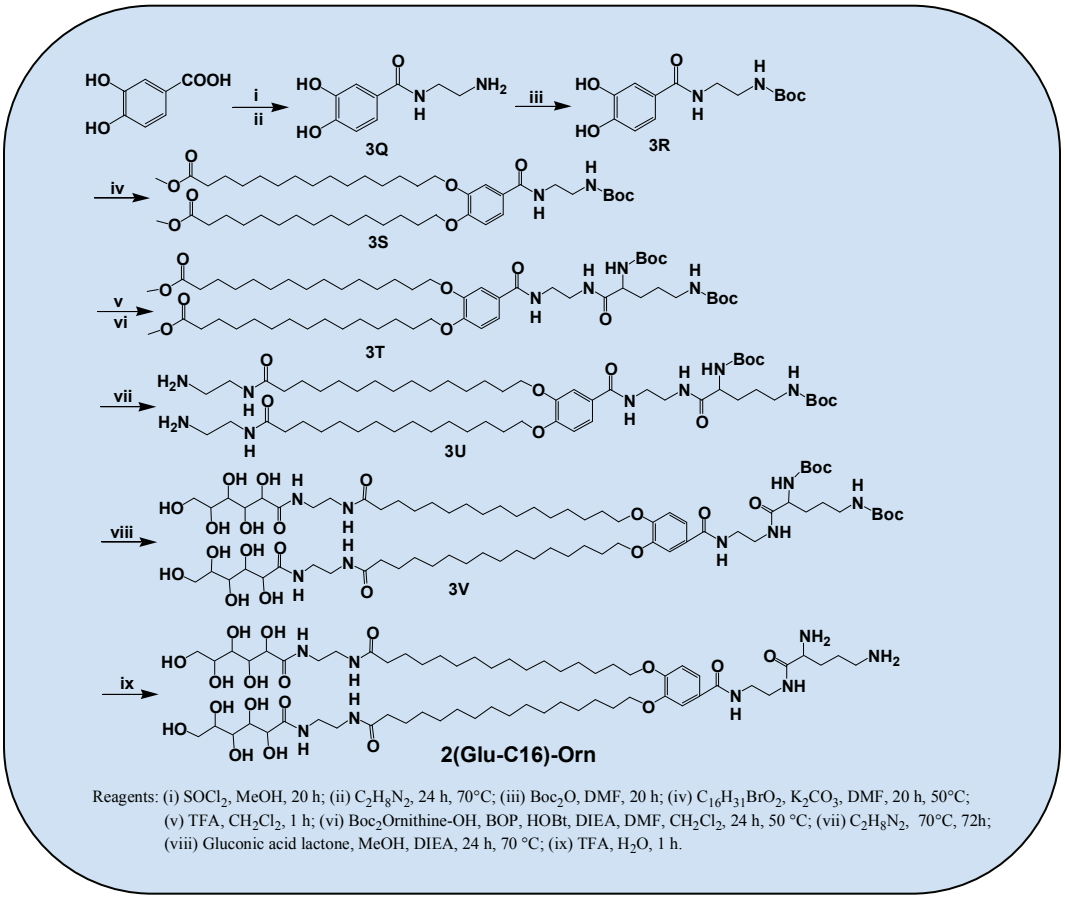

Reagents: (i) $SOCl_2$, MeOH, 20 h; (ii) $C_2H_8N_2$, 24 h, 70°C; (iii) Boc_2O, DMF, 20 h; (iv) $C_{16}H_{31}BrO_2$, K_2CO_3, DMF, 20 h, 50°C; (v) TFA, CH_2Cl_2, 1 h; (vi) Boc_2Ornithine-OH, BOP, HOBt, DIEA, DMF, CH_2Cl_2, 24 h, 50 °C; (vii) $C_2H_8N_2$, 70°C, 72h; (viii) Gluconic acid lactone, MeOH, DIEA, 24 h, 70 °C; (ix) TFA, H_2O, 1 h.

Scheme 3.4. Synthesis of **2(Glu-C16)-Orn**.

3.1 Bolas with Gluconic Headgroup

In order to enhance the hydrophobicity and achieve better self-assembly at micromolar concentrations, we selected as a hydrophobic spacer a long alkyl chain of C20-carbon atoms and a hydrophobic linker composed of an alkyl chain of C16-carbon atoms and an aromatic unit. Based on these modifications, two bolas were synthesized and characterized: **Orn-C20-G** and **Orn-C16-G** (Fig. 3.15).

According to gel electrophoresis results, these bolas showed an excellent affinity to DNA, as complex formation was observed already at N/P 1 (see Fig. 3.16a for the case of **Orn-C16-G**). The results were confirmed by EtBr exclusion assay, where an efficient DNA condensation was also observed at N/P close to 1. The size of the bolaplexes estimated by DLS was ~100 nm at low N/Ps, but increased significantly at higher N/Ps. This unexpected increase in the size with N/P was explained by the charge neutralization of the DNA complexes, which was evidenced from zeta-potential measurements. AFM studies of the bolaplexes revealed their rod-like or spherical nanostructure. More importantly, bolaplexes of **Orn-C16-G** at N/P ≥ 2 showed considerable transfection efficiency in COS-7 cells when helping agents like chloroquine or DOPE were used (Fig. 3.16). The latter results suggested that the key barrier for the internalization of bolaplexes is the endosomal escape. In contrast, **Orn-C20-G** did not show any appreciable transfection efficiency in most of the formulations used. The latter we connected with larger size of its complexes at high N/P ratio. Finally, both bolas presented low cytotoxicity (cell viability >80%).

Thus, gluconic-bolas, particularly **Orn-C16-G**, are good candidates for construction of nonviral gene delivery vectors. However, the further optimization of polar headgroups and hydrophobic spacer in these bolas could lead to vectors with more precisely controlled properties, particularly related to their size and transfection efficiency.

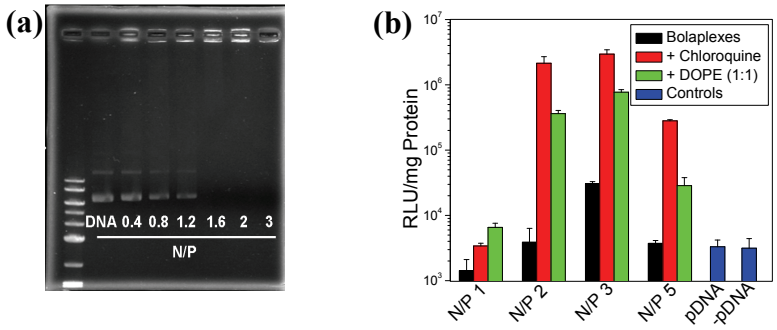

Figure 3.16. (a) Agarose gel electrophoresis (0.9%) of **Orn-C16-G** complexed with pDNA at different N/P ratios. Band at the left of the gel correspond to 10 kbp DNA ladder. The final DNA (phosphate) concentration was 60 μM, while the bola concentration was varied to obtain the final N/P ratio. (b) Transfection efficiency of the Orn-C16-G bolaplexes at different N/P ratios in COS-7 cells without serum. Cells were incubated in serum-free Opti-MEM, with a bolaplex composed of plasmid DNA (1 μg per well), Orn-C16-G and DOPE (when indicated). For some samples the medium contained 100 μM chloroquine. After 3 h, 10 % of FBS was added, while for all the samples with chloroquine the transfection medium was replaced with fresh complete culture medium. The luciferase activity quantification was performed after 48 h of incubation. Transfection efficiency determined from the luciferase assay was expressed as RLU/mg of protein. The negative controls were non-treated cells (–pDNA) and those transfected with naked pDNA (pDNA).

Other gluconic-bolas, such as **Orn-C12-C16-G** and **2(Glu-C16)-Orn** were also characterized. Gel electrophoresis results showed that **Orn-C12-C16-G** and **2(Glu-C16)-Orn** form complexes with pDNA at low N/Ps (Fig. 3.17 a and b respectively), which indicates strong affinity of these bolas towards DNA. In line with the gel electrophoresis data, experiments with ethidium bromide (EtBr) exclusion assay showed a sharp decrease of EtBr fluorescence at N/P ratio around 2 for both **Orn-C12-C16-G** and **2(Glu-C16)-Orn** (Fig. 3.17c), thus confirming that these bolas bind strongly to pDNA by showing a significant level of DNA condensation.

However, DLS studies for these bolas showed the formation of large aggregates. Thus, for N/P > 2, both bolas showed very large particles >5000 nm size. The observed aggregation with **Orn-C12-C16-G** bolaplexes could be due to its large hydrophobic spacer compared to Orn-C16-G that leads to imbalance between hydrophilic and hydrophobic moieties. In the case of **2(Glu-C16)-Orn**, where the hydrophobic-hydrophilic balance should be similar to that of Orn-C16-G, the observed aggregation could be related to a different geometry and the presence of two sugar residues. Thus, V-shaped structure of this bola and additional sugar residue could favor interactions between the bolaplexes, leading to strong aggregation. Because of this aggregation problem, we did not further characterize **Orn-C12-C16-G** and **2(Glu-C16)-Orn**.

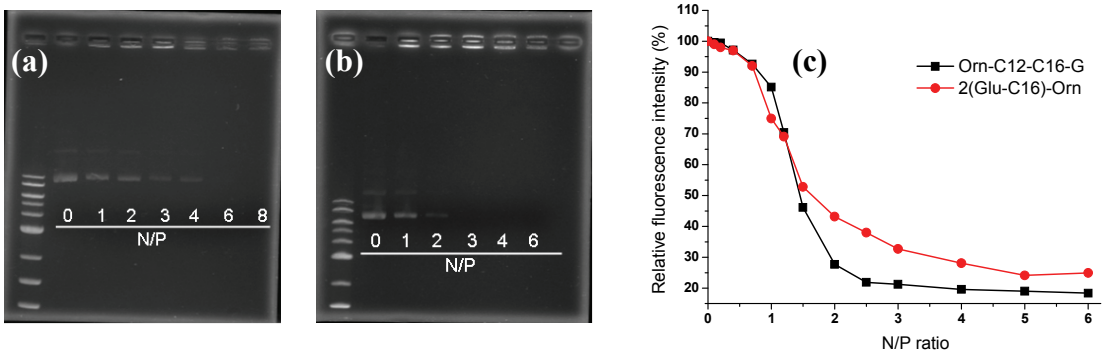

Figure 3.17. Agarose gel electrophoresis (0.9 %) of a) Orn-C12-C16-G and b) 2(Glu-C16)-Orn complexed with pDNA at different N/P ratios. Band on the left of each gel correspond to 10 kb DNA ladder. (c) Exclusion of EtBr from CT-DNA complexes with bolas at different N/P ratios. The fluorescence intensity was normalized to 100% of the initial intensity. The final DNA (phosphate) concentration was 60 µM for gel electrophoresis and 20 µM for EtBr exclusion assay, while the bola concentration was varied to obtain the final N/P ratio.

New unsymmetrical bolaamphiphiles: synthesis, assembly with DNA and application for gene delivery

(Publication 1)

New Unsymmetrical Bolaamphiphiles: Synthesis, Assembly with DNA, and Application for Gene Delivery

Namrata Jain, Youri Arntz, Valérie Goldschmidt, Guy Duportail, Yves Mély, and Andrey S. Klymchenko*

Laboratoire de Biophotonique et Pharmacologie, UMR 7213 CNRS, Université de Strasbourg, Faculté de Pharmacie, 74, Route du Rhin, 67401 ILLKIRCH Cedex, France. Received July 23, 2010; Revised Manuscript Received September 20, 2010

The success in gene therapy relies strongly on new efficient gene delivery vectors. Nonviral vectors based on lipids and polymers constitute an important alternative to the viral vectors. However, the key problem with these vectors is the poor structural control of their DNA complexes. In the present work, following new design we synthesized unsymmetrical bolaamphiphiles, molecules bearing neutral sugar (gluconic acid) and dicationic ornithine head groups connected by different long hydrophobic spacers. Within this design, a positively charged headgroup is expected to bind DNA, the hydrophobic spacer is to drive the formation of a monolayer membrane shell around DNA, while the neutral group is to be exposed outside of the complex. Our fluorescence and gel electrophoresis data showed that self-assembly of bolas and their interaction with DNA depend strongly on the bola structure. The size of bola/DNA complexes (bolaplexes) estimated from dynamic light scattering data was ∼100 nm at low N/P (cationic nitrogen/DNA phosphate molar ratio), while at higher N/Ps it was significantly larger due to neutralization of their surface charge. Atomic force microscopy studies revealed nanostructural rod-shaped or spherical morphology of the bolaplexes. Transfection efficiency of the bolaplexes in vitro was significant when either DOPE or chloroquine were used as helping agents, suggesting that the key barrier for their internalization is the endosomal escape. Finally, all bolas showed low cytotoxicity (cell viability >80%). The present results show that bolas are prospective candidates for construction of nonviral gene delivery vectors. We believe that further optimization of polar head groups and a hydrophobic spacer in the bolas will lead to vectors with controlled small size and high transfection efficiency.

INTRODUCTION

The vast majority of natural and synthetic lipids studied so far are "monopolar" amphiphiles, that is, molecules presenting one polar headgroup and generally two hydrophobic chains. However, bipolar amphiphiles, which are analogues of lipids presenting polar groups at the two opposite sides of the hydrophobic chain(s), so-called bolaamphiphiles (bolas), became the matter of intensive research only in the recent years (*1*). A remarkable feature of bolas is that in contrast to bilayer membranes formed by lipids they can form monolayer membranes (Figure 1), having bolas with membrane-spanning hydrophobic chains, which are believed to be responsible for enhanced physical stability of bola membranes (*1, 2*). In nature, they are mainly present in archaebacteria and ensure the integrity of the bacterial membrane at high temperature (90 °C) and low pH (1−1.5) (*3, 4*). Membranes made from synthetic bolas, forming either nanotubes or vesicles, can also show an exceptional stability, some of them being stable even in the dry phase (*5, 6*) or in some organic solvents (*7*). Unsymmetrical bolas, bearing two different polar head groups, assembled in a parallel fashion can form asymmetric membranes, so that the two opposite sides of the monolayer membrane present different functional groups (Figure 1) (*5, 6*). One of the attractive applications of bolas, which is still in its infancy stage, is gene delivery, a domain for which "monopolar" cationic lipids and other cationic agents are currently maintaining a dominant position.

Gene delivery, which is a main concern in gene therapy, relies heavily on development of new delivery vectors. Nonviral vectors based on lipids are highly attractive, since they can deliver large quantities of genetic information and are weakly immunogenic (*8*). A variety of cationic lipids for gene delivery has been developed in recent decades (*8*−*19*). Their complexes with DNA (lipoplexes) show high transfection efficiency in vitro, though their application for gene therapy in vivo remains a challenge. One of the key problems of cationic lipids is the poor structural control of their lipoplexes (*10, 20*). Indeed, symmetric lipid bilayers made of cationic lipids interact with DNA by forming infinite sandwich-like structures of high polydispersity (Figure 1) (*10*).

In this respect, unsymmetrical bolas bearing positively charged and neutral head groups could be an attractive alternative to the cationic lipids. These molecules could generate asymmetric membranes (in form of vesicles or nanotubes) having positively charged inner and neutral outer surfaces. In such a case, the inner membrane surface can be used to wrap the DNA molecule (Figure 1), while the outer neutral membrane surface, being inert to DNA, would prevent further oligomerization of the complex and could be utilized for efficient exposure of the biological signal for specific targeting. The examples of successful application of bolas for gene delivery, which has been shown only in the recent years, include synthetic unsymmetrical bolas (*21*−*25*) and archaebacteria-derived lipids (*26, 27*). Among unsymmetrical bolas, the most promising were those bearing a sugar (gluconic or lactonic acid) residue on one side and mono- or oligo-cationic ammonium-based group on the other (*21, 23*). Moreover, the galactose-bearing bolas showed some specificity to HepG2 cell line, expressing a galactose receptor of endocytosis (*21, 22*).

In the present work, three new bolaamphiphiles were synthesized, bearing neutral sugar and dicationic ornithine head groups, connected by different hydrophobic spacers. We showed

* To whom correspondence should be addressed. E-mail: andrey.klymchenko@unistra.fr. Fax: +33 368 854313. Tel: +33 368 854255.

10.1021/bc100334t
Published on Web 10/14/2010

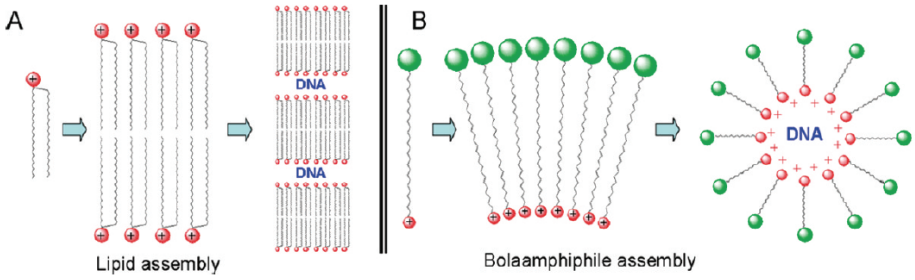

Figure 1. Lipids and bolaamphiphiles assembly with DNA. (A) Schematic presentation of bilayers formed from cationic lipids and further formation of DNA complexes, so-called lipoplexes. (B) Assembly of bolaamphiphiles into asymmetric membranes and formation of DNA complexes, so-called bolaplexes.

that the nature of spacer defines the bola self-assembly, the interaction with DNA and the morphology of the obtained complexes. Moreover, some bolas can transfect efficiently COS-7 cells in the presence of either a helper lipid (DOPE) or an endosomolytic reagent (chloroquine) (*28*). The latter indicates that the key barrier for gene delivery with the present bolas resides in the endosomal escape. This work presents new bolaamphiphile-based nonviral vectors and provides insights for further improvements of their efficiency.

MATERIALS AND METHODS

All chemicals and solvents for synthesis were purchased from Sigma-Aldrich. Mass spectra were measured using Mass Spectrometer Mariner System 5155. LC-MASS was performed on Agilent, 1956 B/MSD. ^{1}H NMR spectra were recorded on Bruker 300 MHz spectrometer.

***N*-Boc-4-aminophenol (1).** 4-Aminophenol (4 g, 36.7 mmol) and Boc_2O (8 g, 36.7 mmol) were dissolved in 30 mL of THF and left stirring overnight. Then 100 mL of water was added and the product was extracted with ethyl acetate (3 × 50 mL) and further dried with sodium sulfate. After solvent evaporation in vacuo, the crude product **1** was used without further purification.

16-(4-tert-Butoxycarbonylaminophenoxy)-hexadecanoic Acid Methyl Ester (2). Boc-protected 4-aminophenol (**1**) (1.8 g, 8.6 mmol) and 16-bromohexadecanoic acid methyl ester (3 g, 8.6 mmol, prepared by methylation of the acid in methanol and thionyl chloride) were dissolved in 10 mL of DMF and supplemented with 1.8 g (13 mmol) of potassium carbonate. After 12 h of stirring at room temperature (RT), the solution was poured in water (50 mL) and the product was extracted with dichloromethane (3 × 30 mL) and dried with sodium sulfate. Then the solvent was removed and the product **2** (1.6 g, 40%) was crystallized from ethanol. ^{1}H NMR ($CDCl_3$, 300 MHz): δ 7.24 (d, 2H), 6.82 (d, 2H), 6.4 (s, 1H), 3.91 (t, 2H), 3.67 (s, 3H), 2.31 (t, 2H), 1.82−1.58 (m, 4H), 1.55−1.48 (m, 9H), 1.46−1.2 (m, 24H). LC-MS (*m*/*z*): found $[M + 1]^+$ = 378.2; calcd for $C_{28}H_{47}NO_5^+$-$C_5H_9O_2$ (Boc) = 378.3.

16-[4-(2,5-Bis-tert-butoxycaronylamino-pentanoylamino)-phenoxy]-hexadecanoic Acid Methyl Ester (3). Boc was removed from **2** (3.14 mmol, 1.5 g) by treating with 5 mL TFA and 3% H_2O for 1 h at RT. The solvent was evaporated and 1.54 g (3.1 mmol) of the obtained deprotected amine was coupled with 2,5-bis-tert-butoxycarbonyl amino-pentanoic acid (3.57 mmol, 1.15 g) using BOP (3.44 mmol, 1.52 g), HOBt (4.3 mmol, 0.58 g), and DIEA (12.6 mmol, 2.2 mL) in DMF (15 mL) and dichloromethane (30 mL). The mixture was stirred overnight at RT. Then, solvent was evaporated and product was crystallized from acetonitrile. The precipitate was filtered off and dried to give compound **3** (1.6 g, 76%). ^{1}H NMR ($CDCl_3$, 300 MHz): δ 8.41 (s, 1H), 7.41 (d, 2H), 6.81 (d, 2H), 5.25 (s, 1H), 4.73 (s, 1H), 4.39 (s, 1H), 3.9 (t, 2H), 3.65 (s, 3H), 3.4 (s, 1H), 3.09 (s, 1H), 2.28 (t, 2H), 1.83−1.69 (m, 4H), 1.67−1.53 (m, 4H), 1.47−1.38 (m, 18H), 1.37−1.16 (m, 22H). LC-MS (*m*/*z*): found $[M + 1]^+$ = 491.2; calcd for $C_{38}H_{65}N_3O_8^+$-$C_{10}H_{18}O_4$ (2Boc) = 491.2.

(1-{4-[15-(2-Amino-ethylcarbamoyl)-pentadecyloxy]-phenylcarbamoyl}-4-tert-butoxycabonylamino-butyl)-carbamic Acid tert-Butyl Ester (4). Methyl ester of **3** (0.7 mmol, 0.5 g) was substituted with ethylenediamine (150 mmol, 10 mL) for 72 h at 70 °C. Then the excess of ethylenediamine was evaporated, 50 mL of water was added and the product **4** was filtered (0.45 g, 87%). ^{1}H NMR ($CDCl_3$, 300 MHz): δ 8.45 (s, 1H), 7.42 (d, 2H), 6.82 (d, 2H), 6.05 (s, 1H), 5.30 (s, 1H), 4.75 (s, 1H), 4.37 (s, 1H), 3.91 (t, 2H), 3.42−3.25 (m, 3H), 3.16−3.02 (m, 1H), 2.84 (t, 2H), 2.17 (t, 2H), 2.06−1.92 (m, 4H), 1.79−1.7 (m, 2H), 1.67−1.54 (m, 4H), 1.48−1.37 (m, 18H), 1.37−1.20 (m, 20H). LC-MS (*m*/*z*): found $[M + 1]^+$ = 720.4; calcd for $C_{39}H_{69}N_5O_7^+$ = 720.4.

[4-tert-Butoxylamino-4-(4-{15-[2-(2,3,4,5,6-pentahydroxy-hexanoylamino)-ethylcabamoyl]-pentadecyloxy}-phenylcarbamoyl)-butyl]-carbamic Acid tert-Butyl Ester (5). D-gluconic acid δ-lactone (0.23 mmol, 0.04 g) was added to solution of **4** (0.11 mmol, 0.1 g) in 15 mL of methanol. Then, DIEA (1.4 mmol, 0.24 mL) was added and the reaction mixture was stirred at 70 °C for about 24 h. Solvents were evaporated in vacuo. Compound **5** (0.09 g, 90%) was crystallized from methanol. ^{1}H NMR (CD_3OD, 300 MHz): δ 7.42 (d, 2H), 6.87 (d, 2H), 4.21 (s, 1H), 4.18−4.06 (m, 2H), 3.96 (t, 2H), 3.83−3.6 (m, 5H), 3.09 (t, 2H), 2.19 (t, 2H), 1.86−1.54 (m, 10H), 1.48−1.41 (m, 18H), 1.39−1.26 (m, 22H). LC-MS (*m*/*z*): found $[M + 1]^+$ = 898.57; calcd for $C_{45}H_{79}N_5O_{13}^+$ = 898.57.

16-[4-(2,5-Diamino-pentanoylamino)-phenoxy]-hexadecanoica-cid[2-(2,3,4,5,6-pentahydroxy-hexanoylamino)-ethyl]-amide (Orn-C16-G). Boc was removed from 50 mg of **5** using 0.5 mL TFA and 3% H_2O (1 h) to get the final product Orn-C16-G (27 mg, 90%). LC-MS (Bruker, HTCultra) (*m*/*z*): found $[M + 1]^+$ = 698.4; calcd for $C_{35}H_{64}N_5O_9^+$ = 698.4.

Fluorescence Measurements. Absorption spectra were recorded on a Cary 400 spectrophotometer (Varian) and fluorescence spectra either on FluoroMax 3.0 or Fluorolog (Jobin Yvon, Horiba) spectrofluorimeters. All the emission spectra were corrected from the background signal of the corresponding blank (corresponding solution without the fluorescent dye). For measurements with 1,8-ANS, 50 nM of the dye dissolved in 20 mM MES buffer (pH 7.4 or 6.0) solution was titrated with increasing quantities of the corresponding bola, added from stock solutions. All spectra were recorded 2 min after each addition. In the ethidium bromide (EtBr) exclusion assay, an aliquot of CT-DNA (final concentration 20 μM) was added to the solution of EtBr (0.4 μM). After 2 min, increasing quantities of the corresponding bola were added from stock solutions (in DMF with 10% of water). Fluorescence intensity recorded at 600 nm (excitation at 550 nm) was recorded 2 min after each addition of bola aliquot.

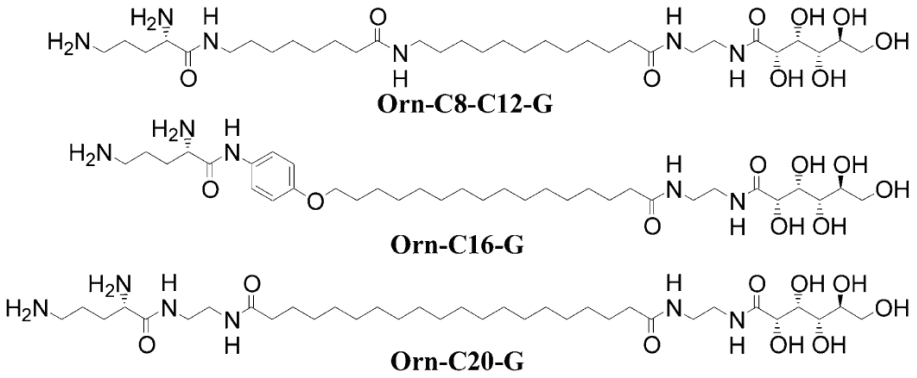

Figure 2. Chemical structures of bolaamphiphiles.

Dynamic Light Scattering (DLS) and ζ-Potential Measurements. The bolaplexes were prepared in 20 mM MES at pH 7.4 by mixing equal volumes of the solutions of calf thymus DNA (CT-DNA) or pCMV-Luc plasmid (pDNA) and the corresponding bolas. The bola solutions were prepared by adding aliquots of their stock solutions (in DMF with 10% of water) to the buffer. The final DNA concentration (expressed in phosphate) was 20 μM, while the bolas concentration was adjusted according to a desired N/P ratio. The N/P ratio between bolas and pDNA was expressed as the molar ratio between all the protonable amino groups of the bolas and the phosphate groups of the DNA. The DLS measurements were performed after 30 min of incubation at room temperature. The average size of the complexes was determined with a Zetasizer Nano ZS (Malvern Instruments) with the following specifications: sampling time, 30 s; medium viscosity, 0.8872 cP; refractive index (RI) medium, 1.33; RI particle, 1.590; scattering angle, 90°; temperature, 25 °C. For particle analysis, the statistics based on particle volume and particle number were presented. For ζ-potential measurements, the same sample preparation was done using CT-DNA at 30 μM concentration. The instrumental specifications were the same, accounting for a solvent dielectric constant of 78.5.

Gel Electrophoresis. The bolaplexes were prepared at different N/P ratios using 60 μM pCMV-Luc plasmid (final phosphate concentration), followed by 30 min incubation at room temperature. Four microliters of loading dye (Lonza, 6×) was added to 20 μL of the prepared complexes and then 12 μL of this mixture was loaded on 0.9% agarose gel prepared with 0.5X TAE (tris-acetate-ethylenediaminetetraacetic acid) buffer. In parallel, a 10 kbp DNA ladder (Lonza) was loaded on the gel. Electrophoresis was carried out with 0.5X TAE buffer at a constant voltage of 100 mV. DNA bands were visualized by UV trans-illuminator (GeneGenius, Syngene) after coloration with EtBr (0.5 μg/mL) for 15 min.

AFM Measurements. AFM measurements were performed using the Solver Pro-M (NT-MDT) instrument. The measurements were performed in liquid phase (MES buffer pH 7.4) by using the tapping mode. The cantilevers used were NSG03 type (NT-MDT) with a typical spring constant of 1.7 N/m, a resonance frequency of 32 kHz in liquid, and a tip curvature radius of 10 nm. Images were acquired with a resolution of 512 × 512 and a scan rate of 2 Hz. The samples were prepared as for DLS measurements, then 100 μL of the solution was deposited on the freshly cleaved mica followed by the addition of 10 μL of a $MgCl_2$ stock solution to obtain a final concentration of 10 mM. The measurements were performed 10 min after sample preparation.

Transfection and Cytotoxicity. COS-7 cells (African Green Monkey kidney fibroblast cell line) were grown in Dulbecco's modified Eagle's medium (Gibco-Intvitogen), supplemented with 10% fetal bovine serum (FBS, Lonza) and 100 U/ml of penicillin and streptomycin (Gibco-Intvitogen) at 37 °C in a humidified atmosphere containing 5% CO_2. Cells were seeded at a density of 1×10^5 cells in a 24-well plate, 24 h before transfection.

Transfection was done by using bola/pDNA (pCMV-Luc plasmid, 1 μg/well) complexes at different N/P ratios in serum-free Opti-MEM (Gibco-Invitrogen) or complete culture medium (DMEM containing 10% of FBS). For this purpose, bolaplexes were prepared in MES buffer (pH 7.4) as for DLS measurements and then added to the cells in Opti-MEM. Chloroquine (100 μM) or DOPE (1:1 molar ratio with respect to bola) was used to enhance transfection efficiency in some formulations. In formulations with DOPE, a mixture of DOPE and a corresponding bola in ethanol was evaporated in a round-bottom flask to obtain a film. Then, MES buffer (pH 7.4) was added and the samples were hydrated overnight at RT. Then, the samples were vortexed vigorously for 1 min and further sonicated in an ultrasonic bath for 15 min. The obtained suspensions were mixed with an equal volume of pDNA in the buffer to obtain a desired N/P ratio. All formulations were incubated at RT for 30 min before addition to the cells. After 3 h of incubation of cells with bolaplexes at 37 °C, 10% of FBS was added to serum-free samples, while for all the samples with chloroquine the transfection medium was replaced with fresh complete culture medium and then cells were cultured for another 45 h. Total incubation time for all samples was 48 h. Luciferase gene expression of lysed cells was quantified using a commercial kit (Invitrogen) and a luminometer (CentroXS^3 LB 960, BERTHOLD Technologies). Results were expressed as relative light units integrated over 10 s per mg of total cell protein lysate (RLU/mg of total protein). The experiments were repeated six times for serum-free samples and three times for samples with serum. The total protein was determined by BC assay (Protein Quantitation Kit, Interchim) using Cary 4000 spectrophotometer. As a positive control in the transfection measurements, commercially available agent jetPEI (Polyplus) was used following protocols provided in the kit.

Cytotoxicity of bolas was evaluated using 3-(4,5-dimethyl-2-thiazolyl)-2,5-diphenyltetrazolium bromide (MTT, Sigma-Aldrich) assay (*29*). COS-7 cells were seeded in a 24-well plate at 1×10^5 cells per well and after 24 h of incubation at 37 °C supplemented with bolas at different concentrations or jetPEI (150 μM, expressed as concentration of nitrogen residues) in serum-free Opti-MEM. After incubation for 3 h at 37 °C, 10% of FBS was added and cells were cultured for another 45 h. Cells were washed with phosphate buffer saline (PBS) and incubated with serum free medium containing 0.5 mg/mL MTT for 3 h at 37 °C. Media was discarded and formazan crystals were resuspended in 0.5 mL MTT solvent (Sigma-Aldrich). Absorbance of formazan solution was measured at 570 nm with

Scheme 1. Synthesis of Bola Orn-C16-G

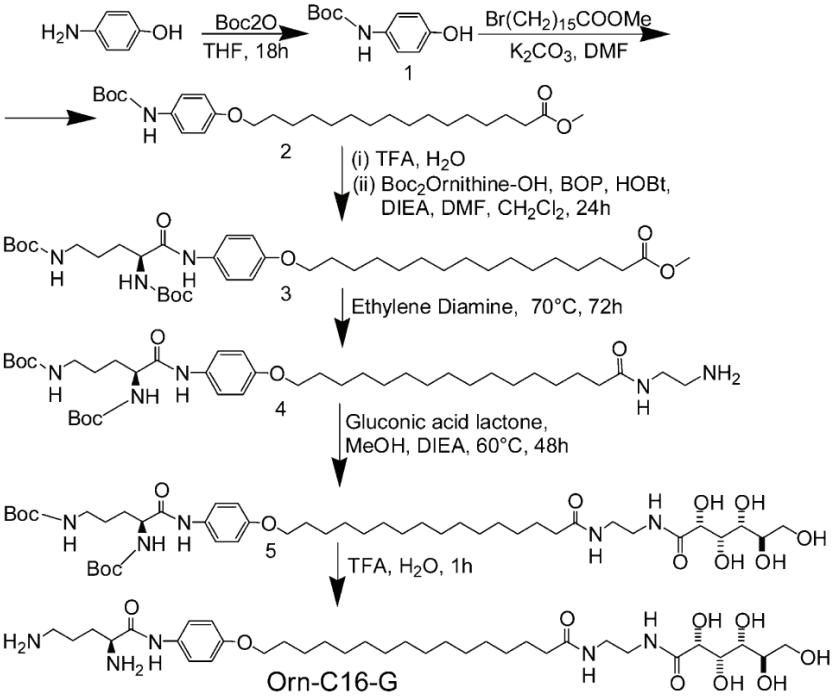

respect to the background at 690 nm using Cary 4000 spectrophotometer. Cell viability was expressed as relative absorbance (%) of the sample versus control cells.

RESULTS AND DISCUSSION

Design and Synthesis. The basic design of bolas relies on one neutral group and one dicationic group connected by a hydrophobic spacer. As neutral group we selected a sugar residue, which is biocompatible and relatively inert. The dicationic headgroup responsible for DNA binding was the ornithine residue (Orn), featuring two amino groups separated by a 4-carbon atom distance. This distance ensures protonation of both amino groups at neutral pH and thereby efficient interaction with negatively charged DNA. On the basis of this design, three new bolaamphiphiles were synthesized, presenting different hydrophobic spacers: (a) a dipeptide composed of end-substituted amino acids of 8- and 12-carbon atoms, Orn-C8-C12-G; (b) a hydrophobic linker composed of an alkyl chain of C16-carbon atoms and an aromatic unit, Orn-C16-G; and (c) a long (20-carbon atoms) alkyl chain, Orn-C20-G (Figure 2). This variation of the hydrophobic spacer could tune the hydrophobic, H-bonding and π-stacking interactions between bolas. An example of synthesis of Orn-C16-G is presented in Scheme 1. Initially, the amino group of 4-aminophenol was protected with Boc-group (**1**) and its hydroxyl was further reacted with methyl 16-bromohexadecanoate. Then, the amino group in the obtained conjugate **2** was further deprotected and substituted with Boc-protected ornithine. The obtained conjugate **3** was further reacted with ethylene diamine giving **4**. The latter was then substituted with D-gluconic acid δ-lactone followed by Boc-removal, affording final bola Orn-C16-G. The yields of the individual steps were systematically >50% and the obtained final bolas in 100−200 mg quantities were sufficiently pure according to NMR, LC-MS and HPLC techniques (see also Supporting Information).

Self-Assembly. 1,8-ANS dye is poorly fluorescent in water, while on binding to lipid membranes it becomes strongly fluorescent (*30*). In the present work, we used this probe to study the concentration-dependent bolas assembly. Solutions at pH 7.4 and 6.0 were tested, which could alter the protonation of the amino groups of bolas in the self-assembled state. It can be seen from Figure 3 that for Orn-C16-G at pH 7.4, fluorescence intensity grows rapidly with bola concentration showing beginning of saturation at higher concentrations. In contrast, at pH 6.0, a moderate increase in fluorescence intensity is followed by rapid increase at concentrations >20 μM. These data suggest that the critical aggregation concentration (CAC) at pH 7.4 is too low to be detected with this method, while at pH 6.0 it is clearly much larger being close to 20 μM. We could speculate that the self-assembly could be accompanied by a partial deprotonation of bola amino groups, so that lower pH may favor disassembly (i.e., higher CAC). In contrast, for bola Orn-C20-G rapid increase of 1,8-ANS fluorescence intensity was observed both at pH 7.4 (see Figure S1 in Supporting Information) and 6.0 (Figure 3). This indicates that CAC of Orn-C20-G is much

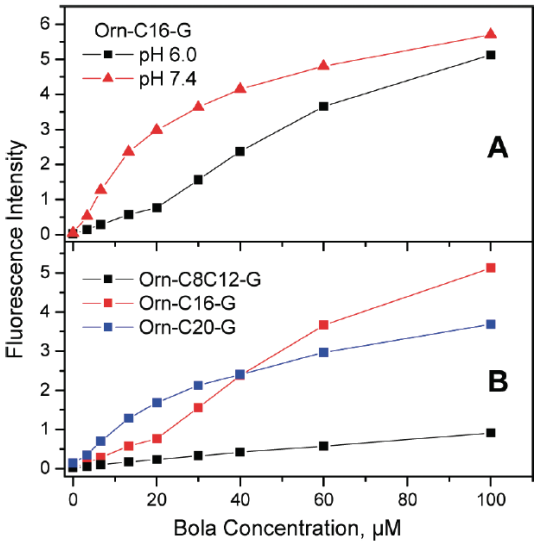

Figure 3. Fluorescence intensity of 1,8-ANS (50 nM) as a function of bolas concentration. (A) Orn-C16-G in MES buffer at pH 7.4 and 6. (B) Three different bolas at pH 6.

Table 1. Dynamic Light Scattering Data of Bolas and Bolaplexes in Aqueous Buffer (pH 7.4)

		volume analysis		
	sample	diameter, nm	amount, %	number analysis mean diameter, nm
Orn-C16-G	bola (100 μM)	110	88	73
		1450	12	
	bola/pDNA N/P 1.2 (12 μM bola)	109	95	90
	bola/pDNA	92	45	152
	N/P 2 (12 μM bola)	510	55	
	bola/pDNA N/P 2 (20 μM bola)	1550	95	1400
	bola/pDNA N/P 5 (50 μM bola)	870	100	925
	bola (100 μM)	140	15	110
		1050	85	
	bola/pDNA	97	20	90
	N/P 1.2 (12 μM bola)	930	80	
Orn-C20-G	bola/pDNA N/P 2 (12 μM bola)	970	100	900
	bola/pDNA N/P 2 (20 μM bola)	1370	100	1200
	bola/pDNA N/P 5 (50 μM bola)	1090	100	1069
	bola/DOPE (100 μM bola)	220	30	140
		1120	70	
Orn-C16-G/DOPE (1:1)	bola/DOPE/pDNA N/P 2 (20 μM bola)	220	100	218
	bola/DOPE/pDNA N/P 3 (30 μM bola)	200	20	190
		800	80	
	bola/DOPE/pDNA N/P 5 (50 μM bola)	1440	100	1350

lower than that of Orn-C16-G, probably because of its hydrophobic spacer, which is longer and does not contain bulky aromatic group, thus ensuring tight bola packing. Finally, Orn-C8-C12-G showed relatively weak increase in the fluorescence of 1,8-ANS with increasing concentration suggesting that it does not assemble at the studied concentration range. The latter result is probably connected to the presence of an amide group within the bola hydrophobic spacer, which may strongly diminish its hydrophobic interactions and thus increase its CAC.

The information about molecular order of bolas assemblies can be provided from fluorescence anisotropy of a rod-shaped molecule TMA-DPH (*31*). The observed values of fluorescence anisotropy for Orn-C16-G and Orn-C20-G assemblies at 100 μM are relatively high (0.30−0.32) at 20 °C and correspond to a rigid and highly ordered environment similar to lipid membranes in solid gel phase (0.32) for DPPC at 20 °C (data not shown) (*32*). These high values of fluorescence anisotropy suggest that bolas are probably organized in monolayers with a transmembrane spanning orientation, thus excluding possible bolas bilayer structure presenting a U-shaped conformation, as reported for some other bolas (*33*).

According to DLS data, Orn-C16-G and Orn-C20-G at 100 μM concentration form a significant fraction of small structures (around 100 nm, Table 1) in line with fluorescence data suggesting self-assembly of bolas at these conditions. These structures were stable for 1−2 h, while after longer incubation some precipitation of the bolas was observed.

Interactions with DNA. To study interactions of bolas with DNA, gel electrophoresis was first used. It can be seen from Figure 4A that Orn-C8-C12-G forms complexes with firefly luciferase plasmid DNA (pDNA) only at high N/P ratios (ratio between cationic groups of bola and phosphate groups of DNA). Indeed, only at N/P > 10 the pDNA band disappears. This indicates a relatively weak affinity of this bola to DNA. In contrast, Orn-C16-G (Figure 4B) and Orn-C20-G (Figure 4C) form complexes with pDNA at N/P values close to 1.0−1.2. It can be noted that Orn-C20-G shows a slightly stronger interaction since the DNA band disappears at lower N/P ratio (1.2) as compared to Orn-C16-G (1.6). By taking into account that all bola molecules are bearing the same dicationic ornithine residue, the stronger interaction of Orn-C16-G and Orn-C20-G with DNA is probably connected with a higher hydrophobicity of their spacers, which in turn favors their self-assembly and their cooperative interaction with DNA. Thus, we can assert that the interaction of the present bolas with DNA is controlled in part by their ability to self-assemble. Finally, a mixture of Orn-C16-G with a helper lipid DOPE (1:1 molar ratio with respect to bola), which was important in our transfection experiments (see below), showed complex formation at slightly higher N/P ratio, being completed at N/P 3 (see Figure S2 in Supporting Information).

The DNA condensation within the bolaplexes can be followed by the ethidium bromide (EtBr) exclusion assay (*34*). This dye when intercalated into DNA is highly fluorescent, while after DNA condensation it is expelled from its intercalation site, thus resulting in a strong decrease of its fluorescence intensity (up to 90%). For these studies, a linear DNA from calf thymus was used as the model. According to our data, Orn-C8-C12-G showed a relatively weak and rather linear decrease of EtBr fluorescence intensity as a function of N/P ratio (Figure 5), which is in line with the gel electrophoresis data showing its

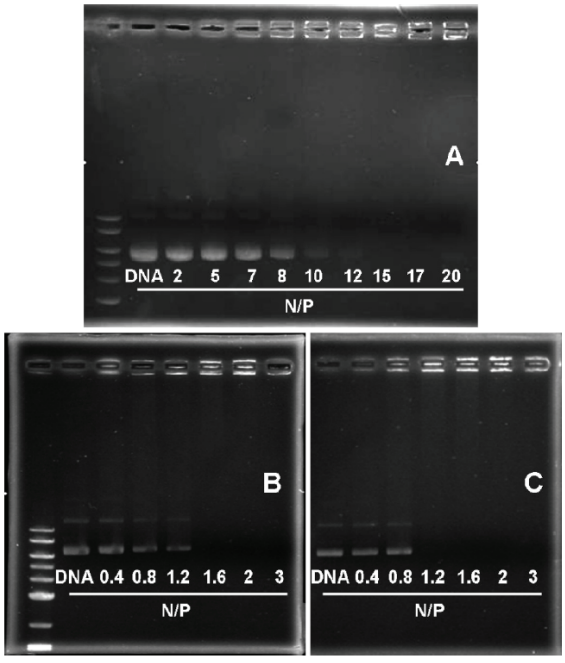

Figure 4. Agarose gel electrophoresis (0.9%) of Orn-C8-C12-G (A), Orn-C16-G (B), and Orn-C20-G (C) complexed with pDNA at different N/P ratios. Bands at the left of gels (A) and (B) correspond to 10 kbp DNA ladder.

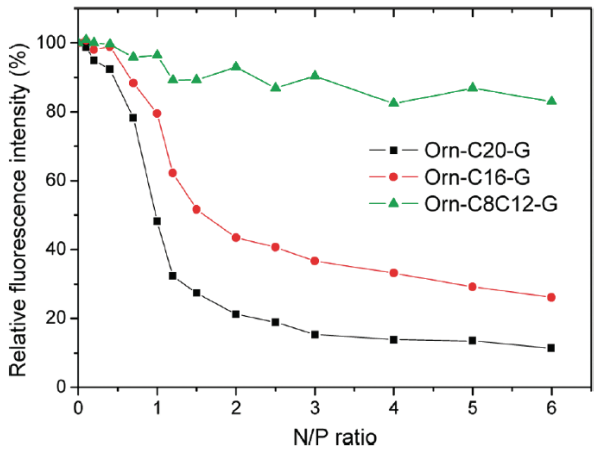

Figure 5. Exclusion of EtBr from CT-DNA complexes with bolas at different N/P ratios. The fluorescence intensity was normalized to 100% of the initial intensity.

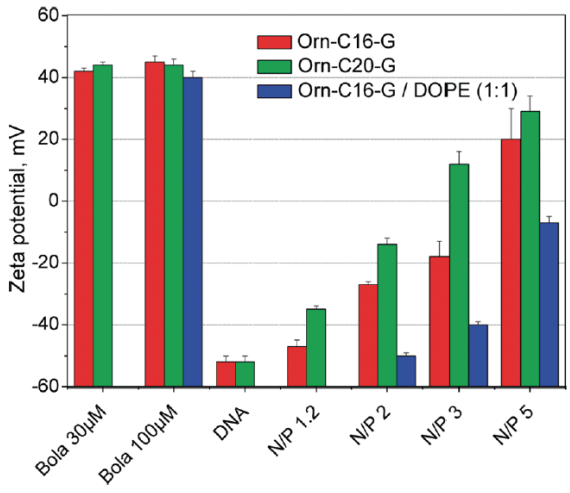

Figure 6. ζ-potential of nanostructures formed by bolas alone and by their formulations with DOPE and CT-DNA in MES buffer (pH 7.4) at different N/P ratios.

weak interaction with DNA. In contrast, both Orn-C16-G and Orn-C20-G showed a sharp decrease of EtBr fluorescence at N/P around 1. Thus, in accordance with the gel electrophoresis data it is confirmed that these bolas bind strongly to DNA by showing a significant level of DNA condensation. It can be also noticed that, similarly to the gel electrophoresis data, Orn-C20-G shows an EtBr fluorescence decrease at lower N/P ratio as compared to Orn-C16-G. Moreover, the fluorescence decrease is stronger for the former bola (ca. 85% for Orn-C20-G as compared to ca. 70% for Orn-C16-G). Thus, we can conclude that Orn-C20-G presents a stronger affinity to DNA and condense it more significantly as compared to Orn-C16-G. This conclusion corroborates with the observed stronger ability of Orn-C20-G to self-assemble without DNA evidenced by 1,8-ANS data. Since Orn-C8-C12-G shows a poor affinity to DNA and almost a negligible DNA condensation ability, we excluded this compound from further characterization, focusing only on Orn-C16-G and Orn-C20-G bolas.

Structural Characterization of Bolaplexes. To estimate the size of the obtained bolaplexes, DLS technique was used. Initially, the bolaplexes at different N/P ratios were prepared by direct addition of increasing quantities of Orn-C16-G from stock to pDNA solution. It was observed that at low N/P ratios, the particle size was relatively small (around 100 nm), while above N/P 1.2, their size increased rapidly reaching a maximum at N/P 2 (700 nm) and then further decreases until N/P 5 (see Supporting Information). In a second approach, the bolaplexes were prepared by mixing equal volumes of bolas and DNA aqueous solutions, followed by 30 min incubation at RT. This method gave similar DLS results for low N/P ratios (1.2 and 2): relatively small particles at N/P = 1.2 and much larger at N/P = 2 (Table 1). It is important to note that for Orn-C16-G at lower concentration the bolaplexes at N/P 2 (30 min incubation) showed much smaller sizes (150 nm). In contrast, after 5 min of incubation, Orn-C16-G/pDNA complexes presented similar small sizes (ca. 150 nm) for both low and high bola concentrations. Thus, the higher bola concentration probably favors aggregation of bolaplexes into larger particles. At N/P 5, this preparation method (with 30 min incubation) also gave relatively large particles as for N/P 2. The observed discrepancy between the two methods of preparation for N/P 5 is probably related to the incubation time, since in the first approach the measurements were done 5 min after each addition. The DLS data obtained with Orn-C20-G were similar to those with Orn-C16-G (Table 1), so that bolaplexes were small at N/P ratio 1.2, while their size increased significantly at higher N/P ratios. Moreover, for Orn-C16-G/DOPE mixture (1:1), a similar increase in the size of the bolaplexes was observed at higher N/P ratios (Table 1). The observation of larger complexes at higher N/Ps differs clearly from behavior of polyplexes and lipoplexes. Indeed, the latter at N/Ps close to 1 show relatively large complexes because of neutral charge of the complex, while at higher N/Ps they are much smaller because of their strong positive charge (*35*−*37*). Interestingly, our observations are in line with recent reports on other bolas featuring cationic group on one end and a neutral sugar residue on the other (*23, 24*). Therefore, we can suggest that the increase in size of bolaplexes at higher N/Ps could be a special feature of this type of bolas, which is probably because their bolaplexes do not become positively charged at higher N/Ps. This hypothesis was verified by measuring the zeta potential of bolaplexes (Figure 6). The bolas alone showed strongly positive ζ-potentials, while the bolaplexes at low N/P ratios were negatively charged and reached neutrality at N/P ratios around 3. At N/P 5, the observed ζ-potential was positive, however, we suspect that it could be due to excess of bola molecules that do not complex with DNA, thus contributing to apparent positive potential values. For Orn-C16-G/DOPE mixture (1:1), the ζ-potentials were systematically more negative, though a clear neutralization of the complexes was observed at N/P 5 (Figure 6). We expect that, as shown in Figure 1B, the positively charged part of bola interacts with DNA, while the neutral sugar residue is exposed at the bolaplex surface. This structure may favor neutrality of the bolaplex at higher N/Ps. Presence of DOPE does not change this tendency, but only shifts the complex neutralization to higher N/P ratios.

To access the nanoscopic architecture of bolaplexes, we performed atomic force microscopy (AFM) measurements in liquid (buffer) phase on a mica surface. An efficient absorption of the bolaplexes (N/P 2 or 1.2) at the mica surface was achieved only in the presence of magnesium cations. This indicates that the bolaplexes at the studied N/P ratios are negatively charged, so that Mg^{2+} ions act as a link between bolaplexes and the negatively charged mica surface. Orn-C16-G bolaplexes with pDNA formed relatively small and spherical structures (Figure 7A). The average height and width of the particles were 12 and 120 nm, respectively, which correspond to an average particle volume of about 1.7×10^5 nm^3 and an equivalent spherical particle diameter of 70 nm. This size is smaller than the one observed by DLS for N/P 2 (12 μM bola). Several reasons may explain this discrepancy. At first, the smaller size particles observed by AFM is based on a particle by particle data analysis, while DLS measures an average size with higher sensitivity to larger particles. Indeed, the DLS data based on particle number

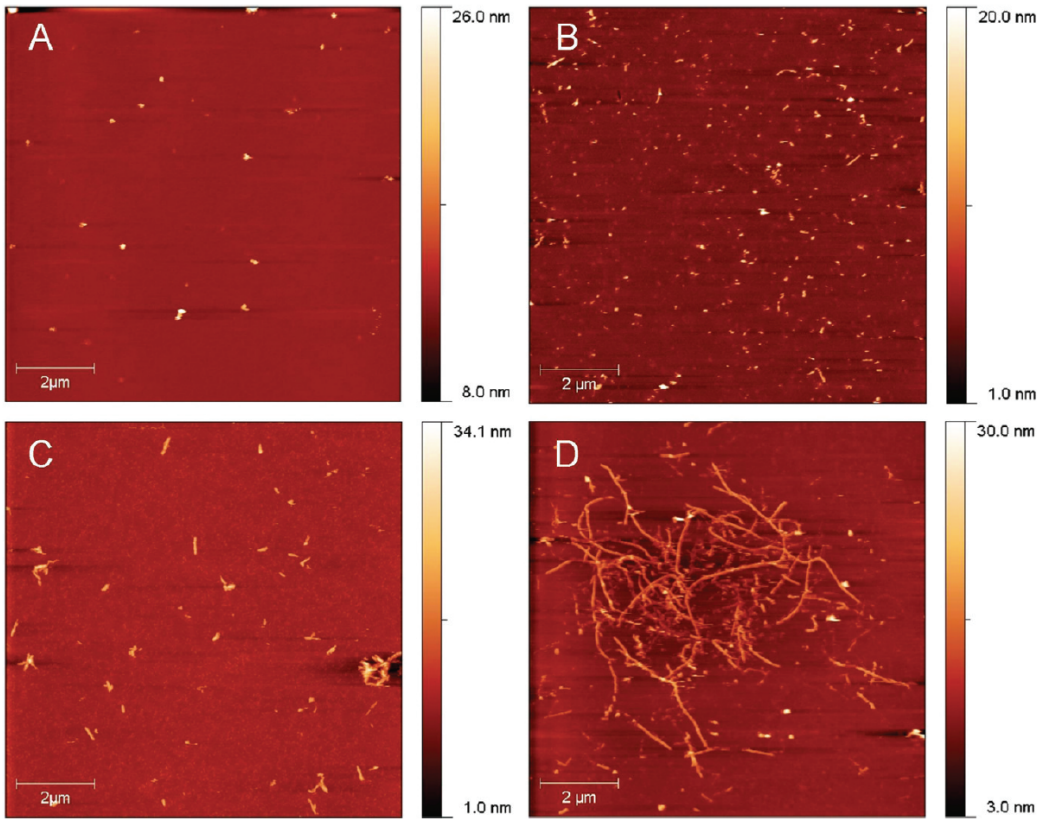

Figure 7. AFM images of Orn-C16-G (A and B, N/P 2) and Orn-C20-G (C and D, N/P 1.2) bolaplexes with pDNA (A and C) and CT-DNA (B and D). Images were obtained by tapping mode.

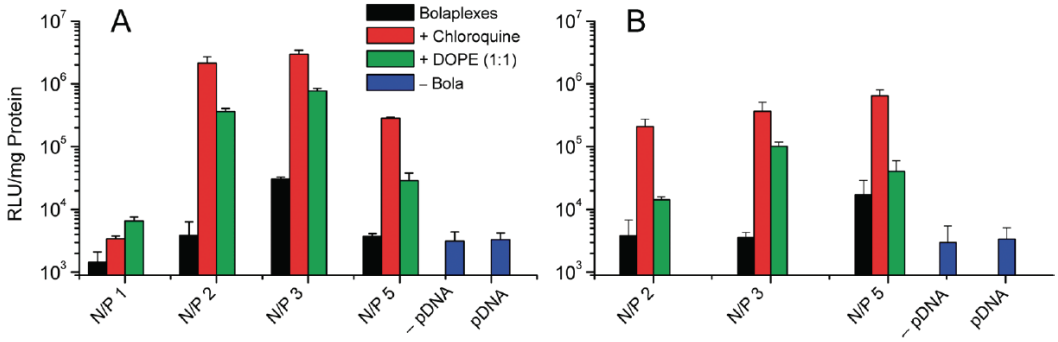

Figure 8. Transfection efficiency of the Orn-C16-G bolaplexes at different N/P ratios in COS-7 cells without (A) and with serum (B). Cells were incubated in serum-free Opti-MEM (A) or complete culture medium, DMEM containing 10% of FBS (B) with a bolaplex composed of plasmid DNA (1 μg per well), Orn-C16-G, and DOPE (when indicated). For some samples, the medium contained 100 μM chloroquine. After 3 h, 10% of FBS was added to the serum-free samples, while for all the samples with chloroquine the transfection medium was replaced with fresh complete culture medium. The luciferase activity quantification was performed after 48 h of incubation. Transfection efficiency determined from the luciferase assay was expressed as RLU/mg of protein. The negative controls were nontreated cells (-pDNA) and those transfected with naked pDNA (pDNA). The experiments were repeated six times for serum-free samples (A) and three times for samples with serum (B).

statistics is much closer to AFM data than those based on volume analysis (Table 1). Moreover, DLS data provides a hydrodynamic size of the particles, which is larger than the real size. Finally, in AFM measurements, the particles are stabilized by adsorption at the surface, while in DLS they are free in solution and can further aggregate to form larger particles. Bolaplexes of Orn-C16-G with CT-DNA showed high polydispersity and formed both spherical and short rodlike structures (Figure 7B). The presence of short rods of 8−10 nm height, 40−60 nm width, and 300−600 nm length could be explained by the linear structure of CT-DNA that favored the formation of elongated structures. In contrast, Orn-C20-G/DNA bolaplexes at N/P 2 were very large and polydisperse, in line with DLS data, which prompted us to study the bolaplexes at N/P 1.2. Remarkably, the complexes at N/P 1.2 showed predominantly rodlike structures for both pDNA and CT-DNA (Figure 7C and D). However, in the case of pDNA, the observed rods were relatively short, having height and width around 10 and 120 nm, respectively, while in the case of CT-DNA, they correspond to very long fibers of 16 nm height and 80 nm width. The formation of these "spaghetti-like" structures was previously reported for cationic lipids (*38*). It was proposed that in this kind of structure, the DNA molecule is located in the core, being surrounded by the lipid membrane. Probably, Orn-C20-G/CT-DNA bolaplexes present a similar structure, where single or multiple DNA strands are surrounded by a monolayer of bola molecules, similarly to the idealistic model in Figure 1B.

Transfection Efficiency and Cytotoxicity. The transfection efficiency of bolaplexes was in serum-free and serum-containing media for the different formulations by using the luciferase expression assay (Figure 8). For serum-free samples (Figure 8A), considerable transfection efficiency was observed for Orn-C16-G bolaplexes at N/P 2, 3, and 5 only in the presence of helper lipid DOPE or the endosomolytic reagent chloroquine (*28*). The better efficiency observed in the presence of DOPE is in line with previously reported data concerning other bolaamphiphiles (*21, 23*). DOPE probably improves the fusion of bolaplexes with cellular and endosomal membranes (*39, 40*). However, the strong effect of chloroquine on bolaplexes delivery is reported for the first time. This result clearly shows that the key barrier for internalization of bolaplexes is related to the endosomal escape. In the presence of serum, the transfection efficiency decreased significantly for all samples with DOPE (Figure 8B), which is in line with previous reports showing that DOPE-containing lipoplexes are highly sensitive to serum (*41*). In the presence of chloroquine, the effect of serum was less important, and the transfection efficiency increased systematically at higher N/P ratio. At N/P = 5, the sample with serum showed even slightly higher transfection efficiency than that without serum (Figure 8). Similar results were reported for lipoplexes, where higher N/Ps increased their resistance to serum (*42*).

On the other hand, bolaplexes of Orn-C20-G displayed relatively poor transfection efficiency for most of the formulations, which can be related to their larger size and spaghetti-like architecture (Figure 7). It should be noted that the observed values of transfection efficiency for Orn-C16-G were significantly lower than that for highly efficient commercial agent jetPEI (3×10^8 RLU/mg protein in the present study), while they were comparable with those recently reported for some other bolaamphiphiles (*21, 22*). Taking into account that the area of bolaamphiphiles as nonviral vectors is still poorly explored, we believe that there is a lot of room for improvement of their transfection efficiency. It will require optimization of bola chemical structure to achieve better control on the size and stability of the bolaplexes as well as on their ability to escape from endosomes. This work is currently in progress and will be reported in due course.

MTT-based assay suggested that new bolas do not show any considerable cytotoxicity. In the concentration range 30−200 μM of bolas with 48 h incubation, the observed cell viability was >80%, while for jetPEI (150 μM, expressed for nitrogen residues) it was only about 60% (see Supporting Information). The MTT results correlated well with the observed relatively high total protein (>80% vs. control) after 48 h of transfection with bolaplexes. This low cytotoxicity of the new bolas is an important advantage compared to polyplexes and lipoplexes. Thus, the obtained results showed the potentials of the new bolas molecules, especially Orn-C16-G, for the elaboration of highly efficient nonviral vectors.

CONCLUSIONS

We have synthesized three new bolaamphiphiles, bearing cationic and neutral groups at opposite sides of a hydrophobic spacer. The two bolaamphiphiles with more hydrophobic spacers exhibit low critical aggregation concentration and stronger affinities to DNA. At low N/P ratio (1.2), these bolas form bolaplexes of relatively small size, showing spherical and rodlike structures, while at higher N/P ratio their size increases due to neutralization of the complexes. Bolaplexes showed considerable transfection efficiency only in presence of the helper lipid DOPE or the endosomolytic agent chloroquine, indicating that the endosomal escape constitutes the main barrier to the internalization of these complexes. The present work provides strong basis for a further development of new efficient gene delivery vectors based on this original class of compounds.

ACKNOWLEDGMENT

This work was supported by Fondation pour la Recherche Médicale (FRM). We thank the groups of J.-S. Remy and B. Frisch for help with luminometry and DLS measurements. We also thank G. Zuber for fruitful discussions.

Supporting Information Available: Procedures for synthesis of Orn-C20-G and Orn-C8-C12-G. Some DLS data. Total protein and MTT-based cytotoxicity assays. This material is available free of charge via the Internet at http://pubs.acs.org.

LITERATURE CITED

(1) Fuhrhop, J. H., and Wang, T. (2004) Bolaamphiphiles. *Chem. Rev. 104*, 2901–2938.
(2) Damste, J. S. S., Schouten, S., Hopmans, E. C., Van Duin, A. C. T., and Geenevasen, J. A. J. (2002) Crenarchaeol: The characteristic core glycerol dibiphytanyl glycerol tetraether membrane lipid of cosmopolitan pelagic crenarchaeota. *J. Lipid Res. 43*, 1641–1651.
(3) Derosa, M., Gambacorta, A., and Gliozzi, A. (1986) Structure, Biosynthesis, And Physicochemical Properties Of Archaebacterial Lipids. *Microbiol. Rev. 50*, 70–80.
(4) Stetter, K. O. (1996) Hyperthermophilic procaryotes. *FEMS Microbiol. Rev. 18*, 149–158.
(5) Shimizu, T., Masuda, M., and Minamikawa, H. (2005) Supramolecular nanotube architectures based on amphiphilic molecules. *Chem. Rev. 105*, 1401–1443.
(6) Kameta, N., Masuda, M., Minamikawa, H., Mishima, Y., Yamashita, I., and Shimizu, T. (2007) Functionalizable organic nanochannels based on lipid nanotubes: Encapsulation and nanofluidic behavior of biomacromolecules. *Chem. Mater. 19*, 3553–3560.
(7) Wang, X., and Liang, Y. (2001) Formation of monolayer lipid membranes in water and ethanol from bolaamphiphiles. *J. Colloid Interface Sci. 233*, 364–366.
(8) Mintzer, M. A., and Simanek, E. E. (2009) Nonviral vectors for gene delivery. *Chem. Rev. 109*, 259–302.
(9) Martin, B., Sainlos, M., Aissaoui, A., Oudrhiri, N., Hauchecorne, M., Vigneron, J. P., Lehn, J. M., and Lehn, P. (2005) The design of cationic lipids for gene delivery. *Curr. Pharm. Des. 11*, 375–394.
(10) Safinya, C. R. (2001) Structures of lipid-DNA complexes: Supramolecular assembly and gene delivery. *Curr. Opin. Struct. Biol. 11*, 440–448.
(11) Chesnoy, S., and Huang, L. (2000) Structure and function of lipid-DNA complexes for gene delivery. *Annu. Rev. Biophys. Biomol. Struct. 29*, 27–47.
(12) Hirko, A., Tang, F., and Hughes, J. A. (2003) Cationic lipid vectors for plasmid DNA delivery. *Curr. Med. Chem. 10*, 1185–1193.
(13) Huang, L., Hung, M.-C., and Wagner, E., Eds. (1999) *Nonviral Vectors for Gene Therapy*, Academic Press, London.
(14) Demeneix, B., Hassani, Z., and Behr, J. P. (2004) Towards multifunctional synthetic vectors. *Curr. Gene. Ther. 4*, 445–455.
(15) Mastrobattista, E., van der Aa, M. A. E. M., Hennink, W. E., and Crommelin, D. J. A. (2006) Artificial viruses: a nanotechnological approach to gene delivery. *Nat. Rev. Drug Discovery 5*, 115–121.
(16) Nishikawa, M., and Huang, L. (2001) Nonviral vectors in the new millennium: Delivery barriers in gene transfer. *Hum. Gene Ther. 12*, 861–870.
(17) Zuber, G., Dauty, E., Nothisen, M., Belguise, P., and Behr, J. P. (2001) Towards synthetic viruses. *Adv. Drug Delivery Rev. 52*, 245–253.
(18) Zuber, G., Zammut-Italiano, L., Dauty, E., and Behr, J. P. (2003) Targeted gene delivery to cancer cells: Directed assembly

of nanometric DNA particles coated with folic acid. *Angew. Chem., Int. Ed. 42*, 2666–2669.
(19) Zhang, S., Zhao, Y., Zhao, B., and Wang, B. (2010) Hybrids of Nonviral Vectors for Gene Delivery. *Bioconjugate Chem. 21*, 1003–1009.
(20) Koltover, I., Salditt, T., Radler, J. O., and Safinya, C. R. (1998) An inverted hexagonal phase of cationic liposome-DNA complexes related to DNA release and delivery. *Science 281*, 78–81.
(21) Gaucheron, J., Santaella, C., and Vierling, P. (2001) In vitro gene transfer with a novel galactosylated spermine bolaamphiphile. *Bioconjugate Chem. 12*, 569–575.
(22) Fabio, K., Gaucheron, J., Di Giorgio, C., and Vierling, P. (2003) Novel galactosylated polyamine bolaamphiphiles for gene delivery. *Bioconjugate Chem. 14*, 358–367.
(23) Brunelle, M., Polidori, A., Denoyelle, S., Fabiano, A. S., Vuillaume, P. Y., Laurent-Lewandowski, S., and Pucci, B. (2009) A structure-activity investigation of hemifluorinated bifunctional bolaamphiphiles designed for gene delivery. *C. R. Chim. 12*, 188–208.
(24) Denoyelle, S., Polidori, A., Brunelle, M., Vuillaume, P. Y., Laurent, S., ElAzhary, Y., and Pucci, B. (2006) Synthesis and preliminary biological studies of hemifluorinated bifunctional bolaamphiphiles designed for gene delivery. *New J. Chem. 30*, 629–646.
(25) Eaton, M. A. W., Baker, T. S., Catterall, C. F., Crook, K., Macaulay, G. S., Mason, B., Norman, T. J., Parker, D., Perry, J. J. B., Taylor, R. J., Turner, A., and Weir, A. N. (2000) A new self-assembling system for targeted gene delivery. *Angew. Chem., Int. Ed. 39*, 4063–4067.
(26) Réthoré, G., Montier, T., Le Gall, T., Delépine, P., Cammas-Marion, S., Lemiègre, L., Lehn, P., and Benvegnu, T. (2007) Archaeosomes based on synthetic tetraether-like lipids as novel versatile gene delivery systems. *Chem. Commun. 20*, 2054–2056.
(27) Lainé, C., Mornet, E., Lemiègre, L., Montier, T., Cammas-Marion, S., Neveu, C., Carmoy, N., Lehn, P., and Benvegnu, T. (2008) Folate-equipped pegylated archaeal lipid derivatives: Synthesis and transfection properties. *Chem.—Eur. J. 14*, 8330–8340.
(28) Cotten, M., Langle-Rouault, F., Kirlappos, H., Wagner, E., Mechtler, K., Zenke, M., Beug, H., and Birnstiel, M. L. (1990) Transferrin-polycation-mediated introduction of DNA into human leukemic cells: Stimulation by agents that affect the survival of transfected DNA or modulate transferrin receptor levels. *Proc. Natl. Acad. Sci. U.S.A. 87*, 4033–4037.
(29) Mosmann, T. (1983) Rapid colorimetric assay for cellular growth and survival: Application to proliferation and cytotoxicity assays. *J. Immunol. Meth. 65*, 55–63.
(30) Slavik, J. (1982) Anilinonaphthalene Sulfonate as a Probe of Membrane-Composition and Function. *Biochim. Biophys. Acta 694*, 1–25.
(31) Lentz, B. R. (1993) Use of fluorescent probes to monitor molecular order and motions within liposome bilayers. *Chem. Phys. Lipids 64*, 99.
(32) M'Baye, G., Mely, Y., Duportail, G., and Klymchenko, A. S. (2008) Liquid ordered and gel phases of lipid bilayers: fluorescent probes reveal close fluidity but different hydration. *Biophys. J. 95*, 1217–1225.
(33) Meister, A., and Blume, A. (2007) Self-assembly of bipolar amphiphiles. *Curr. Opin. Colloid Interface Sci. 12*, 138–147.
(34) Lleres, D., Dauty, E., Behr, J. P., Mely, Y., and Duportail, G. (2001) DNA condensation by an oxidizable cationic detergent. Interactions with lipid vesicles. *Chem. Phys. Lipids 111*, 59–71.
(35) Pitard, B., Oudrhiri, N., Vigneron, J. P., Hauchecorne, M., Aguerre, O., Toury, R., Airiau, M., Ramasawmy, R., Scherman, D., Crouzet, J., Lehn, J. M., and Lehn, P. (1999) Structural characteristics of supramolecular assemblies formed by guanidinium-cholesterol reagents for gene transfection. *Proc. Natl. Acad. Sci. U.S.A. 96*, 2621–2626.
(36) Xu, Y., Hui, S. W., Frederik, P., and Szoka, F. C., Jr. (1999) Physicochemical characterization and purification of cationic lipoplexes. *Biophys. J. 77*, 341–353.
(37) Findeis, M. A., Ed. (2001) *Nonviral Vectors for Gene Therapy: Methods and Protocols*, Humana Press, Clifton, NJ.
(38) Sternberg, B., Sorgi, F. L., and Huang, L. (1994) New structures in complex formation between DNA and cationic liposomes visualized by freeze-fracture electron microscopy. *FEBS Lett. 356*, 361–366.
(39) Felgner, J. H., Kumar, R., Sridhar, C. N., Wheeler, C. J., Tsai, Y. J., Border, R., Ramsey, P., Martin, M., and Felgner, P. L. (1994) Enhanced gene delivery and mechanism studies with a novel series of cationic lipid formulations. *J. Biol. Chem. 269*, 2550–2561.
(40) Farhood, H., Serbina, N., and Huang, L. (1995) The role of dioleoyl phosphatidylethanolamine in cationic liposome mediated gene transfer. *Biochim. Biophys. Acta 1235*, 289–295.
(41) Li, S., Tseng, W. C., Beer Stolz, D., Wu, S. P., Watkins, S. C., and Huang, L. (1999) Dynamic changes in the characteristics of cationic lipidic vectors after exposure to mouse serum: Implications for intravenous lipofection. *Gene Ther. 6*, 585–594.
(42) Yang, J. P., and Huang, L. (1997) Overcoming the inhibitory effect of serum on lipofection by increasing the charge ratio of cationic liposome to DNA. *Gene Ther. 4*, 950–960.

BC100334T

Supporting information

New unsymmetrical bolaamphiphiles: synthesis, assembly with DNA and application for gene delivery

Namrata Jain, Youri Arntz, Valerie Goldschmidt, Guy Duportail, Yves Mely, Andrey S. Klymchenko

1. Synthesis of Orn-C12-G and Orn-C8-C12-G bolas.

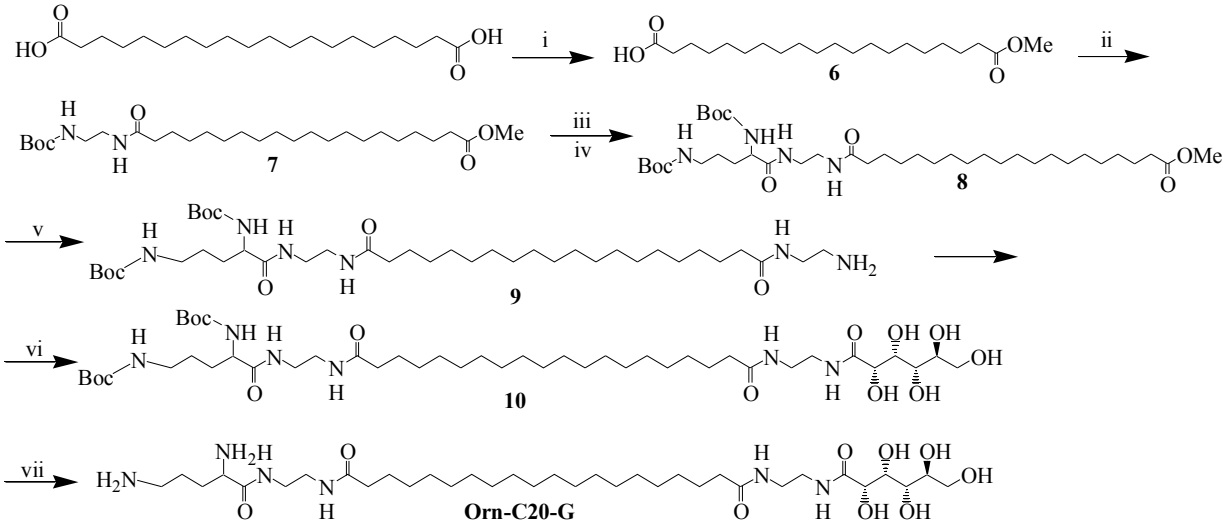

Reagents: (i) MeOH, H_2SO_4, $C_2H_4Cl_2$, 85°C, 24h (25%) ; (ii) BOP, HOBt, DIEA, DMF, CH_2Cl_2, 24h (72%) ; (iii) TFA, H_2O, 1h;
(iv) BOP, HOBt, DIEA, DMF, CH_2Cl_2, 40°C, 24h (70%) ; (v) Ethylene Diamine, 70°C, 72h (93%) ;
(vi) Gluconic acid lactone, MeOH, DIEA ; (vii) TFA, H_2O, 1h (90%).

Scheme S1. Synthesis of **Orn-C20-G.**

Eicosanedioic acid monomethyl ester (6). The procedure was adapted from Ref. (1). Eicosanedioic acid (14.6 mmol, 5 g) was dissolved in 300 ml of ethylene chloride at 85°C. Methanol (7.4 mmol, 0.59 ml) was added to the clear solution, then H_2SO_4 (1.4 ml) was cautiously added, and the reaction was left for reflux overnight at 85°C. The solvent was concentrated and water was added. Three phases were obtained: aqueous, organic and slurry. To the organic phase, which contained mainly di- and mono-esters, carbon tetrachloride was added and placed in a separate funnel. The organic layer was washed with water, then dried over $MgSO_4$ and evaporated. Product was subjected to column chromatography, where di-ester was eluded with dichloromethane and the monoester **6** with ethyl acetate (25 % yield). ^{1}H NMR ($CDCl_3$, 300 MHz): 3.65 (s, 3H), 2.36-2.26 (m, 4H), 1.65-1.56 (m, 4H), 1.39-1.19 (m, 28H).

19-(2-tert-Butoxycarbonylamino-ethylcarbamoyl)-nonadecanoic acid methyl ester (7). *N*-Boc-ethylenediamine (1 mmol, 0.162 g) was coupled with mono-methyl ester **6** (0.84 mmol, 0.3 g) using BOP (0.93 mmol, 0.41 g), HOBt (1.2 mmol, 0.16 g) and DIEA (3.4 mmol, 0.6 ml) in DMF (5 ml) and dichloromethane (20 ml). The mixture was stirred overnight at room temperature. Then the solvent was

evaporated and the product was crystallized from acetonitrile to give product **7** (0.3 g, 72 %). ^{1}H NMR (DMSO, 300 MHz): 7.62 (s, 1H), 6.61 (s, 1H), 3.58 (s, 3H), 3.05 (t, 2H), 2.97 (t, 2H), 2.27 (t, 2H), 2.03 (t, 2H), 1.57-1.42 (m, 4H), 1.4-1.33 (m, 9H), 1.32-1.17 (m, 28H). LC-MS: (m/z) Found $[M+1]^+ = 399.2$ (calcd for $C_{28}H_{54}N_2O_5^+$ - $C_5H_9O_2$ (Boc) = 399.3).

19-[2-(2,5-Bis-tert-butoxycarbonylamino-pentanoylamino)-ethylcarbamoyl]-nonadecanoic acid methyl ester (8). Boc-group was removed from **7** (0.54 mmol, 0.27 g) by treating with 1 ml TFA and 3% H_2O, for 1 h at RT. The solvent was evaporated and obtained de-protected amine was coupled with 2,5-Bis-tert-butoxycarbonyl-aminopentanoic acid (0.62 mmol, 0.207 g) using BOP (0.93 mmol), HOBt (1.2 mmol) and DIEA (3.4 mmol, 0.6 ml) in DMF (10 ml) and dichloromethane (10 ml). The mixture was stirred overnight at 40 °C. Then the solvent was evaporated and the product was crystallized from ethyl acetate. The precipitate was filtered off and dried to give solid crystals of compound **8** (0.34 g, 70 %). ^{1}H NMR ($CDCl_3$, 300 MHz): 6.95 (s, 1H), 6.39 (s, 1H), 5.18 (s, 1H), 4.76 (s, 1H), 4.17 (s, 1H), 3.65 (t, 3H), 3.4-3.2 (m, 5H), 3.11-2.99 (m, 1H), 2.28 (t, 2H), 2.15 (t, 2H), 1.87-1.7 (m, 2H), 1.67-1.5 (m, 8H), 1.46-1.38 (m, 18H), 1.34-1.17 (m, 30H). LC-MS: (m/z) Found $[M+1]^+ = 613.4$ (calcd for $C_{38}H_{72}N_4O_5^+$ - $C_5H_9O_2$ (Boc) = 613.4).

(1-{2-[19-[2-(2-Amino-ethylcarbamoyl)-nonadecanoylamino]-ethylcarbamoyl}-4-tert-butoxycarbonylamino-butyl)-carbamic acid tert-butyl ester (9). Methyl ester **8** (0.4 mmol, 0.3 g) was reacted with ethylenediamine (150 mmol 10 ml) for 72 h at 70°C. Then the excess of ethylenediamine was evaporated and water was poured into the reaction flask. Formed precipitate was filtered off to give compound **9** (0.29 g, 93 %). ^{1}H NMR (CD_3OD, 300 MHz): 3.96 (s, 1H), 3.05 (t, 2H), 2.73 (t, 2H), 2.23-2.16 (m, 4H), 1.67-1.5 (m, 8H), 1.46-1.44 (m, 18H), 1.39-1.23 (m, 30H). LC-MS: (m/z) Found $[M+1]^+ =$ 741.4 (calcd for $C_{39}H_{76}N_6O_7^+ = 741.5$).

[4-tert-Butoxycabonylamino-4-(2-{19-[2-(2,3,4,5,6-pentahydroxy-hexanoylamino)-ethylcarbamoyl]-nonadecanoylamino}-ethylcabamoyl)-butyl]-carbamic acid tert-butyl ester (10). δ-Gulonic-γ-Lactone (0.23 mmol, 0.04 g) was added to solution of **9** (0.13 mmol, 0.1 g) in 10 ml of methanol. Then, DIEA (1.4 mmol, 0.24 ml) was added and reaction mixture was stirred at 70°C for about 24 h. Solvents were evaporated in vacuo. The obtained compound was crystallized from methanol to give product **10** (0.095 g, 95 %). ^{1}H NMR (CD_3OD, 300 MHz): 4.21 (s,1H), 4.1 (s, 1H), 3.98 (s, 1H), 3.84-3.59 (m, 5H), 3.07 (t, 2H), 2.25-2.12 (m, 4H), 1.68-1.49 (m, 8H), 1.49-1.4 (m, 18H), 1.4-1.21 (m, 30H). LC-MS: (m/z) Found $[M+1]^+ = 919.6$ (calcd for $C_{45}H_{86}N_6O_{13}^+ = 919.6$).

Eicosanedioic acid [2-(2,5-diamino-pentnoylamino)-ethyl]-amide[2-(2,3,4,5,6-pentahydroxy-hexanoylamino)-ethyl]-amide (Orn-C20-G). 40 mg of the Boc-protected product **10** was treated with 0.4 ml TFA and 3 % H2O for clean removal of Boc group to get final compound **Orn-C20-G** (27 mg, 90 %). LC-MS: (m/z) Found $[M+1]^+ = 719.5$ (calcd for $C_{35}H_{71}N_6O_9^+ = 719.5$).

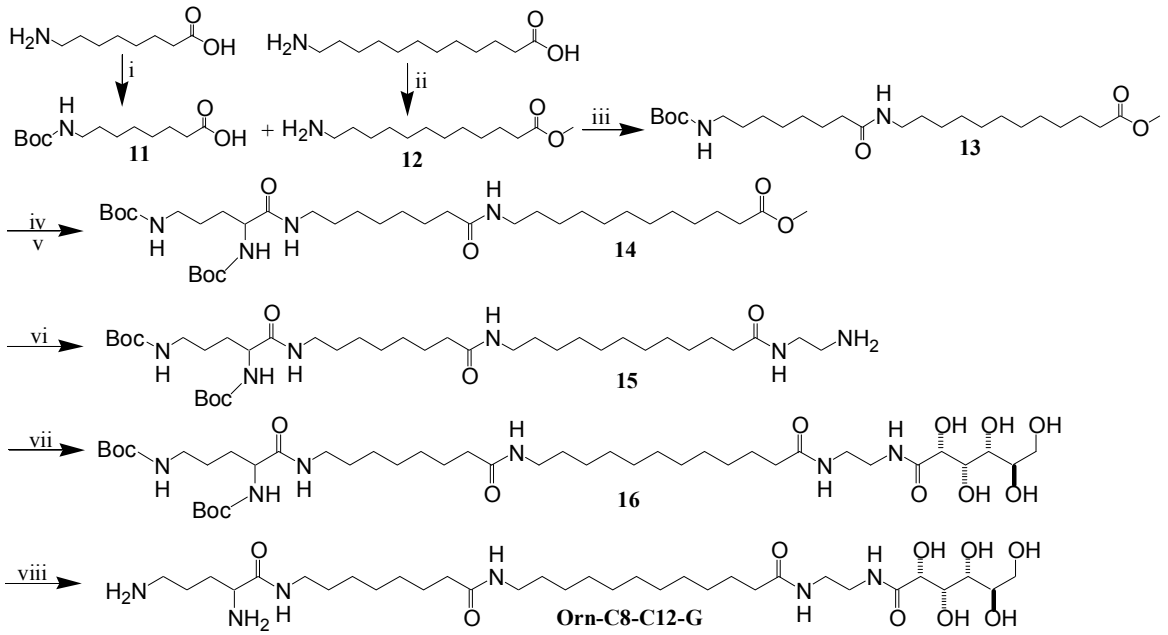

Reagents: (i) Boc_2O, DMF, CH_2Cl_2, 20h (92%); (ii) $SOCl_2$, MeOH, 20h (94%); (iii) BOP, HOBt, DIEA, DMF, CH_2Cl_2, 24h (81%); (iv) TFA, CH_2Cl_2, 1h; (v) BOP, HOBt, DIEA, DMF, CH_2Cl_2, 24h (92%); (vi) $C_2H_8N_2$, 70°C, 72h (96%); (vii) MeOH, DIEA, 70°C, 24h; (viii) TFA, H_2O, 1h (92%).

Scheme S2. Synthesis of **Orn-C8-C12-G.**

8-tert-Butoxycabonylamino-octanoic acid (11). Amino group of 8-Aminooctanoic acid (31.4 mmol, 5 g) was protected by Boc using Di-tert-butyl dicarbonate (34.6 mmol, 7.54 g) in solution of DMF (30 ml) and dichloromethane (40 ml).Then, DIEA (94.2 mmol, 16.38 ml) was added and the reaction mixture was stirred for 20 h at RT. The solvent was evaporated and product was crystallized from dichloromethane. The precipitate was filtered off and dried to give compound **11** (7.5 g, 92 %). ^{1}H NMR ($CDCl_3$, 300 MHz): δ 4.55 (s, 1H), 3.07 (t, 2H), 2.3 (t, 2H), 1.67-1.5 (t, 4H), 1.56-1.37 (t, 9H), 1.37-1.21 (m, 6H).

12-Amino-dodecanoic acid methyl ester (12). Thionyl chloride (103.4 mmol, 7.5 ml) was added drop-wise to 100 ml of methanol at 0 °C and the mixture was stirred for another 20 min. Then, 10 g of 12-aminododecanoic acid (46.5 mmol) was added and reaction mixture was stirred for 20 h at RT. The solvent was evaporated and product was crystallized from heptane to give compound **12** (10 g, 94 %). ^{1}H NMR (DMSO, 300 MHz): δ 7.89 (s, 2H), 3.68 (s, 3H), 2.75 (t, 2H), 2.28 (t, 2H), 1.58-1.15 (m, 18H).

12-(8-tert-Butoxycarbonylamino-octanoylamino)-dodecanoic acid methyl ester (13). Compound **12** (6.5 mmol, 1.5 g) was coupled with **11** (7.2 mmol, 1.87 g) using BOP (7.2 mmol, 3.18 g), HOBt (8.9 mmol, 1.2 g) and DIEA (25.9 mmol, 4.5 ml) in DMF (15 ml) and dichloromethane (30 ml). The reaction mixture was stirred 24 h at RT. Then the solvents were evaporated and product was crystallized from ethyl acetate : heptane (8:2). The precipitate was filtered off and dried to give compound **13** (2.5 g, 81 %). ^{1}H NMR ($CDCl_3$, 300 MHz): δ 5.41 (s, 1H), 4.48 (s, 1H), 3.65 (s, 3H), 3.21 (t, 2H), 3.08 (t, 2H), 2.29 (t, 2H), 2.13 (t, 2H), 1.69-1.15 (m, 39H). LC-MS: (m/z) Found $[M+1]^+$ = 371.2 (calcd for $C_{26}H_{50}N_2O_5^+$ - $C_{10}H_{18}O_4$ (2Boc) = 371.2).

12-[8-(2,5-Bis-tert-butoxycarbonylamino-pentanoylamino)-octanoylamino]-dodecanoic acid methyl ester (14). Boc group of **13** (2.13 mmol, 1 g) was removed in dichloromethane (3 ml) in the presence of 2 ml of TFA for 1 h at RT. The solvent was evaporated and 1 g (2.1 mmol) of the obtained deprotected amine was coupled with 2,5-Bis-tert-butoxycarbonyl amino-pentanoic acid (2.2 mmol, 0.72 g) using BOP (2.4 mmol, 1.04 g), HOBt (2.96 mmol, 0.4 g) and DIEA (8.63 mmol, 1.5 ml) in DMF (5 ml) and dichloromethane (15 ml). The mixture was stirred overnight at RT. Then solvent was evaporated and product **14** (1.3 g, 92 %) was crystallized from acetonitrile. ^{1}H NMR ($CDCl_3$, 300 MHz): δ 6.46 (s, 1H), 5.56 (s, 1H), 5.2 (s, 1H), 4.73 (s, 1H), 4.17 (s, 1H), 3.65 (s, 3H), 3.28-3.04 (m, 6H), 2.28 (t, 2H), 2.13 (t, 2H), 1.66-1.19 (m, 50H). LC-MS: (m/z) Found $[M+1]^+$ = 585.4 (calcd for $C_{36}H_{68}N_4O_8^+$ - $C_{10}H_{18}O_4$ (2Boc) = 585.4).

(1-{7-[11-(2-Amino-ethylcarbamoyl)-undecylcarbamoyl]-heptylcarbamoyl}-4-tert-butoxycarbonylamino-butyl)-carbamic acid tert-butyl ester (15). The methyl ester of **14** (1.75 mmol, 1.2 g) was reacted with ethylenediamine (150 mmol, 10 ml) for 72 h at 70°C. Then the excess of ethylenediamine was evaporated, the water was added and the product **15** was filtered (1.2 g, 96 %). ^{1}H NMR (CD_3OD, 300 MHz): δ 3.99 (s, 1H), 3.28-3.13 (m, 6H), 3.06 (t, 2H), 2.73 (t, 2H), 2.24-2.15 (m, 4H), 1.67-1.28 (m, 50H). LC-MS: (m/z) Found $[M+1]^+$ = 713.4 (calcd for $C_{37}H_{72}N_6O_7^+$ = 713.4).

[4-tert-Butoxycabonylamino-4-(7-{11-[2-(2,3,4,5,6-pentahydroxy-hexanoylamino)-ethylcarbamoyl]-undecylcarbamoyl}-heptylcabamoyl)-butyl]-carbamic acid tert-butyl ester (16). δ-Gulonic-γ-Lactone (0.95 mmol, 0.17 g) was added to solution of **15** (0.56 mmol, 0.4 g) in 30 ml of methanol. Then, DIEA (5.64 mmol, 0.98 ml) was added and the reaction mixture was stirred at 70°C for about 24 h. Solvents were evaporated in vacuo. The obtained compound was crystallized from methanol to get product **16** (0.15 g, 88 %). ^{1}H NMR (DMSO, 300 MHz): δ 7.83-7.61 (m, 4H), 6.8-6.64 (m, 2H), 5.35 (d, 1H), 4.57-4.26 (m, 5H), 4.0-3.75 (m, 3H), 3.61-3.38 (m, 6H), 3.22-2.81 (m, 11H), 2.06-1.95 (m, 4H), 1.54-1.37 (m, 10H), 1.36-1.32 (m, 18H), 1.31-1.11 (m, 24H). LC-MS: (m/z) Found $[M+1]^+$ = 891.6 (calcd for $C_{43}H_{82}N_6O_{13}^+$ = 891.6).

12-[8-(2,5-Diamino-pentanoylamino)-octanoylamino]-dodecanoic acid[2-(2,3,4,5,6-pentahydroxy-hexanoylamino)-ethyl]-amide (Orn-C8-C12-G). Boc group of **16** was removed from 0.1 g (0.11 mmol) of the compound using 1 ml TFA and 3% of H2O to afford the final product **Orn-C8-C12-G** (0.095 g, 92 %). MS: (m/z) Found $[M+1]^+$ = 691.5 (calcd for $C_{33}H_{67}N_6O_9^+$ = 691.5). MS: (m/z) Found $[M+1]^+$ = 691.5 (calcd for $C_{33}H_{67}N_6O_9^+$ = 691.5).

2. 1,8-ANS fluorescence data.

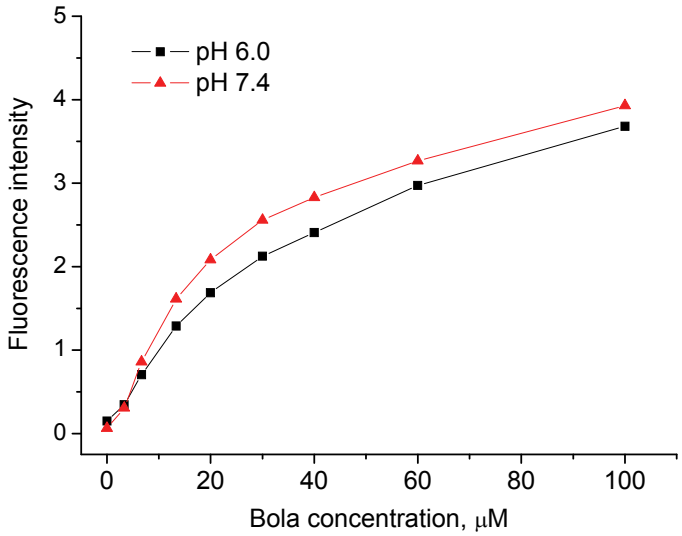

Fig. S1. Fluorescence intensity of 1,8-ANS (50 nM) as a function of Orn-C20-G bola concentration at two different pH.

3. Gel electrophoresis data.

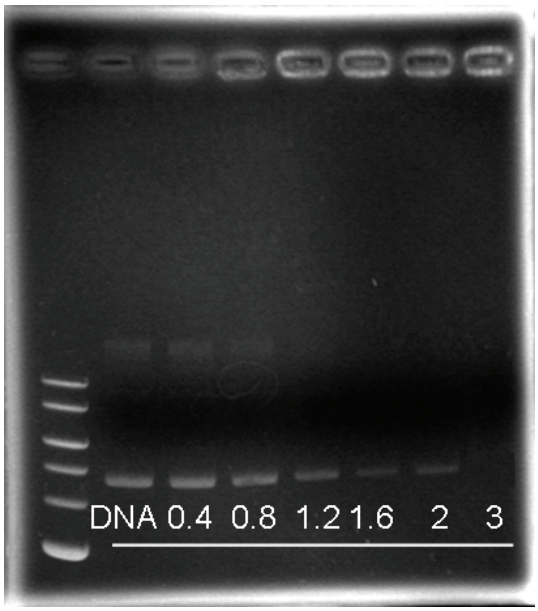

Fig. S2. Agarose gel electrophoresis (0.9%) of Orn-C16-G/DOPE (1:1) mixture complexed with pDNA at different N/P ratios. Bands at the left of the gel correspond to 10 kbp DNA ladder.

4. DLS data

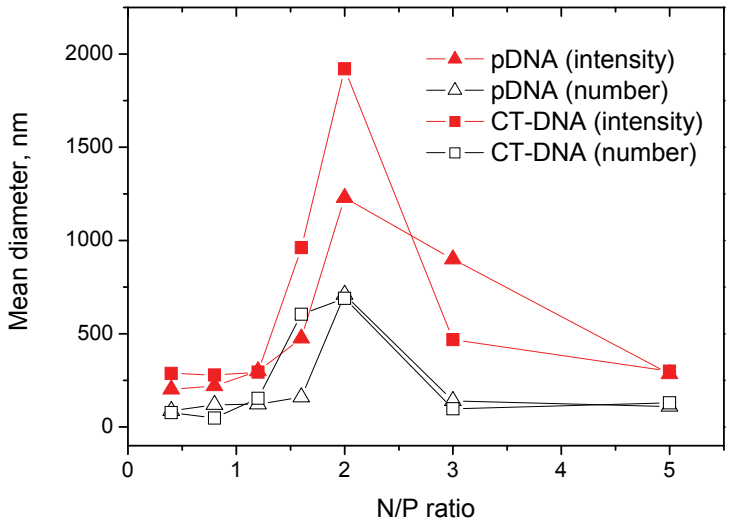

Fig. S3. Mean diameters as measured by DLS of Orn-C16-G complexes with pDNA (triangle) and CT-DNA (square) at different N/P ratios. The experiments were performed in MES buffer (pH 7.4) by addition of increasing quantities of bola stock solution (in DMF/water) to pDNA solution. Each measurement was proceeded 5 min after each addition of bola aliquot. Mean diameters are presented based on statistics of scattered intensity (filled symbols) and particle number (open symbols).

5. Cytotoxicity and total protein assays.

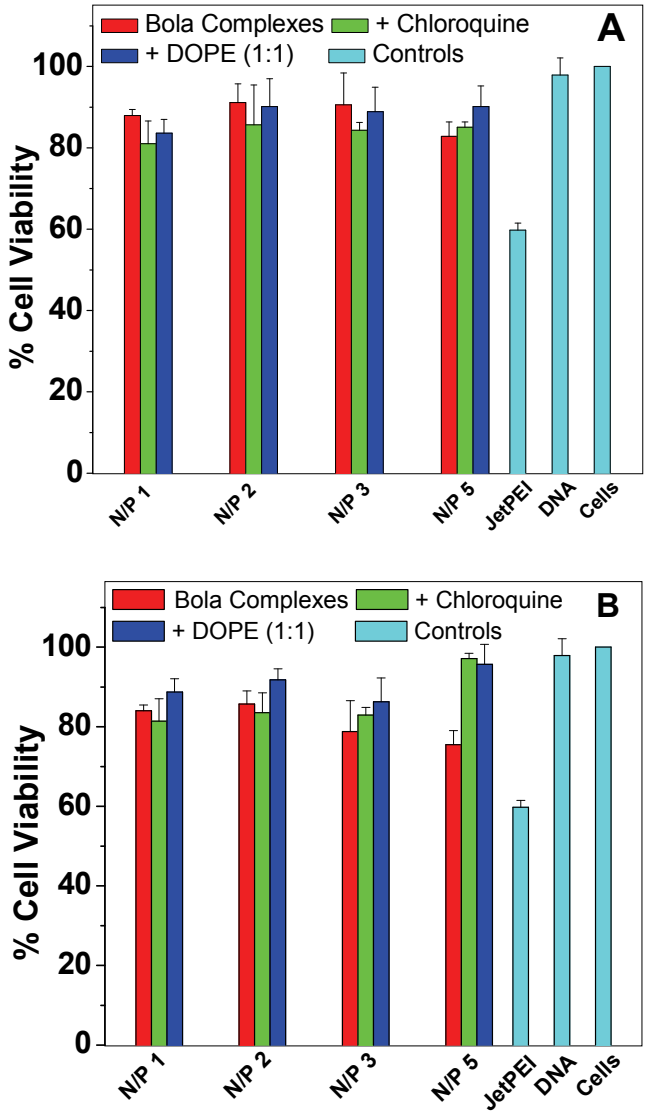

Fig. S4. Total protein concentration from the transfection experiments in COS-7 cells for **Orn-C16-G** (A) and **Orn-C20-G** (B) bolas. The data are normalized to 100% for the control non-treated cells. Cells were incubated in serum-free Opti-MEM with a bolaplex composed of plasmid DNA (1 μg per well), bola and DOPE (when indicated) at pH 7.4. Different N/P ratios were tested. After 3 h, the transfection medium was replaced with fresh complete culture medium, and cells were cultured for an additional 45 h. When indicated the medium contained 100 μM chloroquine. Then cells were lysed and the total protein was estimated using BC assay.

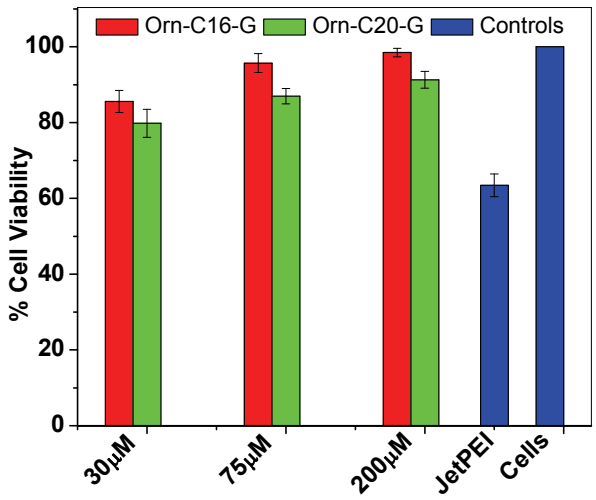

Fig. S5. Cytotoxicity of bolas based on MTT assay. COS-7 cells were incubated for 48 h with the bolas (as described in Fig. S1) at the mentioned concentrations or with JetPEI (150 μM, expressed as concentration of nitrogen residues).

References

(1) Buller, R., Cohen, H., Jensen, T. R., Kjaer, K., Lahav, M.; Leiserowitz, L. (2001) Self-Assembly of Bolaamphiphiles Forming Alternating Layer Arrangements with Lead and Copper Divalent Ions. *J. Phys. Chem. B 105*, 11447–11455.

3.2 Bolas with Lactonic Headgroup

In another set of bolas, namely **Orn-C20-L** and **Orn-C16-L**, a lactonic sugar residue was used as a neutral group. At first, the lactonic residues being much larger than the gluconic ones, should significantly modify the assembly of the bolaplexes. Second, the lactonic residues being specific to hepatocytes (HepG2 cells) containing the asialoglycoprotein receptors could help to enhance the transfection efficiency through the receptor mediated pathway.

According to gel electrophoresis data, lactonic-bolas formed complexes with DNA at significantly higher N/P ratio as compared to their gluconic-bola analogues (Fig. 3.18a). Similar observation was made from the ethidium bromide exclusion assay, where completion of DNA condensation was observed at N/P 5. Nevertheless, similarly to the gluconic-bolas, the size of bolaplexes from lactonic-bolas increased at higher N/Ps, according to DLS data. This increase was connected with the neutralization of the bolaplex charge, as evidenced by zeta-potential measurements. In addition to this trend, an abrupt decrease of the bolaplexes size was observed for lactonic bolas at high N/Ps in the presence of DOPE, used as a helper lipid, which could be explained by their highly positive zeta-potential. AFM data confirmed the small size of the DOPE-containing bolaplexes and showed their spherical morphology. Cellular studies showed that the lactonic-bolas are capable to transfect efficiently different cell lines like HeLa, COS-7 and HepG2. Surprisingly, the transfection efficiency in HeLa and COS-7 cells was generally higher than in HepG2 cells, so that the lactonic group did not provide bolaplexes with specificity to the latter. Both bolas showed a moderate transfection efficiency, when used alone at N/P 10. The transfection efficiency of the bolaplexes was improved significantly with chloroquine and particularly with DOPE (Fig. 3.18b). Importantly, for some formulations with DOPE, the transfection efficiency was close to that of commercial agent jetPEI. The positive effects of DOPE and chloroquine further confirmed that the key barriers for the internalization of these bolaplexes are membrane fusion and endosomal escape, similarly to the gluconic-bolas. Nevertheless, compared to the gluconic-bolas, the lactonic-bolas are more efficient with as well as without helper agents. However, an adverse effect due to the presence of serum in the transfection

medium was observed, though it could not completely abolish the transfection efficiency of bolaplexes. Time dependent mediation of transfection was performed and these studies revealed that the bolas alone can work efficiently after two repetitive transfections for 24 h without the use of any helping agent. The intracellular trafficking studies of the fluorescently labeled bolaplexes, as performed by confocal microscopy, suggested that they were internalized through endocytosis, and then released into cytoplasm by endosomal escape. Finally, MTT-based assay showed that the cytotoxicity of the new bolas is very low.

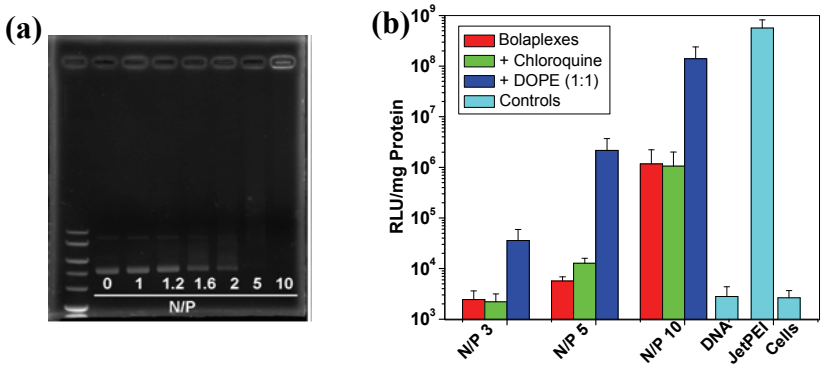

Figure 3.18. (a) Agarose gel electrophoresis (0.9%) of **Orn-C16-L** complexed with pDNA at different N/P ratios. Band at the left of gel correspond to 10 kbp DNA ladder. The final DNA (phosphate) concentration was 60 μM, while the bola concentration was varied to obtain the final N/P ratio. (b) Transfection efficiency of the Orn-C16-L bolaplexes at different N/P ratios in COS-7 cells without serum. Cells were incubated in serum-free Opti-MEM, with a bolaplex composed of plasmid DNA (1 μg per well), Orn-C16-L and DOPE (when indicated). For some samples the medium contained 100 μM chloroquine. After 3 h, 10 % of FBS was added, while for all the samples with chloroquine the transfection medium was replaced with fresh complete culture medium. The luciferase activity quantification was performed after 48 h of incubation. Transfection efficiency determined from the luciferase assay was expressed as RLU/mg of protein. The negative controls were non-treated cells, those transfected with naked pDNA and commercial transfecting agent jetPEI.

Thus, the present work further improves this new concept for construction of nonviral vectors featuring controlled small size, high efficiency and low cytotoxicity. However, the remarkable improvement in transfection efficiency observed for lactonic-bolas compared to their gluconic-bola analogues remains to be understood.

Lactose-ornithine bolaamphiphiles for efficient gene delivery in vitro

(Publication 2)

Will be submitted to J. of Medicinal Chemistry

3.3 Bolas with PEG Headgroup

Unfortunately, both the gluconic- and the lactonic-bolas, when used alone, showed a relatively large size of their bolaplexes at high N/Ps. We hypothesized that sugar groups could probably be responsible for aggregation of the bolaplexes at high N/Ps, when the complexes become uncharged. Therefore, we thought of changing the sugar group by another neutral group, featuring stronger shielding properties. In this respect polyethylene glycol (PEG) groups are the most interesting, since they are largely used for shielding nanostructures and preventing their aggregation. Therefore in this work, we replaced the sugar group by an inert PEG group. Based on this modification, two bolas, bearing PEG residues of different lengths, were synthesized and characterized: **Orn-C16-PEG2000** and **Orn-C16-PEG350**.

Structural Characterization and DNA Interaction Studies

The ability of PEG bolas, **Orn-C16-PEG350** and **Orn-C16-PEG2000,** to complex DNA at different N/P ratios was investigated by gel electrophoresis (Fig. 3.19). It was found that both the bolas were able to complex DNA, though the complex formation and the mobility of the bolaplexes were influenced by their chemical structure. The short-PEG-bola, **Orn-C16-PEG350**, complexed DNA more efficiently than long-PEG-bola **Orn-C16-PEG2000** since pDNA band for the former disappears at lower N/Ps. It should be also noted that for **Orn-C16-PEG350** at low N/P ratios (1-3), the complexes moved slower on the gel, while at N/P>7 mainly immobile complexes were observed. In contrast, for **Orn-C16-PEG2000** only complexes that moved slower on the gel were observed. These results suggested a significant difference in the size and charge of the DNA complexes formed by the two bolas at high N/P ratios.

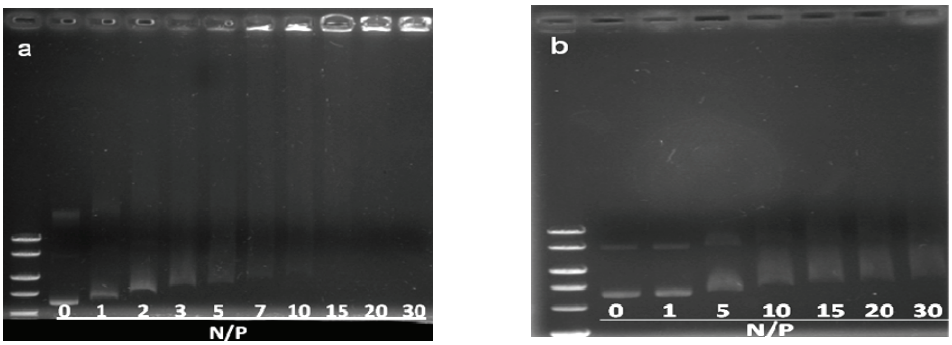

Figure 3.19. Agarose gel electrophoresis (0.9%) of (a) **Orn-C16-PEG350** and (b) **Orn-C16-PEG2000** complexed with pDNA at different N/P ratios. Bands at the left of each gel corresponds to 10 kbp DNA ladder. The final DNA (phosphate) concentration was 60 μM, while the bola concentration was varied to obtain the final N/P ratio.

Ethidium bromide exclusion studies showed that the DNA condensation is more efficient for **Orn-C16-PEG350,** than for **Orn-C16-PEG2000** (Fig. 3.20). Indeed, for **Orn-C16-PEG350** complexes with CT-DNA, the relative fluorescence intensity of EtBr drops rapidly at low N/P to reach a stable minimum level (10%) above N/P 10, thus indicating an efficient bola-DNA interaction and stong DNA condensation. On the other hand, **Orn-C16-PEG2000** showed a slower decrease in the fluorescence intensity without a clear plateau, as the fluorescence intensity at N/P 30 was still ~15% of the initial.

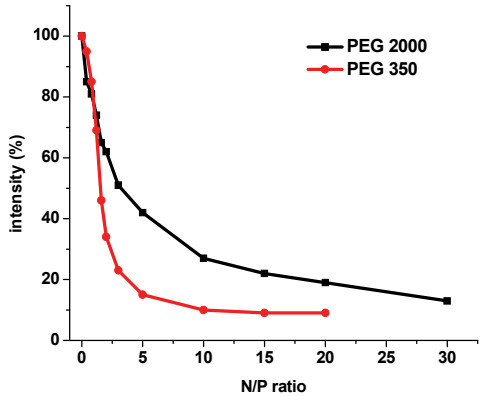

Figure 3.20. Exclusion of EtBr from CT-DNA complexes with PEG-bolas at different N/P ratios. The fluorescence intensity was normalized to 100% of the initial intensity. The final DNA (phosphate) concentration was 20 μM, while the bola concentration was varied to obtain the final N/P ratio.

Particle size measurements by DLS showed that **Orn-C16-PEG350** formed relatively small complexes at lower N/Ps, while their size increased significantly at higher N/Ps (Fig. 3.21). This observation is very similar to those previously made for gluconic- and lactonic-bolas. In contrast, **Orn-C16-PEG2000** formed small bolaplexes for all N/Ps tested and their size decreased at higher N/P (~100 nm for N/P 10). This observation is fully in agreement with gel electrophoresis data. Thus, the observation of immobile complexes of **Orn-C16-PEG350** for N/P>2 is probably connected with the large size of the complexes. In contrast, complexes of **Orn-C16-PEG2000** are much smaller and therefore move on the gel. Formation of small bolaplexes for **Orn-C16-PEG2000** is probably due to the long PEG chain, which provides an efficient shielding of the obtained particles preventing their aggregation.

The zeta potential of bolaplexes formed by **Orn-C16-PEG350** increased with increasing N/Ps, reaching neutrality at N/P 10 (Fig. 3.21). This neutralization of **Orn-C16-EG350** bolaplexes explains the observed increase in the bolaplex size for high N/Ps. In contrast, the zeta potential of bolaplexes formed by **Orn-C16-PEG2000** was close to neutrality for all N/Ps studied, indicating an efficient shielding of the bolaplexes by long-chain PEG groups.

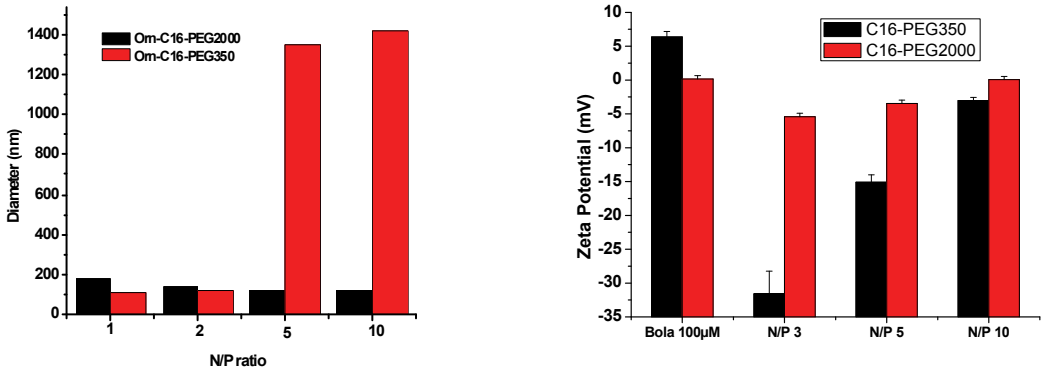

Figure 3.21. DLS and Zeta potential data of 3rd generation PEG-bolas (100 µM) and their complexes with DNA at different N/Ps in aqueous buffer (pH 7). The final DNA (phosphate) concentration was 20 µM for DLS measurements and 30 µM for zeta potential measurements, while the bola concentration was varied to obtain the final N/P ratio.

As **Orn-C16-PEG2000** provides an efficient shielding of the bolaplexes, allowing formation of small-sized particles, we made an attempt to use it to optimize the size of bolaplexes of lactonic-bola **Orn-C16-L** (Fig. 3.22). The latter, being the most efficient transfection agent developed in this work, shows relatively large bolaplexes at high N/P ratio. Therefore, we prepared bolaplexes of **Orn-C16-L** at N/P 10, containing different molar quantities of **Orn-C16-PEG2000.** DLS measurements showed a drastic decrease in size of Orn-C16-L bolaplexes for these formulations. For example, at 33 mol% of **Orn-C16-PEG2000** bolaplex size reached ~ 100 nm, which corresponds to that formed by neat **Orn-C16-PEG2000.** Moreover, for formulations containing ≥ 33 mol% **Orn-C16-PEG2000** the bolaplex size remained invariant for samples prepared after 10 min, 30 min and 3 h (data are not shown), indicating a remarkable stability of the bolaplexes against aggregation. Thus, addition of 33 mol% of **Orn-C16-PEG2000** to **Orn-C16-L** allows reducing size of the bolaplexes by about 20-fold. Thus, we confirmed our hypothesis that shielding of bolaplexes of lactonic-bola with PEG group can prevent their aggregation allowing formation of small and stable bolaplexes.

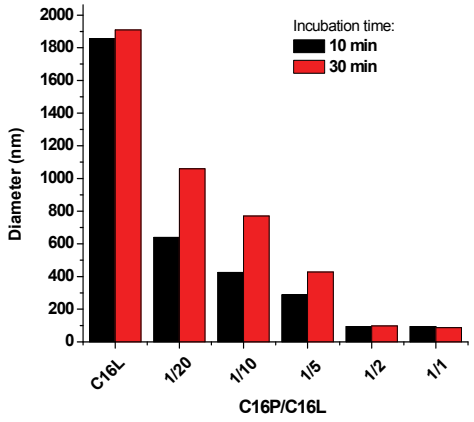

Figure 3.22. DLS data of complexes formed by the mixture of bola Orn-C16-L (N/P 10) and Orn-C16-PEG2000 at different molar ratios with CT-DNA in aqueous buffer (pH 7). The final DNA (phosphate) concentration was 20 μM.

Transfection Efficiency and Cell Viability

The transfection efficiency of **Orn-C16-PEG350** and **Orn-C16-PEG2000** was evaluated for different N/P ratios (3, 5 and 10) in COS-7 cells. Helper lipid DOPE and endosomolytic reagent chloroquine were used for some formulations. For **Orn-C16-PEG350,** no transfection was observed at N/P 3, while for N/P 5 some transfection was observed only in the presence of chloroquine. However, at N/P 10 the transfection efficiency of **Orn-C16-PEG350** was substantially improved. The important property of **Orn-C16-PEG350** is its considerable transfection efficiency when it is used alone without any helping agent (Fig. 3.23). This property was observed so far only for one bola, **Orn-C16-L**. Significantly higher transfection levels were measured for bolaplexes in the presence of DOPE or with chloroquine compared to bola alone, which shows that, similarly to other bolas, the important barrier for the bolaplexes is fusion with biomembranes and endosomal escape. Generally, the results of transfection for **Orn-C16-PEG350** were similar to that of **Orn-C16-L**, though the efficiency of the former with DOPE was found lower. In contrast, **Orn-C16-PEG2000** did not show any transfection efficiency. This could be explained by relatively weak interaction of this bola with DNA, as evidenced by gel electrophoresis and EtBr exclusion assay. In addition the strong shielding of the bolaplexes by the long-chain PEG groups, shown by DLS and zeta potential measurements may be an additional factor decreasing the transfection efficiency of these bolaplexes.

To estimate cell viability, the total cellular protein was measured after transfection with bolaplexes (Fig. 3.23). The obtained results indicated a negligible cytotoxicity of the bolaplexes, which appears much lower than that of jet-PEI and even lower than that of gluconic- and lactonic-bolas. The fact that PEG group is known to be biocompatible and non-toxic may explain the low cytotoxicity that characterizes these compounds.

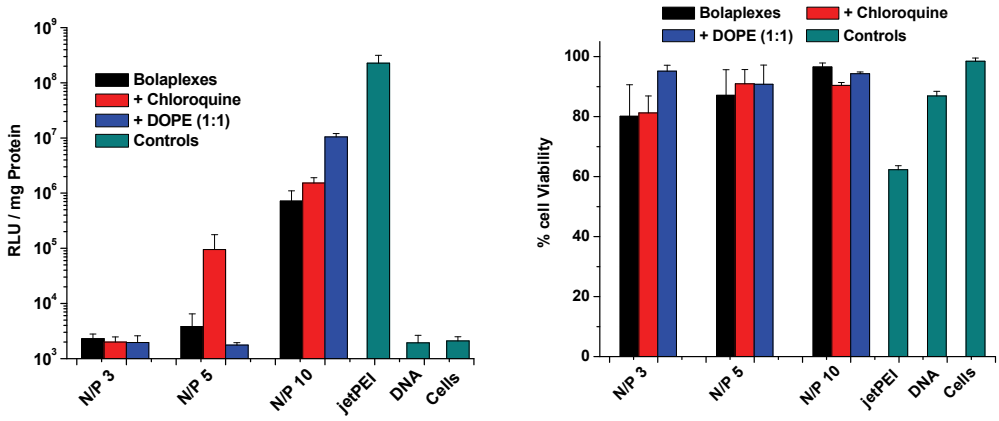

Figure 3.23. Transfection efficiency and cell viability of **C16-PEG350** at different N/P ratios in COS-7 cells without serum. Cells were incubated in serum-free Opti-MEM, with a bolaplex composed of plasmid DNA (1 μg per well), Orn-C16-G and DOPE (when indicated). For some samples the medium contained 100 μM chloroquine. After 3 h, 10 % of FBS was added, while for all the samples with chloroquine the transfection medium was replaced with fresh complete culture medium. The luciferase activity quantification and the total protein were estimated after 48 h of incubation. The negative controls were non-treated cells (cells) and those transfected with naked pDNA (DNA). Transfection efficiency determined from the luciferase assay was expressed as RLU/mg of protein. Cell viability determined using BC assay was normalized to 100% for the control non-treated cells.

Conclusions

In conclusion, a 3rd generation of bolaamphiphiles was synthesized, where the structure of the hydrophobic spacer and the nature of the neutral headgroup were varied. A long alkyl chain of C20-carbon atoms or an alkyl chain of C16-carbon atoms and an aromatic unit were used as hydrophobic spacers, while PEG was used as headgroup in addition to the sugar residues. We found that the increase in the hydrophilicity of the hydrophobic spacer compared to the 2nd generation of bolas improved significantly the interaction of bolas with DNA. For most of bolas, the size of bolaplexes increased with N/P, which was explained by their neutralization at higher N/Ps. Moreover, the obtained bolaplexes of the 3rd generation bolas showed significant transfection efficiency, which was further improved by addition of either a helper lipid DOPE or the lysosomolytic agent chloroquine. The latter fact suggests that the key transfection barrier for these bolaplexes is the fusion with cell membranes and the endosomal escape. When different neutral headgroups were compared, we found that the larger lactonic headgroup decreased slightly the affinity to DNA, but improved strongly the transfection efficiency as compared with the gluconic headgroup. Moreover, PEG of short chain lengths showed properties similar to bolas bearing lactonic group. In contrast, bola bearing a long-chain PEG group showed a very different behavior as compared to other bolas, as the size of its bolaplexes was smaller, especially at higher N/P ratios. This result shows that a long PEG group allows efficient shielding of bolaplexes, preventing their aggregation. This bola can be used in mixture with other bolas in order to decrease the size of their DNA complexes. However, bola bearing a long PEG chain did not show any transfection efficiency, probably because of a too efficient shielding of its complexes and rather weak interaction with DNA within the complex. Thus, achieving high transfection efficiency together with small size of bolaplexes requires a fine optimization of their properties, namely the strength of interaction with DNA, the shielding of the bolaplex from aggregation and its ability to internalize into the cell.

General Conclusions and Future Prospectives

This work presents an innovative direction in the development of non-viral vectors using specially designed unsymmetrical bolaamphiphiles. A variety of bolaamphiphiles, bearing cationic and neutral groups connected by a hydrophobic spacer, were obtained by multi-step organic synthesis. Their characterization by different instrumental techniques suggested that the nature of both headgroups and the hydrophobic spacer defines the bolas self-assembly, their interaction with DNA and the morphology of the bolaplexes.

The first generation of bolaamphiphiles presented a poor solubility and an inefficient DNA interaction. However, these bolas formed asymmetric membranes in form of monolayers or fibrous nano-structures on the surface of mica. These bolas did not show any significant transfection efficiency, while the cytotoxicity was low. Further improvement of bolas structure resulted in the second generation of bolas, bearing di-cationic headgroup. Though these bolas showed much higher solubility, compared to first generation bolas, they lost their ability to self-assemble and kept a poor affinity to DNA resulting in no transfection efficiency together with a maintained low cytotoxicity.

While the first two generations of bolas lack the essential features of nonviral vectors, the final third generation, bearing di-cationic (ornithine) and neutral (sugar or PEG) headgroups connected by enlarged hydrophobic spacer, was found highly promising. This latter generation showed a strong interaction with DNA and significant DNA condensation. These bolas formed small bolaplexes at low N/Ps, showing spherical and rod-like structures, while at higher N/P ratio their size increased due to the neutralization of the complexes. The only exception was a bola bearing long PEG headgroup, which due to the efficient shielding effect of PEG, formed bolaplexes of small size at high N/Ps. The bolaplexes were able to transfect different cell lines, and the transfection efficiency was significantly improved in the presence of the helper lipid DOPE or the endosomolytic agent chloroquine, which suggested that the key barrier for their internalization could be membrane fusion and endosomal escape. Some bolaplex formulations showed transfection efficiency comparable to the best commercial transfection agent jetPEI. Thus, the present work validates a new concept based on unsymmetrical bolaamphiphiles for construction of nonviral vectors featuring controlled small size, high efficiency and low cytotoxicity.

As a future perspective, several aspects should be mentioned. As we found in this work, the major barrier for bola-based vectors is endosomal escape, which explains the poor transfection efficiency for formulation that did not contain helper lipids. Therefore, the next efforts should be focused on modifying the bola structure in order to optimize the endosomal escape of their bolaplexes without use of any helping agent. This can be achieved by introducing a second hydrocarbon chain within the hydrophobic linker. This second chain would promote fusion of the bolaplexes with cell membranes and further biomembrane destabilization, similarly to the effect of DOPE. A second possibility is to introduce a pH sensitive group in the bola that would trigger change in the bola structure inside the endosomes due to lower pH, thus promoting the endosomal escape of the bolaplexes. Once the problems above will be appropriately addressed, it will be important to provide the bolaplexes with high specificity to a particular biological target. For this purpose, the most promising bola-based vectors could be further modified with ligands that are specific to receptors of the target cells. Particularly interesting in this respect are receptors responsible for endocytosis (like asialoglycoprotein and folate receptors), since they will promote ligand driven internalization of the bolaplexes. These studies will be of key importance for specific targeting *in vivo* and future applications of these vectors for gene therapy.

References

(1) **Watson, J. D., and Crick, F. H. (1953) The structure of DNA. *Cold Spring Harb Symp Quant Biol 18*, 123-31.**

(2) **Raphael, Y., and Martin, D. M. (2005) Deafness: lack of regulation encourages hair cell growth. *Gene Ther 12*, 1021-2.**

(3) **Friedmann, T., and Roblin, R. (1972) Gene therapy for human genetic disease? *Science 175*, 949-55.**

(4) **Stribley, J. M., Rehman, K. S., Niu, H., and Christman, G. M. (2002) Gene therapy and reproductive medicine. *Fertil Steril 77*, 645-57.**

(5) **Blaese, R. M. (1997) Gene therapy for cancer. *Sci Am 276*, 111-5.**

(6) **Ledley, F. D. (1995) After gene therapy: issues in long-term clinical follow-up and care. *Adv Genet 32*, 1-16.**

(7) **Cavazzana-Calvo, M., Hacein-Bey, S., de Saint-Basile, G., Le Deist, F., and Fischer, A. (2000) [Gene therapy of severe combined immunodeficiencies]. *Transfus Clin Biol 7*, 259-60.**

(8) **Davidson, H., McLachlan, G., Wilson, A., Boyd, A. C., Doherty, A., MacGregor, G., Davies, L., Painter, H. A., Coles, R., Hyde, S. C., Gill, D. R., Amaral, M. D., Collie, D. D., Porteous, D. J., and Penque, D. (2006) Human-specific cystic fibrosis transmembrane conductance regulator antibodies detect in vivo gene transfer to ovine airways. *Am J Respir Cell Mol Biol 35*, 72-83.**

(9) **Kaplitt, M. G., Feigin, A., Tang, C., Fitzsimons, H. L., Mattis, P., Lawlor, P. A., Bland, R. J., Young, D., Strybing, K., Eidelberg, D., and During, M. J. (2007) Safety and tolerability of gene therapy with an adeno-associated virus (AAV) borne GAD gene for Parkinson's disease: an open label, phase I trial. *Lancet 369*, 2097-105.**

(10) **Yang, Z. R., Wang, H. F., Zhao, J., Peng, Y. Y., Wang, J., Guinn, B. A., and Huang, L. Q. (2007) Recent developments in the use of adenoviruses and immunotoxins in cancer gene therapy. *Cancer Gene Ther 14*, 599-615.**

(11) **Rosenberg, S. A., Aebersold, P., Cornetta, K., Kasid, A., Morgan, R. A., Moen, R., Karson, E. M., Lotze, M. T., Yang, J. C., Topalian, S. L., and et al. (1990) Gene transfer into humans--immunotherapy of patients with advanced melanoma, using tumor-infiltrating lymphocytes modified by retroviral gene transduction. *N Engl J Med 323*, 570-8.**

(12) **Raper, S. E., Chirmule, N., Lee, F. S., Wivel, N. A., Bagg, A., Gao, G. P., Wilson, J. M., and Batshaw, M. L. (2003) Fatal systemic inflammatory response syndrome in a ornithine transcarbamylase deficient patient following adenoviral gene transfer. *Mol Genet Metab 80*, 148-58.**

(13) **Hacein-Bey-Abina, S., Von Kalle, C., Schmidt, M., McCormack, M. P., Wulffraat, N., Leboulch, P., Lim, A., Osborne, C. S., Pawliuk, R., Morillon, E., Sorensen, R., Forster, A., Fraser, P., Cohen, J. I., de Saint Basile, G., Alexander, I., Wintergerst, U., Frebourg, T., Aurias, A., Stoppa-Lyonnet, D., Romana, S., Radford-Weiss, I., Gross, F., Valensi, F., Delabesse, E., Macintyre, E., Sigaux, F., Soulier, J., Leiva, L. E., Wissler, M., Prinz, C., Rabbitts, T. H., Le Deist, F., Fischer, A., and Cavazzana-Calvo, M. (2003) LMO2-associated clonal T cell proliferation in two patients after gene therapy for SCID-X1. *Science 302*, 415-9.**

(14) Bainbridge, J. W., Smith, A. J., Barker, S. S., Robbie, S., Henderson, R., Balaggan, K., Viswanathan, A., Holder, G. E., Stockman, A., Tyler, N., Petersen-Jones, S., Bhattacharya, S. S., Thrasher, A. J., Fitzke, F. W., Carter, B. J., Rubin, G. S., Moore, A. T., and Ali, R. R. (2008) Effect of gene therapy on visual function in Leber's congenital amaurosis. *N Engl J Med 358*, 2231-9.

(15) Maguire, A. M., Simonelli, F., Pierce, E. A., Pugh, E. N., Jr., Mingozzi, F., Bennicelli, J., Banfi, S., Marshall, K. A., Testa, F., Surace, E. M., Rossi, S., Lyubarsky, A., Arruda, V. R., Konkle, B., Stone, E., Sun, J., Jacobs, J., Dell'Osso, L., Hertle, R., Ma, J. X., Redmond, T. M., Zhu, X., Hauck, B., Zelenaia, O., Shindler, K. S., Maguire, M. G., Wright, J. F., Volpe, N. J., McDonnell, J. W., Auricchio, A., High, K. A., and Bennett, J. (2008) Safety and efficacy of gene transfer for Leber's congenital amaurosis. *N Engl J Med 358*, 2240-8.

(16) Haider, M., Hatefi, A., and Ghandehari, H. (2005) Recombinant polymers for cancer gene therapy: a minireview. *J Control Release 109*, 108-19.

(17) Takakura, Y., Mahato, R. I., and Hashida, M. (1998) Extravasation of macromolecules. *Adv Drug Deliv Rev 34*, 93-108.

(18) Lee, C. H., Hsiao, M., Tseng, Y. L., and Chang, F. H. (2003) Enhanced gene delivery to HER-2-overexpressing breast cancer cells by modified immunolipoplexes conjugated with the anti-HER-2 antibody. *J Biomed Sci 10*, 337-44.

(19) Shadidi, M., and Sioud, M. (2003) Identification of novel carrier peptides for the specific delivery of therapeutics into cancer cells. *FASEB J 17*, 256-8.

(20) Davis, M. E. (2002) Non-viral gene delivery systems. *Curr Opin Biotechnol 13*, 128-31.

(21) Hwang, S. W., and Oh, U. (2002) Hot channels in airways: pharmacology of the vanilloid receptor. *Curr Opin Pharmacol 2*, 235-42.

(22) Kircheis, R., Blessing, T., Brunner, S., Wightman, L., and Wagner, E. (2001) Tumor targeting with surface-shielded ligand--polycation DNA complexes. *J Control Release 72*, 165-70.

(23) Nasongkla, N., Bey, E., Ren, J., Ai, H., Khemtong, C., Guthi, J. S., Chin, S. F., Sherry, A. D., Boothman, D. A., and Gao, J. (2006) Multifunctional polymeric micelles as cancer-targeted, MRI-ultrasensitive drug delivery systems. *Nano Lett 6*, 2427-30.

(24) Chang, X. H., Cheng, H. Y., Cheng, Y. X., Ye, X., Guo, H. F., Fu, T. Y., Zhang, L., Zhang, G., and Cui, H. (2008) [Specific immune cell therapy against ovarian cancer in vivo and in vitro]. *Ai Zheng 27*, 1244-50.

(25) Jule, E., Nagasaki, Y., and Kataoka, K. (2003) Lactose-installed poly(ethylene glycol)-poly(d,l-lactide) block copolymer micelles exhibit fast-rate binding and high affinity toward a protein bed simulating a cell surface. A surface plasmon resonance study. *Bioconjug Chem 14*, 177-86.

(26) Qian, Z. M., Li, H., Sun, H., and Ho, K. (2002) Targeted drug delivery via the transferrin receptor-mediated endocytosis pathway. *Pharmacol Rev 54*, 561-87.

(27) Dinauer, N., Balthasar, S., Weber, C., Kreuter, J., Langer, K., and von Briesen, H. (2005) Selective targeting of antibody-conjugated nanoparticles to leukemic cells and primary T-lymphocytes. *Biomaterials 26*, 5898-906.

(28) Paillard, F. (1999) Immunotherapy with T cells bearing chimeric antitumor receptors. *Hum Gene Ther 10*, 151-3.

(29) Peng, L. S., Penichet, M. L., and Morrison, S. L. (1999) A single-chain IL-12 IgG3 antibody fusion protein retains antibody specificity and IL-12 bioactivity and demonstrates antitumor activity. *J Immunol 163*, 250-8.

(30) Vyas, S. P., Katare, Y. K., Mishra, V., and Sihorkar, V. (2000) Ligand directed macrophage targeting of amphotericin B loaded liposomes. *Int J Pharm 210*, 1-14.

(31) Schatzlein, A. G. (2003) Targeting of Synthetic Gene Delivery Systems. *J Biomed Biotechnol 2003*, 149-158.

(32) Wang, S., and Low, P. S. (1998) Folate-mediated targeting of antineoplastic drugs, imaging agents, and nucleic acids to cancer cells. *J Control Release 53*, 39-48.

(33) Uherek, C., and Wels, W. (2000) DNA-carrier proteins for targeted gene delivery. *Adv Drug Deliv Rev 44*, 153-66.

(34) Wagner, E., Zenke, M., Cotten, M., Beug, H., and Birnstiel, M. L. (1990) Transferrin-polycation conjugates as carriers for DNA uptake into cells. *Proc Natl Acad Sci U S A 87*, 3410-4.

(35) Huckett, B., Ariatti, M., and Hawtrey, A. O. (1990) Evidence for targeted gene transfer by receptor-mediated endocytosis. Stable expression following insulin-directed entry of NEO into HepG2 cells. *Biochem Pharmacol 40*, 253-63.

(36) Rosenkranz, A. A., Yachmenev, S. V., Jans, D. A., Serebryakova, N. V., Murav'ev, V. I., Peters, R., and Sobolev, A. S. (1992) Receptor-mediated endocytosis and nuclear transport of a transfecting DNA construct. *Exp Cell Res 199*, 323-9.

(37) Wu, G. Y., and Wu, C. H. (1987) Receptor-mediated in vitro gene transformation by a soluble DNA carrier system. *J Biol Chem 262*, 4429-32.

(38) Cotten, M., Wagner, E., and Birnstiel, M. L. (1993) Receptor-mediated transport of DNA into eukaryotic cells. *Methods Enzymol 217*, 618-44.

(39) Kawasaki, T., and Ashwell, G. (1976) Carbohydrate structure of glycopeptides isolated from an hepatic membrane-binding protein specific for asialoglycoproteins. *J Biol Chem 251*, 5292-9.

(40) Schwartz, A. L., Fridovich, S. E., Knowles, B. B., and Lodish, H. F. (1981) Characterization of the asialoglycoprotein receptor in a continuous hepatoma line. *J Biol Chem 256*, 8878-81.

(41) Wu, G. Y., and Wu, C. H. (1988) Evidence for targeted gene delivery to Hep G2 hepatoma cells in vitro. *Biochemistry 27*, 887-92.

(42) Wagner, E., Ogris, M., and Zauner, W. (1998) Polylysine-based transfection systems utilizing receptor-mediated delivery. *Adv Drug Deliv Rev 30*, 97-113.

(43) Blume, G., Cevc, G., Crommelin, M. D., Bakker-Woudenberg, I. A., Kluft, C., and Storm, G. (1993) Specific targeting with poly(ethylene glycol)-modified liposomes: coupling of homing devices to the ends of the polymeric

chains combines effective target binding with long circulation times. *Biochim Biophys Acta 1149*, 180-4.

(44) Duncan, R., Kopecek, J., Rejmanova, P., and Lloyd, J. B. (1983) Targeting of N-(2-hydroxypropyl)methacrylamide copolymers to liver by incorporation of galactose residues. *Biochim Biophys Acta 755*, 518-21.

(45) Dragsten, P. R., Mitchell, D. B., Covert, G., and Baker, T. (1987) Drug delivery using vesicles targeted to the hepatic asialoglycoprotein receptor. *Biochim Biophys Acta 926*, 270-9.

(46) Rogers, J. C., and Kornfeld, S. (1971) Hepatic uptake of proteins coupled to fetuin glycopeptide. *Biochem Biophys Res Commun 45*, 622-9.

(47) Ashwell, G., and Harford, J. (1982) Carbohydrate-specific receptors of the liver. *Annu Rev Biochem 51*, 531-54.

(48) Duncan, R., Seymour, L. C., Scarlett, L., Lloyd, J. B., Rejmanova, P., and Kopecek, J. (1986) Fate of N-(2-hydroxypropyl)methacrylamide copolymers with pendent galactosamine residues after intravenous administration to rats. *Biochim Biophys Acta 880*, 62-71.

(49) Goto, M., Yura, H., Chang, C.W., Kobayashi, A., Shinoda, T., Maeda, A.,Kojima, S.,Kobayashi, K., Akaike, T. (1994) Lactosecarrying polystyrene as a drug carrier: investigation of body distributions to parenchymal liver cells using 125I-labelled lactosecarrying polystyrene. *J. Control. Release 28*, 223–233.

(50) Meijer, D. K., and van der Sluijs, P. (1989) Covalent and noncovalent protein binding of drugs: implications for hepatic clearance, storage, and cell-specific drug delivery. *Pharm Res 6*, 105-18.

(51) Nishikawa, M., Kamijo, A., Fujita, T., Takakura, Y., Sezaki, H., and Hashida, M. (1993) Synthesis and pharmacokinetics of a new liver-specific carrier, glycosylated carboxymethyl-dextran, and its application to drug targeting. *Pharm Res 10*, 1253-61.

(52) Wilson, G. (1978) Effect of reductive lactosamination on the hepatic uptake of bovine pancreatic ribonuclease A dimer. *J Biol Chem 253*, 2070-2.

(53) Stockert, R. J., Morell, A. G., and Scheinberg, I. H. (1974) Mammalian hepatic lectin. *Science 186*, 365-6.

(54) Lundquist, J. J., and Toone, E. J. (2002) The cluster glycoside effect. *Chem Rev 102*, 555-78.

(55) Kopecek, J., Duncan, R. (1987) Targetable polymeric prodrugs *J.Control. Release 6*, 315–327.

(56) Wiethoff, C. M., Middaugh, C.R. (2003) Barriers to nonviral gene delivery *J Pharm Sci. 92*, 203-17.

(57) Clague, M. J., and Urbe, S. (2001) The interface of receptor trafficking and signalling. *J Cell Sci 114*, 3075-81.

(58) Lukacs, G. L., Haggie, P., Seksek, O., Lechardeur, D., Freedman, N., and Verkman, A. S. (2000) Size-dependent DNA mobility in cytoplasm and nucleus. *J Biol Chem 275*, 1625-9.

(59) Dean, D. A. (1997) Import of plasmid DNA into the nucleus is sequence specific. *Exp Cell Res 230*, 293-302.

(60) Walter, P. (1999) The transport of molecules into and out of the nucleus. *Molecular cell biology* 561–568.

(61) Ryan, K. J., and Wente, S. R. (2000) The nuclear pore complex: a protein machine bridging the nucleus and cytoplasm. *Curr Opin Cell Biol 12*, 361-71.

(62) Mattaj, I. W., and Englmeier, L. (1998) Nucleocytoplasmic transport: the soluble phase. *Annu Rev Biochem 67*, 265-306.

(63) Zanta, M. A., Belguise-Valladier, P., and Behr, J. P. (1999) Gene delivery: a single nuclear localization signal peptide is sufficient to carry DNA to the cell nucleus. *Proc Natl Acad Sci U S A 96*, 91-6.

(64) Branden, L. J., Mohamed, A. J., and Smith, C. I. (1999) A peptide nucleic acid-nuclear localization signal fusion that mediates nuclear transport of DNA. *Nat Biotechnol 17*, 784-7.

(65) Wilke, M., Fortunati, E., van den Broek, M., Hoogeveen, A. T., and Scholte, B. J. (1996) Efficacy of a peptide-based gene delivery system depends on mitotic activity. *Gene Ther 3*, 1133-42.

(66) Bauerschmitz, G. J., Lam, J. T., Kanerva, A., Suzuki, K., Nettelbeck, D. M., Dmitriev, I., Krasnykh, V., Mikheeva, G. V., Barnes, M. N., Alvarez, R. D., Dall, P., Alemany, R., Curiel, D. T., and Hemminki, A. (2002) Treatment of ovarian cancer with a tropism modified oncolytic adenovirus. *Cancer Res 62*, 1266-70.

(67) Takatsuki, K., Obaru, K., Yoshimura, K., and Matsushita, S. (1996) [Gene therapy for AIDS: current trends]. *Nippon Rinsho 54*, 233-41.

(68) Chamberlain, J. S. (2002) Gene therapy of muscular dystrophy. *Hum Mol Genet 11*, 2355-62.

(69) Wei, C. M., Gibson, M., Spear, P. G., and Scolnick, E. M. (1981) Construction and isolation of a transmissible retrovirus containing the src gene of Harvey murine sarcoma virus and the thymidine kinase gene of herpes simplex virus type 1. *J Virol 39*, 935-44.

(70) Shimotohno, K., and Temin, H. M. (1981) Formation of infectious progeny virus after insertion of herpes simplex thymidine kinase gene into DNA of an avian retrovirus. *Cell 26*, 67-77.

(71) Roe, T., Reynolds, T. C., Yu, G., and Brown, P. O. (1993) Integration of murine leukemia virus DNA depends on mitosis. *EMBO J 12*, 2099-108.

(72) Bordignon, C., Notarangelo, L. D., Nobili, N., Ferrari, G., Casorati, G., Panina, P., Mazzolari, E., Maggioni, D., Rossi, C., Servida, P., Ugazio, A. G., and Mavilio, F. (1995) Gene therapy in peripheral blood lymphocytes and bone marrow for ADA- immunodeficient patients. *Science 270*, 470-5.

(73) Stone, D., David, A., Bolognani, F., Lowenstein, P. R., and Castro, M. G. (2000) Viral vectors for gene delivery and gene therapy within the endocrine system. *J Endocrinol 164*, 103-18.

(74) Naldini, L. (1998) Lentiviruses as gene transfer agents for delivery to non-dividing cells. *Curr Opin Biotechnol 9*, 457-63.

(75) Li, Q., Kay, M. A., Finegold, M., Stratford-Perricaudet, L. D., and Woo, S. L. (1993) Assessment of recombinant adenoviral vectors for hepatic gene therapy. *Hum Gene Ther 4*, 403-9.

(76) Quantin, B., Perricaudet, L. D., Tajbakhsh, S., and Mandel, J. L. (1992) Adenovirus as an expression vector in muscle cells in vivo. *Proc Natl Acad Sci U S A 89*, 2581-4.

(77) Shenk, T. (1996) Adenoviridae: the viruses and their application. *Fundamental Virology*, 979-1016.

(78) Doerfler, W., Boehm, P. (1995) The molecular repertoire of adenoviruses. *Springer: Berlin*.

(79) Stewart, P. L., Curiel, D.T. (2002) Adenovirus structure. In adenoviral gene therapy. *Academic press: San diego*, 1-18.

(80) Bergelson, J. M., Cunningham, J. A., Droguett, G., Kurt-Jones, E. A., Krithivas, A., Hong, J. S., Horwitz, M. S., Crowell, R. L., and Finberg, R. W. (1997) Isolation of a common receptor for Coxsackie B viruses and adenoviruses 2 and 5. *Science 275*, 1320-3.

(81) Wickham, T. J., Mathias, P., Cheresh, D. A., and Nemerow, G. R. (1993) Integrins alpha v beta 3 and alpha v beta 5 promote adenovirus internalization but not virus attachment. *Cell 73*, 309-19.

(82) Swisher, S. G., Roth, J. A., Komaki, R., Gu, J., Lee, J. J., Hicks, M., Ro, J. Y., Hong, W. K., Merritt, J. A., Ahrar, K., Atkinson, N. E., Correa, A. M., Dolormente, M., Dreiling, L., El-Naggar, A. K., Fossella, F., Francisco, R., Glisson, B., Grammer, S., Herbst, R., Huaringa, A., Kemp, B., Khuri, F. R., Kurie, J. M., Liao, Z., McDonnell, T. J., Morice, R., Morello, F., Munden, R., Papadimitrakopoulou, V., Pisters, K. M., Putnam, J. B., Jr., Sarabia, A. J., Shelton, T., Stevens, C., Shin, D. M., Smythe, W. R., Vaporciyan, A. A., Walsh, G. L., and Yin, M. (2003) Induction of p53-regulated genes and tumor regression in lung cancer patients after intratumoral delivery of adenoviral p53 (INGN 201) and radiation therapy. *Clin Cancer Res 9*, 93-101.

(83) Roy, I., Holle, L., Song, W., Holle, E., Wagner, T., and Yu, X. (2002) Efficient translocation and apoptosis induction by adenovirus encoded VP22-p53 fusion protein in human tumor cells in vitro. *Anticancer Res 22*, 3185-9.

(84) Anderson, S. C., Johnson, D. E., Harris, M. P., Engler, H., Hancock, W., Huang, W. M., Wills, K. N., Gregory, R. J., Sutjipto, S., Wen, S. F., Lofgren, S., Shepard, H. M., and Maneval, D. C. (1998) p53 gene therapy in a rat model of hepatocellular carcinoma: intra-arterial delivery of a recombinant adenovirus. *Clin Cancer Res 4*, 1649-59.

(85) Cattaneo, R., Miest, T., Shashkova, E. V., and Barry, M. A. (2008) Reprogrammed viruses as cancer therapeutics: targeted, armed and shielded. *Nat Rev Microbiol 6*, 529-40.

(86) Muzyczka, N. (1992) Use of adeno-associated virus as a general transduction vector for mammalian cells. *Curr Top Microbiol Immunol 158*, 97-129.

(87) Rose, J. A., Berns, K. I., Hoggan, M. D., and Koczot, F. J. (1969) Evidence for a single-stranded adenovirus-associated virus genome: formation of a DNA density hybrid on release of viral DNA. *Proc Natl Acad Sci U S A 64*, 863-9.

(88) Srivastava, A., Lusby, E. W., and Berns, K. I. (1983) Nucleotide sequence and organization of the adeno-associated virus 2 genome. *J Virol 45*, 555-64.

(89) El-Aneed, A. (2004) An overview of current delivery systems in cancer gene therapy. *J. Control Release 94*.

(90) Buller, R. M., Janik, J. E., Sebring, E. D., and Rose, J. A. (1981) Herpes simplex virus types 1 and 2 completely help adenovirus-associated virus replication. *J Virol 40*, 241-7.

(91) Janik, J. E., Huston, M. M., Cho, K., and Rose, J. A. (1989) Efficient synthesis of adeno-associated virus structural proteins requires both adenovirus DNA binding protein and VA I RNA. *Virology 168*, 320-9.

(92) Yalkinoglu, A. O., Heilbronn, R., Burkle, A., Schlehofer, J. R., and zur Hausen, H. (1988) DNA amplification of adeno-associated virus as a response to cellular genotoxic stress. *Cancer Res 48*, 3123-9.

(93) Alexander, I. E., Russell, D. W., and Miller, A. D. (1994) DNA-damaging agents greatly increase the transduction of nondividing cells by adeno-associated virus vectors. *J Virol 68*, 8282-7.

(94) Alexander, I. E., Russell, D. W., Spence, A. M., and Miller, A. D. (1996) Effects of gamma irradiation on the transduction of dividing and nondividing cells in brain and muscle of rats by adeno-associated virus vectors. *Hum Gene Ther 7*, 841-50.

(95) Kanazawa, T., Mizukami, H., Okada, T., Hanazono, Y., Kume, A., Nishino, H., Takeuchi, K., Kitamura, K., Ichimura, K., and Ozawa, K. (2003) Suicide gene therapy using AAV-HSVtk/ganciclovir in combination with irradiation results in regression of human head and neck cancer xenografts in nude mice. *Gene Ther 10*, 51-8.

(96) Cusack, J. C., Jr., and Tanabe, K. K. (2002) Introduction to cancer gene therapy. *Surg Oncol Clin N Am 11*, 497-519, v.

(97) Krisky, D. M., Marconi, P. C., Oligino, T. J., Rouse, R. J., Fink, D. J., Cohen, J. B., Watkins, S. C., and Glorioso, J. C. (1998) Development of herpes simplex virus replication-defective multigene vectors for combination gene therapy applications. *Gene Ther 5*, 1517-30.

(98) Lowenstein, P. R., Bain, D., Morrison, E. E., Preston, C. M., Clissold, P., Fournel, S., Epstein, A., and Castro, M. G. (1994) HSV1 vectors to study protein targeting in neurones: are glycosyl-phosphatidylinositol anchors polarized targeting signals in neurones? *Gene Ther 1 Suppl 1*, S32-5.

(99) Lowenstein, P. R., Fournel, S., Bain, D., Tomasec, P., Clissold, P. M., Castro, M. G., and Epstein, A. L. (1995) Simultaneous detection of amplicon and HSV-1 helper encoded proteins reveals that neurons and astrocytoma cells do express amplicon-borne transgenes in the absence of synthesis of virus immediate early proteins. *Brain Res Mol Brain Res 30*, 169-75.

(100) Huard, J., Goins, W. F., and Glorioso, J. C. (1995) Herpes simplex virus type 1 vector mediated gene transfer to muscle. *Gene Ther 2*, 385-92.

(101) Boviatsis, E. J., Chase, M., Wei, M. X., Tamiya, T., Hurford, R. K., Jr., Kowall, N. W., Tepper, R. I., Breakefield, X. O., and Chiocca, E. A. (1994) Gene transfer into experimental brain tumors mediated by adenovirus, herpes simplex virus, and retrovirus vectors. *Hum Gene Ther 5*, 183-91.

(102) Miyanohara, A., Johnson, P. A., Elam, R. L., Dai, Y., Witztum, J. L., Verma, I. M., and Friedmann, T. (1992) Direct gene transfer to the liver with herpes simplex virus type 1 vectors: transient production of physiologically relevant levels of circulating factor IX. *New Biol 4*, 238-46.

(103) Liu, Y., Rabinovitch, A., Suarez-Pinzon, W., Muhkerjee, B., Brownlee, M., Edelstein, D., and Federoff, H. J. (1996) Expression of the bcl-2 gene from a defective HSV-1 amplicon vector protects pancreatic beta-cells from apoptosis. *Hum Gene Ther 7*, 1719-26.

(104) Goya, R. G., Rowe, J., Sosa, Y. E., Tomasec, P., Lowenstein, P. R., and Castro, M. G. (1998) Use of recombinant herpes simplex virus type 1 vectors

for gene transfer into tumour and normal anterior pituitary cells. *Mol Cell Endocrinol 139*, 199-207.

(105) Kay, M. A., Glorioso, J. C., and Naldini, L. (2001) Viral vectors for gene therapy: the art of turning infectious agents into vehicles of therapeutics. *Nat Med 7*, 33-40.

(106) Dolter, K. E., Goins, W. F., Levine, M., and Glorioso, J. C. (1992) Genetic analysis of type-specific antigenic determinants of herpes simplex virus glycoprotein C. *J Virol 66*, 4864-73.

(107) Krisky, D. M., Wolfe, D., Goins, W. F., Marconi, P. C., Ramakrishnan, R., Mata, M., Rouse, R. J., Fink, D. J., and Glorioso, J. C. (1998) Deletion of multiple immediate-early genes from herpes simplex virus reduces cytotoxicity and permits long-term gene expression in neurons. *Gene Ther 5*, 1593-603.

(108) Samaniego, L. A., Neiderhiser, L., and DeLuca, N. A. (1998) Persistence and expression of the herpes simplex virus genome in the absence of immediate-early proteins. *J Virol 72*, 3307-20.

(109) Avery, O. T., Macleod, C. M., and McCarty, M. (1944) Studies on the Chemical Nature of the Substance Inducing Transformation of Pneumococcal Types : Induction of Transformation by a Desoxyribonucleic Acid Fraction Isolated from Pneumococcus Type Iii. *J Exp Med 79*, 137-58.

(110) Sakurai, H., Kawabata, K., Sakurai, F., Nakagawa, S., and Mizuguchi, H. (2008) Innate immune response induced by gene delivery vectors. *Int J Pharm 354*, 9-15.

(111) Kreiss, P., Cameron, B., Rangara, R., Mailhe, P., Aguerre-Charriol, O., Airiau, M., Scherman, D., Crouzet, J., and Pitard, B. (1999) Plasmid DNA size does not affect the physicochemical properties of lipoplexes but modulates gene transfer efficiency. *Nucleic Acids Res 27*, 3792-8.

(112) Behr, J. P. (1994) Gene transfer with synthetic cationic amphiphiles: prospects for gene therapy. *Bioconjug Chem 5*, 382-9.

(113) Wolff, J. A., Malone, R. W., Williams, P., Chong, W., Acsadi, G., Jani, A., and Felgner, P. L. (1990) Direct gene transfer into mouse muscle in vivo. *Science 247*, 1465-8.

(114) Hickman, M. A., Malone, R. W., Lehmann-Bruinsma, K., Sih, T. R., Knoell, D., Szoka, F. C., Walzem, R., Carlson, D. M., and Powell, J. S. (1994) Gene expression following direct injection of DNA into liver. *Hum Gene Ther 5*, 1477-83.

(115) Zhang, G., Vargo, D., Budker, V., Armstrong, N., Knechtle, S., and Wolff, J. A. (1997) Expression of naked plasmid DNA injected into the afferent and efferent vessels of rodent and dog livers. *Hum Gene Ther 8*, 1763-72.

(116) Budker, V., Zhang, G., Knechtle, S., and Wolff, J. A. (1996) Naked DNA delivered intraportally expresses efficiently in hepatocytes. *Gene Ther 3*, 593-8.

(117) Choate, K. A., and Khavari, P. A. (1997) Direct cutaneous gene delivery in a human genetic skin disease. *Hum Gene Ther 8*, 1659-65.

(118) Meyer, K. B., Thompson, M. M., Levy, M. Y., Barron, L. G., and Szoka, F. C., Jr. (1995) Intratracheal gene delivery to the mouse airway: characterization of plasmid DNA expression and pharmacokinetics. *Gene Ther 2*, 450-60.

(119) Gao, X., Kim, K. S., and Liu, D. (2007) Nonviral gene delivery: what we know and what is next. *AAPS J 9*, E92-104.
(120) Coster, H. G. (1965) A quantitative analysis of the voltage-current relationships of fixed charge membranes and the associated property of "punch-through". *Biophys J 5*, 669-86.
(121) Heller, L. C., Ugen, K., and Heller, R. (2005) Electroporation for targeted gene transfer. *Expert Opin Drug Deliv 2*, 255-68.
(122) Neumann, E., Schaefer-Ridder, M., Wang, Y., and Hofschneider, P. H. (1982) Gene transfer into mouse lyoma cells by electroporation in high electric fields. *EMBO J 1*, 841-5.
(123) Hojman, P. Basic principles and clinical advancements of muscle electrotransfer. *Curr Gene Ther 10*, 128-38.
(124) Durieux, A. C., Bonnefoy, R., Busso, T., and Freyssenet, D. (2004) In vivo gene electrotransfer into skeletal muscle: effects of plasmid DNA on the occurrence and extent of muscle damage. *J Gene Med 6*, 809-16.
(125) Yang, N. S., Burkholder, J., Roberts, B., Martinell, B., and McCabe, D. (1990) In vivo and in vitro gene transfer to mammalian somatic cells by particle bombardment. *Proc Natl Acad Sci U S A 87*, 9568-72.
(126) O'Brien, J., and Lummis, S. C. (2002) An improved method of preparing microcarriers for biolistic transfection. *Brain Res Brain Res Protoc 10*, 12-5.
(127) Felgner, P. L., Gadek, T. R., Holm, M., Roman, R., Chan, H. W., Wenz, M., Northrop, J. P., Ringold, G. M., and Danielsen, M. (1987) Lipofection: a highly efficient, lipid-mediated DNA-transfection procedure. *Proc Natl Acad Sci U S A 84*, 7413-7.
(128) Wivel, N. A., and Wilson, J. M. (1998) Methods of gene delivery. *Hematol Oncol Clin North Am 12*, 483-501.
(129) Huang, C. (1969) Studies on phosphatidylcholine vesicles. Formation and physical characteristics. *Biochemistry 8*, 344-52.
(130) Jiskoot, W., Teerlink, T., Beuvery, E. C., and Crommelin, D. J. (1986) Preparation of liposomes via detergent removal from mixed micelles by dilution. The effect of bilayer composition and process parameters on liposome characteristics. *Pharm Weekbl Sci 8*, 259-65.
(131) Madden, T. D., Bally, M. B., Hope, M. J., Cullis, P. R., Schieren, H. P., and Janoff, A. S. (1985) Protection of large unilamellar vesicles by trehalose during dehydration: retention of vesicle contents. *Biochim Biophys Acta 817*, 67-74.
(132) Mayer, L. D., Hope, M. J., and Cullis, P. R. (1986) Vesicles of variable sizes produced by a rapid extrusion procedure. *Biochim Biophys Acta 858*, 161-8.
(133) Yi, S. W., Yune, T. Y., Kim, T. W., Chung, H., Choi, Y. W., Kwon, I. C., Lee, E. B., and Jeong, S. Y. (2000) A cationic lipid emulsion/DNA complex as a physically stable and serum-resistant gene delivery system. *Pharm Res 17*, 314-20.
(134) Choi, B. Y., Chung, J. W., Park, J. H., Kim, K. H., Kim, Y. I., Koh, Y. H., Kwon, J. W., Lee, K. H., Choi, H. J., Kim, T. W., Kim, Y. J., Chung, H., Kwon, I. C., and Jeong, S. Y. (2002) Gene delivery to the rat liver using cationic lipid emulsion/DNA complex: comparison between intra-arterial, intraportal and intravenous administration. *Korean J Radiol 3*, 194-8.

(135) Felgner, J. H., Kumar, R., Sridhar, C. N., Wheeler, C. J., Tsai, Y. J., Border, R., Ramsey, P., Martin, M., and Felgner, P. L. (1994) Enhanced gene delivery and mechanism studies with a novel series of cationic lipid formulations. *J Biol Chem 269*, 2550-61.

(136) Remy, J. S., Sirlin, C., Vierling, P., and Behr, J. P. (1994) Gene transfer with a series of lipophilic DNA-binding molecules. *Bioconjug Chem 5*, 647-54.

(137) Gao, X., and Huang, L. (1995) Cationic liposome-mediated gene transfer. *Gene Ther 2*, 710-22.

(138) Budker, V., Gurevich, V., Hagstrom, J. E., Bortzov, F., and Wolff, J. A. (1996) pH-sensitive, cationic liposomes: a new synthetic virus-like vector. *Nat Biotechnol 14*, 760-4.

(139) Stephan, D. J., Yang, Z. Y., San, H., Simari, R. D., Wheeler, C. J., Felgner, P. L., Gordon, D., Nabel, G. J., and Nabel, E. G. (1996) A new cationic liposome DNA complex enhances the efficiency of arterial gene transfer in vivo. *Hum Gene Ther 7*, 1803-12.

(140) Zhao, D. D., Watarai, S., Lee, J. T., Kouchi, S., Ohmori, H., and Yasuda, T. (1997) Gene transfection by cationic liposomes: comparison of the transfection efficiency of liposomes prepared from various positively charged lipids. *Acta Med Okayama 51*, 149-54.

(141) Serikawa, T., Suzuki, N., Kikuchi, H., Tanaka, K., and Kitagawa, T. (2000) A new cationic liposome for efficient gene delivery with serum into cultured human cells: a quantitative analysis using two independent fluorescent probes. *Biochim Biophys Acta 1467*, 419-30.

(142) Hara, T., Yadi, T. . (2003) In vivo gene delivery to the liver using reconstituted chylomicron remnants as a novel nonviral vector. *Proc. Natl. Acad. Sci. USA 94*, 14547-14552.

(143) Chesnoy, S., and Huang, L. (2000) Structure and function of lipid-DNA complexes for gene delivery. *Annu Rev Biophys Biomol Struct 29*, 27-47.

(144) Templeton, N. S., Lasic, D. D., Frederik, P. M., Strey, H. H., Roberts, D. D., and Pavlakis, G. N. (1997) Improved DNA: liposome complexes for increased systemic delivery and gene expression. *Nat Biotechnol 15*, 647-52.

(145) Pinnaduwage, P., Schmitt, L., and Huang, L. (1989) Use of a quaternary ammonium detergent in liposome mediated DNA transfection of mouse L-cells. *Biochim Biophys Acta 985*, 33-7.

(146) Clamme, J. P., Bernacchi, S., Vuilleumier, C., Duportail, G., and Mely, Y. (2000) Gene transfer by cationic surfactants is essentially limited by the trapping of the surfactant/DNA complexes onto the cell membrane: a fluorescence investigation. *Biochim Biophys Acta 1467*, 347-61.

(147) Freedland, S. J., Malone, R. W., Borchers, H. M., Zadourian, Z., Malone, J. G., Bennett, M. J., Nantz, M. H., Li, J. H., Gumerlock, P. H., and Erickson, K. L. (1996) Toxicity of cationic lipid-ribozyme complexes in human prostate tumor cells can mimic ribozyme activity. *Biochem Mol Med 59*, 144-53.

(148) Leventis, R., and Silvius, J. R. (1990) Interactions of mammalian cells with lipid dispersions containing novel metabolizable cationic amphiphiles. *Biochim Biophys Acta 1023*, 124-32.

(149) Farhood, H., Bottega, R., Epand, R. M., and Huang, L. (1992) Effect of cationic cholesterol derivatives on gene transfer and protein kinase C activity. *Biochim Biophys Acta 1111*, 239-46.

(150) Heyes, J. A., Niculescu-Duvaz, D., Cooper, R. G., and Springer, C. J. (2002) Synthesis of novel cationic lipids: effect of structural modification on the efficiency of gene transfer. *J Med Chem 45*, 99-114.

(151) Vigneron, J. P., Oudrhiri, N., Fauquet, M., Vergely, L., Bradley, J. C., Basseville, M., Lehn, P., and Lehn, J. M. (1996) Guanidinium-cholesterol cationic lipids: efficient vectors for the transfection of eukaryotic cells. *Proc Natl Acad Sci U S A 93*, 9682-6.

(152) Felgner, P. L., and Ringold, G. M. (1989) Cationic liposome-mediated transfection. *Nature 337*, 387-8.

(153) Almofti, M. R., Harashima, H., Shinohara, Y., Almofti, A., Baba, Y., and Kiwada, H. (2003) Cationic liposome-mediated gene delivery: biophysical study and mechanism of internalization. *Arch Biochem Biophys 410*, 246-53.

(154) Pedroso de Lima, M. C., Simoes, S., Pires, P., Faneca, H., and Duzgunes, N. (2001) Cationic lipid-DNA complexes in gene delivery: from biophysics to biological applications. *Adv Drug Deliv Rev 47*, 277-94.

(155) Ross, P. C., and Hui, S. W. (1999) Lipoplex size is a major determinant of in vitro lipofection efficiency. *Gene Ther 6*, 651-9.

(156) Dan, N. (1997) Multilamellar structures of DNA complexes with cationic liposomes. *Biophys J 73*, 1842-6.

(157) Koltover, I., Salditt, T., Radler, J. O., and Safinya, C. R. (1998) An inverted hexagonal phase of cationic liposome-DNA complexes related to DNA release and delivery. *Science 281*, 78-81.

(158) May, S., and Ben-Shaul, A. (1997) DNA-lipid complexes: stability of honeycomb-like and spaghetti-like structures. *Biophys J 73*, 2427-40.

(159) Radler, J. O., Koltover, I., Salditt, T., and Safinya, C. R. (1997) Structure of DNA-cationic liposome complexes: DNA intercalation in multilamellar membranes in distinct interhelical packing regimes. *Science 275*, 810-4.

(160) Hafez, I. M., Maurer, N., and Cullis, P. R. (2001) On the mechanism whereby cationic lipids promote intracellular delivery of polynucleic acids. *Gene Ther 8*, 1188-96.

(161) Hui, S. W., Langner, M., Zhao, Y. L., Ross, P., Hurley, E., and Chan, K. (1996) The role of helper lipids in cationic liposome-mediated gene transfer. *Biophys J 71*, 590-9.

(162) Farhood, H., Serbina, N., and Huang, L. (1995) The role of dioleoyl phosphatidylethanolamine in cationic liposome mediated gene transfer. *Biochim Biophys Acta 1235*, 289-95.

(163) Liu, Y., Mounkes, L. C., Liggitt, H. D., Brown, C. S., Solodin, I., Heath, T. D., and Debs, R. J. (1997) Factors influencing the efficiency of cationic liposome-mediated intravenous gene delivery. *Nat Biotechnol 15*, 167-73.

(164) Bennett, M. J., Nantz, M. H., Balasubramaniam, R. P., Gruenert, D. C., and Malone, R. W. (1995) Cholesterol enhances cationic liposome-mediated DNA transfection of human respiratory epithelial cells. *Biosci Rep 15*, 47-53.

(165) Behr, J. P., Demeneix, B., Loeffler, J. P., and Perez-Mutul, J. (1989) Efficient gene transfer into mammalian primary endocrine cells with lipopolyamine-coated DNA. *Proc Natl Acad Sci U S A 86*, 6982-6.

(166) Gao, X., and Huang, L. (1991) A novel cationic liposome reagent for efficient transfection of mammalian cells. *Biochem Biophys Res Commun 179*, 280-5.

(167) Rose, J. K., Buonocore, L., and Whitt, M. A. (1991) A new cationic liposome reagent mediating nearly quantitative transfection of animal cells. *Biotechniques 10*, 520-5.

(168) Wrobel, I., and Collins, D. (1995) Fusion of cationic liposomes with mammalian cells occurs after endocytosis. *Biochim Biophys Acta 1235*, 296-304.

(169) Hong, K., Zheng, W., Baker, A., and Papahadjopoulos, D. (1997) Stabilization of cationic liposome-plasmid DNA complexes by polyamines and poly(ethylene glycol)-phospholipid conjugates for efficient in vivo gene delivery. *FEBS Lett 400*, 233-7.

(170) Balasubramaniam, R. P., Bennett, M. J., Aberle, A. M., Malone, J. G., Nantz, M. H., and Malone, R. W. (1996) Structural and functional analysis of cationic transfection lipids: the hydrophobic domain. *Gene Ther 3*, 163-72.

(171) Gorman, C. M., Aikawa, M., Fox, B., Fox, E., Lapuz, C., Michaud, B., Nguyen, H., Roche, E., Sawa, T., and Wiener-Kronish, J. P. (1997) Efficient in vivo delivery of DNA to pulmonary cells using the novel lipid EDMPC. *Gene Ther 4*, 983-92.

(172) Solodin, I., Brown, C. S., Bruno, M. S., Chow, C. Y., Jang, E. H., Debs, R. J., and Heath, T. D. (1995) A novel series of amphiphilic imidazolinium compounds for in vitro and in vivo gene delivery. *Biochemistry 34*, 13537-44.

(173) Elouahabi, A., and Ruysschaert, J. M. (2005) Formation and intracellular trafficking of lipoplexes and polyplexes. *Mol Ther 11*, 336-47.

(174) Gershon, H., Ghirlando, R., Guttman, S. B., and Minsky, A. (1993) Mode of formation and structural features of DNA-cationic liposome complexes used for transfection. *Biochemistry 32*, 7143-51.

(175) Ruponen, M., Yla-Herttuala, S., and Urtti, A. (1999) Interactions of polymeric and liposomal gene delivery systems with extracellular glycosaminoglycans: physicochemical and transfection studies. *Biochim Biophys Acta 1415*, 331-41.

(176) Wong, S. Y., Pelet, J.M., Putnam, D. . (2007) Polymer systems for gene delivery—past, present, and future. *Prog Polym Sci 32*, 799–837.

(177) Petersen, H., Merdan, T., Kunath, K., Fischer, D., and Kissel, T. (2002) Poly(ethylenimine-co-L-lactamide-co-succinamide): a biodegradable polyethylenimine derivative with an advantageous pH-dependent hydrolytic degradation for gene delivery. *Bioconjug Chem 13*, 812-21.

(178) LeHoux, J. G., and Grondin, F. (1993) Some effects of chitosan on liver function in the rat. *Endocrinology 132*, 1078-84.

(179) Brown, M. D., Schatzlein, A., Brownlie, A., Jack, V., Wang, W., Tetley, L., Gray, A. I., and Uchegbu, I. F. (2000) Preliminary characterization of novel amino acid based polymeric vesicles as gene and drug delivery agents. *Bioconjug Chem 11*, 880-91.

(180) Shewring, L., Collins, L., Lightman, S. L., Hart, S., Gustafsson, K., and Fabre, J. W. (1997) A nonviral vector system for efficient gene transfer to corneal endothelial cells via membrane integrins. *Transplantation 64*, 763-9.

(181) Pouton, C. W., Lucas, P., Thomas, B. J., Uduehi, A. N., Milroy, D. A., and Moss, S. H. (1998) Polycation-DNA complexes for gene delivery: a comparison of the biopharmaceutical properties of cationic polypeptides and cationic lipids. *J Control Release 53*, 289-99.

(182) Irvin, J. L., and Irvin, E. M. (1947) Spectrophotometric and potentiometric evaluation of apparent acid dissociation exponents of various 4-aminoquino lines. *J Am Chem Soc 69*, 1091-9.

(183) Ohkuma, S., and Poole, B. (1981) Cytoplasmic vacuolation of mouse peritoneal macrophages and the uptake into lysosomes of weakly basic substances. *J Cell Biol 90*, 656-64.

(184) Erbacher, P., Roche, A. C., Monsigny, M., and Midoux, P. (1996) Putative role of chloroquine in gene transfer into a human hepatoma cell line by DNA/lactosylated polylysine complexes. *Exp Cell Res 225*, 186-94.

(185) Ward, C. M., Pechar, M., Oupicky, D., Ulbrich, K., and Seymour, L. W. (2002) Modification of pLL/DNA complexes with a multivalent hydrophilic polymer permits folate-mediated targeting in vitro and prolonged plasma circulation in vivo. *J Gene Med 4*, 536-47.

(186) Mannisto, M., Vanderkerken, S., Toncheva, V., Elomaa, M., Ruponen, M., Schacht, E., and Urtti, A. (2002) Structure-activity relationships of poly(L-lysines): effects of pegylation and molecular shape on physicochemical and biological properties in gene delivery. *J Control Release 83*, 169-82.

(187) Nishikawa, M., Takemura, S., Takakura, Y., and Hashida, M. (1998) Targeted delivery of plasmid DNA to hepatocytes in vivo: optimization of the pharmacokinetics of plasmid DNA/galactosylated poly(L-lysine) complexes by controlling their physicochemical properties. *J Pharmacol Exp Ther 287*, 408-15.

(188) Wolfert, M. A., Dash, P. R., Nazarova, O., Oupicky, D., Seymour, L. W., Smart, S., Strohalm, J., and Ulbrich, K. (1999) Polyelectrolyte vectors for gene delivery: influence of cationic polymer on biophysical properties of complexes formed with DNA. *Bioconjug Chem 10*, 993-1004.

(189) Ohsaki, M., Okuda, T., Wada, A., Hirayama, T., Niidome, T., and Aoyagi, H. (2002) In vitro gene transfection using dendritic poly(L-lysine). *Bioconjug Chem 13*, 510-7.

(190) Okuda, T., Sugiyama, A., Niidome, T., and Aoyagi, H. (2004) Characters of dendritic poly(L-lysine) analogues with the terminal lysines replaced with arginines and histidines as gene carriers in vitro. *Biomaterials 25*, 537-44.

(191) Zhou, X. H., Klibanov, A. L., and Huang, L. (1991) Lipophilic polylysines mediate efficient DNA transfection in mammalian cells. *Biochim Biophys Acta 1065*, 8-14.

(192) Surovoy, A., Flechsler, I., and Jung, G. (1998) A novel series of serum-resistant lipoaminoacid compounds for cellular delivery of plasmid DNA. *Adv Exp Med Biol 451*, 461-7.

(193) Schaffer, D. V., and Lauffenburger, D. A. (1998) Optimization of cell surface binding enhances efficiency and specificity of molecular conjugate gene delivery. *J Biol Chem 273*, 28004-9.

(194) Boussif, O., Lezoualc'h, F., Zanta, M. A., Mergny, M. D., Scherman, D., Demeneix, B., and Behr, J. P. (1995) A versatile vector for gene and oligonucleotide transfer into cells in culture and in vivo: polyethylenimine. *Proc Natl Acad Sci U S A 92*, 7297-301.

(195) Godbey, W. T., Wu, K. K., Hirasaki, G. J., and Mikos, A. G. (1999) Improved packing of poly(ethylenimine)/DNA complexes increases transfection efficiency. *Gene Ther 6*, 1380-8.

(196) Kunath, K., Merdan, T., Hegener, O., Haberlein, H., and Kissel, T. (2003) Integrin targeting using RGD-PEI conjugates for in vitro gene transfer. *J Gene Med 5*, 588-99.

(197) Lungwitz, U., Breunig, M., Blunk, T., and Gopferich, A. (2005) Polyethylenimine-based non-viral gene delivery systems. *Eur J Pharm Biopharm 60*, 247-66.

(198) Kim, Y. H., Park, J. H., Lee, M., Park, T. G., and Kim, S. W. (2005) Polyethylenimine with acid-labile linkages as a biodegradable gene carrier. *J Control Release 103*, 209-19.

(199) Klemm, A. R., Young, D., and Lloyd, J. B. (1998) Effects of polyethyleneimine on endocytosis and lysosome stability. *Biochem Pharmacol 56*, 41-6.

(200) Kichler, A., Leborgne, C., Coeytaux, E., and Danos, O. (2001) Polyethylenimine-mediated gene delivery: a mechanistic study. *J Gene Med 3*, 135-44.

(201) Kircheis, R., Schuller, S., Brunner, S., Ogris, M., Heider, K. H., Zauner, W., and Wagner, E. (1999) Polycation-based DNA complexes for tumor-targeted gene delivery in vivo. *J Gene Med 1*, 111-20.

(202) Fischer, D., Bieber, T., Li, Y., Elsasser, H. P., and Kissel, T. (1999) A novel non-viral vector for DNA delivery based on low molecular weight, branched polyethylenimine: effect of molecular weight on transfection efficiency and cytotoxicity. *Pharm Res 16*, 1273-9.

(203) Godbey, W. T., Wu, K. K., and Mikos, A. G. (2001) Poly(ethylenimine)-mediated gene delivery affects endothelial cell function and viability. *Biomaterials 22*, 471-80.

(204) Han, S., Mahato, R. I., Lee, M., Maheshwari, A., and Kim, S. W. . (2001) Intratumoral delivery of p2CMVmIL-12 using water-soluble lipopolymers. *Mol Ther 4*, 130-8.

(205) Wang, D. A., Narang, A. S., Kotb, M., Gaber, A. O., Miller, D. D., Kim, S. W., and Mahato, R. I. (2002) Novel branched poly(ethylenimine)-cholesterol water-soluble lipopolymers for gene delivery. *Biomacromolecules 3*, 1197-207.

(206) Mahato, R. I. (2005) Water insoluble and soluble lipids for gene delivery. *Adv Drug Deliv Rev 57*, 699-712.

(207) Maheshwari, A., Mahato, R. I., McGregor, J., Han, S., Samlowski, W. E., Park, J. S., and Kim, S. W. (2000) Soluble biodegradable polymer-based cytokine gene delivery for cancer treatment. *Mol Ther 2*, 121-30.

(208) Lynn, D., Langer, R. (2000) Degradable Poly(b-amino esters): Synthesis, Characterization and self Assembly with Plasmid DNA. *J. Am. Chem. Soc. 122*, 10761-10768.

(209) Wang, J., Mao, H. Q., and Leong, K. W. (2001) A novel biodegradable gene carrier based on polyphosphoester. *J Am Chem Soc 123*, 9480-1.

(210) Ahn, C. H., Chae, S. Y., Bae, Y. H., and Kim, S. W. (2002) Biodegradable poly(ethylenimine) for plasmid DNA delivery. *J Control Release 80*, 273-82.

(211) Park, T. G., Jeong, J. H., and Kim, S. W. (2006) Current status of polymeric gene delivery systems. *Adv Drug Deliv Rev 58*, 467-86.

(212) Clark, P. R., Hersh, E. M. . (1999) Cationic lipid-mediated gene transfer: current concepts. *Curr Opin Mol Ther 1*, 158-76.

(213) Meyer, K., Uyechi, L. S. . (1997) Manipulating the intracellular trafficking of nucleic acids. *Gene Therapy for Diseases of the Lung, (Ed. K. L. Brigham), Marcel Dekker. Inc. New York*, 135-80.

(214) Stegmann, T., and Legendre, J. Y. (1997) Gene transfer mediated by cationic lipids: lack of a correlation between lipid mixing and transfection. *Biochim Biophys Acta 1325*, 71-9.

(215) Pires, P., Simoes, S., Nir, S., Gaspar, R., Duzgunes, N., and Pedroso de Lima, M. C. (1999) Interaction of cationic liposomes and their DNA complexes with monocytic leukemia cells. *Biochim Biophys Acta 1418*, 71-84.

(216) Xu, Y., and Szoka, F. C., Jr. (1996) Mechanism of DNA release from cationic liposome/DNA complexes used in cell transfection. *Biochemistry 35*, 5616-23.

(217) Allen, T. M., Hong, K., and Papahadjopoulos, D. (1990) Membrane contact, fusion, and hexagonal (HII) transitions in phosphatidylethanolamine liposomes. *Biochemistry 29*, 2976-85.

(218) Fasbender, A., Zabner, J., Zeiher, B. G., and Welsh, M. J. (1997) A low rate of cell proliferation and reduced DNA uptake limit cationic lipid-mediated gene transfer to primary cultures of ciliated human airway epithelia. *Gene Ther 4*, 1173-80.

(219) Medina-Kauwe, L. K., Xie, J., and Hamm-Alvarez, S. (2005) Intracellular trafficking of nonviral vectors. *Gene Ther 12*, 1734-51.

(220) El Ouahabi, A., Thiry, M., Pector, V., Fuks, R., Ruysschaert, J. M., and Vandenbranden, M. (1997) The role of endosome destabilizing activity in the gene transfer process mediated by cationic lipids. *FEBS Lett 414*, 187-92.

(221) Zhou, X., and Huang, L. (1994) DNA transfection mediated by cationic liposomes containing lipopolylysine: characterization and mechanism of action. *Biochim Biophys Acta 1189*, 195-203.

(222) Ruysschaert, J. M., el Ouahabi, A., Willeaume, V., Huez, G., Fuks, R., Vandenbranden, M., and Di Stefano, P. (1994) A novel cationic amphiphile for transfection of mammalian cells. *Biochem Biophys Res Commun 203*, 1622-8.

(223) Haensler, J., and Szoka, F. C., Jr. (1993) Polyamidoamine cascade polymers mediate efficient transfection of cells in culture. *Bioconjug Chem 4*, 372-9.

(224) Rittner, K., Benavente, A., Bompard-Sorlet, A., Heitz, F., Divita, G., Brasseur, R., and Jacobs, E. (2002) New basic membrane-destabilizing peptides for plasmid-based gene delivery in vitro and in vivo. *Mol Ther 5*, 104-14.

(225) Bieber, T., Meissner, W., Kostin, S., Niemann, A., and Elsasser, H. P. (2002) Intracellular route and transcriptional competence of polyethylenimine-DNA complexes. *J Control Release 82*, 441-54.

(226) Sonawane, N. D., Szoka, F. C., Jr., and Verkman, A. S. (2003) Chloride accumulation and swelling in endosomes enhances DNA transfer by polyamine-DNA polyplexes. *J Biol Chem 278*, 44826-31.

(227) Curiel, D. T., Agarwal, S., Wagner, E., and Cotten, M. (1991) Adenovirus enhancement of transferrin-polylysine-mediated gene delivery. *Proc Natl Acad Sci U S A 88*, 8850-4.

(228) Curiel, D. T., Wagner, E., Cotten, M., Birnstiel, M. L., Agarwal, S., Li, C. M., Loechel, S., and Hu, P. C. (1992) High-efficiency gene transfer mediated by adenovirus coupled to DNA-polylysine complexes. *Hum Gene Ther 3*, 147-54.

(229) Wagner, E., Zatloukal, K., Cotten, M., Kirlappos, H., Mechtler, K., Curiel, D. T., and Birnstiel, M. L. (1992) Coupling of adenovirus to transferrin-polylysine/DNA complexes greatly enhances receptor-mediated gene delivery and expression of transfected genes. *Proc Natl Acad Sci U S A 89*, 6099-103.

(230) James, M. B., and Giorgio, T. D. (2000) Nuclear-associated plasmid, but not cell-associated plasmid, is correlated with transgene expression in cultured mammalian cells. *Mol Ther 1*, 339-46.

(231) Tachibana, R., Harashima, H., Ide, N., Ukitsu, S., Ohta, Y., Suzuki, N., Kikuchi, H., Shinohara, Y., and Kiwada, H. (2002) Quantitative analysis of correlation between number of nuclear plasmids and gene expression activity after transfection with cationic liposomes. *Pharm Res 19*, 377-81.

(232) Zelphati, O., Liang, X., Hobart, P., and Felgner, P. L. (1999) Gene chemistry: functionally and conformationally intact fluorescent plasmid DNA. *Hum Gene Ther 10*, 15-24.

(233) Lechardeur, D., Sohn, K. J., Haardt, M., Joshi, P. B., Monck, M., Graham, R. W., Beatty, B., Squire, J., O'Brodovich, H., and Lukacs, G. L. (1999) Metabolic instability of plasmid DNA in the cytosol: a potential barrier to gene transfer. *Gene Ther 6*, 482-97.

(234) Pollard, H., Toumaniantz, G., Amos, J. L., Avet-Loiseau, H., Guihard, G., Behr, J. P., and Escande, D. (2001) Ca2+-sensitive cytosolic nucleases prevent efficient delivery to the nucleus of injected plasmids. *J Gene Med 3*, 153-64.

(235) Pollard, H., Remy, J. S., Loussouarn, G., Demolombe, S., Behr, J. P., and Escande, D. (1998) Polyethylenimine but not cationic lipids promotes transgene delivery to the nucleus in mammalian cells. *J Biol Chem 273*, 7507-11.

(236) Page, R. L., Butler, S. P., Subramanian, A., Gwazdauskas, F. C., Johnson, J. L., and Velander, W. H. (1995) Transgenesis in mice by cytoplasmic injection of polylysine/DNA mixtures. *Transgenic Res 4*, 353-60.

(237) Zabner, J., Fasbender, A. J., Moninger, T., Poellinger, K. A., and Welsh, M. J. (1995) Cellular and molecular barriers to gene transfer by a cationic lipid. *J Biol Chem 270*, 18997-9007.

(238) Moret, I., Esteban Peris, J., Guillem, V. M., Benet, M., Revert, F., Dasi, F., Crespo, A., and Alino, S. F. (2001) Stability of PEI-DNA and DOTAP-DNA complexes: effect of alkaline pH, heparin and serum. *J Control Release 76*, 169-81.

(239) Godbey, W. T., Barry, M. A., Saggau, P., Wu, K. K., and Mikos, A. G. (2000) Poly(ethylenimine)-mediated transfection: a new paradigm for gene delivery. *J Biomed Mater Res 51*, 321-8.

(240) Chan, C. K., and Jans, D. A. (2002) Using nuclear targeting signals to enhance non-viral gene transfer. *Immunol Cell Biol 80*, 119-30.

(241) Cartier, R., and Reszka, R. (2002) Utilization of synthetic peptides containing nuclear localization signals for nonviral gene transfer systems. *Gene Ther 9*, 157-67.

(242) Vacik, J., Dean, B. S., Zimmer, W. E., and Dean, D. A. (1999) Cell-specific nuclear import of plasmid DNA. *Gene Ther 6*, 1006-14.

(243) Zana, R., Yiv, S., Kale, K.M. (1980) Chemical relaxation and equilibrium studies of association in aqueous solutions of bolaform detergents. 3. Docosane-1,22-bis(trimethylammonium bromide). *J. Colloid Interface Sci. 77*, 456–465.

(244) Fuhrhop, J. H., Mathieu, J. (1984) Routes to functional vesicle membranes without proteins. *Angew. Chem. Int. Ed. Engl. 23*, 100–113.

(245) Brunelle, M., Polidori, A., Denoyelle, S., Fabiano, A. S., Vuillaume, P.Y., Lewandowski, S.L., Pucci, B. (2008) A structure-activity investigation of hemifluorinated bifunctional bolaamphiphiles designed for gene delivery. *C. R. Chimie 12*, 188-208.

(246) Fuhrhop, J. H., and Wang, T. (2004) Bolaamphiphiles. *Chem Rev 104*, 2901-37.

(247) Gliozzi, A., Rolandi, R., De Rosa, M., and Gambacorta, A. (1983) Monolayer black membranes from bipolar lipids of archaebacteria and their temperature-induced structural changes. *J Membr Biol 75*, 45-56.

(248) Gulik, A., Luzzati, V., De Rosa, M., and Gambacorta, A. (1985) Structure and polymorphism of bipolar isopranyl ether lipids from archaebacteria. *J Mol Biol 182*, 131-49.

(249) Sprott, G. D. (1992) Structures of archaebacterial membrane lipids. *J Bioenerg Biomembr 24*, 555-66.

(250) Fan, Q., Relini, A., Cassinadri, D., Gambacorta, A., and Gliozzi, A. (1995) Stability against temperature and external agents of vesicles composed of archael bolaform lipids and egg PC. *Biochim Biophys Acta 1240*, 83-8.

(251) Yamauchi, K., Doi, K., Yoshida, Y., and Kinoshita, M. (1993) Archaebacterial lipids: highly proton-impermeable membranes from 1,2-diphytanyl-sn-glycero-3-phosphocholine. *Biochim Biophys Acta 1146*, 178-82.

(252) Gliozzi, A., Relini, A., Chong, P.L.-G. . (2002) Structure and permeability properties of biomimetic membranes of bolaform archaeal tetraether lipids. *Journal of Membrane Science 206* 131–147.

(253) Fuhrhop, J. H., Fritsch, D. (1986) Bolaamphiphiles form ultrathin, porous and unsymmetric monolayer lipid membranes. *Acc. Chem. Res. 19*.

(254) Sprott, G. D., Tolson, D. L., and Patel, G. B. (1997) Archaeosomes as novel antigen delivery systems. *FEMS Microbiol Lett 154*, 17-22.

(255) Cornell, B. A., Braach-Maksvytis, V. L., King, L. G., Osman, P. D., Raguse, B., Wieczorek, L., and Pace, R. J. (1997) A biosensor that uses ion-channel switches. *Nature 387*, 580-3.

(256) Yan, Y., Lu, T., and Huang, J. (2009) Recent advances in the mixed systems of bolaamphiphiles and oppositely charged conventional surfactants. *J Colloid Interface Sci 337*, 1-10.

(257) Brard, M., Richter, W., Benvegnu, T., and Plusquellec, D. (2004) Synthesis and supramolecular assemblies of bipolar archaeal glycolipid analogues

containing a cis-1,3-disubstituted cyclopentane ring. *J Am Chem Soc 126*, 10003-12.

(258) Shimizu, T., Masuda, M., and Minamikawa, H. (2005) Supramolecular nanotube architectures based on amphiphilic molecules. *Chem Rev 105*, 1401-43.

(259) Clary, L., Gadras, C., Greiner, J., Rolland, J. P., Santaella, C., Vierling, P., and Gulik, A. (1999) Phase behavior of fluorocarbon and hydrocarbon double-chain hydroxylated and galactosylated amphiphiles and bolaamphiphiles. Long-term shelf-stability of their liposomes. *Chem Phys Lipids 99*, 125-37.

(260) Fuhrhop, J. H., Spiroski, D., Boettcher, C. (1993) Molecular Monolayer Rods and Tubules Made of α-(L-Lysine),ω-(Amino) Bolaamphiphiles. *J. Am. Chem. Soc. 115*, 1600-1601.

(261) Franceschi, S., Viguerie, N., Riviere, M., Lattes, A. (1999) Synthesis and aggregation of two-headed surfactants bearing amino acid moieties. *New J. Chem. 23*, 447-452.

(262) Qiu, F., Chen, Y., Tang, C., Zhou, Q., Wang, C., Shi, Y. K., and Zhao, X. (2008) De novo design of a bolaamphiphilic peptide with only natural amino acids. *Macromol Biosci 8*, 1053-9.

(263) Masuda, M., and Shimizu, T. (2001) Multilayer structure of an unsymmetrical monolayer lipid membrane with a 'head-to-tail' interface. *Chem Commun (Camb)*, 2442-3.

(264) Sirieix, J., Lauth-de Viguerie, N., Riviére, M. R., Lattes, A. . (2000) From unsymmetrical bolaamphiphiles to supermolecules. *New J. Chem. 24*, 1043-1048.

(265) Masuda, M., and Shimizu, T. (2004) Lipid nanotubes and microtubes: experimental evidence for unsymmetrical monolayer membrane formation from unsymmetrical bolaamphiphiles. *Langmuir 20*, 5969-77.

(266) Meister, A., Weygand, M. J., Brezesinski, G., Kerth, A., Drescher, S., Dobner, B., and Blume, A. (2007) Evidence for a reverse U-shaped conformation of single-chain bolaamphiphiles at the air-water interface. *Langmuir 23*, 6063-9.

(267) Roussel, M., Lognone, V., Plusquellec, D., and Benvegnu, T. (2006) Monolayer lipid membrane-forming dissymmetrical bolaamphiphiles derived from alginate oligosaccharides. *Chem Commun (Camb)*, 3622-4.

(268) Schneider, J., Messerschmidt, C., Schulz, A., Gnade, M., Schade, B., Luger, P., Bombicz, P., Hubert, V., Fuhrhop, J. H. . (2000) Odd-Even Effects in Supramolecular Assemblies of Diamide Bolaamphiphiles. *Langmuir 16*, 8575-8584.

(269) Shimizu, T., Masuda, M. (1997) Stereochemical Effect of Even−Odd Connecting Links on Supramolecular Assemblies Made of 1-Glucosamide Bolaamphiphiles. *J. Am. Chem. Soc. 119*, 2812–2818.

(270) Zelphati, O., Uyechi, L. S., Barron, L. G., and Szoka, F. C., Jr. (1998) Effect of serum components on the physico-chemical properties of cationic lipid/oligonucleotide complexes and on their interactions with cells. *Biochim Biophys Acta 1390*, 119-33.

(271) Bally, M. B., Harvie, P., Wong, F. M., Kong, S., Wasan, E. K., and Reimer, D. L. (1999) Biological barriers to cellular delivery of lipid-based DNA carriers. *Adv Drug Deliv Rev 38*, 291-315.

(272) Ferkol, T., Perales, J. C., Mularo, F., and Hanson, R. W. (1996) Receptor-mediated gene transfer into macrophages. *Proc Natl Acad Sci U S A 93*, 101-5.

(273) Erbacher, P., Bousser, M. T., Raimond, J., Monsigny, M., Midoux, P., and Roche, A. C. (1996) Gene transfer by DNA/glycosylated polylysine complexes into human blood monocyte-derived macrophages. *Hum Gene Ther 7*, 721-9.

(274) Kawakami, S., Sato, A., Nishikawa, M., Yamashita, F., and Hashida, M. (2000) Mannose receptor-mediated gene transfer into macrophages using novel mannosylated cationic liposomes. *Gene Ther 7*, 292-9.

(275) Choi, Y. H., Liu, F., Park, J. S., and Kim, S. W. (1998) Lactose-poly(ethylene glycol)-grafted poly-L-lysine as hepatoma cell-tapgeted gene carrier. *Bioconjug Chem 9*, 708-18.

(276) Hashida, M., Takemura, S., Nishikawa, M., and Takakura, Y. (1998) Targeted delivery of plasmid DNA complexed with galactosylated poly(L-lysine). *J Control Release 53*, 301-10.

(277) Kawakami, S., Yamashita, F., Nishikawa, M., Takakura, Y., and Hashida, M. (1998) Asialoglycoprotein receptor-mediated gene transfer using novel galactosylated cationic liposomes. *Biochem Biophys Res Commun 252*, 78-83.

(278) Kawakami, S., Fumoto, S., Nishikawa, M., Yamashita, F., and Hashida, M. (2000) In vivo gene delivery to the liver using novel galactosylated cationic liposomes. *Pharm Res 17*, 306-13.

(279) Remy, J. S., Kichler, A., Mordvinov, V., Schuber, F., and Behr, J. P. (1995) Targeted gene transfer into hepatoma cells with lipopolyamine-condensed DNA particles presenting galactose ligands: a stage toward artificial viruses. *Proc Natl Acad Sci U S A 92*, 1744-8.

(280) Eaton, M. A., Baker, T. S., Catterall, C. F., Crook, K., Macaulay, G. S., Mason, B., Norman, T. J., Parker, D., Perry, J. J., Taylor, R. J., Turner, A., and Weir, A. N. (2000) A New Self-Assembling System for Targeted Gene Delivery We thank the BBSRC Chiroptical Service for CD studies, Brian McManus (Optokem Instruments, Nercyws, Flintshire) for assistance with the light-scattering studies, Dr. Clive Roberts (Molecular Profiles Ltd.) for AFM studies, Professor J.-H. Fuhrhop for many discussions, Dr. I. S. Blagbrough for related synthetic work, the EPSRC for support, and the Royal Society for a Leverhulme Trust Senior Research Fellowship (D.P.). *Angew Chem Int Ed Engl 39*, 4063-4067.

(281) Weissig, V., and Torchilin, V. P. (2001) Cationic bolasomes with delocalized charge centers as mitochondria-specific DNA delivery systems. *Adv Drug Deliv Rev 49*, 127-49.

(282) Yoshimura, T., Hasegawa, S., Hirashima, N., Nakanishi, M., and Ohwada, T. (2001) Anchoring and bola cationic amphiphiles for nucleotide delivery. Effects of orientation and extension of hydrophobic regions. *Bioorg Med Chem Lett 11*, 2897-901.

(283) Ren, T., Zhang, G., and Liu, D. (2001) Synthesis of galactosyl compounds for targeted gene delivery. *Bioorg Med Chem 9*, 2969-78.

(284) Gaucheron, J., Santaella, C., and Vierling, P. (2001) In vitro gene transfer with a novel galactosylated spermine bolaamphiphile. *Bioconjug Chem 12*, 569-75.

(285) Fabio, K., Gaucheron, J., Di Giorgio, C., and Vierling, P. (2003) Novel galactosylated polyamine bolaamphiphiles for gene delivery. *Bioconjug Chem 14*, 358-67.

(286) Denoyelle, S., Polidori, A., Brunelle, M., Vuillaume, P.Y., Laurent, S., ElAzhary, Y. (2006) Synthesis and preliminary biological studies of hemifluorinated bifunctional bolaamphiphiles designed for gene delivery. *New J Chem 30*, 629–46.

(287) Graminski, G. F., Carlson, C. L., Ziemer, J. R., Cai, F., Vermeulen, N. M., Vanderwerf, S. M., and Burns, M. R. (2002) Synthesis of bis-spermine dimers that are potent polyamine transport inhibitors. *Bioorg Med Chem Lett 12*, 35-40.

(288) Kan, P. L., Papahadjopoulos-Sternberg, B., Wong, D., Waigh, R. D., Watson, D. G., Gray, A. I., McCarthy, D., McAllister, M., Schätzlein, A. G., Uchegbu, L. F. (2004) Highly Hydrophilic Fused Aggregates (Microsponges) from a C12 Spermine Bolaamphiphile. *J. Phys. Chem. B 108*, 8129-8135.

(289) Ehrenpreis, S., and Kellock, M. G. (1960) The interaction of quarternary ammonium compounds with hyaluronic acid. *Biochim Biophys Acta 45*, 525-8.

(290) Morawetz, H. (1966) Reactivity of organic crystals. *Science 152*, 705-11.

(291) Jeong, Y. I., Seo, S. J., Park, I. K., Lee, H. C., Kang, I. C., Akaike, T., and Cho, C. S. (2005) Cellular recognition of paclitaxel-loaded polymeric nanoparticles composed of poly(gamma-benzyl L-glutamate) and poly(ethylene glycol) diblock copolymer endcapped with galactose moiety. *Int J Pharm 296*, 151-61.

(292) Gillies, E. R., Goodwin, A. P., and Frechet, J. M. (2004) Acetals as pH-sensitive linkages for drug delivery. *Bioconjug Chem 15*, 1254-63.

(293) Lleres, D., Weibel, J. M., Heissler, D., Zuber, G., Duportail, G., and Mely, Y. (2004) Dependence of the cellular internalization and transfection efficiency on the structure and physicochemical properties of cationic detergent/DNA/liposomes. *J Gene Med 6*, 415-28.

(294) Pastukhov, A. V., and Ropson, I. J. (2003) Fluorescent dyes as probes to study lipid-binding proteins. *Proteins 53*, 607-15.

(295) Kirk, W. R., Kurian, E., and Prendergast, F. G. (1996) Characterization of the sources of protein-ligand affinity: 1-sulfonato-8-(1')anilinonaphthalene binding to intestinal fatty acid binding protein. *Biophys J 70*, 69-83.

(296) Ory, J. J., and Banaszak, L. J. (1999) Studies of the ligand binding reaction of adipocyte lipid binding protein using the fluorescent probe 1, 8-anilinonaphthalene-8-sulfonate. *Biophys J 77*, 1107-16.

(297) Rye, H. S., Yue, S., Wemmer, D. E., Quesada, M. A., Haugland, R. P., Mathies, R. A., and Glazer, A. N. (1992) Stable fluorescent complexes of double-stranded DNA with bis-intercalating asymmetric cyanine dyes: properties and applications. *Nucleic Acids Res 20*, 2803-12.

(298) Zuber, G., Dauty, E., Nothisen, M., Belguise, P., and Behr, J. P. (2001) Towards synthetic viruses. *Adv Drug Deliv Rev 52*, 245-53.

(299) Remy-Kristensen, A., Clamme, J. P., Vuilleumier, C., Kuhry, J. G., and Mely, Y. (2001) Role of endocytosis in the transfection of L929 fibroblasts by polyethylenimine/DNA complexes. *Biochim Biophys Acta 1514*, 21-32.

(300) Fuhrhop, J. H., Schnieder, P., Boekema, E., Helfrich, W. (I988) Lipid Bilayer Fibers from Diastereomeric and Enantiomeric N-Octylaldonamides. *J. Am. Chem. SOC. 110*, 2861-2867.

(301) Chittimalla, C., Zammut-Italiano, L., Zuber, G., and Behr, J. P. (2005) Monomolecular DNA nanoparticles for intravenous delivery of genes. *J Am Chem Soc 127*, 11436-41.

Appendix

In addition to my dissertation work, I had the opportunity to collaborate on other projects that are presented in papers shortly introduced below:

1) Article "Excited-State Intramolecular Proton Transfer Distinguishes Microenvironments in Single-And Double-Stranded DNA"

The development of environment sensitive dyes is one of the main topics of research of our research team. The efficient interaction of an environment-sensitive fluorophore that undergoes excited-state intramolecular proton transfer (ESIPT) with DNA has been studied by conjugation of a 3-hydroxychromone (3HC) moiety with polycationic spermine. The designed conjugate exhibits a change of 16-folds in the ratio of the two emission bands on binding to double-stranded DNA that suggests an efficient screening from the water molecules. On the contrary, only a moderate change is observed on binding to a single-stranded DNA, indicating a much higher exposure to water at the binding site. Thus, these dyes are promising to monitor the interaction of polycationic molecules with DNA and to probe the microenvironment of their DNA binding sites

2) Article "Virus-sized DNA nanoparticles for gene delivery based on micelles of cationic calixarenes"

In this work, we characterized the self-assembly of new amphiphilic calixarenes (synthesized by Dr. Roman V. Rodik) by fluorescent probes, fluorescence correlation spectroscopy, dynamic light scattering, gel electrophoresis and atomic force microscopy. We found that, in contrast to short-chain (propyl) analogue, calixarenes bearing long alkyl chains (octyl) self-assemble into micelles of 6 nm diameter at low CMC and present the unique ability to condense DNA into small nanoparticles of about 50 nm diameter which resulted in better gene transfection efficiency *in vitro*, indicating that gene delivery of calixarene/DNA complexes depends strongly on their structure. Moreover, all cationic calixarenes studied showed low cytotoxicities. Thus, this work presents a two-step hierarchical concept of construction of small DNA nanoparticles for gene delivery based on amphiphilic cone-shaped cationic calixarenes.

Excited-State Intramolecular Proton Transfer Distinguishes Microenvironments in Single-And Double-Stranded DNA

(Publication 3)

Excited-State Intramolecular Proton Transfer Distinguishes Microenvironments in Single- And Double-Stranded DNA

Andrey S. Klymchenko,* Volodymyr V. Shvadchak, Dmytro A. Yushchenko, Namrata Jain, and Yves Mély

Photophysique des Interactions Biomoléculaires, UMR 7175 du CNRS, Faculté de Pharmacie, Université Louis Pasteur, 67401, Illkirch, France

Received: February 11, 2008

Herein, the efficient interaction of an environment-sensitive fluorophore that undergoes excited-state intramolecular proton transfer (ESIPT) with DNA has been realized by conjugation of a 3-hydroxychromone (3HC) with polycationic spermine. On binding to a double-stranded DNA (dsDNA), the ratio of the two emission bands of the 3HC conjugates changes up to 16-fold, so that emission of the ESIPT product increases dramatically. This suggests an efficient screening of the 3HC fluorophore from the water molecules in the DNA complex, which is probably realized by its intercalation into dsDNA. In sharp contrast, the 3HC conjugates show only moderate changes in the dual emission on binding to a single-stranded DNA (ssDNA), indicating a much higher fluorophore exposure to water at the binding site. Thus, the 3-hydroxychromone fluorophore being conjugated to spermine discriminates the binding of this polycation to dsDNA from that to ssDNA. Consequently, ESIPT-based dyes are promising for monitoring the interaction of polycationic molecules with DNA and probing the microenvironment of their DNA binding sites.

Introduction

Solvatochromic (environment-sensitive) fluorescent dyes are highly useful for obtaining new information about biomolecules and their interactions.[1−3] However, applications of these dyes for DNA research remains a challenge and only few examples are available in the literature. For instance, a dansyl fluorophore has been used to estimate the microenvironment polarity in the major groove of double-stranded DNA (dsDNA).[4,5] Moreover, DNA dynamics has been monitored by the time-resolved solvent relaxation of a coumarin.[6] In recent reports, a PRODAN-based fluorophore was conjugated with DNA bases[7−9] to evidence differences in the microenvironment of the major and minor grooves of A-, B- and Z-DNA. Environment-sensitive fluorophores having cationic groups, can bind DNA and report on the local properties of the DNA binding sites. For instance, the polarity of the minor groove of dsDNA has been estimated using the polycationic bisbenzimide (Hoechst 33258).[10] Similarly, a cationic anthracene derivative[11] and cationic acridizinium salts[12] provide a site-specific fluorescence signal on binding to DNA. Consequently, environment-sensitive fluorophores are highly promising for detecting the interaction of small molecules with DNA and probing the microenvironment of their binding site. In this respect, a prospective approach, which has not been realized so far, is to use a fluorophore undergoing excited-state intramolecular proton transfer (ESIPT) reaction as a building block of a DNA probe. ESIPT results in the formation of a new long-wavelength emission band.[13−16] This reaction is highly sensitive to the environment, so that solvent polarity and H-bonding may strongly modulate the relative intensity of the ESIPT product.[17−19] In this respect, 3-hydroxychromone (3HC) derivatives are probably among the best candidates for DNA applications. They undergo ESIPT between their 3-hydroxyl and 4-carbonyl groups[20] resulting in the emission of both normal excited-state (N*) and phototautomer (T*) species (Scheme 1).

SCHEME 1: 3-Hydroxychromone Derivative and Its Excited State Intramolecular Proton Transfer (ESIPT) Reaction (A) and, for Comparison, the Structure of a Natural Base Pair (dA-dT) (B)

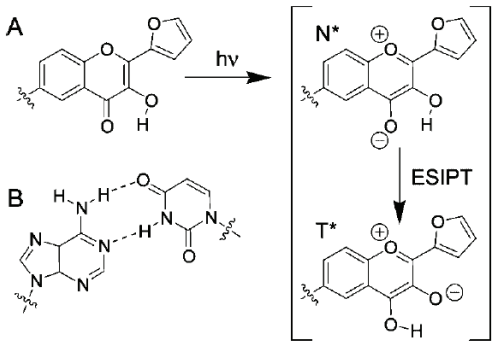

The dual emission of 3HCs is highly sensitive to the environment,[17,18,21−23] since an increase in the polarity and H-bond donor ability of solvents inhibits the ESIPT reaction and thus, decreases the relative intensity of the T* band.[23,24] Moreover, the position of the maximum of the T* band in 3HCs is insensitive to solvent polarity, but exhibits high sensitivity to H-bond donor ability.[24] Thus, 3HCs provide two independent spectroscopic channels allowing a detailed characterization of their environment. These unique properties of 3HCs have already been applied for probing proteins, lipid bilayers and cell membranes.[25−28] However, application of 3HCs for DNA probing has never been shown so far. For this purpose, 2-(2-furanyl)-3-hydroxychromone is probably the most convenient fluorophore among known 3HCs, since it is a flat molecule with a size close to that of a base pair (Scheme 1), and exhibiting dual emission in aqueous media with a satisfactory fluorescence quantum yield.[29] In the present work, we conjugated 2-(2-furanyl)-3HC to an amino group of a natural polyamine, spermine, which is a polycation at neutral pH. In eukaryotic

* Corresponding author. E-mail: aklymchenko@pharma.u-strasbg.fr.

10.1021/jp8058068 CCC: $40.75
Published on Web 09/03/2008

SCHEME 2: Synthesis of Conjugates 1 and 2[a]

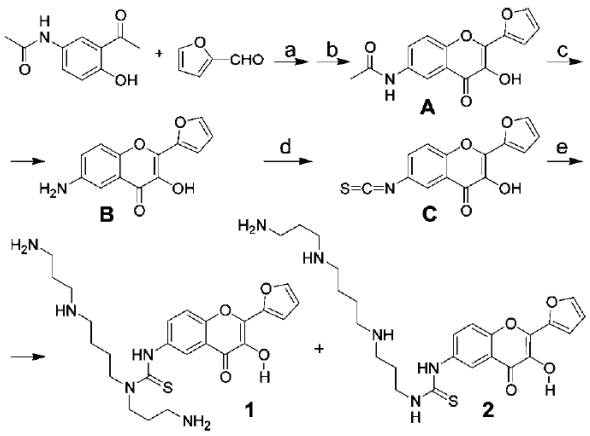

[a] Reagents: (a) DMF, MeONa; (b) H_2O_2, EtOH, NaOMe; (c) 10% HCl; (d) DPT, THF; (e) spermine, DMF.

cells, spermine and its shorter analog spermidine form strong complexes with DNA and, thus, stabilize chromatin and prevent DNA damage.[30−32] Moreover, their lipid conjugates are efficient gene delivery vectors.[33] Our results show that binding of 3HC-spermine conjugates to dsDNA strongly increases the relative intensity of the T* state, indicating a low polar surrounding of the fluorophore inside DNA probably due to an intercalation of the dye between the DNA bases. In contrast, in complex with single-stranded DNA (ssDNA), a different dual emission profile is observed, indicating a significantly higher polarity of the fluorophore surrounding. Thus, our environment-sensitive dye conjugated with spermine can distinguish between ssDNA and dsDNA. Application of environment-sensitive dyes undergoing ESIPT constitutes thus a new approach for DNA probing.

Materials and Methods

Reagents and Solvents. All the reagents were purchased from Aldrich-Sigma Chemical Company. Solvents for synthesis were of reagent quality, they were appropriately dried if necessary. For absorption and fluorescence studies the solvents were of spectroscopic grade. Calf thymus DNA (CT-DNA) and single-stranded polydeoxyadenylic acids poly(dA) and poly(dT) were from Sigma.

Synthesis of 3HC Conjugates with Spermine (See Scheme 2). 5′-Acetamido-2′-hydroxyacetophenone and furfural were condensed into the corresponding chalcone in dry DMF in the presence of sodium methoxide (RT, 24 h). The reaction mixture was diluted with several volumes of ethanol and treated with 10 mol excess of hydrogen peroxide and 12 mol excess of sodium methoxide. Refluxing the mixture for 5 min afforded corresponding 3-hydroxychromone (**A**) with yield 55%. ^{1}H NMR (300 MHz, DMSO-d6) δ 10.25 (s, 1H, OH), 9.95 (br.s, 1H, NH), 8.43 (d, J = 2.5 Hz, 1H, ArH), 8.03 (br.s, 1H, HetH), 7.97 (dd, J = 9 Hz, J = 2.5 Hz,1H, ArH), 7.69 (d, J = 9 Hz, 1H, ArH), 7.29 (d, J = 3.5 Hz, 1H, HetH), 6.8 (dd, J = 3.5 Hz, J = 1.5 Hz, 1H, HetH), 2.09 (s, 3H, $COCH_3$); m/z 286.4 (M++H).

The above-obtained acetamide (**A**) was hydrolyzed in 10% HCl under refluxing during 7 h (100 °C). Then water was added and the mixture was neutralized with base to pH 7. The obtained product was filtrated and dried to give the corresponding amine (**B**) with yield 90%. ^{1}H NMR (300 MHz, DMSO-d_6) δ 9.63 (s, 1H, OH), 7.99 (s, 1H, HetH), 7.44 (d, J = 9 Hz, 1H, ArH), 7,23 (m, 2H, ArH, HetH), 7.08 (dd, J = 9 Hz, J = 2.5 Hz,1H, ArH), 6.77 (dd, J = 3.5 Hz, J = 1.5 Hz, 1H, HetH), 5.47 (br.s, 2H, NH_2); m/z 244.2 (M^+ + H).

A 0.2 g (0.82 mmol) sample of 6-amino-2-furan-2-yl-3-hydroxychromone (**B**) was dissolved in 10 mL of dry THF and 0.35 g (1.5 mmol) of DPT (1,1′-thiocarbonyldi-2(1*H*)pyridone) was added to this solution. The reaction mixture was stirred under Ar at room temperature for 2 h. The solvent was removed in vacuo, and the product was purified by column chromatography (CH_2Cl_2/cyclohexane = 50/50) to give 0.17 g (72%) of pure isothiocyanate (**C**). ^{1}H NMR (300 MHz, DMSO-d_6) δ 10.26 (s, 1H, OH), 8.07 (m, 2H, ArH), 7.82 (s, 2H, HetH), 7.32 (d, J = 4 Hz 1H, ArH), 6.82 (dd, J = 3.5 Hz, J = 1.5 Hz, 1H, HetH); m/z 286.3 (M^+ + H).

A solution of 30 mg of **C** (2-furan-2-yl-3-hydroxy-6-isothiocyanato-chromen-4-one) in 1 mL of DMF was added dropwise to 100 μL of spermine with constant stirring for 2 h at rt. Crude mixture of two isomers (**1** and **2**) was applied to a reversed-phase C8 high-pressure liquid chromatography (HPLC) column (5 μm particle size) eluted with (A) aqueous TFA (0.05%, v/v), and (B) 70% of MeCN, 30% of water, with addition of TFA (0.05%, v/v). Linear gradient from 10 to 30% of B in 30 min was used. Fractions were collected at a flow rate of 4 mL/min and the eluant was monitored by adsorption at 360 nm. Fractions containing compounds **1** and **2** were freeze-dried to give lyophilized powders. For compound **1**, ^{1}H NMR (300 MHz, D_2O + drop of TFA) δ 7.65 (m, 2H, ArH), 7.28 (m, 3H, ArH), 6.64 (dd, J = 3.5 Hz, J = 1.5 Hz, 1H, HetH), 3.65 (m, 2H, C**H**$_2$NC=S), 2.84 (m, 10H, C**H**$_2$N), 1.92 (m, 2H, NCH$_2$C**H**$_2$CH$_2$N), 1.76 (m, 2H, NCH$_2$C**H**$_2$CH$_2$N), 1.54 (m, 4H, CH$_2$C**H**$_2$C**H**$_2$CH$_2$). For Compound **2**, ^{1}H NMR (300 MHz, D_2O + drop of TFA) δ 7.69 (m, 2H, ArH), 7.38 (m, 3H, ArH), 6.66 (dd, J = 3.5 Hz, J = 1.5 Hz, 1H, HetH), 3.8 (m, 2H, C**H**$_2$NHC=S), 3.6 (m, 2H, C**H**$_2$NHC=S), 2.88 (m, 8H, C**H**$_2$N), 1.99 (m, 2H, NCH$_2$C**H**$_2$CH$_2$N), 1.86 (m, 2H, NCH$_2$C**H**$_2$CH$_2$N), 1.65 (m, 4H, CH$_2$C**H**$_2$C**H**$_2$CH$_2$).

Instrumentation. Proton NMR spectra were recorded on a 300 MHz Bruker spectrometer and mass spectra were recorded on a Mariner System 5155 mass spectrometer using the electrospray ionization (ESI) method. All column chromatography experiments were performed on silica gel (Merck, Kieselgel 60H, Art 7736). Purification was carried out on a Shimadzu SPD-20A HPLC using a C8 column (uptisphere 300A, 5 μm; 250 × 10, Interchim, France) with a 10 to 70% linear gradient and monitoring the 3HC dye absorption at 360 nm. Absorption and fluorescence spectra were recorded on a Cary 400 spectrophotometer (Varian) and FluoroMax 3.0 spectrofluorimeter (Jobin Yvon, Horiba), respectively. For fluorescence studies, the dyes were used at 0.1 to 1 μM concentrations. Excitation wavelength was 340 nm. Fluorescence quantum yields were determined using quinine sulfate in 0.5 M sulfuric acid as a reference (quantum yield, φ = 0.577).[34] For the experiments in water, 10 mM phosphate buffer (pH 7.0) was used systematically. Hybridization of poly(dA) with poly(dT) was performed by annealing their equimolar mixture (100 μM, expressed in phosphate groups) in the phosphate buffer containing 100 mM NaCl at 95 °C for 10 min, followed by slow cooling (within *ca* 6 h) to room temperature. For the spectroscopic measurements, the obtained stock solution of the hybridized DNA, poly(dA-dT), was diluted to a final concentration (1 μM) using 10 mM phosphate buffer.

Results and Discussion

Initially, we synthesized a fluorophore building block **A** starting from 2-hydroxyacetonenone and 2-furaldehyde. The **A**

TABLE 1: Spectroscopic Properties of the Parent Dye A, and the Conjugates 1 and 2 in Different Organic Solvents, in Buffer, and as Bound to Different ssDNAs and dsDNAs[a]

media	dye	λ_{N^*}, nm	λ_{T^*}, nm	I_{T^*}/I_{N^*}	Q, %
water ($\alpha = 1.17$,[b] $\epsilon = 78.4$)	**A**	431	506	0.62	2.4
	1	433	510	0.90	0.5
	2	435	510	1.14	0.7
MeOH ($\alpha = 0.43$, $\epsilon = 32.6$)	**A**	421	532	1.14	6.3
	1	423	537	1.01	1.0
	2	425	537	1.32	1.0
EtOH ($\alpha = 0.37$, $\epsilon = 24.9$)	**A**	422	532	2.88	6.2
	1	422	538	2.08	1.0
	2	422	537	2.56	0.94
1-octanol ($\alpha = 0.37$, $\epsilon = 9.86$)	**A**	418	534	4.83	14.6
	1	421	536	5.00	3.0
	2	421	538	5.00	2.8
DMF ($\alpha = 0$, $\epsilon = 37.2$)	**A**	420	540	9.30	8.2
	1	425	543	7.52	1.3
	2	431	543	5.49	2.0
acetone ($\alpha = 0$, $\epsilon = 20.5$)	**A**	411	536	13.9	8.6
	1	419	538	7.4	1.7
	2	420	539	5.8	2.4
EtOAc ($\alpha = 0$, $\epsilon = 5.99$)	**A**	413	535	19.8	12.1
	1	417	537	14.9	3.9
	2	419	537	10.8	5.9
CT-DNA	**1**	435	539	7.70	1.3
	2	439	539	18.2	6.7
poly(dA)	**1**	436	535	1.15	0.7
	2	442	535	1.79	1.2
poly(dT)	**1**	431	532	1.35	0.7
	2	432	535	1.90	0.7
CT-DNA 83 °C	**1**	440	532	0.97	–
	2	444	539	1.88	–
poly (dA-dT)	**1**	430	537	6.35	1.4
	2	433	539	10.4	2.6

[a] Key: Q, fluorescence quantum yield, measured using quinine sulfate in 0.5 M sulfuric acid as a reference; λ_{N^*} and λ_{T^*}, position of the N* and T* emission band maximum, respectively; I_{T^*}/I_{N^*}, intensity ratio of the two emission bands. A 10 mM phosphate buffer was used. α: Abraham's H-bond donor ability (from ref 35). ϵ: dielectric constant. [b] The presented value of α corresponds to the H-bond donor ability introduced by Kamlet−Taft.[36]

compound was further hydrolyzed in hydrochloric acid and the obtained 6-amino derivative was converted into the 6-isothiocyanate derivative of 2-(2-furanyl)-3HC by using DPT (Scheme 2). The resulting derivative was further reacted with spermine giving two products of nearly equal quantities. After isolation with HPLC, we identified compounds **1** and **2**, corresponding to spermine modified with 3HC at the secondary and primary amino groups, respectively. Since the amino group of spermine used for conjugation cannot be protonated, conjugate **2** can be considered as a derivative of spermidine.

Spermine conjugates **1** and **2** as well as compound **A** which corresponds to the fluorophore, were studied in organic solvents of different polarity and H-bond donor ability (Table 1). The compound **A**, similarly to its parent 2-(2-furanyl)-3-hydroxychromone, exhibits dual emission highly sensitive to solvent properties.[24] In aprotic solvents, the I_{T^*}/I_{N^*} ratio is large, so that the emission of the ESIPT product T* dominates. On increase in solvent polarity within aprotic solvents from ethyl acetate to DMF, a decrease in the I_{T^*}/I_{N^*} ratio is observed (Table 1). In protic solvents, the emission of the ESIPT product is strongly decreased, due to the H-bonding perturbation of the ESIPT by the H-bond donor ability of the protic solvents.[17,24] Thus, comparison of protic and aprotic solvents of similar polarity, such as DMF and methanol, shows that in protic solvents, the relative intensity of the ESIPT product T*, the I_{T^*}/I_{N^*} ratio is much lower than in aprotic solvents (where the H-bond donor ability close to 0) (Table 1). Moreover, in protic solvents the dual emission of A varies also as a function of solvent polarity, so that in the polar solvent methanol, the I_{T^*}/I_{N^*} ratio is nearly 5-fold lower than in the less polar 1-octanol. Thus, both the H-bond donor ability and the solvent polarity hamper the ESIPT reaction and thus the emission of the T* form in **A**. As a result, in water, where both parameters are extremely high, the I_{T^*}/I_{N^*} ratio exhibits the lowest values (Table 1). Spectroscopic studies of conjugates **1** and **2** in organic solvents show that the 3HC moiety keeps its dual emission (Figure 1), and thus, undergoes ESIPT. Moreover, the positions of the two bands and the ratio of their intensities, I_{T^*}/I_{N^*} are not strongly modified on conjugation with spermine, as it can be seen by comparison of conjugates **1** and **2** with the parent dye **A** in most of the studied solvents (Table 1, some deviations are observed in water and aprotic solvents, see below). However, **1** and **2** show significantly lower fluorescence quantum yields than **A**, indicating a quenching of 3HC likely by the amine groups of spermine.[37] Similarly to **A**, the nature of the solvent affects strongly the dual emission of **1** and **2**. Indeed, for both conjugates the I_{T^*}/I_{N^*} ratio is much higher in aprotic than in protic solvents. Moreover, an increase in solvent polarity from 1-octanol to methanol also decreases the I_{T^*}/I_{N^*} ratio (Figure 1, Table 1). Noteworthy, the I_{T^*}/I_{N^*} ratio of **1** and **2** varies in a less broad range with solvent properties than that of **A** (its value being higher in water and lower in aprotic solvents, Table 1). This poorer spectroscopic sensitivity of **1** and **2** to solvent could be explained by a screening of the 3HC fluorophore by the spermine backbone. In water, spermine probably decreases the local polarity and H-bond donor ability around the fluorophore, while in aprotic solvents, it may considerably increase the local H-bond donor ability (due to presence of its NH-protons). Thus, similarly to the parent fluorophore A and other 3HC analogs,[17,18,22−24] conjugates **1** and **2** exhibit high sensitivity of their emission to solvent polarity and H-bond donor ability. These two solvent parameters also affect the fluorescence quantum yield of the dyes, so that it is the highest in the apolar aprotic ethyl acetate and the lowest in water.

Since water is a key solvent that modulates the local polarity and H-bond donor ability in biomolecules, we studied the influence of water in the aprotic acetone solvent on the dual emission of conjugates **1** and **2**. The fluorescence spectra of conjugates **1** and **2** exhibit a strong decrease in the I_{T^*}/I_{N^*} ratio on increase in the water content in acetone (Figure 1), so that water hampers the ESIPT process and thus decreases the emission of the ESIPT product. Moreover, the increase in water content shifts considerably the T* band maximum to the blue (Table 1), which according to our previous studies is likely due to the high H-bond donor ability of water.[24,29] Thus, both the ratio of the two emission bands and the position of the tautomer band of 3HC dyes provides information on the water content in their surrounding, so that being bound to biomolecules, 3HC fluorophore can report on its exposure to water.

Addition of dsDNA (calf thymus DNA, CT-DNA) to conjugates **1** and **2** in buffer changes dramatically their fluorescence spectra (Figure 2), while dye **A** does not show any spectroscopic response to dsDNA (data not shown). Thus, conjugation with spermine enables the 3HC fluorophore to bind dsDNA. This binding strongly increases the fluorescence intensity of the T* band and decreases the intensity of the N* band, so that the I_{T^*}/I_{N^*} ratio increases (Table 1). Thus, binding to dsDNA favors the emission of the ESIPT product (T*). Noticeably, the increase in the T* emission on binding to

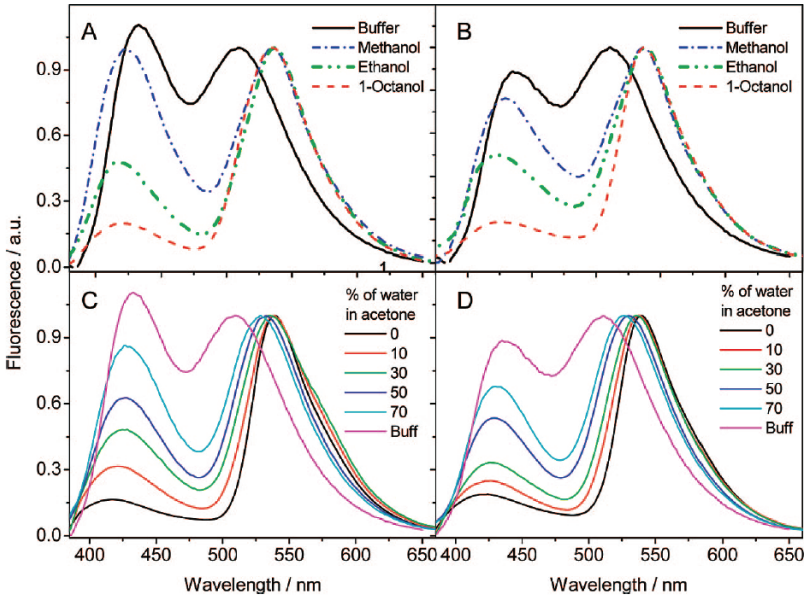

Figure 1. Effect of solvents on the dual emission of conjugates **1** and **2**. A and B: Fluorescence spectra of **1** and **2**, respectively, in different protic solvents. C and D: Fluorescence spectra of **1** and **2**, respectively, in acetone−water mixtures. The spectra were normalized at the maximum of the long wavelength T* band. Excitation wavelength was 340 nm.

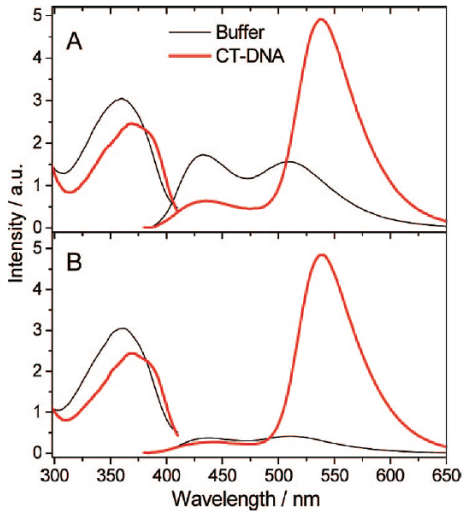

Figure 2. Absorption (left) and fluorescence (right) spectra of **1** (A) and **2** (B) in buffer (thin black curves) and in the presence of CT-DNA (thick red curves). 10 mM phosphate buffer (pH 7.0) was used. Concentration of **1** and **2** was 0.1 μM. The concentration of CT-DNA base pairs was 1 μM. Excitation wavelength was 340 nm.

dsDNA is more pronounced for **2** than for **1** (Figure 2). Moreover, both **1** and **2** exhibit shifts of their T* band to the red (Figure 2, Table 1). According to the data in solvents, the observed spectroscopic effects suggest that on binding to dsDNA, the environment of the 3HC fluorophore changes from a highly polar aqueous one with high H-bond donor ability (high exposure to water) to a less polar one with low H-bond donor ability (low exposure to water). On binding to dsDNA, the absorbance of **1** and **2** decreases by 20−25% (hypochromic effect), and the absorption maximum shifts to the red (from 361 to 369 nm) (Figure 2), strongly suggesting an intercalation of the 3HC fluorophore between the DNA bases. Remarkably, an increase in the fluorescence quantum yield accompanies the binding of **1** and **2** to dsDNA (Table 1), while many fluorescent dyes are quenched by DNA bases.[11,38] This increase in the quantum yield on intercalation of 3HC between the DNA bases can be explained by a screening of the 3HC fluorophore from the bulk aqueous environment and a decreased quenching by the amino groups of spermine. Remarkably, the I_{T^*}/I_{N^*} ratio in dsDNA for both conjugates is significantly lower than in any protic solvent including the low polar 1-octanol (Table 1), confirming the absence in the probe vicinity of water molecules, which are the major H-bond donors in the DNA surrounding. According to previous studies using other environment sensitive dyes, the polarity of the minor and major grooves of dsDNA is rather high, namely $\varepsilon \approx 20$[10] and 40−60[4] respectively, indicating a significant amount of water molecules in the grooves. The poor water exposure of the 3HC fluorophore of our conjugates in dsDNA declines its possible localization in the DNA grooves, but confirms that the fluorophore is probably intercalated between the DNA bases, where the amount of water molecules is limited. Interestingly, a highly efficient ESIPT was also observed for a 2-(2′-hydroxyphenyl)benzoxazole derivative incorporated in dsDNA opposite an abasic site, in line with a low-polar and aprotic environment between the base pairs.[39]

What should happen then on binding of **1** and **2** to ssDNA, where intercalation is not expected? Addition of the poly(dA) ssDNA also modifies the fluorescence spectra of both conjugates (Figure 3), but the resulting spectra are strongly different from those with dsDNA. Indeed, the I_{T^*}/I_{N^*} ratio with poly(dA) is 7−10 fold lower than with dsDNA, while the T* band position with ssDNA is slightly shifted to the blue (Table 1). Importantly, on binding to another ssDNA, poly(dT), the conjugates **1** and **2** exhibit very close fluorescence spectra to those in poly(dA) (Figure 3). Similar fluorescence spectra were also obtained when CT-DNA was melted at 83 °C (Table 1).[40] Finally, annealing of poly(dA) with poly(dT) changes dramatically the spectra of **1** and **2**, so that they become very close to the spectrum with double-stranded CT-DNA (Figure 3, Table 1). Thus, irrespective to the DNA sequence, the spectra with ssDNA are strongly different from those with dsDNA, the relative intensity of the ESIPT product (i.e., I_{T^*}/I_{N^*} ratio) being strongly decreased in ssDNA (Table 1). Moreover, the fluorescence quantum yields of **1** and **2** bound to ssDNA are systematically lower compared to dsDNA (Table 1). Finally, ssDNAs modify the absorption spectra of **1** and **2** to a much lower extent than dsDNAs,

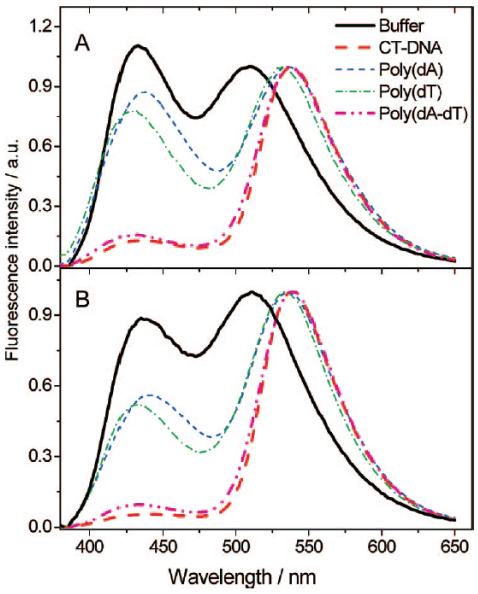

Figure 3. Fluorescence spectra of 0.1 μM of conjugates **1** (A) and **2** (B) in 10 mM phosphate buffer (pH 7) in the absence and in the presence of an excess of dsDNA (CT-DNA and poly(dA-dT) at 20 °C) or ssDNA (poly(dA) and poly(dT)). Concentration of dsDNA (base pairs) and ssDNA (bases) was 1 μM. The spectra were normalized at the T* band maximum. Excitation wavelength was 340 nm.

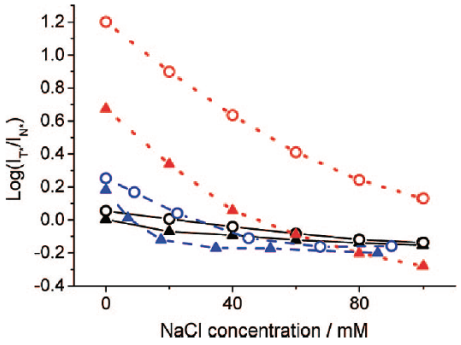

Figure 4. Salt effect on log(I_{T*}/I_{N*}) of conjugates **1** (▲) and **2** (○) in free form (solid curve and symbols in black), bound to CT-DNA (dotted curve and symbols in red) or to poly(dA) (dashed curve and symbols in blue). Conditions were as in Figure 3.

providing only a 5−7% hypochromism and *ca* 5 nm red shift. These data suggest that the 3HC fluorophore of the spermine conjugates is much more exposed to water in ssDNA than in dsDNA, probably because an efficient screening of the fluorophore from the bulk water due to intercalation between the base pairs can only be realized in dsDNAs. Thus, the ESIPT-based fluorophore allows us to clearly distinguish between ssDNAs and dsDNAs, simply by the ratio of the two emission bands.

Due to the polycationic nature of conjugates **1** and **2**, their interaction with DNA should be mainly electrostatic, and therefore, it should strongly depend on salt concentration. In line with our expectations, log(I_{T*}/I_{N*}), which is a function of the I_{T*}/I_{N*} ratio exhibiting a linear correlation with solvent parameters,[23,41] strongly decreases with increasing salt concentrations for **1** and **2** complexed with dsDNA (CT-DNA), while in DNA-free buffer the salt effect is negligible (Figure 4). For both conjugates, the log(I_{T*}/I_{N*}) values at high salt concentrations approach the values in DNA-free buffer, indicating that the complexes of **1** and **2** with dsDNA are probably dissociated. Noticeably, the salt effect is stronger for conjugate **1,** suggesting that it forms weaker complexes with DNA than conjugate **2**. Relatively weak complexes are formed with poly(dA), since the log(I_{T*}/I_{N*}) values of their complexes with **1** and **2** decrease very rapidly with increasing salt concentrations (Figure 4). Titrations in 30 mM NaCl confirm that both conjugates bind dsDNA much stronger than ssDNA, since the binding constants for **1** and **2** with dsDNA are $(2.5 \pm 0.5) \times 10^7$ M^{-1} and $(9.1 \pm 1.4) \times 10^7$ M^{-1}, respectively, while for ssDNA, the corresponding values are $(1.0 \pm 0.5) \times 10^6$ M^{-1} and $(2 \pm 1) \times 10^6$ M^{-1}. The binding constants for dsDNA correspond well to the literature values for spermidine in low-salt buffer.[42] Moreover, the higher affinity of both conjugates to dsDNA as compared to ssDNA is in line with the reported preference of spermine and spermidine for dsDNA.[42] Finally, the higher affinity of **2** compared to **1** can be understood considering that the modification of a primary amino group of spermine (in **2**) perturbs less the binding to DNA than modification of its secondary amino group (in **1**). In case of **2**, the cationic spermidine residue likely binds to the dsDNA minor or major grooves,[43,44] while the long and flexible fluorophore spacer (Figure 1) enables the fluorophore to intercalate between the bases. The appropriate size, the flat aromatic structure (Scheme 1) and the hydrophilicity of the 3HC fluorophore are likely the key factors that favor its intercalation into dsDNA. In case of **1** bound to dsDNA, the 3HC fluorophore is probably locked between the cationic groups, and, therefore, due to insufficient freedom intercalates less efficiently. This reduced intercalation is evidenced by the significantly lower I_{T*}/I_{N*} ratio and thus, the higher water accessibility of **1** compared to **2** in complex with dsDNA. This poorer intercalation could be an additional factor of the lower affinity of **1** compared to **2** for dsDNA.

In conclusion, we have conjugated an environment-sensitive 3HC fluorophore undergoing ESIPT to spermine. On binding to dsDNA and ssDNA, the conjugates show dramatic change in their dual emission. This enables to directly monitor their interaction with DNA by recording the ratio of the two emission bands. In complex with dsDNA, the enhanced emission of the ESIPT product indicates an efficient screening of the 3HC fluorophore from the bulk water, probably due to its intercalation in dsDNA. A very different spectral profile is observed on binding to ssDNA, suggesting that in ssDNA the fluorophore is much less screened from water molecules. Thus, our dyes can clearly distinguish between ssDNA and dsDNA. Consequently, this study shows that labeling of a polycationic molecule (like spermine) with 3HC allows monitoring its interaction with nucleic acids as well as probing the microenvironment of local binding sites.

Acknowledgment. This work was supported by FRM, TRIoH, and ANR research grants, as well as by ARCUS. V.V.S. and D.A.Y. acknowledge the financial support of the Eiffel Fellowship Program. We thank Alain Burger and Rachid Benhida for fruitful discussions.

References and Notes

(1) Cohen, B. E.; McAnaney, T. B.; Park, E. S.; Jan, Y. N.; Boxer, S. G.; Jan, L. Y. *Science* **2002**, *296*, 1700.
(2) Sloan, D. J.; Hellinga, H. W. *Protein Eng.* **1998**, *11*, 819.
(3) Altschuh, D.; Oncul, S.; Demchenko, A. P. *J. Molecular Recognition* **2006**, *19*, 459.
(4) Jadhav, V. R.; Barawkar, D. A.; Ganesh, K. N. *J. Phys. Chem. B* **1999**, *103*, 7383.
(5) Barawkar, D. A.; Ganesh, K. N. *Nucleic Acids Res.* **1995**, *23*, 159.
(6) Somoza, M. M.; Andreatta, D.; Murphy, C. J.; Coleman, R. S.; Berg, M. A. *Nucleic Acids Res.* **2004**, *32*, 2494.
(7) Kimura, T.; Kawai, K.; Majima, T. *Org. Lett.* **2005**, *7*, 5829.
(8) Kimura, T.; Kawai, K.; Majima, T. *Chem. Commun.* **2006**, 1542.

(9) Tainaka, K.; Tanaka, K.; Ikeda, S.; Nishiza, K.; Unzai, T.; Fujiwara, Y.; Saito, I.; Okamoto, A. *J. Am. Chem. Soc.* **2007**, *129*, 4776.
(10) Jin, R; Breslauer, K. J. *Proc. Natl. Acad. Sci. U.S.A.* **1988**, *85*, 8939.
(11) Kumar, C. V.; Asuncion, E. H. *J. Am. Chem. Soc.* **1993**, *115*, 8547.
(12) Granzhan, A.; Ihmels, H.; Viola, G. *J. Am. Chem. Soc.* **2007**, *129*, 1254.
(13) Formosinho, S. J.; Arnaut, L. G. *J. Photochem. Photobiol. A: Chem.* **1993**, *75*, 21.
(14) Douhal, A.; Lahmani, F.; Zewail, A. H. *Chem. Phys.* **1996**, *207*, 477.
(15) Henary, M.; Fahrni, C. *J. Phys. Chem. A* **2002**, *106*, 5210.
(16) Santra, S.; Krishnamoorthy, G.; Dogra, S. K. *Chem. Phys. Lett.* **1999**, *311*, 55.
(17) McMorrow, D.; Kasha, M. *J. Phys. Chem.* **1984**, *88*, 2235.
(18) Chou, P. T.; Martinez, M. L.; Clements, J. H. *J. Phys. Chem.* **1993**, *97*, 2618.
(19) Chou, P.; Yu, W.; Cheng, Y.; Pu, S.; Yu, Y.; Lin, Y.; Huang, C.; Chen, C. *J. Phys. Chem. A* **2004**, *108*, 6487.
(20) Sengupta, P. K.; Kasha, M. *Chem. Phys. Lett.* **1979**, *68*, 382.
(21) Ormson, S. M.; Brown, R. G; Vollmer, F.; Rettig, W. *J. Photochem. Photobiol. A: Chem.* **1994**, *81*, 65.
(22) Swinney, T. C.; Kelley, D. F. *J. Chem. Phys.* **1993**, *99*, 211.
(23) Klymchenko, A. S.; Demchenko, A. P. *Phys. Chem. Chem. Phys.* **2003**, *5*, 461.
(24) Klymchenko, A. S.; Kenfack, C.; Duportail, G.; Mely, Y. *J. Chem. Sci.* **2007**, *119*, 83.
(25) Klymchenko, A. S.; Avilov, S. V.; Demchenko, A. P. *Analyt. Biochem.* **2004**, *329*, 43.
(26) Klymchenko, A. S.; Duportail, G.; Mely, Y.; Demchenko, A. P *Proc. Natl. Acad. Sci. U.S.A.* **2003**, *100*, 11219.
(27) Shynkar, V. V.; Klymchenko, A. S.; Duportail, G.; Demchenko, A. P.; Mely, Y. *Biochim. Biophys. Acta* **2005**, *1712*, 128.
(28) Shynkar, V. V.; Klymchenko, A. S.; Kunzelmann, C.; Duportail, G.; Muller, C. D.; Demchenko, A. P.; Freyssinet, J. M.; Mely, Y. *J. Am. Chem. Soc.* **2007**, *129*, 2187.
(29) Klymchenko, A. S.; Demchenko, A. P. *New J. Chem.* **2004**, *28*, 687.
(30) Feuerstein, B. G.; Pattabiraman, N.; Marton, L. J. *Proc. Natl. Acad. Sci. U.S.A.* **1986**, *83*, 5948.
(31) Feuerstein, B. G.; Pattabiraman, N.; Marton, L. J. *Nucleic Acids Res.* **1990**, *18*, 1271.
(32) Khan, A. U.; Mei, Y. H.; Wilson, T. *Proc. Natl. Acad. Sci. U.S.A.* **1992**, *89*, 11426.
(33) Behr, J. P.; Demeneix, B.; Loeffler, J. P.; Perez-Mutul, J. *Proc. Natl. Acad. Sci. U.S.A.* **1989**, *86*, 6982.
(34) Eastman, J. W. *Photochem. Photobiol.* **1967**, *6*, 55–72.
(35) Abraham, M. H. *J. Phys. Org. Chem.* **1993**, *6*, 660–684.
(36) Kamlet, M. J.; Abboud, J. L. M.; Abraham, M. H.; Taft, R. W. *J. Org. Chem.* **1983**, *48*, 2877–2887.
(37) Gordon, M., Ware, W. R., Eds. *The Exiplex*; Academic Press: New York, 1975.
(38) Yang, X.; Liu, W.-H.; Jin, W.-J.; Shen, G.-L.; Yu, R.-Q. *Spectrochim. Acta A* **1999**, *55*, 2719.
(39) Ogawa, A. K.; Abou-Zied, O. K.; Tsui, V.; Jimenez, R.; Case, D. A.; Romesberg, F. E. *J. Am. Chem. Soc.* **2000**, *122*, 9917–9920.
(40) At the molar ratio dye/base pairs = 1/10, **1** and **2** do not modify considerably the melting point of CT-DNA, according to measurements of absorbance at 260 nm vs temperature (data not shown).
(41) Klymchenko, A. S.; Pivovarenko, V. G.; Ozturk, T.; Demchenko, A. P. *New. J. Chem.* **2003**, *27*, 1336.
(42) Morgan, J. E.; Blankenship, J. W.; Matthews, H. R. *Arch. Biochem. Biophys.* **1986**, *246*, 225.
(43) Schmid, N.; Behr, J. P. *Biochemistry* **1991**, *30*, 4357–4361.
(44) Yuki, M.; Grukhin, V.; Lee, C.-S.; Haworth, I. S. *Arch. Biochem. Biophys.* **1996**, *325*, 39–46.

JP8058068

Virus-sized DNA nanoparticles for gene delivery based on micelles of cationic calixarenes

(Publication 4)

Résumé en Français

de la Thèse de Doctorat de l'Université de Strasbourg

de Mlle Namrata JAIN

"Vecteurs de Gènes Non-Viraux Basés sur de Nouveaux Bolaamphiphiles Dissymétriques"

INTRODUCTION

La thérapie génique est un domaine de recherches en constant développement et une importante promesse thérapeutique pour le futur. Les vecteurs non-viraux basés sur les lipides cationiques sont très intéressants, car ils peuvent délivrer une grande quantité de matériel génétique et sont faiblement immunogènes. Bien que leurs complexes avec l'ADN (lipoplexes) démontrent une forte efficacité de transfection *in-vitro*, leur application en thérapie génique *in-vivo* reste cependant à confirmer. Notamment, l'un des inconvénients majeurs de ces lipoplexes est leur grande variabilité structurelle.

Les amphiphiles bipolaires appelées bolaamphiphiles (bolas), qui sont des analogues de lipides présentant des groupements polaires aux deux extrémités opposées de chaînes hydrophobes, ont progressivement gagné en intérêt ces dernières années étant donné leur aptitude à former des nanostructures supramoléculaires bien définies. Dans ce contexte, des bolas dissymétriques portant des têtes positivement chargées et neutres peuvent s'avérer une alternative intéressante aux lipides cationiques pour la délivrance de gènes.

Le but de cette thèse vise au développement de nouveaux vecteurs non-viraux basés sur de tels bolaamphiphiles dissymétriques. Pour cela, de nouveaux bolaamphiphiles ont été synthétisés, leur interaction avec l'ADN a été caractérisée par différentes techniques expérimentales et leur efficacité de transfection ainsi que leur trafic intracellulaire ont été testés sur différentes lignées cellulaires.

RÉSULTATS

Conception et synthèse des bolaamphiphiles

La conception de nos vecteurs non-viraux est basée sur des bola-molécules portent d'un coté un résidu neutre, soit sucre (dérivés du mannose, lactose, glucose) ou PEG et de l'autre un groupement mono- ou di-cationique basés sur des groupements amines, reliés par différents espaceurs hydrophobes (Fig. 1). Ces molécules peuvent générer des membranes asymétriques, en forme de vésicules ou de nanotubes, avec des surfaces interne et externe respectivement positivement chargée et neutre. Dans ce cas, la surface interne de la membrane devrait envelopper la molécule d'ADN alors que la surface externe neutre, étant inerte vis-à-vis de l'ADN, devrait empêcher toute agrégation des complexes et pouvoir être utilisée pour une exposition efficace d'un signal biologique pour un ciblage spécifique.

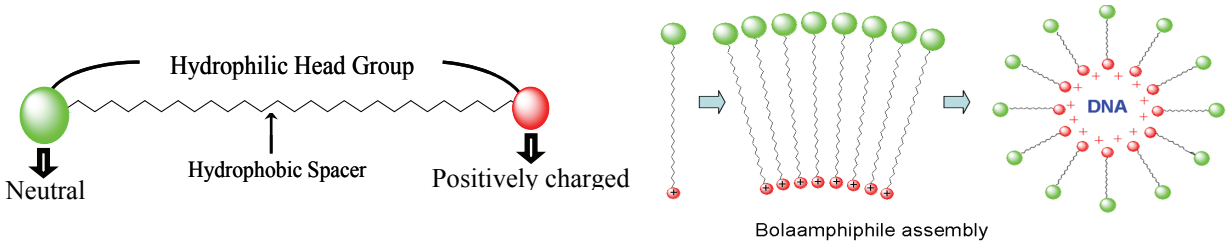

Figure1. Représentation schématique d'un bolaamphiphile et de son assemblage.

A partir de ce concept, 17 molécules de bolaamphiphiles ont été synthétisées et purifiées. Chacune de ces molécules a nécessité de 6 à 9 étapes de synthèse. Leur caractérisation et leur pureté ont été confirmées par HPLC, spectrométrie de masse et ^{1}H-NMR. Ces nouveaux bolas ont été classés en trois générations, et présentés ainsi dans ce travail.

Caractérisation structurale et études cellulaires

1ère Génération de Bolas portant une tête mono-cationique.

La première génération de bolas avec une tête mono-cationique (exemple : M-C8-C12-EDA, Fig. 2) n'a montré qu'une faible interaction avec l'ADN, ceci par électrophorèse sur gel. En outre, les mesures de diffusion de lumière (DLS) ont montré qu'avec ou sans ADN, la taille des nanostructures obtenues n'était pas stable, du fait d'une agrégation continue. La microscopie de force atomique (AFM) a révélé que certains bolas s'auto-assemblaient, sur une surface de mica, en une monocouche membranaire de 3-4 nm d'épaisseur. Par ailleurs, des nanotubes de ~30 nm de diamètre on été observés par microscopie électronique. Finalement, les essais de transfection des complexes sur des cellules HeLa (essai à la luciférase) se sont révélés inefficaces, avec une faible cytotoxicité. Ces résultats nous ont incité à effectuer des modifications de structure pour les bolas afin d'obtenir une meilleure interaction avec l'ADN ainsi qu'une meilleure solubilité.

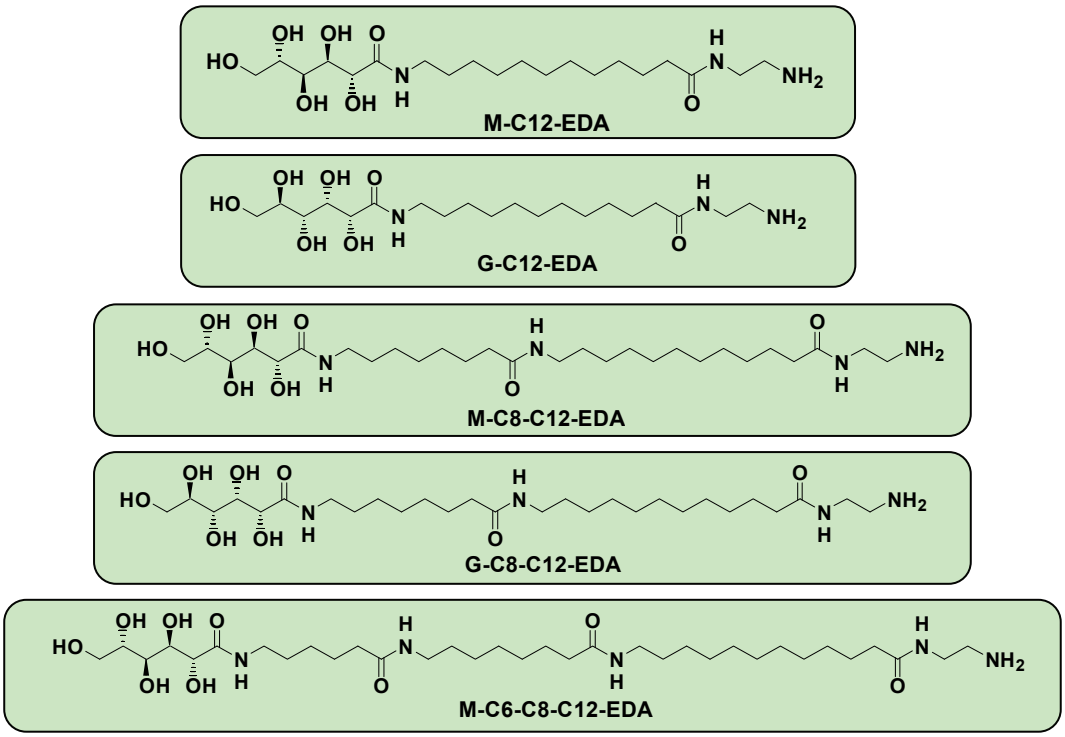

Figure 2. Structures chimiques de la 1ère Génération de bolas-molécules.

2nde Génération de Bolas portant une tête di-cationique.

Afin de surmonter les problèmes constatés avec la 1ére génération de bolas, nous avons choisi un résidu di-amine (ornithine) en place de l'amine initiale afin d'accroître la charge positive de la tête polaire. Cette modification s'est traduite par une augmentation de solubilité aqueuse significative et une moindre agrégation des bolas en l'absence d'ADN, ceci à concentration micromolaire. En outre, ces bolas ont montré une plus forte interaction avec l'ADN, bien que celle-ci ne soit totale qu'à des rapports N/P >7, comme l'ont montré les expériences d'électrophorèse sur gel et d'exclusion du bromure d'éthidium. La taille des bolaplexes obtenus, mesurés par DLS et AFM, est également moindre. Cependant, malgré ces résultats a priori favorables, cette 2nde génération de bolaplexes, testée sur des cellules HeLa et COS-7, ne montre toujours aucune efficacité de transfection. Afin de remédier à cette situation, de nouvelles modifications de la structure des bolas sont apparues nécessaires afin d'améliorer leur capacité à former des complexes avec l'ADN.

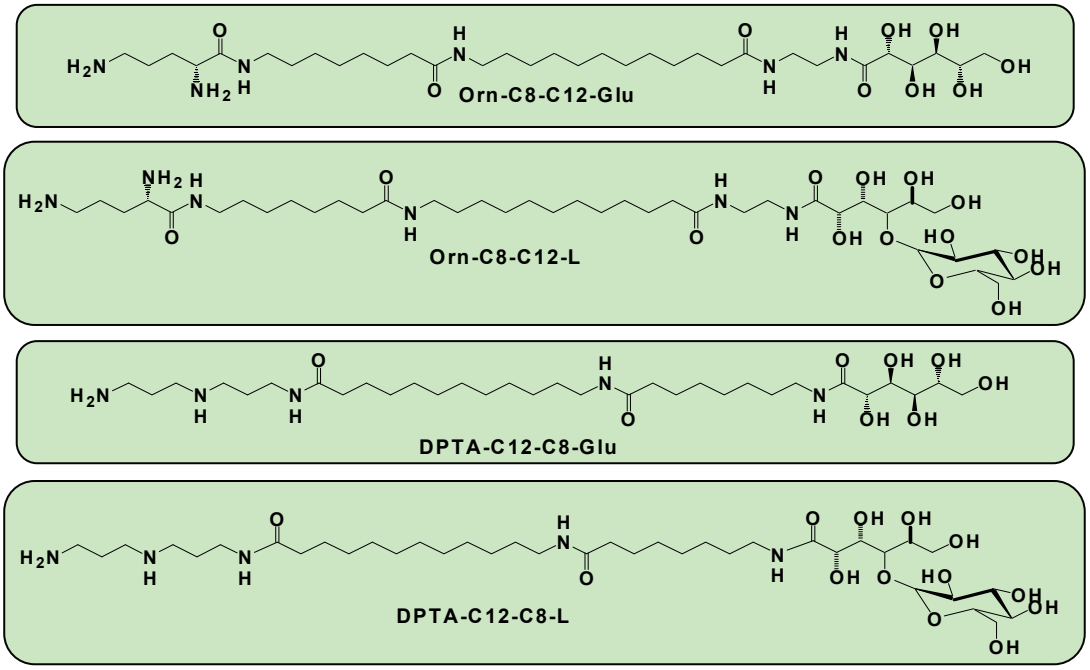

Figure 3. Structures chimiques de la 2nde Génération de bolas-molécules.

3ème Génération de Bolas portant une tête di-cationique et une tête sucre ou PEG, avec différents espaceurs hydrophobes.

En dernier lieu, nous avons synthétisé des bolas portant toujours une tête di-cationique ornithine, mais dont les espaceurs ont été modifiés afin d'augmenter leur hydrophobicité et ainsi d'améliorer leur capacité d'auto-association aux concentrations micromolaires. Par ailleurs, les têtes sucres ont dans certains cas été remplacés par une tête polyéthyléne glycol (PEG) (300 Da ou 2000 Da), également neutre et biocompatible.

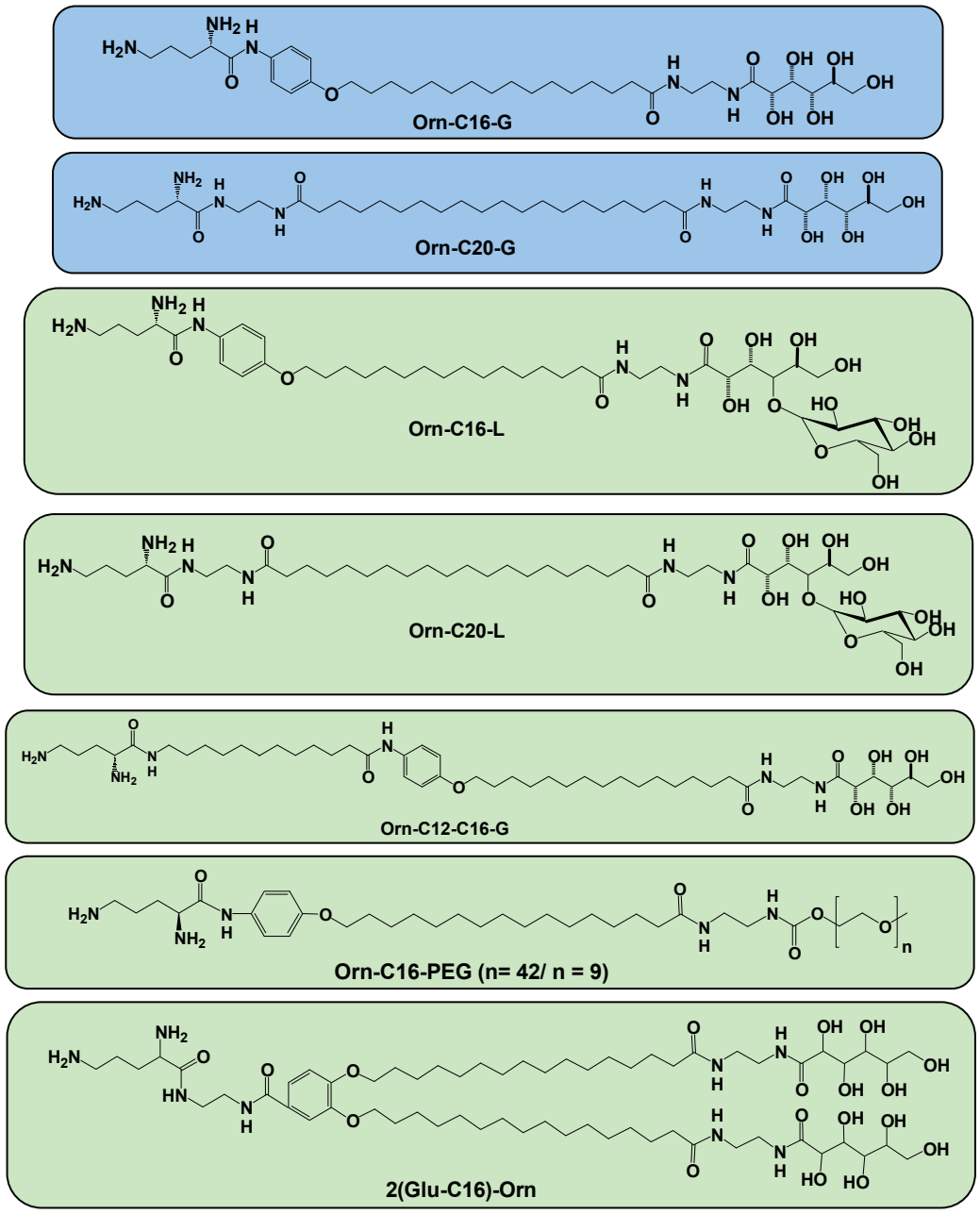

Figure 4. Structures chimiques de la 3ème Génération de bolas-molécules.

Ces nouveaux bolas gardent une excellente solubilité aqueuse et, en contraste avec la 2nde génération de bolas, leur auto-association conduit à des nanostructures de petite taille (100-200 nm par DLS) à concentration micromolaire (Tableau 1). Nous privilégierons dans ce résumé les résultats obtenus avec les bolas **Orn-C16-G** et **Orn-C20-G** (Fig.4, en bleu).

Tableau 1. Mesure de tailles de bolas et de bolaplexes par diffusion de la lumière (DLS) en solution aqueuse tamponnée (pH 7.4).

Sample		Volume analysis		Number analysis Mean diameter, nm
		Diameter, nm	Amount, %	
Orn-C16-G	Bola (100µM)	110	88	73
		1450	12	
	Bola/pDNA N/P 1.2 (12µM Bola)	109	95	90
	Bola/pDNA N/P 2 (12µM Bola)	92	45	152
		510	55	
	Bola/pDNA N/P 2 (20µM Bola)	1550	95	1400
	Bola/pDNA N/P 5 (50µM Bola)	870	100	925
Orn-C20-G	Bola (100µM)	140	15	110
		1050	85	
	Bola/pDNA N/P 1.2 (12µM Bola)	97	20	90
		930	80	
	Bola/pDNA N/P 2 (12µM Bola)	970	100	900
	Bola/pDNA N/P 2 (20µM Bola)	1370	100	1200
	Bola/pDNA N/P 5 (50µM Bola)	1090	100	1069
Orn-C16-G/ DOPE (1:1)	Bola/DOPE (100µM bola)	220	30	140
		1120	70	
	Bola/DOPE/pDNA N/P 2 (20µM Bola)	220	100	218
	Bola/DOPE/pDNA N/P 3 (30µM Bola)	200	20	190
		800	80	
	Bola/DOPE/pDNA N/P 5 (50µM Bola)	1440	100	1350

Les expériences d'électrophorése sur gel et d'exclusion du bromure d'éthidium (Fig. 5) indiquent une interaction forte avec l'ADN et une condensation importante de celui-ci.

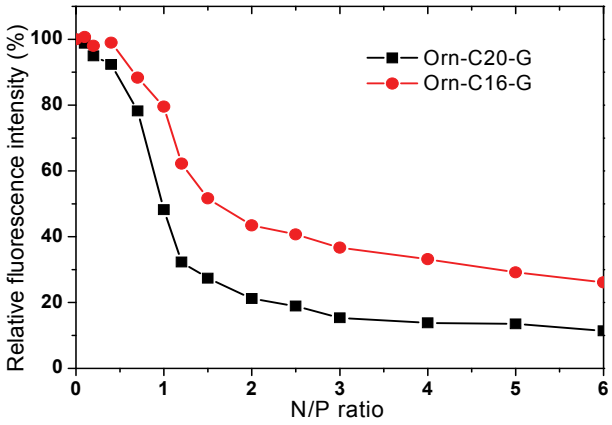

Figure 5. Expériences d'exclusion du bromure d'éthidium sur des complexes d'ADN de thymus de veau avec des bolas à différents rapports N/P. L'intensité de fluorescence est normalisée à 100% de l'intensité initiale.

Une augmentation en taille des bolaplexes a été observée par DLS aux rapports N/P élevés pour la plupart des bolas (Tableau 1), ce qui peut être lié à une neutralisation des complexes, en accord avec les mesures de potentiel Zeta (Fig. 6).

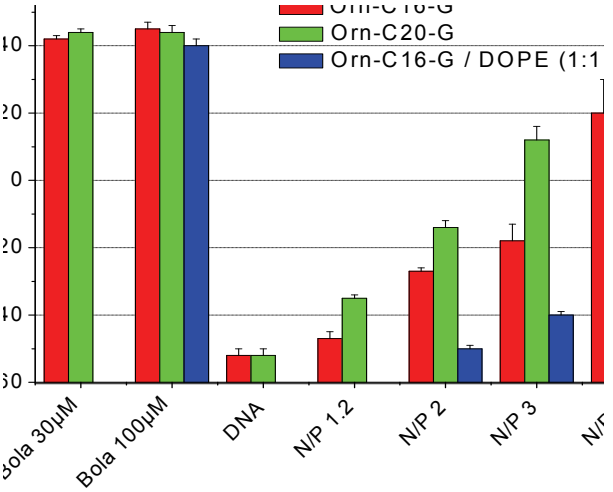

Figure 6. Potentiel Zeta de nanostructures formées uniquement de bolas ou de leurs formulations en présence de DOPE et d'ADN de thymus de veau à différents rapports N/P (tampon MES, pH 7.4).

Une diminution brutale de la taille des bolaplexes a été observée pour les bolas portant un dérivé lactose, ceci aux hauts rapports N/P et en présence de DOPE, ce qui a pu être expliqué par leur potentiel Zeta positif. Une autre exception concerne les bolas portant une tête PEG-2000, donnant des complexes de petite taille (ca 100 nm) même aux rapports N/P élevés. Il est possible d'en conclure que la présence de ce type de PEG empêche l'agrégation des bolaplexes à ces N/P, permettant ainsi un contrôle de leur taille. Afin d'accéder à la structure nanoscopique des bolaplexes, nous avons effectué des mesures de microscopie en force

atomique (AFM) en phase liquide tamponnée sur une surface en mica. Comme le montre la Fig. 7, les bolaplexes obtenus présentent des structures soit sphériques, soit en bâtonnet, selon la formulation du bola utilisé.

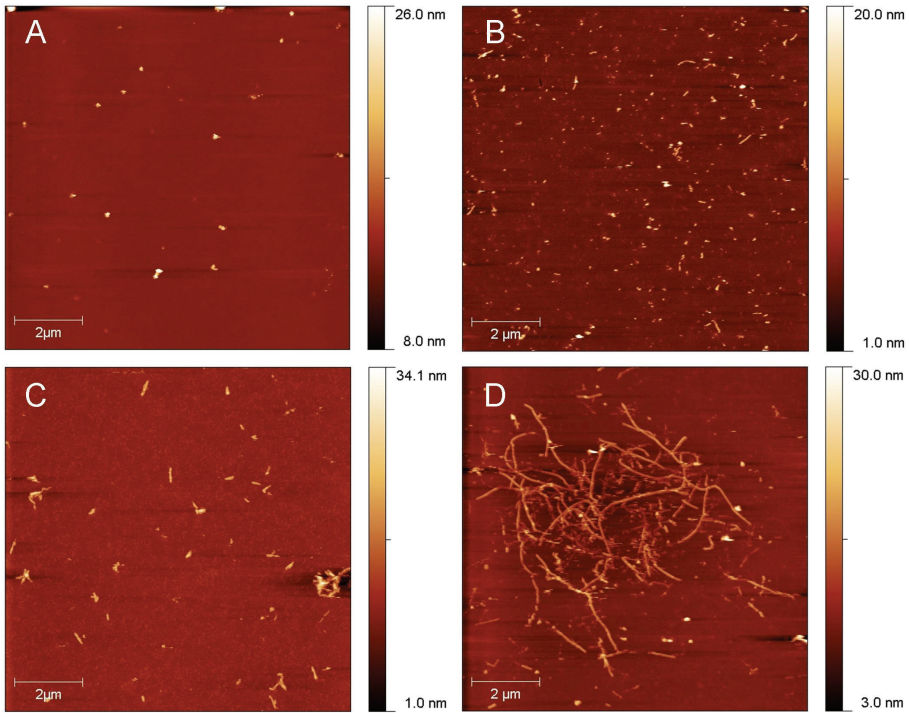

Figure 7. Images d'AFM de bolaplexes de Orn-C16-G (A et B, N/P 2) et de Orn-C20-G (C et D, N/P 1.2) obtenus avec de l'ADN plasmidique (A and C) et de l'ADN de thymus (B and D). Les images sont obtenues par "tapping mode".

Des études de transfection menées avec cette 3ème génération de bolas se sont révélées positives sur différentes lignées cellulaires (HeLa, COS-7 and HepG2). Leur efficacité de transfection augmente significativement en présence de DOPE ou de chloroquine, ce qui montre que les étapes clefs pour leur internalisation concernent leur fusion avec la membrane et leur sortie de l'endosome. Certaines formulations de bolaplexes contenant de la DOPE montrent une très forte efficacité de transfection, proche de celle observée pour un vecteur commercial tel le jetPEI. Cependant, la présence of sérum diminue significativement (mais non totalement) l'efficacité de transfection de ces bolaplexes, les formulations les plus sensibles à la présence de sérum étant celles contenant de la DOPE.

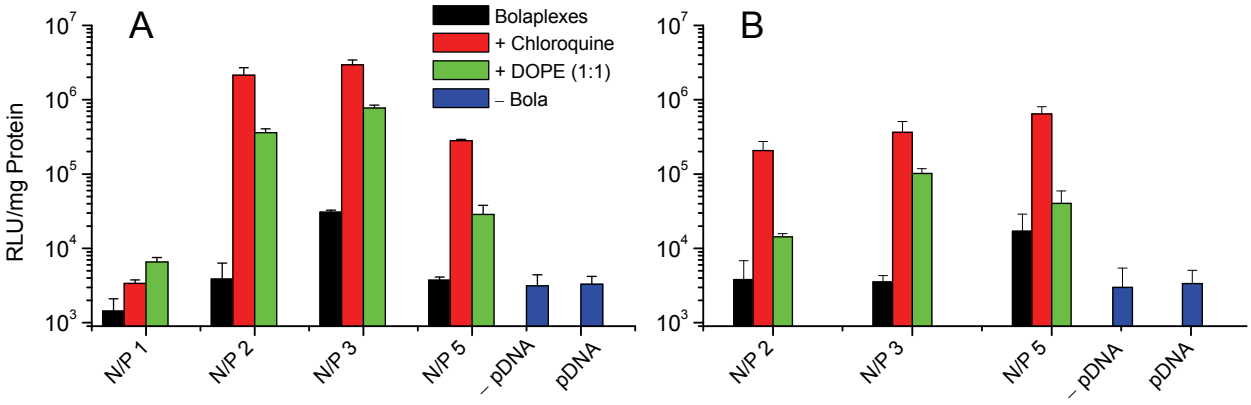

Figure 8. Efficacité de transfection de bolaplexes d'Orn-C16-G à différents rapports N/P sur des cellules COS-7 sans (A) et avec sérum (B). Les cellules on été incubées en serum-free Opti-MEM (A) ou en milieu de culture complet, DMEM, contenant 10 % de FBS (B), avec un bolaplexe composé d'ADN plasmidique (1 µg par puit), d'Orn-C16-G et de DOPE (lorsque indiqué). Pour quelques échantillons, le milieu contient 100 µM de chloroquine. Après 3 h, 10 % de FBS ont été ajoutés aux échantillons serum-free, alors que pour les échantillons avec chloroquine le milieu de transfection a été remplacé par du milieu de culture complet. L'activité luciférase a été mesurée après 48 h d'incubation. L'efficacité de transfection déterminée par l'essai à la luciférase est exprimée en RLU/mg de protéine. Les contrôles négatifs ont été réalisés avec des cellules non traitées (–pDNA) et des cellules transfectées avec de l'ADN nu (pDNA). Les expériences ont été répétées six fois pour les échantillons serum-free (A) et trois fois pour les échantillons avec sérum (B).

Les études de trafic intracellulaire de bolaplexes marqués par fluorescence, effectuées par microscopie confocale, montrent une internalisation par endocytose suivie d'une sortie des endosomes (Fig. 9). Enfin, des tests MTT montrent également une très faible cytotoxicité de cette génération de bolas.

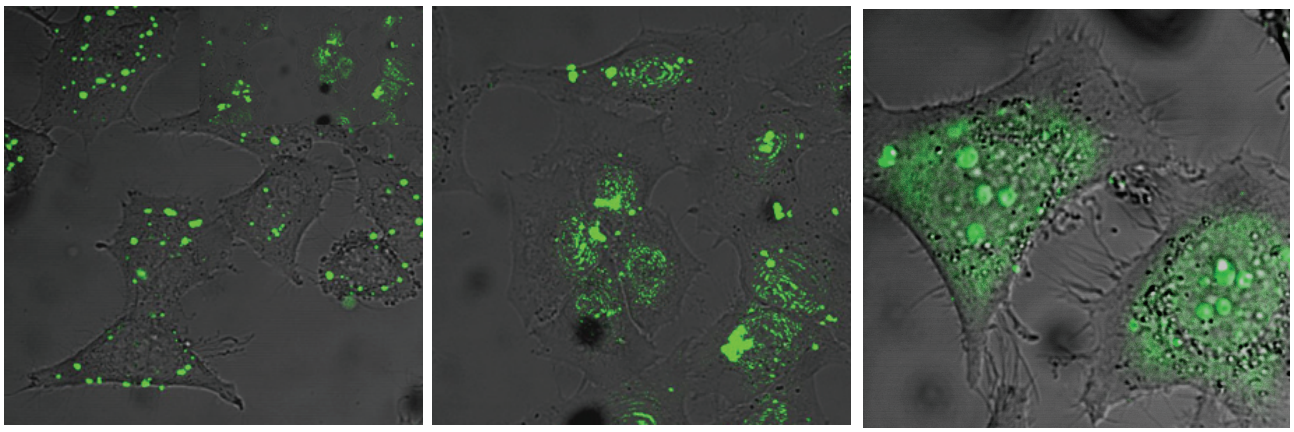

Figure 9. Images de microscopie de fluorescence obtenues avec des bolaplexes Orn-C16-L + DOPE au rapport N/P = 10 marqués au YOYO-1, pour des cellules HeLa à différents temps d'incubation: 1 h, 6h et 24 h.

CONCLUSIONS

Ce travail présente une alternative originale pour le développement de vecteurs non-viraux par l'utilisation de molécules bolaamphiphiles dissymétriques spécialement conçues dans ce but. Une grande variété de bolas, portant des groupements cationiques et neutres séparés par un espaceur hydrophobe, a été obtenue par synthèse organique multi-étapes. Leur caractérisation physicochimique par différentes techniques suggère que la nature de ces groupements et de l'espaceur hydrophobe conditionne l'auto-assemblage des bolas, leur interaction avec l'ADN et la morphologie des bolaplexes obtenus. Les deux premières générations de bolas synthétisés ne sont pas révélées posséder les propriétés nécessaires pour générer de bons vecteurs non-viraux. Par contre, la troisième génération s'est révélée très prometteuse. En effet, nous avons pu mettre en évidence pour nombre de ces derniers bolaamphiphiles une forte interaction avec l'ADN, une formation de bolaplexes de petite taille et une bonne efficacité de transfection pour plusieurs lignées cellulaires. L'augmentation de cette efficacité de transfection en présence DOPE et/ou de chloroquine indique que les étapes clefs de l'internalisation des complexes résident dans la fusion membranaire et la sortie de l'endosome. Il est à remarquer que certaines formulations de bolaplexes montrent une efficacité de transfection comparable aux meilleurs agents commerciaux. Le présent travail valide donc un nouveau concept visant à la construction de vecteurs non-viraux possédant une petite taille facile à contrôler, une efficacité élevée et une faible cytotoxicité.

PERSPECTIVES

Une modification complémentaire de la structure de ces molécules peut à nouveau s'envisager afin d'augmenter l'efficacité de transfection des bolaplexes, ceci en favorisant la sortie de l'endosome en l'absence de tout agent facilitateur. Ceci pourrait se réaliser en introduisant une seconde chaîne hydrocarbonée dans l'espaceur hydrophobe, afin de favoriser la fusion membranaire. Une seconde possibilité pourrait être l'introduction de groupements pH-sensibles, ce qui modifierait la structure des bolas à l'intérieur des endosomes, déclenchant ainsi la sortie de l'ADN. Enfin, les plus prometteurs des vecteurs ainsi obtenus pourront être fonctionnalisés par des ligands spécifiques afin de cibler des cellules particulières *in vivo*, ce qui est d'une importance cruciale pour de futures applications en thérapie génique.

Publications

Publications

Articles Published or In Press

Namrata Jain, Youri Arntz, Valérie Goldschmidt, Guy Duportail, Yves Mély, Andrey S. Klymchenko. New unsymmetrical bolaamphiphiles: synthesis, self-assembly, interactions with DNA and application for gene delivery. Bioconjugate Chem., 2010**,** 21, 2110–2118.

Andrey S. Klymchenko, Volodymyr V. Shvadchak, Dmytro A. Yushchenko, **Namrata Jain**, Yves Mély. Excited-State Intermolecular Proton Transfer Distinguishes Microenvironments in Single-And Double-Stranded DNA. J. Phys. Chem. B, 2008, 112 (38), pp 12050–12055.

Article Submitted

Roman V. Rodik, Andrey S. Klymchenko, **Namrata Jain**, Stanislav I. Miroshnichenko, Ludovic Richert, Vitaly I. Kalchenko, Yves Mély**.** Cationic amphiphilic calixarenes: hierarchical assembly of DNA nanoparticles for gene delivery. (Chemistry A European Journal)

Articles in Preparation

Namrata Jain, Valérie Goldschmidt, Youri Arntz, Guy Duportail, Yves Mély, Andrey S. Klymchenko. Gene delivery vectors based on lactose-ornithine bolaamphiphiles.

Namrata Jain, Sebnem Ercelen, Youri Arntz, Guy Duportail, Yves Mély, Andrey S. Klymchenko. Spontaneous monolayer formation of bolaamphiphiles on mica surface.

Posters

Namrata Jain, Youri Arntz, Guy Duportail, Yves Mely, Andrey S. Klymchenko. Self Assembled Nanostructures from Organic Bolaamphiphiles for application as Gene Delivery Vectors. Journees Campus d'Illkirch. 16-17th April, 2009.

Namrata Jain, Youri Arntz, Valerie Goldschmidt, Guy Duportail, Yves Mely, Andrey S. Klymchenko. Self Assembled Nanostructures from Organic Bolaamphiphiles for application as Gene Delivery Vectors. Journees Campus d'Illkirch. 3-4th May, 2010.

Namrata Jain, Youri Arntz, Valerie Goldschmidt, Guy Duportail, Yves Mely, Andrey S. Klymchenko. Self Assembled Nanostructures from Organic Bolaamphiphiles for Gene Delivery. Third International Nanobio Conference 2010, ETH Zurich, Switzerland, August 24-27th, 2010.

Résumé

Le succès de la thérapie génique repose sur la découverte de nouveaux et efficaces vecteurs de gènes. Les vecteurs non-viraux présentent un intérêt certain, car ils peuvent délivrer du matériel génétique en grande quantité et sont faiblement immunogéniques. Dans ce contexte, des molécules bolaamphiphiles dissymétriques (bolas) portant deux têtes polaires hydrophiles différentes reliées par un espaceur hydrophobe peuvent s'avérer être une alternative intéressante, car ils peuvent former des nano-structures supramoléculaires bien définies (nano-vésicules ou nanotubes) et plus stables que celles formées par des lipides. Le but du présent travail fût donc de développer de nouveaux vecteurs de transfection basés sur des bolas à même de former de telles nano-structures pouvant héberger une molécule d'ADN et exposer à leur surface externe des ligands neutres. Dans ce but, plusieurs types de bolas, portant des groupements cationiques et neutres reliés par un espaceur hydrophobe, ont été obtenus par synthèse organique multi-étapes. Leur caractérisation par différentes techniques démontre que la nature aussi bien des têtes polaires que de l'espaceur hydrophobe conditionne l'auto-assemblage des bolas, leur interaction avec l'ADN et la morphologie des complexes obtenus (bolaplexes). Les deux premières générations de bolas n'ont pas présentés les caractéristiques essentielles de bons vecteurs non-viraux. La troisième génération, au contraire, est apparue très prometteuse. Celle-ci montre une forte interaction avec l'ADN, la formation de bolaplexes de petites tailles et une bonne efficacité de transfection pour plusieurs lignées cellulaires. L'augmentation de l'efficacité de transfection en présence de DOPE ou de chloroquine suggère que l'étape essentielle pouvant limiter leur internalisation pourrait être leur fusion avec la membrane ou leur sortie des endosomes. Certaines formulations de bolaplexes présentent une efficacité comparable aux meilleurs agents de transfection commerciaux. Le présent travail introduit donc une nouvelle classe d'agents de transfection efficaces sur la base de bolaamphiphiles dissymétriques.

Abstract

The success in gene therapy relies strongly on new efficient gene delivery vectors. Non-viral vectors are highly attractive, since they can deliver large quantities of genetic information and are low immunogenic. In this respect, unsymmetrical bolaamphiphiles (bolas) bearing two different hydrophilic head-groups connected by a hydrophobic spacer could be an attractive alternative for vector design, as they can form well-defined supramolecular nanostructures (nanovesicles and nanotubes) that are more stable than those formed with lipids. The aim of the present work was to develop new gene delivery vectors based on bolas capable to form such nanostructures hosting a DNA molecule and exposing at their external surface neutral ligands. For this purpose, a variety of bolas, bearing cationic and neutral groups connected by a hydrophobic spacer, were obtained by multi-step organic synthesis. Their characterization by different instrumental techniques suggested that the nature of the head groups as well as the hydrophobic spacer defines the bola self-assembly, their interaction with DNA and the morphology of their complexes (bolaplexes). While the first two generations of bolas lack the essential features of nonviral vectors, the final third generation was found highly promising. The latter showed a strong interaction with DNA, the formation of small bolaplexes and a good transfection efficiency in different cell lines. The increase in transfection efficiency in presence of DOPE or chloroquine suggested that the key barrier for their internalization could be the lipid fusion and the endosomal escape. Some bolaplex formulations showed a transfection efficiency comparable to the best commercial transfection agents. Thus, the present work introduces a new class of efficient transfection agents based on unsymmetrical bolaamphiphiles.